

**STUDIES ON SENSING AND BIOLOGICAL  
APPLICATIONS OF FLUORESCENT  
CARBON DOTS DERIVED FROM  
NATURAL SOURCES**



**THESIS SUBMITTED TO THE UNIVERSITY OF CALICUT IN PARTIAL  
FULFILLMENT OF THE REQUIREMENTS FOR THE AWARD OF THE  
DEGREE OF DOCTOR OF PHILOSOPHY IN CHEMISTRY**

By  
**VIDYA N.**

**POST GRADUATE AND RESEARCH  
DEPARTMENT OF CHEMISTRY  
SREE NEELAKANTA GOVERNMENT SANSKRIT COLLEGE  
PATTAMBI – 679306  
JUNE – 2023**




**POST GRADUATE AND RESEARCH  
DEPARTMENT OF CHEMISTRY  
SREE NEELAKANTA GOVERNMENT  
SANSKRIT COLLEGE, PATTAMBI**



**CERTIFICATE**

This is to certify that the thesis entitled “**STUDIES ON SENSING AND BIOLOGICAL APPLICATIONS OF FLUORESCENT CARBON DOTS DERIVED FROM NATURAL SOURCES** ” bound herewith is a bonafide work done by Mrs. Vidya N. under my supervision in the Department of Chemistry, S.N.G.S. College, Pattambi in partial fulfillment of the requirement for the award of degree of **Doctor of Philosophy** in chemistry of the University of Calicut, and that the work has not been included in any other thesis submitted previously for the award of any other degree.

Place: Pattambi  
Date: 01.06.23

  
**Dr. P. Venugopalan**  
Professor  
(Supervising Teacher)  
Department of Chemistry  
S.N.G.S. College, Pattambi






**POST GRADUATE AND RESEARCH  
DEPARTMENT OF CHEMISTRY  
SREE NEELAKANTA GOVERNMENT  
SANSKRIT COLLEGE, PATTAMBI**



**CERTIFICATE**

This is to certify that the thesis entitled “**STUDIES ON SENSING AND BIOLOGICAL APPLICATIONS OF FLUORESCENT CARBON DOTS DERIVED FROM NATURAL SOURCES** ” bound herewith is a bonafide work done by Mrs. Vidya N. under my supervision in the Department of Chemistry, S.N.G.S. College, Pattambi in partial fulfillment of the requirement for the award of degree of **Doctor of Philosophy** in chemistry of the University of Calicut. I also certify that the corrections/suggestions from adjudicators have been incorporated in the revised thesis.

Place: Pattambi  
Date: 01.06.23

  
**Dr. P. Venugopalan**  
Professor  
(Supervising Teacher)  
Department of Chemistry  
S.N.G.S. College, Pattambi



## **DECLARATION**

I declare that the work presented in the thesis “**STUDIES ON SENSING AND BIOLOGICAL APPLICATIONS OF FLUORESCENT CARBON DOTS DERIVED FROM NATURAL SOURCES** ” is an authentic record of the original work done by me under the guidance of Dr. P. Venugopalan, Professor, Department of Chemistry S.N.G.S. College, Pattambi in partial fulfillment of the requirement for the award of degree of Doctor of Philosophy in chemistry of the University of Calicut, and further that no part of thereof has been included in any other thesis submitted previously for the award of any other degree of this university.

Place: Pattambi  
Date: 01.06.23

**Vidya N.**



## **ACKNOWLEDGEMENTS**

*As I contemplate upon all the years in obtaining my Ph.D. degree, I would like express my gratitude towards all those people who have contributed to my journey in different ways and made an everlasting impact on my life.*

*At this moment of accomplishment, first and foremost, I would like to convey my heartfelt thanks and appreciation to my supervisor, Dr. P. Venugopalan, who provided me a platform for pursuing Ph.D. He has been the guiding spirit for me since the day I started studies under him as a graduate student. It was his cordial behaviour, continuous guidance and support that encouraged me to take up Ph.D. I was able to learn the intricacies of research from him. Under his guidance, I was able to overcome the tough times in my research. I can happily credit him for bringing out the best in me. He provided me the freedom and a favourable environment for work which helped in achieving this feat in a short span of time. It was indeed an exciting and memorable experience working under him for all the years.*

*I wish to express my venerable thanks to the former and present Principals, Sree Neelakanta Government Sanskrit College Pattambi, Dr. K. S. Sheela, Dr. M. Jothiraj, Dr.Saji Stephen D., Dr. Sunil John J. and Dr. T. Subhash for providing the support and freedom for accessing various facilities in the centre.*

*I would also like to express my sincere thanks to research advisory committee (RAC) members, for their constructive criticism and precious suggestions which influenced my thought process.*

*I express my sincere thanks to Dr. Resmi M.R., Dr. Manoj T.P., Dr. Anjali Mathew and all other faculty members in the Department of*

*Chemistry, Sree Neelakanta Government Sanskrit College Pattambi for their valuable suggestions and generous help throughout the course of this work. I offer my sincere gratitude to all the lab assistants for their cooperation and help during the entire period.*

*I would like to express my sincere thanks to all my friends at Sree Neelakanta Government Sanskrit College Pattambi, for their support and cooperation.*

*I extend my gratitude to University of Calicut and FIST program of DST for providing the facilities. SAIF Cochin, SAIF, Mahatma Gandhi University, Kottayam and PSG IAS Coimbatore are acknowledged for experimental support.*

*Of course acknowledgements would be incomplete without thanking my family. Their countless blessings and great support made me sail through all the difficulties during the entire course of this work.*

*Above all, I am greatly thankful to God Almighty, for endowing me with inner strength, self-confidence and patience throughout my Ph.D.*

**Vidya N.**

## **PREFACE**

The newest member of the family of carbon nanomaterials, zero dimensional, fluorescent carbon dots (CDs), has tremendous promise for use in a variety of industries. It acquires the significant importance in almost every field owing to its versatile potentiality and environmental friendliness. The commendable biocompatibility and water solubility of this tiny luminary make it more users friendly. The biocompatibility of the CDs can further be increased by the introduction of biogenic carbon dots. Biogenic carbon dots are generated from natural resources and have a biological origin.

There has recently been an increasing interest in one-pot CDs synthesis, mostly to decrease waste and by-products. Many natural carbon sources, including food, plant biomass, biowaste, and animal products, have been investigated as potential raw materials for the production of CDs. In general, plant parts such as flowers, fruits, seeds, and stems that contain multiple acidic, basic, and neutral bioactive compounds are intriguing as powerful and sustainable biosources for the production of CDs in aqueous media. These green sources provide various advantages, including simple availability, low cost, relatively clean reactions, and non-toxicity.

Hence this thesis presents synthesis, characterisation of CDs from natural resources and they are evaluated for potential sensing applications against various aquatic pollutants and food adulterants.

Apart from this, the biological activities of prepared CDs system were also examined.

The thesis is organised into ten chapters. **Chapter 1** provides an overview of carbon dots with a particular emphasis on their classification, synthetic procedures, characterisation, features, and applications. The chapter also describes the research challenge and discusses the significance of the current inquiry. **Chapter 2**, which deals with the assessment of the literature, gives a succinct overview of carbon dots made from natural resources and their uses, notably in biological applications and the detection of metal and organic pollutants. There is also a brief overview of the natural resources that were chosen for the current work. Materials, chemicals, and characterisation instruments utilised in the investigation are listed in **Chapter 3**. The typical methods used are also briefly described.

The preparation of fluorescent CDs from mango ginger rhizomes is demonstrated in **Chapter 4**. It is known as MGCDs and works well as a fluorescence sensor for the harmful aquatic contaminant hexavalent chromium in aqueous media. This probe successfully completed a real sample analysis. In addition, the fluorescence quenching mechanism underlying this sensing is examined using several techniques and attributed to the inner filter effect (IFE).

**Chapter 5** discusses synthesis and application of fluorescent carbon dots known as LLCs, derived from the wild lemon leaves. The fluorescence of the LLCs is used to



create a tetracycline sensor in water. The sensing is based on the specific interaction of LLCs with tetracycline that results in the quenching of fluorescence. Real environmental water sample analysis also produced positive outcomes. Besides, the mechanism of the fluorescence quenching is also examined and ascribed to static quenching mechanism.

The BCDs, carbon dots that are synthesised from bilimbi fruit extract, is the subject of **Chapter 6**, a fascinating bit of work. The BCDs is employed for multiple sensing tasks. It is primarily intended to function as a Cu(II) sensor in an aqueous medium based on the quenching of fluorescence. And using the fluorescence recovery approach, this BCDs with Cu(II) (abbreviated as BCDs@Cu(II)) is once more utilised as a sensor against the pesticide quinalphos. The mechanism of quenching as well as fluorescence recovery is investigated and static quenching is determined to be the reason. Using successful findings, real sample quinalphos analysis is also performed using rice and tea samples.

The CDs from sweet flag rhizomes are discussed in **Chapter 7** and are designated as SFCDs. Based on the unique way that SFCDs interact with 4-NP, this fluorescent CDs system is put into operation as a 4-NP sensor in water. Real sample analysis is also illustrated, with favourable results. After a thorough investigation using the available techniques, the process of fluorescence quenching sensing was eventually ascribed to a combination of static and IFE mechanism.

CDs from long pepper, designated as LPCDs is the subject in **Chapter 8**. The fluorescence of this system is used for the development of nano sensor against Sudan I, a carcinogenic dye commonly encountered as food adulterant. Real sample analysis is also performed with chilli powder samples. The mechanism behind the fluorescence quenching is accredited to FRET.

The biological properties of the selected CDs systems were discussed in **Chapter 9**. The antioxidant and *in vitro* cytotoxic properties of LPCDs (long pepper derived CDs) and SFCDs (sweet flag derived CDs) are discussed in this chapter. The systems are subjected for the evaluation of biological properties like antioxidant and *in vitro* cytotoxicity against DLA cell lines. Both the systems exert good antioxidant capacity and moderate level of cytotoxicity against the DLA cell lines.

**Chapter 10** includes the overall summary and recommendations of the present investigations.

## LIST OF ABBREVIATIONS

4-NP	4-nitrophenol
$\mu\text{M}$	Micromolar
CDs	Carbon dots
DLA	Dalton's Lymphoma Ascites
DLS	Dynamic light scattering
DPPH	1,1-diphenyl-2-(2,4,6-trinitrophenyl)hydrazine
$\text{EC}_{50}$	Effective concentration for 50 % of scavenging
$E_g$	Band gap energy
FRET	Förster resonance energy transfer
FTIR	Fourier transform infrared spectroscopy
IFE	Inner filter effect
LOD	Limit of detection
nM	Nanomolar
PBS	Phosphate buffered saline
PET	Photo induced electron transfer
PL	Photoluminescence spectroscopy
QC	Quantum confinement
QY	Quantum yield
S %	Scavenging activity percentage
SAED	Selected area electron diffraction
TEM	Transmission electron microscopy
W	Watt
XRD	X-ray diffraction



# LIST OF PUBLICATIONS AND CONFERENCE PAPERS

## Publications

- [1] P. Venugopalan, N. Vidya, Green synthesis of mango ginger (*Curcuma amada*) derived fluorescent carbon dots—a potent label-free probe for hexavalent chromium sensing in water, *Spectroscopy Letters*. 55 (2022) 373–388.  
<https://doi.org/10.1080/00387010.2022.2082483>
- [2] P. Venugopalan, N. Vidya, Microwave-assisted green synthesis of carbon dots derived from wild lemon (*Citrus pennivesiculata*) leaves as a fluorescent probe for tetracycline sensing in water, *Spectrochimica Acta Part A: Molecular and Biomolecular Spectroscopy*. 286 (2023) 122024.  
<https://doi.org/10.1016/j.saa.2022.122024>
- [3] P. Venugopalan, N. Vidya, Bilimbi (*Averrhoa bilimbi*) fruit derived carbon dots for dual sensing of Cu(II) and quinalphos, *International Journal of Environmental Analytical Chemistry*. (2022) 1–14.  
<https://doi.org/10.1080/03067319.2022.2149331>
- [4] P. Venugopalan, N. Vidya, Microwave assisted green synthesis of carbon dots from sweet flag (*Acorus calamus*) for fluorescent sensing of 4-nitrophenol, *Journal of Photochemistry and Photobiology A: Chemistry*. 439 (2023) 114625.  
<https://doi.org/10.1016/j.jphotochem.2023.114625>
- [5] P. Venugopalan, N. Vidya, Long pepper (*Piper longum*) derived carbon dots as fluorescent sensing probe for sensitive detection of Sudan I, *Luminescence*. 38 (2023) 401-409.  
<https://doi.org/10.1002/bio.4459>

## Conference papers

- [1] P. Venugopalan and N. Vidya, " Microwave assisted green synthesis of fluorescent carbon dots from sweet flag (*Acorus calamus*) for fluorescent sensing of 4-nitrophenol", presentation at National conference on Emerging Frontiers in Chemical Sciences (EFCS-2022), The Postgraduate and Research Department of Chemistry, Farook College (Autonomous), Farook.
- [2] P. Venugopalan and N. Vidya, Fluorescent carbon dots derived from long pepper (*Piper longum*) as fluorescent sensing probe for sensitive detection of Sudan I, presentation at International Research Conclave on Advances in Science & Technology (IRCAST-2023), Department of chemistry, NSS College, Ottapalam (Online mode).

# CONTENTS

	<i>Page No.</i>
<b>CHAPTER 1</b>	
<b>INTRODUCTION</b>	
1.1 Nanomaterials	1
1.2 Carbon nanomaterials	2
1.3 Carbon dots (CDs) - The emergence of fluorescent star	3
1.4 Classification of carbon dots	5
1.5 Synthetic approaches	8
1.5.1 Top-down approaches	9
1.5.2 Bottom-up approaches	13
1.6 Characterisation techniques for CDs	20
1.7 Characteristic properties of CDs	24
1.7.1 Biocompatibility, water solubility and lesser toxicity	25
1.7.2 Optical properties	25
1.7.3 Catalytic properties	36
1.7.4 Electrochemical properties	36
1.8 Applications of CDs	37
1.8.1 Sensing applications	38
1.8.2 Biomedical applications	40
1.8.3 Energy applications	44
1.9 Importance of present investigation	47
1.10 Description of research problem	48
1.11 References	51
<b>CHAPTER 2</b>	
<b>REVIEW OF LITERATURE</b>	
2.1 Introduction	63
2.2 CDs from natural sources	64

2.3 Sensing applications of CDs derived from natural sources	67
2.3.1 Metal ion sensing	68
2.3.2 Organic pollutant sensing	77
2.4 Biological applications of CDs derived from natural resources	85
2.5 Plant sources used in the present investigation	89
2.6 References	100
<b>CHAPTER 3</b>	
<b>MATERIALS, INSTRUMENTS AND METHODS</b>	
3.1 Introduction	125
3.2 Materials used	125
3.2.1 Plant sources	125
3.2.2 Chemicals	126
3.3 Instruments	129
3.3.1. Transmission electron microscope	129
3.3.2. Raman microscope	129
3.3.3. Fourier transform infrared spectrometer	130
3.3.4. X-ray diffractometer	130
3.3.5 Dynamic light scattering instrument	130
3.3.6 UV-Vis spectrophotometer	130
3.3.7. Fluorescence spectrophotometer	131
3.4 Methods	131
3.4.1 Synthesis of CDs	131
3.4.2 Sensing studies	132
3.4.3 Fluorescence quantum yield determination	132
3.4.4 XRD interlayer spacing calculations	133
3.4.5 Fluorescence lifetime measurements	133
3.4.6 Real sample analysis	134
3.4.7 Antioxidant activity- DPPH scavenging assay	135
3.4.8 <i>In vitro</i> cytotoxic activity – Trypan blue exclusion method	136



3.5 References	137
<b>CHAPTER 4</b>	
<b>MANGO GINGER DERIVED CARBON DOTS</b>	
4.1 Introduction	139
4.2 Experimental	141
4.2.1 Synthesis of MGCDs	141
4.2.2 Sensing of chromium(VI)	142
4.2.3 Real water analysis	143
4.3 Results and discussion	143
4.3.1 Formation of MGCDs	143
4.3.2 Characterisation of MGCDs	144
4.3.3 Fluorescence quantum yield and fluorescence stability of MGCDs	151
4.3.4 Selectivity studies	153
4.3.5 Sensing studies with chromium(VI)	154
4.3.6 Determination of chromium(VI) in environmental water samples	156
4.3.7 Mechanism of quenching	158
4.4 Conclusions	164
4.5 References	166
<b>CHAPTER 5</b>	
<b>WILD LEMON LEAVES DERIVED CARBON DOTS</b>	
5.1 Introduction	171
5.2 Experimental	173
5.2.1 Synthesis of LLCs	173
5.2.2 Detection of tetracycline	174
5.2.3 Environmental water analysis	175
5.3 Results and discussions	176
5.3.1 Formation of LLCs	176
5.3.2 Characterisation	177
5.3.3 Fluorescence quantum yield and fluorescence stability of LLCs	183

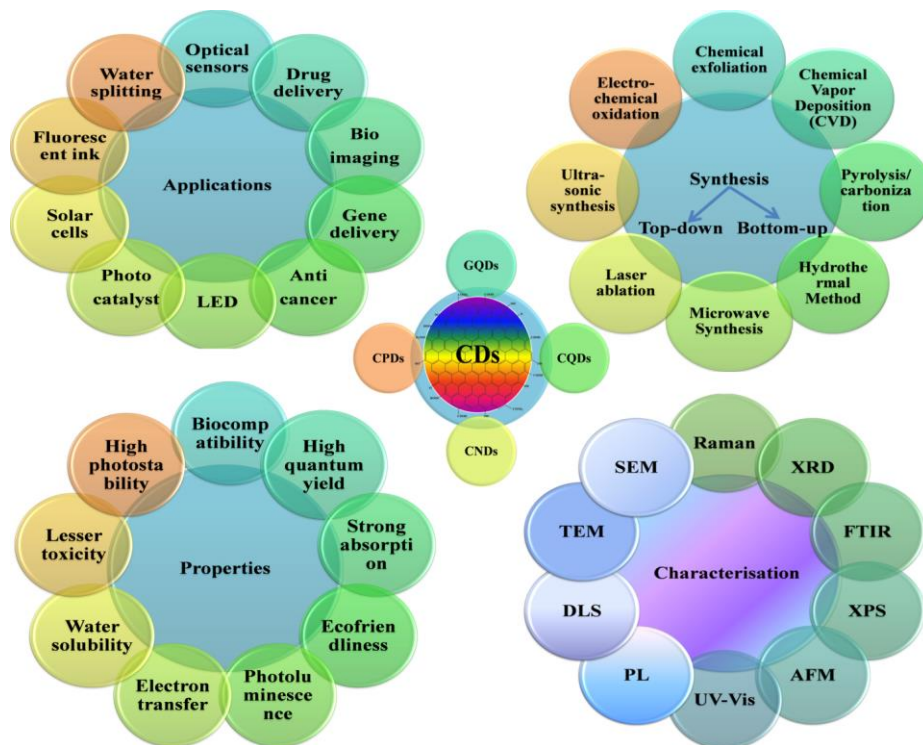
5.3.4 Selectivity studies	185
5.3.5 Sensing studies with tetracycline	186
5.3.6 Determination of tetracycline in environmental water samples	191
5.3.7 Fluorescence quenching mechanism	192
5.4 Conclusions	195
5.5 References	196
<b>CHAPTER 6</b>	
<b>BILIMBI FRUIT DERIVED CARBON DOTS</b>	
6.1 Introduction	201
6.2 Experimental	202
6.2.1 Synthesis of BCDs	202
6.2.2 Cu(II) and quinalphos detection	203
6.2.3 Real sample analysis	204
6.3 Results and discussion	205
6.3.1 Formation of BCDs	205
6.3.2 Characterisation	206
6.3.3 Fluorescence quantum yield and fluorescence stability of BCDs	211
6.3.4 Selectivity studies on BCDs	212
6.3.5 Sensing studies with Cu(II) on BCDs	213
6.3.6 Selectivity studies on BCDs@Cu(II)	216
6.3.7 Sensing studies with quinalphos on BCDs@Cu(II)	217
6.3.8 Analysis of quinalphos in rice and tea samples	220
6.3.9 Probable sensing mechanism	222
6.4 Conclusions	225
6.5 References	226
<b>CHAPTER 7</b>	
<b>SWEET FLAG DERIVED CARBON DOTS</b>	
7.1 Introduction	231
7.2 Experimental	233

7.2.1 Synthesis of SFCDs	233
7.2.2 Detection of 4-NP	233
7.2.3 Real water analysis	235
7.3 Results and discussion	235
7.3.1 Formation of SFCDs	235
7.3.2 Characterisation	236
7.3.3 Fluorescence quantum yield and fluorescence stability of SFCDs	243
7.3.4 Selectivity studies	244
7.3.5 Sensing studies with 4-NP	246
7.3.6 Detection of 4-NP in real samples	249
7.3.7 Fluorescence quenching mechanism	249
7.4 Conclusions	254
7.5 References	255
<b>CHAPTER 8</b>	
<b>LONG PEPPER DERIVED CARBON DOTS</b>	
8.1 Introduction	259
8.2 Experimental	261
8.2.1 Synthesis of LPCDs	261
8.2.2 Detection of Sudan I	262
8.2.3 Real sample analysis	263
8.3. Results and discussion	264
8.3.1 Formation of LPCDs	264
8.3.2 Characterisation	264
8.3.3 Fluorescence quantum yield and fluorescence stability of LPCDs	271
8.3.4 Selectivity studies	271
8.3.5 Sensing studies with Sudan I	272
8.3.6 Analysis of Sudan I in chilli powder	275
8.3.7 Fluorescence quenching mechanism	276
8.4 Conclusions	280

8.5 References	282
<b>CHAPTER 9</b>	
<b>BIOLOGICAL STUDIES ON LPCDs AND SFCDS</b>	
9.1 Introduction	285
9.2 Experimental	287
9.2.1 Antioxidant activity – DPPH method	287
9.2.2 <i>In vitro</i> cytotoxicity – Trypan blue exclusion method	288
9.3 Results and discussion	289
9.3.1 Antioxidant activity of LPCDs and SFCDS	289
9.3.2 Mechanism of DPPH scavenging by CDs	291
9.3.3 <i>In vitro</i> cytotoxicity of LPCDs and SFCDS	292
9.4 Conclusions	295
9.5 References	296
<b>CHAPTER 10</b>	
<b>CONCLUSION AND RECOMMENDATION</b>	
10.1 Conclusions	299
10.2 Recommendations	302

# Chapter 1

## INTRODUCTION



This chapter gives a brief introduction to the carbon dots with a primary focus on the classification, synthetic approaches, characterisation, properties and applications. The chapter also includes the importance of present investigation and description of the research problem.



## 1.1 Nanomaterials

One of the most cutting-edge fields of scientific study in recent decades has been the field of nanotechnology. The investigations on the size dependent physical and chemical properties of nano structures have prompted the researchers to discover its wide spectrum of applications [1]. Such an embarrassing progress is mainly credited to its countless applicability. These materials are of great interest since it bridges the gap between the bulk and molecular levels. It opens up new avenues for versatile applications, particularly in the fields of electronics, optoelectronics and biology.

Nanomaterials are materials having external dimensions within the nanometric range (1-100 nm), at least in one dimension. Nanomaterials have significantly different properties from bulk materials mainly due to increased relative surface area and quantum effects. These factors can change or enhance properties such as reactivity, strength and electrical properties. As particle size decreases, surface area increases and consequently greater proportion of atoms are found at the surface compared to bulk material. Thus nanomaterials have more surface atoms per unit mass compared with bulk material and as a result, they exhibit unusual mechanical, electrical, optical and magnetic properties compared to the bulk material [2].

Based on the chemical composition, nanomaterials are classified into carbon, inorganic, organic and hybrid nanomaterials [3]. Among different nanostructures, carbon based materials are found to be more abundant over the others, a later identified uniqueness of the

most abundant element in the living world. The exceptional ability of carbon atoms to form robust covalent bonds with other carbon atoms in distinct hybridization states ( $sp$ ,  $sp^2$ ,  $sp^3$ ) or with nonmetallic elements enables them to form a wide range of structures, from small molecules to long chains [4]. The prevalence of carbon-based nanomaterials is largely due to this capability.

## **1.2 Carbon nanomaterials**

Carbon nanomaterials are basically the nano allotropes of carbon, considered as the most studied and investigated area in the field of nanoscience. The family of carbon nanomaterials comprised with different nano allotropes including, 2D nanoallotropes such as graphene, graphene nanoribbons; 1D nanoallotropes like carbon nanotubes (CNTs), carbon nanohorns (CNHs) and carbon nano fibers (CNFs) (although the latter are organized into 3D aggregates), and 0D carbon nanostructures such as fullerenes, onion-like carbon (OLC) structures, nanodiamonds, and carbon dots (CDs) [4].

The corridors of carbon research were broadened by the innovations in the field of nano allotropes. All the carbon nano allotropes find promising and significant applications in different fields of science and technologies and they are the hot topic of research in the past few decades. However, lower biocompatibility and lesser water solubility of carbon nanomaterials pull it backward in some fields of applications. But, carbon dots (CDs), the zero-dimensional nano allotropes of carbon can effectively overcome the aforementioned difficulties faced by the other carbon nano materials.



### 1.3 Carbon dots (CDs) - The emergence of fluorescent star

Carbon dots (CDs) are the most emerging member from the family of carbon based nanomaterials. They are zero dimensional (0D) luminescent nanocarbon with size under 10 nm [5]. The structure of CDs is encompass with  $sp^2$  and  $sp^3$  carbon atoms with large number of different functional groups or polymer chains tailored on to its surfaces [6]. The exact structure of CDs is still not clear. However, from the available literature a possible structure is given in **Figure 1.1**.

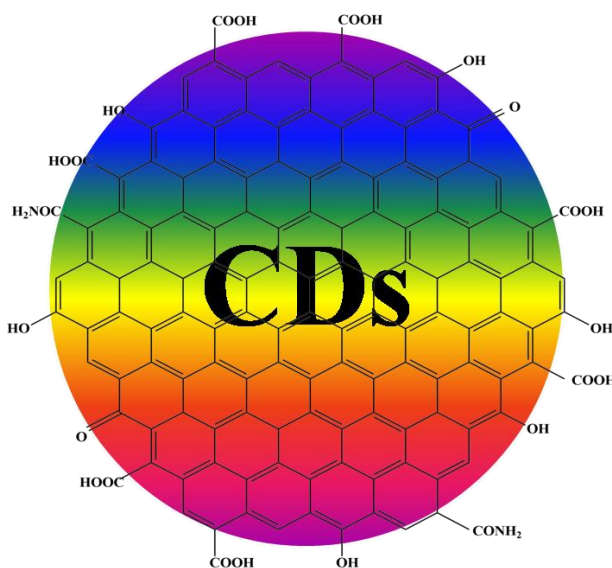


**Figure 1.1:** Schematic structure of CDs

CDs have gathered substantial attraction from the scientific world, owing to their considerable and excellent characteristics, such as excellent electron conductivity, photobleaching and photo blinking properties, high photoluminescent quantum yield, fluorescence property, resistance to photodecomposition, alterable excitation and emission attributes, increased electro-catalytic activity, good solubility

in aqueous media, excellent biocompatibility, long-term chemical stability, cost-effectiveness, negligible toxicity, and acquaintance of large effective surface area-to-volume ratio [7].

The discovery of CDs is quite much interesting; it was in 2004, by Xu et al. the accidental and ground breaking discovery of highly fluorescent carbon material during the purification of SWCNT (single walled carbon nanotube) was happened, which were now named as carbon dots (CDs) [8]. At the primary stage the inventors called it as carbon quantum dots due to its resemblance with the well known semiconductor quantum dots in many aspects like, nano dimensions and fluorescence behaviour.

Semiconductor quantum dots are “artificial atoms”, or quantum dots (QDs), nanometer-sized semiconductor crystals, exhibit variety of optoelectronic properties including, tuneable, effective and narrow emissive photoluminescence and excellent photochemical stability due to its quantum size effects [9,10]. Owing to these properties, QDs have been included in wide range of devices and applications as active element [11]. Now some of these applications are commercialized and are associated with our daily life like, QD-based QLED displays [12]. Even though it being a part of several technologies the synthesis characterisation and applications are still growing research area. However, the lesser biocompatibility and health risks associated with these quantum dots build from toxic metals, pull it down in several fields. The aggregation up on storage of these QDs may release lethal heavy metal ions from the core to the outer surface. This disadvantage was partially resolved by the launch of non-heavy metal based

semiconductors like ZnS, ZnO, ZnSe, silicon based quantum dots, etc [13,14].

So the circumstance demands for the opening of much more biocompatible and eco-friendly fluorescent systems. As expected, the aforementioned drawbacks of QDs can be resolved by the CDs since it well known for its environmental benign and biocompatibility properties. Further studies on CDs reveal that it can be act as an alternative to the non-toxic semiconductor quantum dots since it not only covers almost all the advantages offered by the quantum dots but also solves the major difficulties associated with semiconductor quantum dots.

The urge for the fabrication of non-toxic eco-friendly fluorescent materials sufficiently enhance the acceptance of CDs. This fact was clear from the exponential growth in the number of research articles focusing on the synthesis, properties and applications of CDs. The tuneable luminescent properties of the CDs are the major driving force in the considerable development of CDs research, for the same reason it plays significant role in the nanotechnology revolution by generating new applications in several fields including sensing, bioimaging , energy harvesting etc [15,16].

#### **1.4 Classification of carbon dots**

CDs are primarily classified into four sub categories namely; graphene quantum dots (GQDs), carbon quantum dots (CQDs), carbon nanodots (CNDs), and carbonized polymer dots (CPDs) in the basis of their formation mechanism, carbon core structure, surface functional groups, and properties [6,17], the classification is given in **Figure 1.2**.

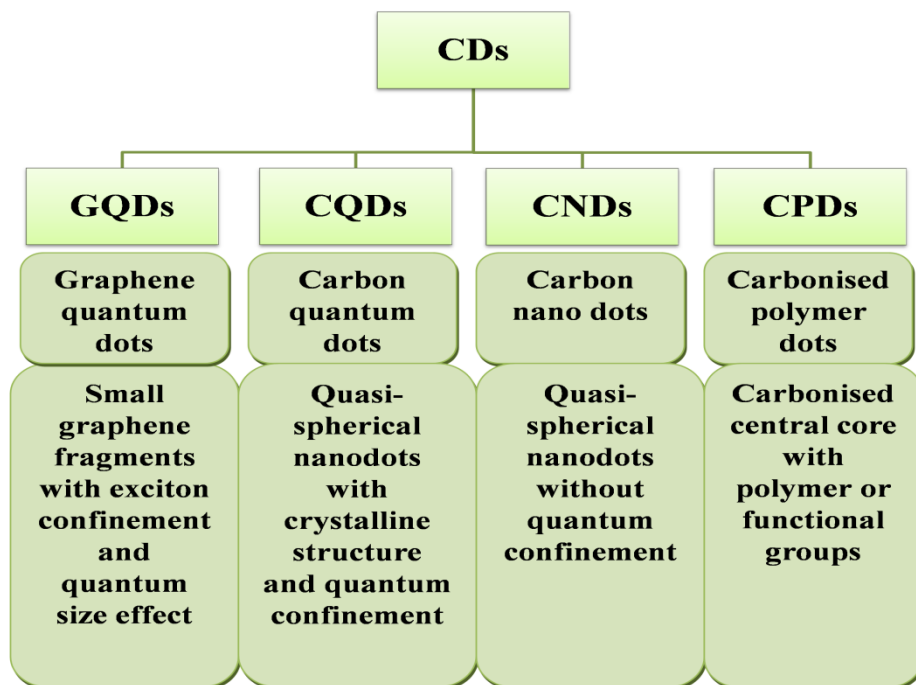


**Figure 1.2:** Classifications of CDs

GQDs are small graphene fragments comprised of single or multiple layers of graphene sheets that have chemical groups on their surfaces, edges, or interlayer spaces. In most cases, they are produced through "top-down" oxide cutting from larger graphitized carbon materials such as graphite powder, carbon rods, carbon fibres, carbon nanotubes, carbon black, or graphene oxide. In addition to having anisotropic features, they have lateral dimensions that are larger than their height. The presence and size of  $\pi$ -conjugated domains, as well as surface/edge effects that result from functions in the GQDs' edge/surface, are what essentially account for these nanostructures' intrinsic optical features [6,17].

Whereas, CQDs are typically nanospheres, with crystalline behaviours, exhibit multiple-layer graphite structures with of large number of surface connected chemical functional groups. The surface effect induced intrinsic state luminescence and quantum confinement effect of CQDs contributes to its luminescence characteristics [6,16,17].

At the same time, CNDs are nanosphere materials with high degree of carbonization and edge effects, but their crystalline or polymeric structures are not disclosed. Besides, quantum confinement effect is found to be missing in CNDs. Both CQDs and CNDs are generally synthesised often produced from small molecules, or biomass by assembling, polymerisation, cross-linking, and carbonization through “bottom-up” approach [6,16,17].

The CPDs typically contains central carbonized core surrounded by polymeric chains or functional groups and is considered as the cross-linked nanohybrids of carbon and aggregated polymers. Usually the CPDs are synthesised via “bottom-up” methods. The special “core-shell” nanostructures, consisting of carbon cores less than 20 nm with highly dehydrated cross-linking polymer frames or slight graphitization and shells of abundant functional groups/polymer chains, which endow CPDs with higher stability, better compatibility, easier modification and functionalization, as well as wider applications [6,16–18].

The optical properties of CPDs are different from that of GQDs, CQDs and CNDs. The molecular state and crosslink enhanced emission (CEE) effect, of CPDs mainly contributes to the optical

properties and thus performance of CPDs more handy in nature [6,16–18].

### 1.5 Synthetic approaches

During the last decade, various methods have been adopted to fabricate the CDs with appropriate properties for different applications. Generally, these synthetic strategies of CDs are classified into “top-down” and “bottom-up” approaches.

In the top-down method, bulk carbonaceous materials are sliced or cut into small nano-sized fragments, while the bottom-up approach includes the building up of nanosized particles through carbonization and stepwise integration of small molecules [7,16,19]. **Figure 1.3** displays the schematic presentation of the two synthetic approaches.

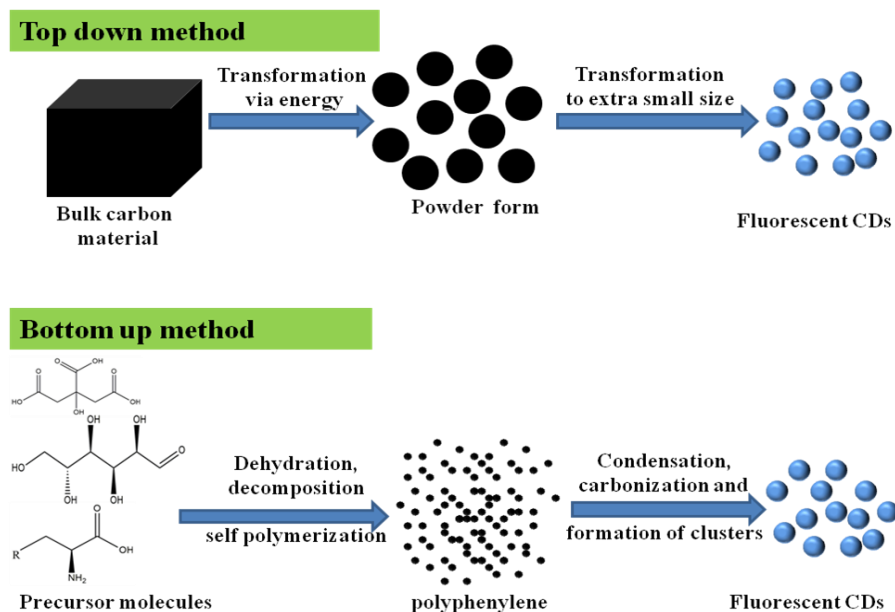


**Figure 1.3** Synthetic approaches for CDs

### 1.5.1 Top-down approaches

In general, top-down approaches are more suitable for the mass production of the materials and it requires long processing time, harsh reaction conditions and expensive instruments and raw materials. The most common synthetic methods from the list of top-down approaches are chemical exfoliation, laser ablation, ultrasonic synthesis and electrochemical oxidation (**Figure 1.4**). Normally, synthesis of GQDs is achieved by this “top-down” policy from macroscopic carbon structures having graphene lattices. Some of these type synthetic methods are detailed below.

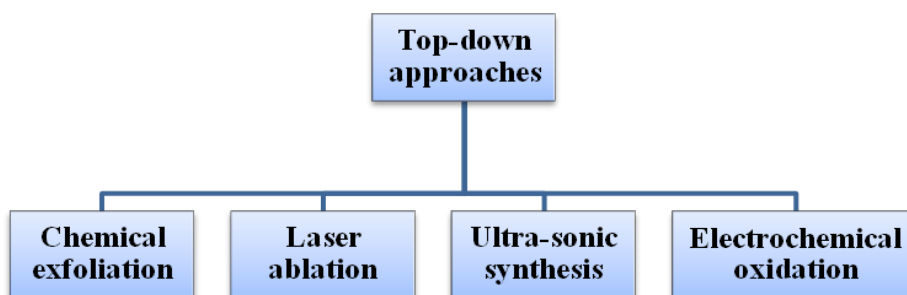


**Figure 1.4:** Different top-down approaches

#### **Chemical exfoliation**

Chemical exfoliation is a facile and convenient method for mass production of high-quality CDs without complicated devices but it generally requires harsh chemical conditions. Strong acids or oxidizing agents are commonly used for the cleavage of the carbon precursor materials, including carbon fibers, graphene oxide and carbon nanotubes.

The fabrication of fluorescent GQDs by the chemical exfoliation was firstly reported by Mao and co-workers in 2007. Different sized GQDs were synthesised from candle soot by the treatment of  $\text{HNO}_3$  under a relatively high temperature [20].

Though it is convenient method for large scale production of CDs, the purification part of the synthesis is a tedious one, and thus increasing the overall synthesis cost. Moreover, the usages of harsh chemicals reduced its greener nature. The purification part gets simplified when mild oxidizing agents are used instead of strong acids and such produced CDs could be more environmental friendly and applicable for the biological studies. indicating that the acid-free strategy is simple and environmentally benign [16].

### **Laser Ablation**

This is termed as unique and potential synthetic route, in which laser ablation is applied for the preparation of CDs in short period of time with simple operations. As mentioned before, operational simplicity has considered as main advantages of this ablation technique, at the same time it lead to generate different types of nanostructures [7]. This method uses a high-energy laser pulse to irradiate surface of the precursor substances in to a thermo-dynamic mood that generates high temperatures and pressures. The heat produced through this is results to the evaporation of the precursor into a plasma mood. At last, the vapour is crystallized into nano dimensional materials [21].



In 2010, Gonçalves et al. use direct laser ablation on carbon targets submerged in water to create carbon nanoparticles, by using UV pulsed laser irradiation of 248 nm, KrF [22].

However, large amount of carbonaceous material as precursor is required to acquire the carbon targets. Moreover, the produced carbon nanoparticles having different sizes and dimensionality consequently the efficiency of this technique is less and utilized rarely as compared with other methods [7,16,21].

### **Ultra-sonic assisted Treatment**

It has been well known that the ultrasound can be used to generate high and low pressure wave in the liquid medium resulting the development and distribution of little vacuum bubbles. The act of cavitations that is the formation and collapse of the vacuum bubbles result in the formation powerful hydro-dynamic shear force. These hydrodynamic shear forces can be successfully utilized for the cutting of bulk carbon precursor in to nano dimensional CDs. [21,23].

The development of GQDs from graphene through the ultrasonic treatment was reported by Zhuo et al. in 2012 [24].

This approach has the advantage of operational simplicity and size controllability simply altering the instrument's parameters. Generally, ultrasonic power, reaction time and the ratio of carbon sources and solvents are the major adjustable parameters to obtain desired CDs [7,16,21].

### **Electrochemical oxidation method**

It is one of the simplest methods to prepare the nanoparticles, and it can be conducted under standard temperature and pressure [21,25]. The electrochemistry based technique considered as one of the acceptable methods for the synthesis of CDs, due to the advantages offered by this method. The major merits include higher purity, affordability, higher yield, particle size controllability, repeatability, bulk production and PL performance of synthesised CQDs.

In this method, CDs are electrochemically synthesised under normal pressure and temperature, through oxidation-reduction reactions. By regulation of redox reactions and electrolyte components, functionalization of CDs can be carried out by incorporating hydrophilic groups such as  $-NH_2$ ,  $-COOH$ ,  $-OH$  to the surface of CDs.

This method was adopted by Ahirwar and team in 2017 for the preparation of GQDs from grapheme rods by using a combination of citric acid and alkali hydroxide in water as the electrolyte [26].

The electrolytes and the electrode materials are crucial for the synthesis, because they have the ability to produce CDs with distinct features in terms of their fluorescence emission, cytotoxicity and surface states [7].

### 1.5.2 Bottom-up approaches

Bottom-up approaches are comparatively time saving and economical than the top-down approaches, however it used for the small scale productions. CQDs, CNDs and CPDs are usually synthesised from small molecular precursors, for example glucose, sucrose, and citric acid, through the bottom-up approaches. Chemical vapour deposition, pyrolysis/carbonization, solvothermal/hydrothermal reactions, and microwave pyrolysis are the major synthetic methods from the bottom-up strategy (**Figure 1.5**). These methods exhibit small amount of defects and high controllability [7,16]. Brief description of the listed methods is given below.

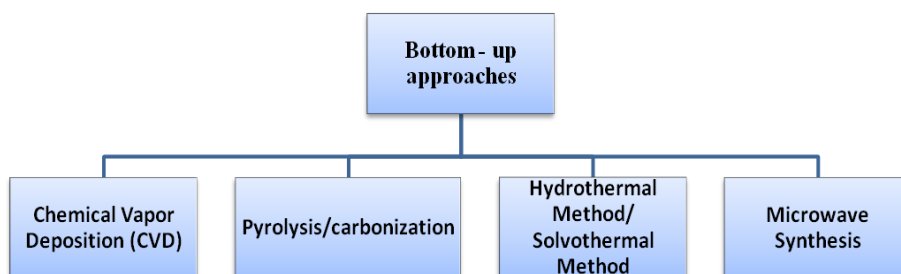


**Figure 1.5:** Different bottom-up approaches

#### **Chemical vapour deposition (CVD)**

It is the well known synthetic approach for the synthesis of nanomaterials. The nanoparticles are formed on the heated substrate, the substrate is exposed to the volatile precursors which react or decompose on the substrate surface and finally the desired product is deposited on the substrate. As a renowned approach, chemical vapour

deposition (CVD) method is used to fabricate CDs, and has also been widely explored in recent years.

In a CVD method, carbon source, growth time, flow rate of the hydrogen (H<sub>2</sub>) and temperature of the substrate determines the size and morphology of the final products, so the tuning of these parameters results in the desired product formation.

Fluorescent carbon quantum dots with graphitic structure were synthesis by this method for the first time was reported by Yan et al. in 2016. With this approach, the synthesised CQDs exhibit excellent crystalline graphitic nature [27].

Controllable morphology and high yield is the major merits of this method however, complicated operational conditions and thereby high cost are the major encountered demerits of this technique [16].

### **Pyrolysis/carbonization**

Pyrolysis is a simple and powerful technique to develop fluorescent CDs. Short reaction time, low cost, easy operation; solvent-free approaches and scalable production make it more advantageous. Under high temperature, the organic carbon precursors converted in to CDs and it involves four main steps; heating, dehydration, degradation and carbonization. They play the critical role in the formation of CDs [16].

This method is adopted by various research teams for the preparation of CDs. And a one-pot pyrolysis preparation of CDs was

reported by Hu et al. in 2019 by tuning the carbonization degree of ammonium citrate [28].

Non-uniform size distribution of the particles, difficulty in separation process and high temperature requirements are the major disadvantage of this process [16].

### **Hydrothermal Method/ Solvothermal Method**

Solvothermal strategy is one of the most accepted preparation technique for CDs, and it refers to the decomposition of carbonaceous materials with a suitable solvent in high temperature and pressure. The method withholds advantages of low cost and operational simplicity [16,29].

In general, the precursor molecules in solution or mixture of solutions were enclosed with Teflon lined autoclave in an oven and allowed to react at high pressure and high temperature. When the solvent used for the preparation is water it is termed as hydrothermal method.

As said earlier, it may be the most used preparation technique for CDs; different research groups from the world wide utilized this approach for the preparation of high purity and well dispersed CDs.

Unsatisfactory uniformity of product size, and morphology, poor control over size is the marked demerit of this method [16].

## **Microwave Synthesis**

According to the reports, microwave assisted method has been considered to be one of the greenest, rapid and cost-effective method of preparation widely applied for the synthesis of CDs.

Microwaves radiation hold a wide range of electromagnetic waves from 1 mm to 1 m and these waves can produce accelerated energies. This energy can be utilized for the chemical bond decomposition of the precursor molecules. The following advantages of the microwave-assisted method make it appropriate for the synthesis of CDs; operational easiness, highly affordability, quite rapid with less reaction times, and uniform heat production for the homogeneous distribution of CDs [7].

The homogeneous heating technology behind this method enhances its merits by effectively reducing the by-products formation and it may simplify the purification process, however the lesser size controllability and inefficiency for large scale production are the main issues faced by this method [21,30].

Major advantages and disadvantages of the synthetic methods generally adopted for CDs synthesis are given in **Table 1.1**

**Table 1.1:** Advantages and disadvantages of different synthetic approaches of CDs

<b>Method</b>	<b>Advantages</b>	<b>Disadvantages</b>	<b>Synthesis route</b>	<b>References</b>
<b>Chemical exfoliation</b>	<ul style="list-style-type: none"> <li>• Mass production of high quality CDs</li> </ul>	<ul style="list-style-type: none"> <li>• Usage of harsh chemicals</li> <li>• Complicated purification</li> </ul>	Top-down	[16,20]
<b>Laser Ablation</b>	<ul style="list-style-type: none"> <li>• Tuneable Surface states</li> <li>• Controllable morphology and size and high purity</li> <li>• Good reproducibility</li> </ul>	<ul style="list-style-type: none"> <li>• Low quantum yield</li> <li>• High cost</li> <li>• Complicated operation</li> <li>• Limits in large-scale production</li> </ul>	Top-down	[31–33]
<b>Ultra-sonic assisted Treatment</b>	<ul style="list-style-type: none"> <li>• Simple, easy to control</li> <li>• Good crystal structure</li> </ul>	<ul style="list-style-type: none"> <li>• Poor size control</li> <li>• Long reaction time</li> </ul>	Top-down	[7,16,21]
<b>Electrochemical oxidation method</b>	<ul style="list-style-type: none"> <li>• Controllable size</li> <li>• High purity</li> <li>• Good reproducibility</li> </ul>	<ul style="list-style-type: none"> <li>• Difficult to control</li> <li>• Complex purification process</li> </ul>	Top-down	[31,33,34]

	<ul style="list-style-type: none"> <li>• Process under the normal temperature and pressure</li> </ul>			
<b>Chemical vapor deposition</b>	<ul style="list-style-type: none"> <li>• Controllable morphology</li> <li>• High yield</li> </ul>	<ul style="list-style-type: none"> <li>• Complicated operational conditions</li> <li>• High cost</li> </ul>	Bottom-up	[16]
<b>Pyrolysis/carbonization</b>	<ul style="list-style-type: none"> <li>• Simple process</li> <li>• Economically feasible</li> <li>• Mass production of highly emissive CDs</li> </ul>	<ul style="list-style-type: none"> <li>• High temperature is required</li> <li>• Difficult to separate CDs and other small molecules of the raw materials</li> <li>• Non-uniform size distribution</li> </ul>	Bottom-up	[33,35]
<b>Hydrothermal Method/ Solvothermal Method</b>	<ul style="list-style-type: none"> <li>• High purity</li> <li>• Good dispersion</li> <li>• Economical</li> </ul>	<ul style="list-style-type: none"> <li>• High vapour pressure</li> <li>• Low yield and purity</li> <li>• Unsatisfactory uniformity of product size, and morphology</li> </ul>	Bottom-up	[33,36,37]



<b>Microwave Synthesis</b>	<ul style="list-style-type: none"><li>• Homogeneous temperature distribution</li><li>• Direct heat of the target molecules</li><li>• Lower reaction temperatures</li><li>• Possibility of very fast synthesis</li><li>• Good quality</li></ul>	<ul style="list-style-type: none"><li>• Use of small reactors limit the large scale production</li><li>• Lesser size controllability</li></ul>	Bottom-up	[30,33]
----------------------------	--	--	-----------	---------

## 1.6 Characterisation techniques for CDs

The characterisation of CDs has become very relevant to explore its physical as well as chemical properties. Various techniques are used for characterisation purpose including microscopic and spectroscopic techniques and are generally rapid and non-destructive [38].

The major analytical techniques used for the characterisation of CDs for illustrating physical characteristics, crystalline structure and identification of surface functionalities are listed as; Transmission electron microscopy (TEM), Scanning Electron Microscopy (SEM), Raman spectroscopy, X-ray powder diffraction (XRD), Fourier transform infrared spectroscopy (FTIR), X-ray photoelectron spectroscopy (XPS), Atomic Force Microscopy (AFM), Dynamic Light Scattering (DLS) and Zeta Potential Measurements and Photoluminescence and Ultraviolet-Visible Spectroscopy (PL and UV-Vis) (**Figure 1.6**). Brief descriptions of the mentioned techniques are given below.

**Transmission electron microscopy (TEM):** It is the primary analytical and visualisation method for CDs. It reveals the relevant information about the particle size morphology, size distribution and crystalline behaviours. High-resolution TEM (HRTEM) can be used to reveal the fine structure of CDs that is whether they are crystalline or amorphous and selected area electron diffraction pattern (SAED) provides additional morphology of the materials. Altogether, HRTEM

and SAED offer the detailed structural details and deprived crystallinity based information of CDs [15,38,39].

**Scanning electron microscopy (SEM):** Like TEM, this analysis also produces images from the interaction of high-energy electron beam with sample, and provides the information about the morphology, topography, chemical composition, granular orientation, crystallographic details of CDs [7].

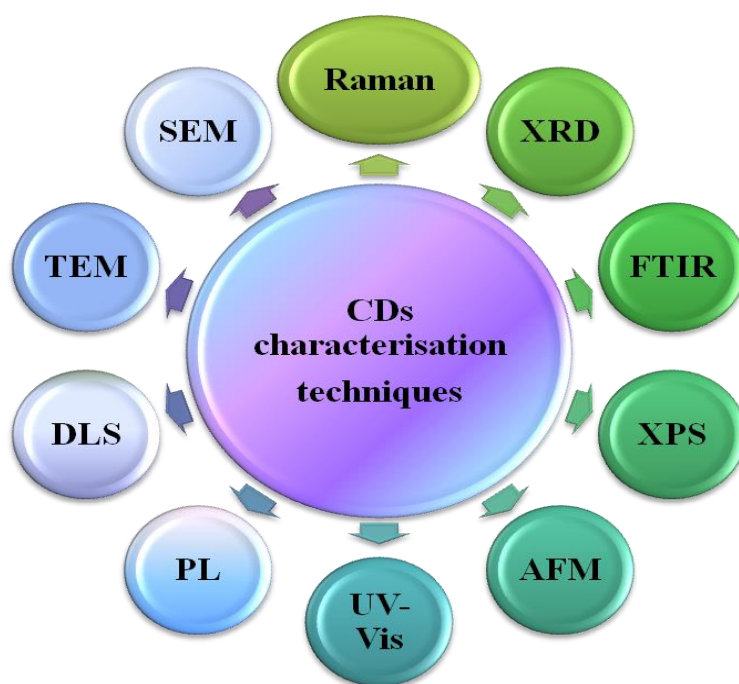


**Figure 1.6** Characterisation techniques of CDs

**Raman spectroscopy:** Raman analysis frequently used to provide the structural data that, optical and electrical characteristics, crystalline or amorphous nature of CDs [39]. This reveals the extent of disorder in the structure of CDs. A typical Raman spectrum of consist of two

eminent peaks corresponds to D and G bands. The former one is appears nearly around  $1350\text{ cm}^{-1}$  and is representing the disordered  $\text{sp}^2$  carbons. While, the latter one originates from the in-plane stretching vibration mode  $\text{E}_{2\text{g}}$  of crystalline graphite carbons. The intensity ratio of these bands ( $I_{\text{D}}/I_{\text{G}}$ ) gives the relative abundance of  $\text{sp}^3$  and  $\text{sp}^2$  carbons in the materials [15].

**X-ray powder diffraction (XRD):** It is an important tool for the study of crystalline nature of the CDs. It gives information about the crystal spacing and unit cell dimension of crystalline carbon core. In general the diffraction peak and lattice spacing of the material is compared with that of graphite to analyse the crystalline behaviour [15].

**Fourier transform infrared spectroscopy (FTIR):** This technique is used to identify the functionalities associated at the CDs based on the detection of electromagnetic radiation absorption in the wavelength range of  $4000$  to  $400\text{ cm}^{-1}$  [39]. Most of the CDs surface contains hydroxyl, carboxyl, carbonyl and ether groups and these groups plays vital role in the characteristics of CDs. So the explorations of functionalities are very relevant in the characterisation and he elucidation carried out by providing different peaks through recording different bond vibrations.

**X-ray photoelectron spectroscopy (XPS):** This method of analysis is an effective tool for surface chemical examination and elemental characterisation of nano-scale materials. It gives information about the electrical structure, elemental composition and qualification and

chemical states of the materials. Surface chemical modifications, components of CDs and core-shell topology of CDs can also be examined from the XPS data [39].

**Atomic force microscopy (AFM):** This technique gives the topographical image of the sample surface from the interactions between a tip and a sample surface. This high-resolution scanning probe microscopic method facilitates the characterisation of CDs by capturing their two-dimensional (2D) as well as three-dimensional (3D) surface images. The CDs dimensions can be calculated through random computation of the particles' heights on the 2D images, whereas 3D images determine the morphology of the surface of CDs [7].

**Dynamic light scattering (DLS) and Zeta potential measurements:** The DLS analysis used hydrodynamic particle size determination of CDs in liquid state. The radii of CDs determined through the measurement of diffusion rate of CDs in the liquid media, and thereby the particle size distribution of CDs can be calculated. Whereas zeta-potential measurements can be used to find out the surface charge and particle size of CDs, the zeta-potential indicates the degree of repulsion between the similarly charged and adjacent particles in dispersion and providing an idea about the stability of CDs. Besides, this method also provides the double layer characteristics of CDs with different hydrophilic groups [7].

**Ultraviolet-Visible spectroscopy (UV-Vis):** This spectroscopy method is broadly employed for exploring the optical characteristics of

CDs. Usually all forms of CDs show their activities in the UV-Vis region of the electromagnetic spectrum. The position of UV-Vis absorption peak strongly depending on the method of synthesis and surface groups present in the CDs. Generally CDs shows strong absorption peaks in the UV and visible region. The major transition resulting these peaks are  $\pi$ - $\pi^*$  and  $n$ - $\pi^*$  transitions of aromatic domains and surface functionalities of CDs [39]. Additionally, this can be particularly used for calculation of the quantum yield (QY) of CDs along with fluorescence spectroscopy.

**Photoluminescence spectroscopy (PL):** This technique may be the most studied characterisation method of CDs because; the elegant fluorescence behaviour is the most attractive part of CDs. Fluorescence, phosphorescence behaviour and excitation dependent emission nature of the CDs can be investigated by this method. Furthermore, PL spectroscopy is used for the fluorescence lifetime measurements of CDs [16,39].

### **1.7 Characteristic properties of CDs**

CDs exhibit entirely different properties than the macroscopic black carbon. Owing to the stupendous properties offered by CDs, they are extensively implemented in several areas. General properties of CDs depicted in **Figure 1.7**. In this section, some of the selected properties of CDs, which make them appropriate candidates for different applications, are discussed.

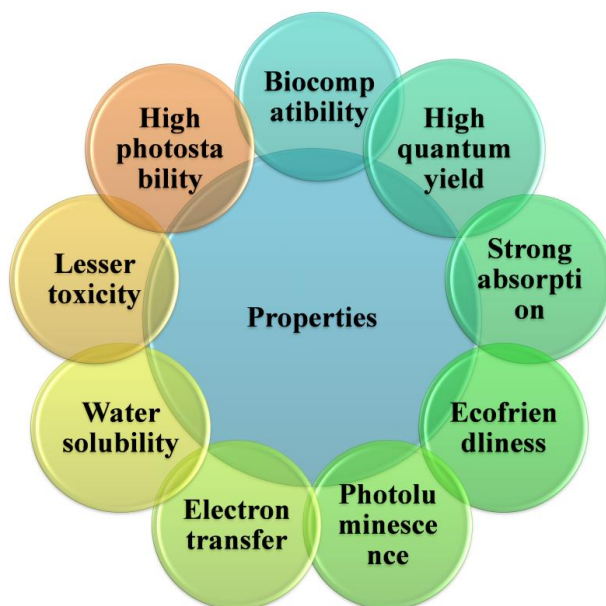


**Figure 1.7:** General properties of CDs

### **1.7.1 Biocompatibility, water solubility and lesser toxicity**

These are the major features which make the CDs as the greenest material among the carbon nano sector. The combined effect of excellent water solubility, non-toxicity and biocompatibility of CDs are enhances the eco-friendliness. The commendable water solubility is mainly accredited to the hydrophilic functionalities attached to the exterior part of CDs, which make it suitable for several applications including biomedical fields and agricultural sectors [40].

### **1.7.2 Optical properties**

As mentioned before, the most appealing features of CDs are their optical properties. Lion share of the applications of CDs are based on this optical properties, especially in the field of fluorescent sensing,

bioimaging, biosensing, and phototherapy. So it is of great importance to understand the optical properties of CDs. Optical properties of CDs comprises with absorption and photoluminescence, chemiluminescence and electroluminescence (**Figure 1.8**).

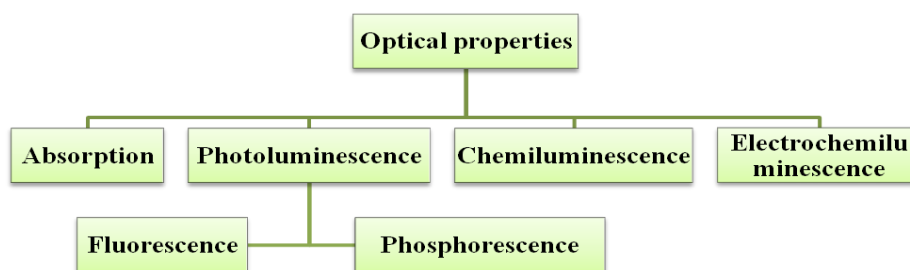


**Figure 1.8** Optical properties of CDs

### **Absorption**

Usually, CDs exhibit strong absorption in the UV region (250–350 nm) and a comparatively weak absorption tail in the visible spectrum. The whole absorption spectrum is comprised with three bands, specifically, (i) the core band, (ii) edge or molecular band, and (iii) surface band. The core band is generated from the  $\pi$ - $\pi^*$  transition from the core- $sp^2$  carbon network, and this peak appears at around 200 - 240 nm whereas the edge and molecular band correspond to the  $n$ - $\pi^*$  transitions of C=O and C=N bonds (from the N- and O-containing functionalities) at the edge of carbon structures, and is generally appears in the range of 290 - 360 nm. The surface band is the extended one which is usually appearing in the visible region of the spectrum



believed to be arises from the lower energy surface states. Sometimes bands at visible region related to the amino functionalities of the CDs [41].

The peaks from the UV region arising due to  $\pi-\pi^*$  transitions usually do not make effective contribution to emission characteristics of CDs. The broad spectral characteristics of CDs in the absorption spectrum are majorly due to the surface defects associated with the CDs [42,43]. Importantly, the absorbance range of CDs highly depends up on the core structure as well as surface functionalities of CDs [16].

### **Photoluminescence (PL)**

Photoluminescence (PL) by definition, it is the emission of light from a substance by the absorption of light (photon). Fluorescence and phosphorescence are the two types of photoluminescence exhibited by materials. In which, fluorescence is the prompt photoluminescence that happens very shortly after the absorption of light, and subsequent photoexcitation by the substance. In this type of PL, the radiative transition is an allowed transition since it does not require a change in the spin multiplicity. In contrast, phosphorescence is the delayed fluorescence and is the long-lived photoluminescence, which continues after the photoexcitation has shut down. The radiative transition in this PL is associated with a change in the spin multiplicity. Unless otherwise noted, the word "PL" is generally used synonymously with the fluorescence that is frequently observed in CDs [41]. Here we are mainly focussing on the

fluorescence behaviour of the CDs, and is briefly explained in the following parts.

### **(a) Fluorescence**

It is one of the most appealing features of CDs, both fundamentally and practically. Unfortunately, it is also the most contentious topic in terms of understanding, because the luminescence mechanisms of CDs are not precisely understood due to incomplete experimental and theoretical understanding. This significantly slows the development of CDs with desirable optical properties. Being the most charming property of CDs, fluorescence behaviour is the most studied area of CDs and still the origin of fluorescence under debate [41].

In general, CDs gives fluorescence emission at higher wavelength than the excitation wavelength, this type of emission known as Stokes fluorescence emission. Another interesting fluorescent features of CDs is the excitation dependent emission behaviour; the emission peak position altered with excitation wavelength, and this behaviour is mainly due to the polydispersity of the CDs [44].

Theories about the origin of fluorescence have gradually matured alongside the evolution of CDs. To date, three theories that explain excitation-dependent fluorescence have received the most attention, namely, (1) size-dependent emission (core emission), which is related to the quantum confinement effect and conjugated  $\pi$ -domains

of the carbon core; (2) the surface states, which are interconnected to the functional groups that are attached to the carbon core structure; (3) the molecular state, where the emission originates from free or bonded fluorescent molecules in the CDs [41,45–47].

(1) *Size-dependent emission(quantum confinement effect) or the core emission*: So many published research works from this area suggest that quantum confinement (QC) in CDs is to bear responsibility for excitation-dependent emission, and some provide strong evidence for this. The QC theory is seems to be very natural to consider because metal-based quantum dots are well known to emit light based on this phenomenon. This phenomenon is actually related to the size of nanoparticle, and the size distribution of CDs is usually less than 10 nm, which matches up to the quantum size range [41,45,46]. It is this confined area in the CDs that allows for electrons to be strongly contained and quantized.

The principle of quantum confinement is presented in **Figure 1.9**. When a photon with the appropriate band gap energy ( $E_g$ ) is absorbed, electrons in the valence band are excited and transferred to the conduction band. Consequently, a hole is formed in the valence band, which results in the formation of an exciton. However, because electrons and holes are confined in all three spatial dimensions in quantum dots, the size of excitons can be tailored, allowing for the measurement of electronic properties [48].

Quantum confinement appears to occur when a nanoparticle approaches the exciton Bohr radius (the distance between the electron-

hole probability distribution in an exciton), result in changes in the density of the electronic state and energy level separation. Consequently, discrete energy levels are observed near to the band edge. The bandgap widens as the size of the CDs gets smaller. With decreasing size, the energy separation between the band edge levels also increases. As more energy is released when the nanoparticle is returned to its ground state after excitation, there is a colour shift from red to blue in the light emitted [48–50].

When the size of CDs is smaller than the exciton Bohr radius, they exhibit a particle size-dependent fluorescence behaviour pattern, which is caused by the energy band-gap transition of conjugated  $\pi$ -domains in the  $sp^2$ -carbon-core [51].

Carbon-core states participate in CDs fluorescence via radiative recombination of electrons and holes in the core, which results from  $\pi - \pi^*$  transitions of  $sp^2$  clusters aided by the quantum confinement effect. The core emission is typically at shorter wavelengths with low quantum yield, but the presence of graphitic nitrogen and hybridised oxygen functional groups with the core allows the emission properties to be red-shifted [52,53].

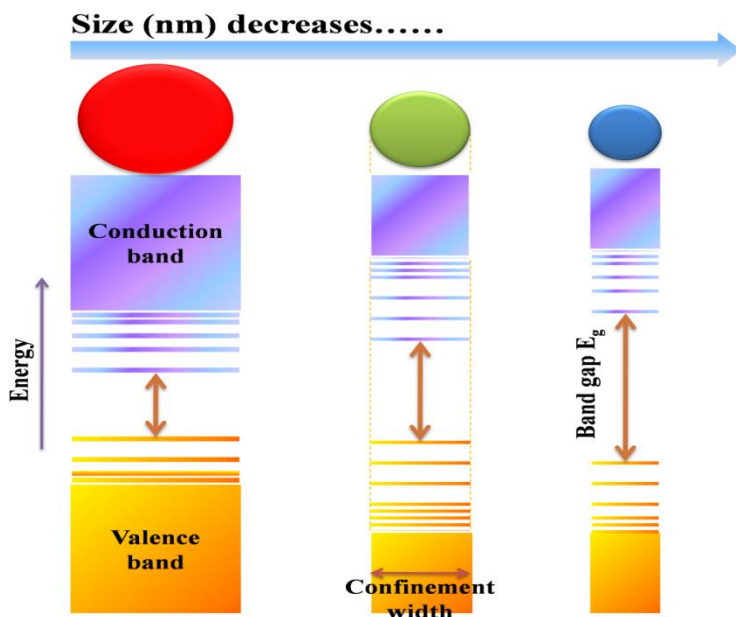


**Figure 1.9** Schematic representation of principle of quantum confinement effect

The relationship between fluorescence emission and  $sp^2$ -domain size has been illustrated theoretically through a series of calculations. It is important to note that the size of  $sp^2$ -domains is the primary controlling factor of the quantum confinement effect, despite the fact that particle size appears to have a comparable algebraic relationship with fluorescence emission [47].

Though some researchers provide compelling evidence for QC theory, numerous published papers lack the data to support this theory, so it is not the most widely accepted theory. Most investigators in recent years haven't employed quantum confinement as the sole factor for the fluorescence mechanism of CDs, but rather it is frequently used in combination with another principle [45].

(2) *Surface state*: The theory of surface states is widely used and has thus achieved widespread acceptance for the mechanism of CDs fluorescence. According to this theory, CDs emission is controlled by the surface state [41].

The surface state of CDs is determined by the hybridization of carbon backbones and functional groups connected to CDs, and their energy gap is correlated to the extent of the  $\pi$ -electron system and surface chemistry [51]. Surface states in CDs are connected with (i) functional groups, (ii) defects (supplemented by a substantial amount of non-perfect  $sp^2$  domains), and (iii) heteroatom dopants. These surface states can function as a capture centre for excitons, resulting in surface state-related fluorescence. Distinct functional groups on CDs have different structural configurations and thus different energy states, tends to result in more recombination possible scenarios for electrons and holes captured by surface states [41,54].

The various surface functional groups connected with CDs can construct widely dispersed surface states, resulting in a large number of transition modes. These states take on predominant roles under various excitations, resulting in a variation of fluorescence peak positions and intensities, which is known as the excitation dependent behaviour [41,55].

The studies with CDs having similar particle sizes but different surface states (particularly the degree of oxidation) show that as the incorporation of oxygen species into their surface structures increases, the band gap gradually decreases, resulting in a red shift in the

emission peak. It is interesting to note that the energy states are determined by surface groups (degree of oxidation) and structures rather than particle size, implying that surface states were the dominant factor controlling fluorescence variations [41,43].

(3) *Molecular state*: In accordance with this theory, various "fluorescent molecular fragments" are synthesised that are either free or attached to the surface of CDs during the bottom-up CDs preparation process [41].

Because bottom-up CDs synthetic methods support highly reactive conditions, other side reactions are also possible. In other words, during CDs synthesis, small molecules or even molecular luminophores can be produced, which can attach to the surface of CDs backbones and give them bright emission properties [41,46].

Though several papers are available with strong evidence, the scope of this theory is limited to the precursors like citric acid/ fluorescent precursors and also this theory cannot completely explain the excitation-dependent emission that CDs usually possess [41,45].

Altogether, the structural characteristics of CDs are the most important factor in determining the fluorescence emissions. The fluorescence emission of CDs is tuneable by adjusting the size of conjugated  $\pi$ -domains and controlling the surface functionalities [16]. Based on the current literatures and studies, fluorescence of CDs believed to be originating from the carbon core and surface states. In which surface state mechanism plays the vital role, controlling the surface functional state is the easiest and primary pathway to modulate

the fluorescence emission of CDs. Different functional groups can form different defect state and there by introducing different energy level band gaps. Besides, elemental doping can also take part in the fluorescence modulation. For example, nitrogen doped CDs generally exhibit improved fluorescence. For the case of CDs with large  $\pi$ -domains and lesser surface groups, the  $\pi$ -domains is the key factor determining the fluorescence, in such cases the modulation of fluorescence will be difficult since, the control over  $\pi$ -domains is not easy as functional group controlling [56].

Up-conversion fluorescence, this is another type of fluorescence exerted by CDs in which excitation wavelength is greater than the emission wavelength. Generally CDs produced through ultrasonic treatments exhibits this up-conversion fluorescence property. And it happens due to the sequential absorption of two or more photons and it is an anti-Stokes type emission [16].

### **(b) Phosphorescence**

Phosphorescence or delayed fluorescence is another interesting photoluminescent property exhibited by CDs. The long lifetime of phosphorescence property of CDs is making it applicable in energy, information and biomedical fields [57]. Generally CDs with enormously cross-linked structures containing non-conjugated groups shows this delayed fluorescence. Phosphorescence is observed when there is suppression of non-radiative transitions by restricting rotation and vibration, or any factors which facilitate the intersystem crossing ability of CDs by enriching the spin-orbit coupling through the use of transition metals. Several studies have suggested that carbonyl groups



attached to the surface of CDs produce excited triplet states, which are responsible for CDs phosphorescence [41]. However phosphorescence is very rare in aqueous media, because phosphorescence is quenched by the solvent-assisted relaxation, and also by the presence of dissolved oxygen [16].

### **Chemiluminescence**

Chemiluminescence is another important optical characteristics exhibited by the CDs. It is the light emission process as a result of chemical reactions. CDs can generate chemiluminescence in aqueous medium under suitable conditions of redox reactions. The unstable products formed from the intermediate radicals of such reactions leads to the chemiluminescence. CDs can produce chemiluminescence either through their excitation after direct oxidation or via enhancement or inhibition of their luminescence [16]. The chemiluminescent properties of CDs is well applicable in the fields of chemical detection in bioanalysis [58]. Nonetheless, investigations based on the chemiluminescence of CDs are still in their infancy and it is one of the less studied optical properties of CDs.

### **Electrochemiluminescence**

This is another intriguing optical property of CDs. The electrochemiluminescence process involves light emission by species formed at the electrode as a result of high energy electron transfer reactions. The ability of CDs to emit photons in the visible region under appropriate electrical excitation results in the electrochemiluminescence. On account to the presence of higher

amount of  $sp^2$  carbon in CDs, which results in enhanced electron transfer results to a stable electro-chemiluminescence. This fascinating property of CDs mainly utilized in the field of bioanalysis [16,59]. Like in the case of chemiluminescence, the studies of electrochemiluminescence of CDs are in the early stage.

### **1.7.3 Catalytic properties**

The catalytic capabilities of CDs are of tremendous importance because, as was stated at the outset, CDs can replace semiconductor quantum dots, which are well-known for their catalytic properties.

Efficient light absorption and electron transfer ability is the core reason for the catalytic properties of CDs. Along with large surface to volume ratio and ability for the formation of hole–electron pair up on irradiation of light and the lesser recombination of this pair due to surface traps make it apt for the catalytic purposes. Due to an excellent photocatalytic activity, CDs were widely applied in photocatalytic field for improving activity of catalysts. This properties is well utilized for the light mediated photodegradation applications [60].

The catalytic properties of CDs are one of the fastest-evolving areas; more research on the mechanism and origin of this property is currently under progress.

### **1.7.4 Electrochemical properties**

The electrochemical properties associated with CDs make it apt for the applications in the area of electrochemistry and electrocatalysis.

The major electrochemical properties of CDs are follows; the exceptional charge transferability, electroconductivity. Due to excellent electrical conductivity CDs can easily transfer the electrons during electrochemical reactions. All these features make it apt for electrochemical applications [7].

### 1.8 Applications of CDs

Outstanding and commendable features of CDs make it one of the potential contestants for broad spectrum of applications in several fields, major applications are depicted in **Figure 1.10**; some of the applications relevant to the present work are detailed in the upcoming sections.

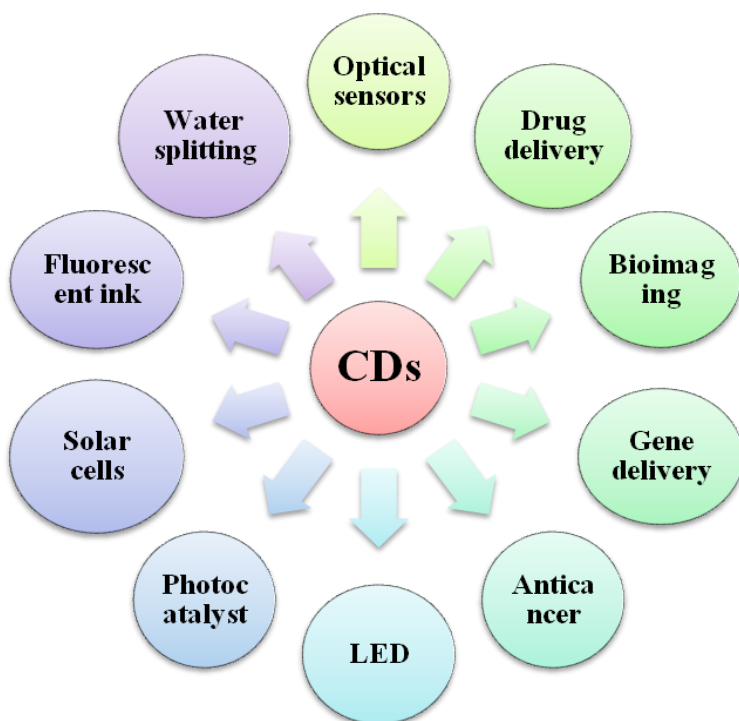


**Figure 1.10:** Major applications of CDs

### 1.8.1 Sensing applications

As mentioned before, fluorescence is the charming feature of CDs effectively used for the sensing applications, based on the changes in the fluorescence (reduction or enhancement of fluorescence intensity) by the presence of foreign species. It has been broadly used as fluorescent nanoprobe for the detection of several analytes in biological as well as environmental samples. Substantial fluorescence, fast responses, high selectivity and sensitivity, low cost, user friendliness, higher biocompatibility, water solubility and abundant surface functional groups are some of the reasons by which CDs can act as fluorescent sensors. Generally, different types of analytes can be detected through this fluorescent sensing with good level of selectivity and sensitivity, which includes metal ions, anions, organic pollutants, biomolecules, and adulterants etc [16,61,62].

The mechanism of this reduction or enhancement of fluorescence, by the addition of analyte depends up on the structure and optical properties of CDs [63]. This CDs sensing application is based on the principle that when the analyte and CDs interact, fluorescence is either quenched or increased. However, the majority of CDs sensing research is based on fluorescence quenching. In general, there are five major types of sensing mechanisms (quenching mechanisms), which are static quenching mechanisms, dynamic quenching mechanisms, inner filter effect (IFE), Förster resonance energy transfer (FRET), and photo induced electron transfer (PET) [64].

- (1) *Static quenching mechanism*: It actually occurs when CDs and quenchers interact to form a non-fluorescent ground state complex.
- (2) *Dynamic quenching mechanism*: This type of quenching can be explained by the fact that the excited state of CDs returns to the ground state as a result of a collision between the quencher and the CDs that involves either energy transfer or electron transfer.
- (3) *Inner filter effect (IFE)*: It appears to happen when the quencher's absorption spectrum overlaps with either the excitation or emission spectra of the CDs. This mechanism operates via a shield operation.
- (4) *Förster resonance energy transfer (FRET)*: It is an electrodynamic phenomenon that occurs between CDs in the excitation state and quenchers in the ground state when the emission spectrum of the CDs overlaps with the absorption spectrum of the quencher.
- (5) *Photo induced electron transfer (PET)*: It can be explained that CDs and quencher participate in an electron transfer reaction that results in the formation of cation and anion radicals. In this process, a complex formed between the electron donor and acceptor can return to the ground state without emitting photons, resulting in fluorescence quenching.

The literature includes an array of intriguing studies based on CDs' use in optical sensing, and according to publishing data, it is the most explored application of CDs.

### **1.8.2 Biomedical applications**

Owing to the lesser toxicity and higher biocompatibility of CDs, it is dominantly used in the field of biomedical applications including, drug delivery, bioimaging, biosensing, anticancer treatments, nano-medicine developments, biosample staining, etc. CDs shows good selective and sensitive interaction with biomolecules like DNA, protein, amino acids and enzymes, which are associated with health issues and certain diseases. Through this interaction CDs can give informative insights in the early diagnosis of certain severe diseases. Similarly, for the same reasons and more emphasize to fluorescence nature, CDs can be an efficient and promising probe for the targeting and imaging of cancer cells [65,66].

It comes as no surprise that one of the most intriguing and widely discussed uses of CDs is in biomedicine. The low toxicity or nontoxicity and great biocompatibility of CDs, even at high concentration levels, are demonstrated by *in vitro* cytotoxicity experiments on a variety of cell lines [17,67]. According to *in vivo* tests, CDs are swiftly eliminated by the hepatobiliary and/or kidney systems. Also, according to blood biochemistry and haematological research, rats' brains, hearts, lungs, livers, spleens, kidneys, testicles, and bladders do not exhibit any notable signs of inflammation [68,69].

These studies indicate that, CDs can be used safely for biomedical purposes.

Moreover, CDs are a prospective substitute for conventional fluorescent materials in disease detection, therapy, and healthcare supplements due to their low cost, small size, customizable surface functionalities, high photostability, unique down-conversion PL, multiphoton PL, and high brightness [17]. This section describes CDs' uses in biomedicine, including bioimaging, phototherapy, drug/ gene delivery, and nanomedicine.

### **Bioimaging**

Bioimaging is a technology that uses probes and detectors to directly and non-invasively view biological activities. Due to its simplicity, cheap cost, high sensitivity, noninvasiveness, and long-term observation, fluorescence imaging has emerged as a potent method for clinical diagnosis [17].

The introduction of CDs to this field is prompted by the toxicity issues or poor fluorescence performance of traditional fluorophores like QDs and organic dyes. CDs are the next-generation fluorescent probes for both *in vitro* and *in vivo* bioimaging due to their high photostability, great biocompatibility, straightforward synthesis methods, adaptability, multicolor emission, deep red/NIR emission, and two-/multiphoton PL.

Many CDs have been extensively utilised to image cells, microbes, and plant tissue. According to the different nanostructures of

CDs and types of cells, CDs can enter cells quickly through energy-/temperature dependent macropinocytosis, clathrin, caveolae, and/or lipid raft-mediated endocytosis and are distributed into mitochondria, lysosomes, endoplasmic reticulum, Golgi apparatus, and/or nucleolus [17,70].

### **Phototherapy**

Phototherapy, including photodynamic therapy (PDT) and photothermal therapy (PTT), is a form of noninvasive therapeutic treatment that converts the irradiating light into reactive oxygen species and heat with the help of photosensitizers, inducing local apoptosis of cancer cells. CDs have gained much attention as promising phototherapeutic agents due to their unique optical properties, high water solubility, and high photostability [17].

### **Drug/Gene Delivery**

In addition to anticancer phototherapies, CDs can create image-guided nanohybrids by fusing imaging tools with drugs or genes to increase the effectiveness of drug delivery or to enhance the therapeutic approach. Drug delivery, the safe and effective therapy, entails transporting the medication to a specified area of the body and releasing it gradually. In order to maximise local therapeutic benefits and reduce adverse effects on healthy, non-cancerous tissue, regulated drug release and strong selectivity in drug delivery systems are essential. Due to their fluorescent features, CDs are advantageous for observing drug accumulation and activity at diseased locations, which



is essential for determining the therapeutic efficacies of drugs [17,71,72].

Gene therapy is viewed as a long-lasting and potentially curative therapeutic approach for a variety of disorders, including hereditary human diseases and cancers, in contrast to other treatment methods. CDs have minimal toxicity, various functional groups, and great biocompatibility. Significantly, the relatively small size of CDs leads to optimal cellular absorption and improves the effectiveness of gene transfection. Its distinctive fluorescence may also be employed to monitor the internalisation of genes. CDs will therefore be a desirable non-viral choice in gene therapy [17,73,74].

### **Nanomedicine**

Besides being carriers, CDs themselves behave with therapeutic performances such as antibacterial activity [75], anticancer activity [76], antiviral activity [77], and antioxidant activity [78]. CDs produced from drug molecules typically display therapeutic performances that are comparable to or better than those of the precursor drug, and it may be due to the preservation of pharmacophores in their structures or the development of novel active structures. More significantly, when compared to drug molecules, these drug-CDs exhibit brighter fluorescence, higher biocompatibility, and water solubility, make them effective theragnostic bioimaging probes [17,75,77].

### 1.8.3 Energy applications

Due to the excellent electron acceptor/donor characteristics, large specific surface area, low cost, low toxicity, and electronic conductivity, CDs promise to be used in a variety of energy-related fields, including photo and electrocatalysts, LEDs, solar cells, and supercapacitors [17].

#### Catalysis

CDs have been used as catalyst in different ways, that is it can act as photocatalyst, electrocatalyst, and photoelectrocatalyst depending on the structural differences and intrinsic properties [17].

Photocatalysis become the most useful application which utilizes the solar energy for the degradation of pollutants, water splitting applications, and chemical reactions [79]. Broad light absorption, charge separation, photostability and low cost features of CDs make it apt for the photocatalytic applications. Exponential growth in the number of reports from this area indicates the acceptance of CDs as photocatalyst [60]. The electrocatalytic application of CDs are performed on accounts to the low cost, chemical inertness, electron mobility, large surface area, surface defects and active site [17].

In addition to facilitating effective interfacial electron transport, CDs with nitrogen atoms at the aromatic domain's edge locations also promote the production of hydrogen from water via photocatalysis [80]. To enhance the photocatalytic activity, CDs are typically hybridised with other nanomaterials ( $\text{Fe}_2\text{O}_3$ ,  $\text{g-C}_3\text{N}_4$ ). These materials

act as the light absorber and/or the electron acceptor in the heterojunction [81].

The key energy conversion mechanisms between chemical energy and electric power are the oxygen reduction reaction (ORR), oxygen evolution reaction (OER), and hydrogen evolution reaction (HER). Due to the inexpensive price, chemical inertness, wide specific surface area, high electron mobility, plentiful surface defects, and active sites, CDs have emerged as a formidable rival to traditional Pt- and Ir/Ru-based electrocatalysts [17].

Applications of CDs for photoelectrocatalysis are primarily found in the water splitting. CDs serve as electron media to encourage charge separation in semiconductors as well as photosensitizers to increase solar energy absorption in the photoelectrochemical (PEC) water splitting and wastewater treatment processes [82].

### **CDs based light emitting diodes (CLEDs)**

LEDs are devices which converts electrical energy in to light, have secured relevant importance in scientific research. It can be used for the full-colour displays, liquid crystal displays and illumination devices. As a biocompatible ecofriendly fluorescent material CDs can replace the toxic and expensive rare-earth based phosphors and metal based semiconductors in LEDs, due to the merits of CDs like, low-cost, abundance, tuneable fluorescence emissions, eco-friendliness. In general, CDs act as phosphors or active layers in these types of devices [17,83].

## **Solar cells**

CDs have been widely studied for its solar cell applications and the addition of small amount of CDs to the bulk hetero-junction improve the efficiency to large extend. The major reasons for this behaviour are significant optical properties, high electron mobility, abundance of surface functionalities, etc. The commendable features of CDs like, photogeneration of electron–hole pair, suppression of their recombination, broad range of light absorption, helps to play its role in solar devices [17,84].

## **Supercapacitors**

CDs have garnered a lot of attention recently and have demonstrated excellent application potential as a high-performance supercapacitor. With higher specific capacitance, higher energy density, and better durability, CDs (either as a bare electrode or a composite) offer a new way to improve supercapacitor performances [85].

Supercapacitors have rapid charge/discharge rates, high power densities, and long cycle lives, but their lower energy densities restrict their usefulness as energy storage devices. Supercapacitors' electrochemical performance has reportedly improved when CDs are hybridised with other carbon materials, polymers, or metal oxides [17,86].

## 1.9 Importance of present investigation

As discussed through the above sections, the CDs, fluorescent star from the carbon nanomaterial family acquire the significant importance in almost every field owing to its versatile potentiality and environmental friendliness. The commendable biocompatibility and water solubility of this tiny luminary make it more users friendly. The biocompatibility of the CDs can further be increased by the introduction of biogenic carbon dots. Biogenic carbon dots are CDs with biological origin that is CDs derived from natural resources.

There has recently been an increasing interest in one-pot CDs synthesis, mostly to decrease waste and by-products. Many natural carbon sources, including food, plant biomass, biowaste, and animal products, have been investigated as potential raw materials for the production of CDs. In general, plant parts such as flowers, fruits, seeds, and stems that contain multiple acidic, basic, and neutral bioactive compounds are intriguing as powerful and sustainable biosources for the production of CDs in aqueous media.

Eco-friendly raw materials, in contrast to synthetic precursors, are rich in carbon and nitrogen supplies in the form of proteins and carbohydrates and also act as self-passivating agents to produce surface-functionalized CDs. Green sources provide various advantages, including simple availability, low cost, relatively clean reactions, and non-toxicity.

Importantly, there is no requirement for an external dopant in the case of green sources because they are comprised with different organic molecules and can be considered as organic reservoirs. Furthermore, various phytochemical constituents present in a certain precursor not only influence reaction kinetics, but also the surface functional groups on the CDs, and hence their reactivity. Besides that, the quantum yield of CDs is affected by the kind of phytoconstituents, particle size, solvent, and dopants used.

These types of CDs production without using any hazardous chemicals not only make it economical and eco-friendly but also give value addition to the precursor. Thereby more exploration of natural resources can also be carried out. CDs made from green resources have nearly identical properties with improved biocompatibility to their synthetic counterparts, and hence can handle nearly all of the application area of CDs in a better way.

### **1.10 Description of research problem**

We are interested in the synthesis, characterisation and applications of novel CDs from the natural resources. In the present investigation, we fabricated five different CDs system from five different natural resources that are easily available and economical through a complete greener approach. All of them are successfully implemented as fluorescent sensors for different species, including aquatic pollutants and food adulterants, and some of them are used for the biological applications.

Hereby, we focused on the truly green synthesis, characterisation and application of the CDs prepared from selected natural resources. Simple, fast, easy to perform, less expensive eco-friendly method, microwave assisted synthesis was adopted for the preparation of CDs systems, without using any other chemical reagents. Microwave heating enables simultaneous homogeneous and effective heating, resulting in a shorter reaction time due to a higher reaction rate. And because of direct heating via resonance with the vibrational frequencies of the molecules in the reaction media, this technique of preparation is found to be favourable. The exponential growth in the number of reports dealing with microwave assisted synthesis of CDs in the literature also supports its great acceptance and it is logical to attempt the synthesis through the most environmental benign method. Synthesis of all the CDs systems in the present work were carried out in a conventional domestic microwave oven. The power and time for the synthesis of CDs found out through trial and error. The reactions were found to be qualitatively reproducible.

Sensing of aquatic pollutants and food adulterants are of great importance, since it adversely affect the health and living of all beings in the nature. Fluorescent sensing is considered as one the simplest sensing method from the analytical view point. CDs can act as an alternative for the conventionally used toxic fluorescent materials. The developed fluorescent CDs systems employed as fluorescent sensors for the selective and sensitive detection of chromium(VI), tetracycline, quinalphos, 4-nitrophenol and sudan I and the real sample analysis of

the analytes were also conducted for all the five systems, with satisfactory level of statistical parameters.

On account to its enhanced biocompatibility, water solubility and pharmacological background of the precursors; the antioxidant potential and *in-vitro* cytotoxic activity against cancerous cells of the CDs systems were also investigated.



## 1.11 References

- [1] R.P. Feynman, Plenty of Room at the Bottom, *Science*. 254 (1991) 1300–1301. [https://web.pa.msu.edu/people/yang/RFeynman\\_plentySpace.pdf](https://web.pa.msu.edu/people/yang/RFeynman_plentySpace.pdf)
- [2] G.A. Ozin, A.C. Arsenault, *Nanochemistry: A Chemical Approach to Nanomaterials*, Royal Society of Chemistry, 2005. [https://books.google.com/books?id=DXUoDwAAQBAJ&printsec=frontcover&dq=Nanochemistry:+A+Chemical+Approach+to+Nanomaterials&hl=en&newbks=1&newbks\\_redir=1&sa=X&ved=2ahUKewjDqoSHqp\\_-AhXPT2wGHdmJBv0Q6AF6BAgDEAI](https://books.google.com/books?id=DXUoDwAAQBAJ&printsec=frontcover&dq=Nanochemistry:+A+Chemical+Approach+to+Nanomaterials&hl=en&newbks=1&newbks_redir=1&sa=X&ved=2ahUKewjDqoSHqp_-AhXPT2wGHdmJBv0Q6AF6BAgDEAI)
- [3] A. Barhoum, M.L. García-Betancourt, J. Jeevanandam, E.A. Hussien, S.A. Mekkawy, M. Mostafa, M.M. Omran, M. S. Abdalla, M. Bechelany, Review on Natural, Incidental, Bioinspired, and Engineered Nanomaterials: History, Definitions, Classifications, Synthesis, Properties, Market, Toxicities, Risks, and Regulations, *Nanomaterials*. 12 (2022) 177. <https://doi.org/10.3390/nano12020177>
- [4] V. Georgakilas, J.A. Perman, J. Tucek, R. Zboril, Broad Family of Carbon Nanoallotropes: Classification, Chemistry, and Applications of Fullerenes, Carbon Dots, Nanotubes, Graphene, Nanodiamonds, and Combined Superstructures, *Chem. Rev.* 115 (2015) 4744–4822. <https://doi.org/10.1021/cr500304f>
- [5] S. Sagbas, N. Sahiner, 22 - Carbon dots: preparation, properties, and application, in: A. Khan, M. Jawaid, Inamuddin, A.M. Asiri (Eds.), *Nanocarbon and Its Composites*, Woodhead Publishing, 2019: pp. 651–676. <https://doi.org/10.1016/B978-0-08-102509-3.00022-5>
- [6] C. Xia, S. Zhu, T. Feng, M. Yang, B. Yang, Evolution and Synthesis of Carbon Dots: From Carbon Dots to Carbonized Polymer Dots, *Adv. Sci.* 6 (2019) 1901316. <https://doi.org/10.1002/advs.201901316>
- [7] B.D. Mansuriya, Z. Altintas, Carbon Dots: Classification, Properties, Synthesis, Characterisation, and Applications in Health Care—An Updated Review (2018–2021), *Nanomaterials*. 11 (2021) 2525. <https://doi.org/10.3390/nano11102525>

- [8] X. Xu, R. Ray, Y. Gu, H.J. Ploehn, L. Gearheart, K. Raker, W.A. Scrivens, Electrophoretic Analysis and Purification of Fluorescent Single-Walled Carbon Nanotube Fragments, *J. Am. Chem. Soc.* 126 (2004) 12736–12737. <https://doi.org/10.1021/ja040082h>
- [9] Zh.I. Alferov, The history and future of semiconductor heterostructures, *Semiconductors.* 32 (1998) 1–14. <https://doi.org/10.1134/1.1187350>
- [10] M.A. Cotta, Quantum Dots and Their Applications: What Lies Ahead?, *ACS Appl. Nano Mater.* 3 (2020) 4920–4924. <https://doi.org/10.1021/acsanm.0c01386>
- [11] S. Kubendhiran, Z. Bao, K. Dave, R.-S. Liu, Microfluidic Synthesis of Semiconducting Colloidal Quantum Dots and Their Applications, *ACS Appl. Nano Mater.* 2 (2019) 1773–1790. <https://doi.org/10.1021/acsanm.9b00456>
- [12] Y. Shirasaki, G.J. Supran, M.G. Bawendi, V. Bulović, Emergence of colloidal quantum-dot light-emitting technologies, *Nature Photon.* 7 (2013) 13–23. <https://doi.org/10.1038/nphoton.2012.328>
- [13] X. Bellanger, P. Billard, R. Schneider, L. Balan, C. Merlin, Stability and toxicity of ZnO quantum dots: interplay between nanoparticles and bacteria, *J Hazard Mater.* 283 (2015) 110–116. <https://doi.org/10.1016/j.jhazmat.2014.09.017>
- [14] C. Zhu, Z. Chen, S. Gao, B.L. Goh, I.B. Samsudin, K.W. Lwe, Y. Wu, C. Wu, X. Su, Recent advances in non-toxic quantum dots and their biomedical applications, *Prog. Nat. Sci.: Mater. Int.* 29 (2019) 628–640. <https://doi.org/10.1016/j.pnsc.2019.11.007>
- [15] R. Jelinek, *Carbon Quantum Dots*, Springer International Publishing, Cham, 2017. <https://doi.org/10.1007/978-3-319-43911-2>
- [16] L. Cui, X. Ren, M. Sun, H. Liu, L. Xia, *Carbon Dots: Synthesis, Properties and Applications*, *Nanomaterials.* 11 (2021) 3419. <https://doi.org/10.3390/nano11123419>
- [17] J. Liu, R. Li, B. Yang, Carbon Dots: A New Type of Carbon-Based Nanomaterial with Wide Applications, *ACS Cent. Sci.* 6 (2020) 2179–2195. <https://doi.org/10.1021/acscentsci.0c01306>

- [18] M. Han, S. Zhu, S. Lu, Y. Song, T. Feng, S. Tao, J. Liu, B. Yang, Recent progress on the photocatalysis of carbon dots: Classification, mechanism and applications, *Nano Today*. 19 (2018) 201–218. <https://doi.org/10.1016/j.nantod.2018.02.008>
- [19] M.L. Liu, B.B. Chen, C.M. Li, C.Z. Huang, Carbon dots: synthesis, formation mechanism, fluorescence origin and sensing applications, *Green Chem.* 21 (2019) 449–471. <https://doi.org/10.1039/C8GC02736F>
- [20] H. Liu, T. Ye, C. Mao, Fluorescent Carbon Nanoparticles Derived from Candle Soot, *Angew. Chem. Int. Ed.* 46 (2007) 6473–6475. <https://doi.org/10.1002/anie.200701271>
- [21] S. Tajik, Z. Dourandish, K. Zhang, H. Beitollahi, Q.V. Le, H.W. Jang, M. Shokouhimehr, Carbon and graphene quantum dots: a review on syntheses, characterisation, biological and sensing applications for neurotransmitter determination, *RSC Adv.* 10 (2020) 15406–15429. <https://doi.org/10.1039/D0RA00799D>
- [22] H. Gonçalves, P.A.S. Jorge, J.R.A. Fernandes, J.C.G. Esteves da Silva, Hg(II) sensing based on functionalized carbon dots obtained by direct laser ablation, *Sens. Actuators, B.* 145 (2010) 702–707. <https://doi.org/10.1016/j.snb.2010.01.031>
- [23] Z. Ma, H. Ming, H. Huang, Y. Liu, Z. Kang, One-step ultrasonic synthesis of fluorescent N-doped carbon dots from glucose and their visible-light sensitive photocatalytic ability, *New J. Chem.* 36 (2012) 861–864. <https://doi.org/10.1039/C2NJ20942J>
- [24] S. Zhuo, M. Shao, S.-T. Lee, Upconversion and Downconversion Fluorescent Graphene Quantum Dots: Ultrasonic Preparation and Photocatalysis, *ACS Nano.* 6 (2012) 1059–1064. <https://doi.org/10.1021/nn2040395>
- [25] S. Anwar, H. Ding, M. Xu, X. Hu, Z. Li, J. Wang, L. Liu, L. Jiang, D. Wang, C. Dong, M. Yan, Q. Wang, H. Bi, Recent Advances in Synthesis, Optical Properties, and Biomedical Applications of Carbon Dots, *ACS Appl. Bio Mater.* 2 (2019) 2317–2338. <https://doi.org/10.1021/acsabm.9b00112>

- [26] S. Ahirwar, S. Mallick, D. Bahadur, Electrochemical Method To Prepare Graphene Quantum Dots and Graphene Oxide Quantum Dots, *ACS Omega*. 2 (2017) 8343–8353. <https://doi.org/10.1021/acsomega.7b01539>
- [27] L. Yan, Y. Yang, C.-Q. Ma, X. Liu, H. Wang, B. Xu, Synthesis of carbon quantum dots by chemical vapor deposition approach for use in polymer solar cell as the electrode buffer layer, *Carbon*. 109 (2016) 598–607. <https://doi.org/10.1016/j.carbon.2016.08.058>
- [28] Y. Hu, Y. Wang, C. Wang, Y. Ye, H. Zhao, J. Li, X. Lu, C. Mao, S. Chen, J. Mao, L. Wang, Q. Xue, One-pot pyrolysis preparation of carbon dots as eco-friendly nanoadditives of water-based lubricants, *Carbon*. 152 (2019) 511–520. <https://doi.org/10.1016/j.carbon.2019.06.047>
- [29] L. Ndlwana, N. Raleie, K.M. Dimpe, H.F. Ogutu, E.O. Oseghe, M.M. Motsa, T.A.M. Msagati, B.B. Mamba, Sustainable Hydrothermal and Solvothermal Synthesis of Advanced Carbon Materials in Multidimensional Applications: A Review, *Materials*. 14 (2021) 5094. <https://doi.org/10.3390/ma14175094>
- [30] T.V. de Medeiros, J. Manioudakis, F. Noun, J.-R. Macairan, F. Victoria, R. Naccache, Microwave-assisted synthesis of carbon dots and their applications, *J. Mater. Chem. C*. 7 (2019) 7175–7195. <https://doi.org/10.1039/C9TC01640F>
- [31] Z. Li, L. Wang, Y. Li, Y. Feng, W. Feng, Frontiers in carbon dots: design, properties and applications, *Mater. Chem. Front*. 3 (2019) 2571–2601. <https://doi.org/10.1039/C9QM00415G>
- [32] R. Atchudan, T.N.J.I. Edison, D. Chakradhar, S. Perumal, J.-J. Shim, Y.R. Lee, Facile green synthesis of nitrogen-doped carbon dots using *Chionanthus retusus* fruit extract and investigation of their suitability for metal ion sensing and biological applications, *Sens. Actuators, B*. 246 (2017) 497–509. <https://doi.org/10.1016/j.snb.2017.02.119>
- [33] S.D. Torres Landa, N.K. Reddy Bogireddy, I. Kaur, V. Batra, V. Agarwal, Heavy metal ion detection using green precursor derived carbon dots, *IScience*. 25 (2022) 103816. <https://doi.org/10.1016/j.isci.2022.103816>

- [34] M. Pan, X. Xie, K. Liu, J. Yang, L. Hong, S. Wang, Fluorescent Carbon Quantum Dots—Synthesis, Functionalization and Sensing Application in Food Analysis, *Nanomaterials*. 10 (2020) 930. <https://doi.org/10.3390/nano10050930>
- [35] C.-W. Lai, Y.-H. Hsiao, Y.-K. Peng, P.-T. Chou, Facile synthesis of highly emissive carbon dots from pyrolysis of glycerol; gram scale production of carbon dots/mSiO<sub>2</sub> for cell imaging and drug release, *J. Mater. Chem.* 22 (2012) 14403–14409. <https://doi.org/10.1039/C2JM32206D>
- [36] Y. Lou, X. Hao, L. Liao, K. Zhang, S. Chen, Z. Li, J. Ou, A. Qin, Z. Li, Recent advances of biomass carbon dots on syntheses, characterisation, luminescence mechanism, and sensing applications, *Nano Sel.* 2 (2021) 1117–1145. <https://doi.org/10.1002/nano.202000232>
- [37] J. Zhang, S.-H. Yu, Carbon dots: large-scale synthesis, sensing and bio-imaging, *Mater. Today*. 19 (2016) 382–393. <https://doi.org/10.1016/j.mattod.2015.11.008>
- [38] V. Manikandan, N.Y. Lee, Green synthesis of carbon quantum dots and their environmental applications, *Environ. Res.* 212 (2022) 113283. <https://doi.org/10.1016/j.envres.2022.113283>
- [39] A. Kanwal, N. Bibi, S. Hyder, A. Muhammad, H. Ren, J. Liu, Z. Lei, Recent advances in green carbon dots (2015–2022): synthesis, metal ion sensing, and biological applications, *Beilstein J. Nanotechnol.* 13 (2022) 1068–1107. <https://doi.org/10.3762/bjnano.13.93>
- [40] J. Praneerad, N. Thongsai, P. Supchocksoonthorn, S. Kladsomboon, P. Paoprasert, Multipurpose sensing applications of biocompatible radish-derived carbon dots as Cu<sup>2+</sup> and acetic acid vapor sensors, *Spectrochim. Acta, Part A*. 211 (2019) 59–70. <https://doi.org/10.1016/j.saa.2018.11.049>
- [41] P. Kumar, S. Dua, R. Kaur, M. Kumar, G. Bhatt, A review on advancements in carbon quantum dots and their application in photovoltaics, *RSC Adv.* 12 (2022) 4714–4759. <https://doi.org/10.1039/D1RA08452F>

- [42] A. Sharma, T. Gadly, S. Neogy, S.K. Ghosh, M. Kumbhakar, Addition to “Molecular Origin and Self-Assembly of Fluorescent Carbon Nanodots in Polar Solvents,” *J. Phys. Chem. Lett.* 8 (2017) 5861–5864. <https://doi.org/10.1021/acs.jpcllett.7b02991>
- [43] H. Ding, S.-B. Yu, J.-S. Wei, H.-M. Xiong, Full-Color Light-Emitting Carbon Dots with a Surface-State-Controlled Luminescence Mechanism, *ACS Nano.* 10 (2016) 484–491. <https://doi.org/10.1021/acsnano.5b05406>
- [44] J. Peng, W. Gao, B.K. Gupta, Z. Liu, R. Romero-Aburto, L. Ge, L. Song, L.B. Alemany, X. Zhan, G. Gao, S.A. Vithayathil, B.A. Kaiparettu, A.A. Marti, T. Hayashi, J.-J. Zhu, P.M. Ajayan, Graphene Quantum Dots Derived from Carbon Fibers, *Nano Lett.* 12 (2012) 844–849. <https://doi.org/10.1021/nl2038979>
- [45] K.J. Mintz, Y. Zhou, R.M. Leblanc, Recent development of carbon quantum dots regarding their optical properties, photoluminescence mechanism, and core structure, *Nanoscale.* 11 (2019) 4634–4652. <https://doi.org/10.1039/C8NR10059D>
- [46] B. Zhi, X. Yao, Y. Cui, G. Orr, C.L. Haynes, Synthesis, applications and potential photoluminescence mechanism of spectrally tunable carbon dots, *Nanoscale.* 11 (2019) 20411–20428. <https://doi.org/10.1039/C9NR05028K>
- [47] L. Li, T. Dong, Photoluminescence tuning in carbon dots: surface passivation or/and functionalization, heteroatom doping, *J. Mater. Chem. C.* 6 (2018) 7944–7970. <https://doi.org/10.1039/C7TC05878K>
- [48] F.T. Rabouw, C. de Mello Donega, Excited-State Dynamics in Colloidal Semiconductor Nanocrystals, *Top Curr Chem (Z).* 374 (2016) 58. <https://doi.org/10.1007/s41061-016-0060-0>
- [49] C. de M. Donegá, Synthesis and properties of colloidal heteronanocrystals, *Chem. Soc. Rev.* 40 (2011) 1512–1546. <https://doi.org/10.1039/C0CS00055H>
- [50] L. Jacak, A. Wójs, P. Hawrylak, *Quantum Dots*, Springer, Berlin, Heidelberg, 1998. <https://doi.org/10.1007/978-3-642-72002-4>

- [51] H. Ding, X.-H. Li, X.-B. Chen, J.-S. Wei, X.-B. Li, H.-M. Xiong, Surface states of carbon dots and their influences on luminescence, *J. Appl. Phys.* 127 (2020) 231101. <https://doi.org/10.1063/1.5143819>
- [52] S.H. Jin, D.H. Kim, G.H. Jun, S.H. Hong, S. Jeon, Tuning the Photoluminescence of Graphene Quantum Dots through the Charge Transfer Effect of Functional Groups, *ACS Nano.* 7 (2013) 1239–1245. <https://doi.org/10.1021/nn304675g>
- [53] C.M. Carbonaro, R. Corpino, M. Salis, F. Mocci, S.V. Thakkar, C. Olla, P.C. Ricci, On the Emission Properties of Carbon Dots: Reviewing Data and Discussing Models, *Journal of Carbon Research.* 5 (2019) 60. <https://doi.org/10.3390/c5040060>
- [54] K.K. Chan, S.H.K. Yap, K.-T. Yong, Biogreen Synthesis of Carbon Dots for Biotechnology and Nanomedicine Applications, *Nano-Micro Lett.* 10 (2018) 72. <https://doi.org/10.1007/s40820-018-0223-3>
- [55] Z. Sun, X. Li, Y. Wu, C. Wei, H. Zeng, Origin of green luminescence in carbon quantum dots: specific emission bands originate from oxidized carbon groups, *New J. Chem.* 42 (2018) 4603–4611. <https://doi.org/10.1039/C7NJ04562J>
- [56] F. Yan, Z. Sun, H. Zhang, X. Sun, Y. Jiang, Z. Bai, The fluorescence mechanism of carbon dots, and methods for tuning their emission color: a review, *Microchim Acta.* 186 (2019) 583. <https://doi.org/10.1007/s00604-019-3688-y>
- [57] H. Kang, J. Zheng, X. Liu, Y. Yang, Phosphorescent carbon dots: Microstructure design, synthesis and applications, *New Carbon Materials.* 36 (2021) 649–664. [https://doi.org/10.1016/S1872-5805\(21\)60083-5](https://doi.org/10.1016/S1872-5805(21)60083-5)
- [58] C.-L. Shen, Q. Lou, K.-K. Liu, L. Dong, C.-X. Shan, Chemiluminescent carbon dots: Synthesis, properties, and applications, *Nano Today.* 35 (2020) 100954. <https://doi.org/10.1016/j.nantod.2020.100954>
- [59] F. Arcudi, L. Đorđević, S. Rebecani, M. Cacioppo, A. Zanut, G. Valenti, F. Paolucci, M. Prato, Lighting up the Electrochemiluminescence of Carbon Dots through Pre- and Post-

- Synthetic Design, *Adv. Sci.* 8 (2021) 2100125.  
<https://doi.org/10.1002/advs.202100125>
- [60] K. Akbar, E. Moretti, A. Vomiero, Carbon Dots for Photocatalytic Degradation of Aqueous Pollutants: Recent Advancements, *Adv. Opt. Mater.* 9 (2021) 2100532. <https://doi.org/10.1002/adom.202100532>
- [61] M. Batoool, H.M. Junaid, S. Tabassum, F. Kanwal, K. Abid, Z. Fatima, A.T. Shah, Metal Ion Detection by Carbon Dots—A Review, *Critical Reviews in Analytical Chemistry.* (2020) 1–12.  
<https://doi.org/10.1080/10408347.2020.1824117>
- [62] G.S. Das, J.P. Shim, A. Bhatnagar, K.M. Tripathi, T. Kim, Biomass-derived Carbon Quantum Dots for Visible-Light-Induced Photocatalysis and Label-Free Detection of Fe(III) and Ascorbic acid, *Sci Rep.* 9 (2019) 15084. <https://doi.org/10.1038/s41598-019-49266-y>
- [63] S. Chahal, J.-R. Macairan, N. Yousefi, N. Tufenkji, R. Naccache, Green synthesis of carbon dots and their applications, *RSC Adv.* 11 (2021) 25354–25363. <https://doi.org/10.1039/D1RA04718C>
- [64] F. Zu, F. Yan, Z. Bai, J. Xu, Y. Wang, Y. Huang, X. Zhou, The quenching of the fluorescence of carbon dots: A review on mechanisms and applications, *Microchim. Acta.* 184 (2017) 1899–1914.  
<https://doi.org/10.1007/s00604-017-2318-9>
- [65] G. Ge, L. Li, D. Wang, M. Chen, Z. Zeng, W. Xiong, X. Wu, C. Guo, Carbon dots: synthesis, properties and biomedical applications, *J. Mater. Chem. B.* 9 (2021) 6553–6575.  
<https://doi.org/10.1039/D1TB01077H>
- [66] L. Đorđević, F. Arcudi, M. Cacioppo, M. Prato, A multifunctional chemical toolbox to engineer carbon dots for biomedical and energy applications, *Nat. Nanotechnol.* 17 (2022) 112–130.  
<https://doi.org/10.1038/s41565-021-01051-7>
- [67] S. Zhu, Q. Meng, L. Wang, J. Zhang, Y. Song, H. Jin, K. Zhang, H. Sun, H. Wang, B. Yang, Highly Photoluminescent Carbon Dots for Multicolor Patterning, Sensors, and Bio-imaging, *Angew. Chem., Int. Ed.* 52 (2013) 3953–3957. <https://doi.org/10.1002/anie.201300519>



- [68] J. Liu, Y. Geng, D. Li, H. Yao, Z. Huo, Y. Li, K. Zhang, S. Zhu, H. Wei, W. Xu, J. Jiang, B. Yang, Deep Red Emissive Carbonized Polymer Dots with Unprecedented Narrow Full Width at Half Maximum, *Adv. Mater.* 32 (2020) 1906641. <https://doi.org/10.1002/adma.201906641>
- [69] J. Liu, D. Li, K. Zhang, M. Yang, H. Sun, B. Yang, One-Step Hydrothermal Synthesis of Nitrogen-Doped Conjugated Carbonized Polymer Dots with 31% Efficient Red Emission for In Vivo Imaging, *Small.* 14 (2018) 1703919. <https://doi.org/10.1002/smll.201703919>
- [70] Y. Liu, J. Liu, J. Zhang, X. Li, F. Lin, N. Zhou, B. Yang, L. Lu, Noninvasive Brain Tumor Imaging Using Red Emissive Carbonized Polymer Dots across the Blood–Brain Barrier, *ACS Omega.* 3 (2018) 7888–7896. <https://doi.org/10.1021/acsomega.8b01169>
- [71] S.-Y. Sung, Y.-L. Su, W. Cheng, P.-F. Hu, C.-S. Chiang, W.-T. Chen, S.-H. Hu, Graphene Quantum Dots-Mediated Theranostic Penetrative Delivery of Drug and Photolytics in Deep Tumors by Targeted Biomimetic Nanosponges, *Nano Lett.* 19 (2019) 69–81. <https://doi.org/10.1021/acs.nanolett.8b03249>
- [72] C. Scialabba, A. Sciortino, F. Messina, G. Buscarino, M. Cannas, G. Roscigno, G. Condorelli, G. Cavallaro, G. Giammona, N. Mauro, Highly Homogeneous Biotinylated Carbon Nanodots: Red-Emitting Nanoheaters as Theranostic Agents toward Precision Cancer Medicine, *ACS Appl. Mater. Interfaces.* 11 (2019) 19854–19866. <https://doi.org/10.1021/acsami.9b04925>
- [73] S. Ghosh, K. Ghosal, S.A. Mohammad, K. Sarkar, Dendrimer functionalized carbon quantum dot for selective detection of breast cancer and gene therapy, *Chem. Eng. J.* 373 (2019) 468–484. <https://doi.org/10.1016/j.cej.2019.05.023>
- [74] J. Han, K. Na, Transfection of the TRAIL gene into human mesenchymal stem cells using biocompatible polyethyleneimine carbon dots for cancer gene therapy, *J. Ind. Eng. Chem.* 80 (2019) 722–728. <https://doi.org/10.1016/j.jiec.2019.02.015>
- [75] P. Li, S. Liu, W. Cao, G. Zhang, X. Yang, X. Gong, X. Xing, Low-toxicity carbon quantum dots derived from gentamicin sulfate to

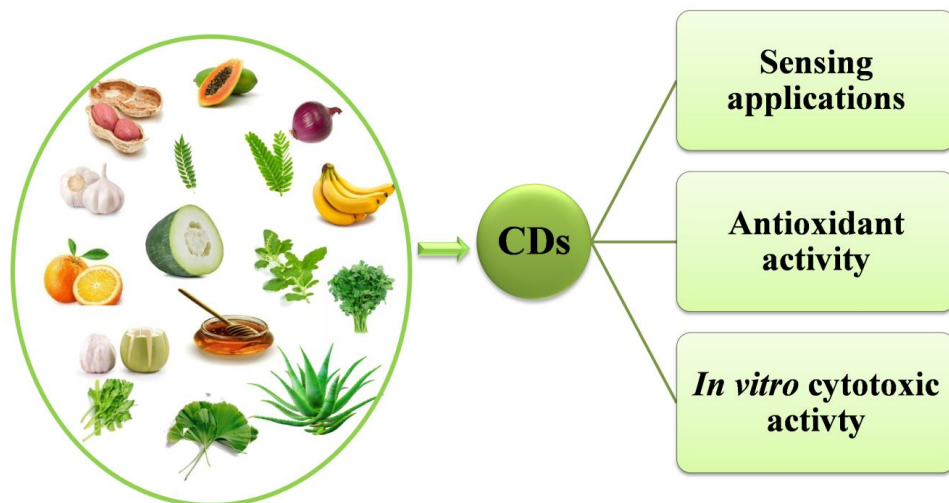
- combat antibiotic resistance and eradicate mature biofilms, *Chem. Commun.* 56 (2020) 2316–2319. <https://doi.org/10.1039/C9CC09223D>
- [76] S. Lu, L. Liu, H. Wang, W. Zhao, Z. Li, Z. Qu, J. Li, T. Sun, T. Wang, G. Sui, Synthesis of dual functional gallic-acid-based carbon dots for bio-imaging and antitumor therapy, *Biomater. Sci.* 7 (2019) 3258–3265. <https://doi.org/10.1039/C9BM00570F>
- [77] T. Tong, H. Hu, J. Zhou, S. Deng, X. Zhang, W. Tang, L. Fang, S. Xiao, J. Liang, Glycyrrhizic-Acid-Based Carbon Dots with High Antiviral Activity by Multisite Inhibition Mechanisms, *Small.* 16 (2020) 1906206. <https://doi.org/10.1002/sml.201906206>
- [78] R. Chen, G. Liu, X. Sun, X. Cao, W. He, X. Lin, Q. Liu, J. Zhao, Y. Pang, B. Li, A. Qin, Chitosan derived nitrogen-doped carbon dots suppress osteoclastic osteolysis via downregulating ROS, *Nanoscale.* 12 (2020) 16229–16244. <https://doi.org/10.1039/D0NR02848G>
- [79] S. Cailotto, M. Negrato, S. Daniele, R. Luque, M. Selva, E. Amadio, A. Perosa, Carbon dots as photocatalysts for organic synthesis: metal-free methylene–oxygen-bond photocleavage, *Green Chem.* 22 (2020) 1145–1149. <https://doi.org/10.1039/C9GC03811F>
- [80] S. Bhattacharyya, F. Ehrat, P. Urban, R. Teves, R. Wyrwich, M. Döblinger, J. Feldmann, A.S. Urban, J.K. Stolarczyk, Effect of nitrogen atom positioning on the trade-off between emissive and photocatalytic properties of carbon dots, *Nat Commun.* 8 (2017) 1401. <https://doi.org/10.1038/s41467-017-01463-x>
- [81] S. Wang, L. Li, Z. Zhu, M. Zhao, L. Zhang, N. Zhang, Q. Wu, X. Wang, G. Li, Remarkable Improvement in Photocatalytic Performance for Tannery Wastewater Processing via SnS<sub>2</sub> Modified with N-Doped Carbon Quantum Dots: Synthesis, Characterisation, and 4-Nitrophenol-Aided Cr(VI) Photoreduction, *Small.* 15 (2019) 1804515. <https://doi.org/10.1002/sml.201804515>
- [82] T. Zhou, S. Chen, L. Li, J. Wang, Y. Zhang, J. Li, J. Bai, L. Xia, Q. Xu, M. Rahim, B. Zhou, Carbon quantum dots modified anatase/rutile TiO<sub>2</sub> photoanode with dramatically enhanced photoelectrochemical performance, *Appl. Catal. B.* 269 (2020) 118776. <https://doi.org/10.1016/j.apcatb.2020.118776>

- [83] P. He, Y. Shi, T. Meng, T. Yuan, Y. Li, X. Li, Y. Zhang, L. Fan, S. Yang, Recent advances in white light-emitting diodes of carbon quantum dots, *Nanoscale*. 12 (2020) 4826–4832.  
<https://doi.org/10.1039/C9NR10958G>
- [84] A. Kim, J.K. Dash, P. Kumar, R. Patel, Carbon-Based Quantum Dots for Photovoltaic Devices: A Review, *ACS Appl. Electron. Mater.* 4 (2022) 27–58. <https://doi.org/10.1021/acsaelm.1c00783>
- [85] F.A. Permatasari, M.A. Irham, S.Z. Bisri, F. Iskandar, Carbon-Based Quantum Dots for Supercapacitors: Recent Advances and Future Challenges, *Nanomaterials (Basel)*. 11 (2021) 91.  
<https://doi.org/10.3390/nano11010091>
- [86] H. Jia, Y. Cai, J. Lin, H. Liang, J. Qi, J. Cao, J. Feng, W. Fei, Heterostructural Graphene Quantum Dot/MnO<sub>2</sub> Nanosheets toward High-Potential Window Electrodes for High-Performance Supercapacitors, *Adv. Sci.* 5 (2018) 1700887.  
<https://doi.org/10.1002/advs.201700887>



# Chapter 2

## REVIEW OF LITERATURE



---

This chapter provides a concise review of carbon dots derived from natural resources and their applications, particularly in metal and organic pollutant sensing and biological applications. A brief description of the natural resources selected in the present work is also included.



## 2.1 Introduction

As discussed in the Chapter 1, during the last few years, a rapid growth has been noticed in the synthesis, properties, and applications of carbon dots (CDs), as it is reviewed by Baker et al. [1] Lim et al. [2] Lee et al. [3] Ray et al. [4], etc. Most of the works gives attention to only the characteristics and applications of CDs, disregard the significance of carbon sources. The synthesis of CDs has been carried out using several carbon rich substances including both synthetic and natural compounds as precursors. However, conventional methods with synthetic starting materials generally demand the use of hazardous and expensive chemicals, sophisticated instruments and high energy. Besides, it probably leads to complicated environmental as well as economical issues. Hence, greener approach of synthesis with harmless or less harmful precursors receives substantial importance [5].

Biomass is an excellent carbon resource for the synthesis of CDs. In actual fact, biomass based carbon resources are the most eco-friendly precursors, compared to other synthetic carbon sources and it possess several advantages, like being economically viable, easy to obtain, abundant, ease of synthesis, enhanced biocompatibility and eco-friendliness [6]. Furthermore, the production of CDs from natural biomass provides value addition to the precursor. That is, a low-value biomass waste can converted into valuable and useful materials [7]. Apart from this, the hetero atoms present in the biomass can effectively acts as surface passivating agents for CDs, in contrast to the CDs made

out of man-made carbon sources require the addition of external hetero atoms sources for the surface passivation [8]. Biogenic carbon dots originate from biobased precursors resolve most of the aforementioned difficulties and recently various reports are coming from this area, since green synthesis of nanomaterials is the most promising subject in the field of nanotechnology, and hence CDs from natural products based synthetic strategies have been mesmerizing the researchers in the field. In recent years, various biomasses have been used as carbon sources to prepare CDs.

This chapter examines recent developments in the detection of food additives, aquatic contaminants, and biological applications with a special focus on the cytotoxicity and antioxidant properties of CDs made with various natural products as carbon sources.

## **2.2 CDs from natural sources**

CDs from natural resources follow the same synthetic strategies of CDs as we discussed in the Chapter 1, by utilizing the natural products as carbon precursors. In general, the preparation of these CDs takes up the bottom-up approach. It is achieved by the fusion of organic molecules by the aid of appropriate external energy. Normally, the bottom-up method results in a high yield and it is more convenient for the heteroatom doping during the synthetic process [7]. To date, different methods for preparing CDs have been established, and most studies search to achieve good-quality CDs through simple, greener and cost-effective synthetic methods.



As mentioned earlier, there are several reports in the literature discussing about the synthesis and applications of CDs from natural products. In general, vegetables, fruits, leaves and rhizomes etc. are widely used as a carbon source to prepare CDs (Figure 2.1). Almost of them are successfully employed in various significant applications. Some of the most recent and relevant works and corresponding applications are enlisted in the Table 2.1



**Figure 2.1:** Different natural products used for the synthesis of CDs

**Table 2.1:** CDs from natural resources and applications

Source	Method	Size (nm)	Quantum yield (%)	Application	Reference
Garlic	Hydrothermal	10.7	17.5	Bioimaging	[8]
Winter melon	Hydrothermal	4.5 – 5.2	7.51	Bioimaging	[9]
Coriander leaves	Hydrothermal	1.5 – 2.98	6.48	Detecting Fe <sup>3+</sup>	[10]
Papaya	Hydrothermal	3.4	18.98	Detecting Fe <sup>3+</sup>	[11]
Onion	Hydrothermal	9	28	Bioimaging	[12]
Pomelo peel	Hydrothermal	2-4	6.9	Detecting Hg <sup>2+</sup>	[13]
Orange juice	Hydrothermal	1.5-4.5	26	Bioimaging	[14]
Soy milk	Hydrothermal	25	2.6	Electrocatalyst	[15]
Banana juice	Hydrothermal	3	8.95	Not reported	[16]
Peach gum	Hydrothermal	2-5	28.46	Detecting Au <sup>3+</sup>	[17]
Linseed	Hydrothermal	4-8	14.2	Biosensor and bioimaging	[18]
Black tea	Hydrothermal	4.6	x	Detecting Fe <sup>3+</sup>	[19]
Prawn shell	Hydrothermal	6	54	Drug delivery	[20]
Cabbage	Hydrothermal	2-6	16.5	Bioimaging	[21]
Bamboo leaves	Hydrothermal	2-6	7.1	Detecting Cu <sup>2+</sup>	[22]
Honey	Hydrothermal	2	19.8	Detecting Fe <sup>3+</sup>	[23]
Willow bark	Hydrothermal	1-4	6	Biosensing and photocatalyst	[24]
Lemon peel	Hydrothermal	1-3	14	Detecting Cr(VI)	[25]
Cornflour	Hydrothermal	2-6	7.7	Bioimaging and detecting Cu <sup>2+</sup>	[26]
Starch	Hydrothermal	2.25-3.5	21.7	Bioimaging	[27]
Eggshell membrane	Microwave	5	14	Biosensor	[28]
Goose feather	Microwave-hydrothermal	21.5	17.1	Detecting Fe <sup>3+</sup>	[29]

Coconut water	Microwave-hydrothermal	1-6	54	Detecting thiamine and $\text{Cu}^{2+}$	[30]
Silkworm chrysalis	Microwave	19	46	Bioimaging	[31]
Natural lignocellulose	Microwave	2-3	x	Bioimaging	[32]
Eutrophic algal blooms	Microwave	8	13	Bioimaging	[33]
Jackfruit seeds	Microwave	3-7	17.91	Bioimaging and detecting $\text{Au}^{3+}$	[34]
Cow manure	Chemical oxidation	4	65	Bioimaging	[35]
Rice husk	Pyrolysis	3-6	15	Bioimaging	[36]
Urine	Pyrolysis	20.6	14	Detecting $\text{Hg}^{2+}$ and $\text{Cu}^{2+}$	[37]
Konjac flour	Pyrolysis	3.37	22	Bioimaging and detecting $\text{Fe}^{3+}$ and lysine	[38]
Peanut shell	Pyrolysis	0.4-2.4	9.91	Bioimaging	[39]

x: Not reported

According to the literature, CDs are widely engaged in metal ion sensing and biological applications, the following sections focusing on the sensing of toxic metal ions and organic molecules, particularly in aquatic medium, by green precursor derived CDs.

### 2.3 Sensing applications of CDs derived from natural sources

CDs derived from natural resources have a wide range of applications in the field of sensing, owing to their fluorescence behaviour. The majority of these sensors used the fluorescence emission quenching or enhancing method. The sensing sector includes several analyte molecules like metals, organic pollutants and food

additives or food adulterants, etc. Sensing of these substances has gained much attention since they are very compatible in aquatic environments and directly and indirectly leads to several health issues to all beings. Some of the applications from the field of sensing of metal and organic pollutants are discussed in the subsequent sections.

### **2.3.1 Metal ion sensing**

Industrialisation and contemporaneous agricultural practices plays major role in the contamination of the planet, and the input of heavy metal ions to this is inevitable. Generally Hg(II), Pb(II), Cd(II) and Cr(VI) are considered as the most hazardous metal ions under use [40]. The extensive usage of these metals adversely affects the environmental system, accumulation even at lower concentration leads to several serious health hazards in all beings. Thus it is crucial to screen the contaminants particularly in water bodies since nearly all of the industrial effluents are directly released in to water resources without any kind of pre-treatments, and the compatibility of these pollutants with water intensify the adverse effects. Therefore, an effective and fast responsive analytical method is highly demandable for the detection of these metal ions.

The typical methods for the detection of metal ions including colorimetric analysis [41], photo electrochemical method [42], surface-enhanced Raman scattering [43], headspace gas chromatography [44], electro catalytic detection [45], and inductively coupled plasma mass spectrometry (ICP – MS) [46]. Most of them are expensive and complicated, while some are lacking of sensitivity [47]. Recently, the

acceptance of fluorescence spectroscopy over the other detection methods increased with higher rate, since it involves comparatively simple operational procedures, cost-effectiveness, fast responses and high sensitivity [48].

Organic molecules, quantum dots, and metal nanoparticles are the most commonly used fluorescent sensor probes for metal ion sensing [49–51]. Although, lesser water solubility, minor biocompatibility, complicated synthetic procedures of these probes make it difficult from the applications and leads for the search of alternatives, which can resolves all the defects. Biocompatible fluorescent carbon dots can easily be posted for this purpose since; the majority of aforementioned difficulties can be solved by this new candidate.

There are numerous reports in the literature on toxic metal ion sensing with biogenic carbon dots, some of which are discussed below.

### **Hg(II)**

Mercury exists as Hg(0), Hg(I) and Hg(II) in our environment (water and air), in which Hg(II) is the most toxic member for living organisms and the eco-system [52]. Accumulation of Hg(II) in trace level particularly in aquatic systems, results in serious health issues to all beings, it adversely effects the major organs like, kidney, liver, cardiovascular, and central nervous system (CNS). As per the guidelines by WHO the maximum in-take level of mercury through water is 1 mg/L and through air is 2 mg/kg body weight per day [53].

Therefore, the detection of Hg(II) is highly demandable for protecting the environment and health.

Mercury sensing is carried out by different types of efficient fluorescent CDs derived from natural precursors. CDs from flour by microwave assisted synthesis have been effectively used for the detection of Hg(II) was reported in 2013, with limit of detection (LOD) of 0.5 nM by Qin et al. [54]. Similarly, in 2014 CDs from cucumber juice has been reported by Wang et al. for the Hg(II) detection through fluorescence decrease of CDs on interaction with the ion with detection limit of 180 nM [55].

In the very next year, rapid and sensitive of Hg(II) with CDs was also reported by Yu et al. by using finger citron bergamot fruit as the carbon precursor via hydrothermal heating with a LOD of 5.5 nM. The fluorescence turn-off behaviour of the CDs with Hg(II) is investigated by the team and finally attributed to the dynamic quenching mechanism [56]. Likewise, in the same year, Li et al. used Chinese yams as raw material for the preparation of highly fluorescent CDs and were effectively utilized as sensing probe towards Hg(II) in aqueous medium with LOD 1.26 nM [57].

By 2016, Gu et al. created a nano probe for the sensing of Hg(II) from readily available lotus root, enriched with various amino acids through microwave heating. These CDs had comparatively higher quantum yield since it contains N-containing groups from the precursor and act as surface passivation reagents. The CDs exhibited remarkable selectivity and sensitivity with Hg(II) (LOD of 18.7 nM)

and it was attributed to relatively higher and faster chelating kinetics of the Hg(II) with surface functionalities of CDs and it leads to static fluorescence quenching [58].

Zhao et al. have fabricated nanohybrid in 2017, based on CDs derived from corn bract exhibiting bright fluorescence due to chlorophyll based porphyrin aromatic rings and used as the sensor for Hg(II) detection through fluorescence quenching with detection limit as low as 9 nM [59]. In the same year, casein, a milk protein based CDs were developed and effectively used as fluorescent probe for the detection for Hg(II) with limit of detection of 6.5 nM by Xu et al. [60]. In the same way, in 2018 fluorimetric sensing of Hg(II) was also carried out by using CDs developed from pineapple peel as carbon source with LOD of 4.5 nM [61].

Blue fluorescent CDs with good quantum yield were reported in the same year with good stability and water solubility. It was synthesised from tamarind leaves comprised with several proteins; carbohydrates and vitamin-C; the research group have adopted hydrothermal treatment for the synthesis. The prepared CDs displays efficient binding capacity towards Hg(II) by the S atoms in the surface resulting the fluorescence turn-off sensing with LOD of 6 nM [62].

Likewise, the next year there is an another work utilizing ethanolic extract of bamboo leaves, for preparation of CDs by Liu et al. CDs nano hybrid was used as dual ratiometric sensor for Hg(II) and Pb(II) ions. Flavonoids and chlorophyll contents in the extract successfully converted into multi-emissive nanohybrids and its

specific binding of Hg(II) and Pb(II) to the flavonoid and porphyrin moieties leads to fluorescence quenching with LODs of 0.22 nM and 0.14 nM, respectively [63].

There are several other reports from the same area and all are tabulated in **Table 2.2**.

### **Pb(II)**

Lead (Pb) is a toxic metal ion, very well known for its harmful disorders in the human body [64,65]. Lead exists in three different oxidation states; Pb(0), Pb(II), and Pb(IV), and is primarily existed as Pb(II) in the environment [66]. Trace level concentration of Pb (II) in blood is highly hazardous and even cause death. Mental disability, anemia, memory loss and migraine are the other serious health issues due to this toxic element. As per the Environmental Protection Agency (EPA) the maximum allowed level of Pb in-take in drinking water should be less than 15.0 ppb (72 nM) [67–69].

The lead detection by green precursor derived CDs are very common in literature, and the most commonly known herb source tulsi leaves derived CDs was synthesised by Kumar et al. in 2017 by means of hydrothermal method. The starting material enriched with different functional groups including carvacrol, several acids (rosmarinic, oleanolic and ursolic), alcohols, aldehydes and ketones, and were attached in to the surface of CDs devoid of any surface passivating agents. The green fluorescent system as-obtained were used for lead (Pb(II)) ion detection through fluorescence quenching with LOD of



0.59 nM and it was successfully implemented in water as well as live cells [70].

Bandi and co-workers demonstrated the synthesis of highly fluorescent N-doped CDs by utilizing lantana berries and ethylenediamine as C and N precursors respectively by the year 2018. It was used as a selective and sensitive sensing probe towards Pb(II) through fluorescence turn-off mechanism with LOD of 9.64 nM. Moreover, this CDs with polar surface functionalities was applied for the sensing of Pb(II) in the real samples including water, human serum and urine [71].

The main works describing Pb (II) sensing via green precursor generated CDs have been tabulated in **Table 2.2**.

## **Cd(II)**

As mentioned before, like other heavy metals Cd(II) can adversely affect the health system especially the central nervous system and other organs and leads to several diseases, like high blood pressure, neuro disorders and kidney related issues [72].

Selective and sensitive detection of Cd(II) ions was effectively carried out by fluorescent CDs, from curry leaves via hydrothermal treatment was reported in 2020 with LOD of 0.29 nM. The native fluorescence of CDs was quenched by the Cd(II) through dynamic fluorescence quenching by ligand-to-metal charge transfer (LMCT) mechanism [73].

In the same year, Chauhan and co-workers reported a coconut waste-derived fluorescent carbon dots prepared through thermal calcinations and successfully demonstrated it as a fluorescent turn-on sensor for Cd(II) with LOD 0.18 nM. The developed system was effectively checked over different water sources with satisfactory parameters [74].

Later on, Sariga et al. reported CDs based fluorescence turn-off probe for Cd(II) sensing in water samples by utilizing Ashoka tree leaves as starting material through a green and facile method. The suggested method exhibits a LOD of 2.4 nM and it was successfully implemented in real samples of water and industrial effluents [75]. There few more reports from the same area and are tabulated in **Table 2.2**.

### **Cr(VI)**

Chromium(VI) is the another very important toxic metal ion considered as one of the primary aquatic pollutant and is carcinogenic in nature. As per the regulation of World Health Organization (WHO) the limit of Cr(VI) in drinking water should be less than 50 µg/L [64].

Different green precursor produced CDs are widely used for the sensing of Cr(VI) in aquatic environment, some of the reports are discussed here. Lemon peel derived CDs were reported by Tyagi et al. in 2016. The prepared system with an average size range of 1 - 3 nm and high photostability, tested for the sensing of Cr (VI) in drinking water and reported a LOD of 73 nM. The possible fluorescence

quenching by Cr(VI) was accredited to the non-radiative recombination of electron-hole pairs because of low redox potentials and low-lying d-d transition states, including functional groups on the surface of CD [25].

Similarly, tulsi leaves-derived CDs were reported by Bhatt et al. in 2018 and successfully used as fluorescent probe against Cr(VI) with LOD of 86.54 nM and also employed in real water samples with good level of recovery [76]. In 2019, Feng et al. developed a fluorescent probe using natural kelp CDs and it was employed for the determination of Cr(VI) in environmental water samples with sufficient recoveries [77]. In the above two cases the quenching mechanism was attributed to combination of IFE and static quenching, which is confirmed through different methods [76,77].

The main works describing Cr(VI) sensing via natural products derived CDs have been tabulated in **Table 2.2**.

**Table 2.2:** Green precursor based CDs for toxic metal ion sensing

Precursor	Analyte species	LOD (nM)	Reference
Flour	Hg(II)	0.5	[54]
Cucumber juice	Hg(II)	180	[55]
Finger citron bergamot fruit	Hg(II)	5.5	[56]
Chinese yam	Hg(II)	1.26	[57]
Lotus root	Hg(II)	18.7	[58]
Corn bract	Hg(II)	9	[59]
Casein	Hg(II)	6.5	[60]

Pineapple peel	Hg(II)	4.5	[61]
Tamarind leaves	Hg(II)	6	[62]
Strawberry juice	Hg(II)	3	[52]
Pomelo peel	Hg(II)	0.23	[13]
Honey	Hg(II)	1.02	[78]
Coconut milk	Hg(II)	16.5	[79]
Muskmelon	Hg(II)	330	[80]
Tulsi leaves	Pb(II)	0.59	[70]
Lantana berries and ethylenediamine	Pb(II)	9.64	[71]
Ginkgo leaves	Pb(II)	0.055	[81]
Table sugar	Pb(II)	67	[82]
Potato-dextrose agar	Pb(II)	0.11	[68]
Curry leaves	Cd(II)	0.29	[73]
Coconut waste	Cd(II)	0.18	[74]
Ashoka tree leaves	Cd(II)	2.4	[75]
Tea residue	Cd(II)	x	[83]
Lemon peel	Cr(VI)	73	[25]
Tulsi leaves	Cr(VI)	86.54	[76]
Kelp	Cr(VI)	520	[77]
Shallot	Cr(VI)	3500	[84]
Flax straw	Cr(VI)	190	[85]
Shrimp shell	Cr(VI)	100	[48]
Groundnuts	Cr(VI)	1923	[86]

x: Not reported

*NB: Some values were recalculated for uniformity in the corresponding units with respect to other reports.*

### **2.3.2 Organic pollutant sensing**

Like in the case of inorganic toxic metal pollutants, some non-biodegradable organic contaminants also stay in the environment for long time and enter to the food chain, leading to several health hazards. Specifically, organic pollutants like nitrophenols widely used in various fields like in the manufacturing of pharmaceuticals, agrochemicals, explosives and dyes. As they are carcinogenic, its extensive usages and discharge to water resources without any pre-treatments leading to serious health issues. Similarly, the modern agricultural practices made use of neurotoxic pesticides to control the pests and there by minimize the crop loss. Superfluous usages of these toxic pesticides leads to water pollution since it can be easily reach to the water resources. As in the case of pesticides, several antibiotics are now used in the field of agriculture and livestock to increase crop productivity and as growth promoters. The over usage of these antibiotics make it as primary water pollutant and it will reach in to the body of non-targeted beings, resulting severe health issues. The sensing of these hazardous organic water pollutants are of great importance.

Similar to the case of aquatic organic pollutants, some of our food products were also contaminated by some synthetic chemicals and generally they are known by the name of food adulterants. The main ideology at the back of food adulterants are of increasing the colour appeal, fragrance and taste of the food materials. Some of these synthetic food additives are carcinogenic and majority of them are

prohibited in almost all the countries in the world. However, some of them are still under use through illegal routes. Therefore the detection of such adulterants in the food materials is of great concern.

CDs are successfully entered to the field of organic pollutants sensing by utilizing its luminescence ability. There are several reports in the literature from this area; some of them are discussed below.

### **Nitrophenols**

Nitrophenols, a class of compounds with appended nitro and phenolic groups, are well-known for its explosive nature. In practical analytical applications, it is critical to detect nitrophenol compounds. There are several reports in the literature that discuss nitrophenol sensing with green CDs, few of them are discussed below.

Walter's dogwood leaves derived CDs was reported by Wang et al. and were successfully implemented as fluorescent CDs for the detection of 4-nitrophenol (4-NP) with LOD of 17.5 nM [87]. Similarly, Chatzimarkou et al. described an efficient and environmentally friendly method for producing biomass CDs from apple seeds. The resulted N-doped CDs were shown to be a sensitive as well as efficient fluorescent probe, which were quenched by 4-nitrophenol via the FRET quenching mechanism [88]. The proposed approach outperforms previously reported approaches due to its low LOD (13 nM) and good recoveries.

In addition to 4-NP, other nitrophenols like 2-nitrophenol, 3-nitrophenol, 2,4-dinitrophenol (DNP) and 2,4,6-trinitrophenol (TNP)

were also simultaneously detected by green precursor derived CDs through fluorescence based sensing method. Such a work was reported in 2018 by Soni and co-workers, in which Palm shell powder and triflic acid based N, S co-doped CDs was synthesised. The as obtained CDs was effectively employed as a sensor for 4-NP, DNP, TNP with LOD in the nanomolar scale and the values are found to be 79 nM (4-NP), 165 nM (DNP) and 82 nM (TNP) [89].

There are some more related works in the literature and the important reports with details are listed in **Table 2.3**.

## **Pesticides**

Some investigators have recently used natural product-based CDs to create pesticide probes. Organophosphorus pesticides are considered to be a significant agrochemical capable of increasing crop yield. There are numbers of studies in the literature deal with pesticide sensing especially, organophosphorous pesticides using bioprecursor derived CDs; some of them are mentioned as follows.

Bera and Mohapatra developed highly fluorescent CDs from chitosan, that were used for ultrasensitive glyphosate detection via effective photoelectron transfer between CdTe and CDs with a LOD of 0.002 nM. The CdTe-CQD integrated probe's specific and selective recognition of glyphosate, even in the presence of other organophosphorus pesticides, makes it suitable for practical applications [90].

Similarly, such an integration probe was also synthesised by Zheng et al. The team created fluorescent CDs with a variety of functional groups using lycii fructus. The prepared CDs were then used as stabilisers in the green synthesis of CDs-AgNPs. The cross-linking of CDs-AgNPs with phoxim causes the CDs-modified AgNPs to aggregate, resulting in colour variations ranging from yellow to red. The phoxim LOD for this probe was 40 nM, and it was successfully used to detect phoxim in water and fruit samples with good recoveries [91].

Hou et al. on the other hand, generated a turn-on fluorescent sensor for glyphosate detection based on CDs derived from Japanese pagoda leaves. Electron transfer was discovered between  $\text{Fe}^{3+}$  and the as-prepared CDs. As a result,  $\text{Fe}^{3+}$  demonstrated a distinct dynamic-quenching behaviour towards CDs. Glyphosate, on the other hand, inhibited the electron transfer process, therefore the addition of glyphosate restored the fluorescence of the quenched CDs/ $\text{Fe}^{3+}$  system. It was caused by the strong complexation of  $\text{Fe}^{3+}$  with the functional groups in the glyphosate molecule. The LOD value of the CDs/ $\text{Fe}^{3+}$  fluorescent probe as prepared is found to be 51.75 nM [92].

Apart from the discussed, several additional related works with different pesticides are available in the literature, and **Table 2.3** lists the significant reports with specific information.



## **Antibiotics**

Antibiotics are chemicals that inhibit the development of other cells and are typically used to treat infectious diseases caused by bacteria. Tetracycline is one of the antibiotics that have been widely used. Tetracycline levels in the human body that are too high can cause a variety of diseases such as hepatotoxicity, nephrotoxicity, and others [93,94]. Fluorescent based sensing of antibiotics by biogenic CDs is well documented in the literature. About a few of them are discussed below.

Feng et al. describe the synthesis of CDs using rose flowers and  $P_2O_5$ . Based on the tetracycline-induced quenching in the fluorescence of CDs, it was used as a tetracycline sensing probe. It was assumed that the interactions between the surface groups of CDs and tetracycline would explain this process [94].

Similar to this, Miao et al. achieved the quantitative detection by differentiating three tetracyclines using tobacco-derived CDs as a sensor. Three tetracyclines reacted with CDs in distinct ways. Tetracycline specifically quenched the fluorescence without causing a fluorescence shift because of the IFE quenching process. Meanwhile, CDs responded to chlortetracycline, and as a result of the expanded energy band gap, their fluorescence displayed a blue shift. Additionally, the band gap narrowing brought about by the introduction of oxytetracycline resulted in a red-shift emission. The quantitative analytical method was constructed using the data from this investigation, and the LODs for tetracycline, chlortetracycline, and

oxytetracycline were 5.18 nM, 14 nM, and 6.06 nM, respectively [95]. In a similar fashion, Guo et al. synthesised CDs from crab shells in 2020. The CDs had good fluorescence due to functional groups made of nitrogen that were generated from the starting material. The prepared CDs were successfully used by the researchers to detect traces of tetracycline, and they had good stability and a low LOD value (0.011 nM). The prepared CDs have good potential for analysing actual sewage and can be used to quantitatively detect tetracycline in the majority of acidic solutions [96].

In addition to the ones mentioned, there are a number of biogenic CDs in the literature that are utilised as fluorescence sensors for various types of antibiotics; **Table 2.3** summarises the noteworthy reports with details.

### **Food adulterants**

Food adulterants are substances that are introduced to food products as additives and can be either natural or manufactured chemicals, as was aforementioned. Previous research has demonstrated that CDs made from natural sources can be used to identify some food contaminants. Because each molecule has unique characteristics, some of them can either increase or decrease the fluorescence of CDs, depending on the nature of the molecules [93].

Sudan I is an azo dye that is commonly used as a red colourant in the food industry and is classified as a carcinogenic chemical by the World Health Organization. In 2018, Anmei et al. created an efficient

fluorescent sensor for the Sudan I dye using CDs derived from the hydrothermal treatment of cigarette filters. The prepared system has a LOD value of 950 nM, and satisfactory results were obtained when the method was applied to Sudan I determination in food samples [97].

Similarly, Tartrazine is another food colorant or simply yellow synthetic chemical that are widely utilised as a colouring agent in the food business. Tartrazine reported to have very harmful effects to the nervous and reproductive systems [98].

In 2015, Xu and his colleagues employed aloe to create tartrazine-quenchable CDs. The as prepared CDs reacted with tartrazine to create a complex, resulting in the quenching of fluorescence. At a LOD of 73 nM, this fluorescent probe successfully detected tartrazine in food samples (steamed buns, honey and candy) [98]. Similar CDs from Russian olive were reported by Ghereghlou et al. in 2021. The produced CDs utilised as tartrazine sensor with LOD of 86 nM. Additionally, they have attempted to assess the sensing system for the detection of tartrazine in real samples also [99].

In addition to the ones already described, there are a few more CDs made from bioprecursors that have been used as fluorescence sensors for various food additives; **Table 2.3** summarises all the interesting publications with details.

**Table 2.3:** Green precursor based CDs for organic pollutant sensing

Precursor for CDs	Analyte species	LOD (nM)	Reference
Apple seeds	4-NP	13	[88]
Palm shell powder and triflic acid	4-NP, DNP, TNP	79 (4-NP) 165(DNP) 82(TNP)	[89]
Celery leaves and glutathione	2-NP 3-NP 4-NP	39 (2-NP) 43(3-NP) 26(4-NP)	[100]
Sweet chestnut rose	2-NP	15.2	[101]
Shaddock peel and HCl	TNP	37.1	[102]
Walter's dogwood leaves	4-NP	17.5	[87]
Chitosan	Glyphosate	0.002	[90]
Pork rib bones	Dimethoate	64	[103]
Lycii Fructus	Phoxim	40	[91]
Flavonoid from ginkgo leaves (a) N-CD-FLA (b) NS-CD-FLA (c) NSB-CD-FLA	Fenitrothion Dithianon Dinoseb	0.36 0.28 0.66	[104]
Feather, H <sub>2</sub> O <sub>2</sub> and NH <sub>3</sub>	Dichlorvos	3.8	[105]
Jatropha fruits	Chlorpyrifos	7.701	[106]
Japanese pagoda leaves	Glyphosate	51.75	[92]
Dried beet powder	Amoxicillin	475	[107]
Plum	Doxorubicin	120	[108]
Rose flower and P <sub>2</sub> O <sub>5</sub>	Tetracycline	3.3	[94]
Crab shell	Tetracycline	0.011	[96]

Rice residue and lysine	Tetracycline	236.7	[109]
	Chlortetracycline	279.1	
	Terramycin	373.9	
Tobacco	Tetracycline,	5.18	[95]
	Chlotetracycline	14	
	Oxytetracycline	6.06	
Hawthorn powder	Chlortetracycline	152.44	[110]
Cigarette filter	Sudan I	950	[97]
Sugarcane molasses	Sunset yellow	399	[111]
Tulsi leaves	Malachite green	18	[112]
Bael patra fruit	Allura red	607	[113]
Aloe	Tartrazine	73	[98]
Lemon peels	Tartrazine	200	[114]
Russian olive	Tartrazine	86	[99]

4-NP: 4-nitrophenol; 3-NP: 3-nitrophenol; 2-NP: 2-nitrophenol; DNP: 2,4-dinitrophenol; TNP: 2,4,6-trinitrophenol

*NB: Some values were recalculated for uniformity in the corresponding units with respect to other reports.*

#### **2.4 Biological applications of CDs derived from natural resources**

Biogenic carbon dots are well established in the field of biology, mainly due to its commendable biocompatibility and water solubility. According to the literature, CDs majorly engaged in the bioapplication including, bioimaging, drug delivery, anticancer agents, antioxidant, photothermal and photodynamic therapy, chemotherapy and gene delivery. Here we are going to discuss about the antioxidant potential and *in-vitro* cytotoxic activity against cancer cell lines of natural products derived CDs, both are found to be relevant to the present works.

### **Antioxidant activity of CDs**

As said earlier, very less but sound evidences are available in the literature dealing with the antioxidant potentiality of CDs. The majority of the antioxidant activity was monitored using the DPPH scavenging method, in which antioxidant activity was determined by the visual colour change of DPPH caused by the addition of CDs.

The antioxidant activity of the green precursor derived CDs was reported by Sachdev and Gopinath in 2015 from coriander leaves and the prepared system exerts good level of antioxidant potential and it was evaluated by the DPPH assay method [10]. Almost similar studies was also reported by Chunduri and co-workers in 2016 and they were used coconut husk for the synthesis of CDs [115].

Likewise, Rodríguez-Varillas et al. studied the antioxidant activity of CDs from tomato. The team also uses the DPPH scavenging assay for evaluating the antioxidant potential. The mechanism behind the antioxidant activity of CDs was investigated by the research group and it was accredited to the hydrogen donating capacity of the surface functionalities associated in the CDs [116].

The antioxidant capability of the sulphur functionalised CDs from turmeric were well studied by Roy et al. and the team used the same DPPH method for the evaluation [117]. Likewise, CDs with great antioxidant potential were also developed by Bhattacharya and co-workers from the red onion peel. The antioxidant study of the system was demonstrated through DPPH assay [118].

A novel work was described by Guo et al. in which the red pitaya peels were used for the synthesis of CDs and the antioxidant potentiality of the same system was investigated through the DPPH assay and reports a comparatively good antioxidant activity than the standard ascorbic acid [119]. The same DPPH assay was utilized by Rajamanikandan et al. in 2022 for the antioxidant activity studies of the developed CDs from the pineapple peels [120].

Altogether, the literature describes the antioxidant potentiality of the natural product derived CDs and opens up a more biocompatible antioxidant moiety in the nano dimension. In the most cases the CDs having higher activity than the corresponding precursor, the comparative studies were found to be less in literature. However, the mechanism behind the increased antioxidant capacity of CDs than the precursor is still unclear and one of probable reason may be the increased surface area to volume ratio.

### ***In vitro* cytotoxic activity of CDs**

A compound's cytotoxic activity often denotes that the substances under examination are hazardous to cells. When it comes to normal cell lines, cytotoxicity is a sign of a substance's negative effects, however when it comes to cancerous cell lines, cytotoxicity is a sign of a substance's anticancer characteristics.

*In vitro* cytotoxic activities of CDs are pretty much available in the literature. The Trypan blue exclusion and MTT assay [(3-(4,5-dimethylthiazol-2-yl)-2,5-diphenyltetrazolium bromide) tetrazolium

reduction assay] are the most widely used assays for the evaluation of *In vitro* cytotoxicity.

Chen et al. conducted *in vitro* cytotoxic studies of six different CDs derived from two species of bamboo, wood, stem and root of the Chinese mahonia herb and two different pineapple roots through MTT assay [121]. Similar to the above study orange juice derived CDs cytotoxicity against Human colorectal carcinoma (HCT 116) and human embryonic kidney (HEK 293) cell lines was evaluated by MTT assay. The results reveal the cytotoxic potency of the prepared system with good level of activity [122].

Using the human cancer cell lines PC3, MCF-7, and HT-29, Arkan and team used the MTT techniques to assess the cytotoxic potential of walnut CDs. Caspase-3 and Caspase-9 activation as well as mitochondrial membrane potential (MMP) approaches were used to investigate the mode of cell death in order to better understand the mechanism of action [123].

Paul and Kurian used trypan blue exclusion method with Dalton's Lymphoma Ascites cells (DLA) for the examination of *in vitro* cytotoxicity of two CDs derived from jackfruit peel and tamarind peel. The comparison of the two CDs shows that N-CDs from jackfruit peel have more predominately anticancerous activity than that from the tamarind peel [124].

Thus the cytotoxicity against cancer cell lines directly implies the anticancer activity of the samples. Numerous reports on the



cytotoxic activity of CDs are coming up and each claiming with improved potentiality and wide applicability against different cell lines.

## 2.5 Plant sources used in the present investigation

Five distinct pharmaceutically relevant biosources have been employed to produce CDs in the current investigation. The subsequent paragraphs provide a succinct explanation of the sources that were used.

### Mango ginger rhizomes

Mango ginger (*Curcuma amada*) (**Figure 2.2**) is a unique spice with important pharmacological activities and is distinguished by its mango flavour, which makes it appealing as a fragrant as well as for other industrial and medicinal applications. It is originated in the Indo-Malayan region and widely distributed in the tropics of Asia to Africa and Australia. In India it is allocated in the wild and cultivated forms [125].



**Figure 2.2** Mango ginger rhizomes

The significant constituents found in the rhizomes are starch, curcuminoids (curcumin, demethoxycurcumin, bis-demethoxycurcumin), terpinoids (difurocumenol, amadaldehyde and amadannulen.), phenolic compounds (gallic acid, caffeic acid, ferulic acid, gentisic acid and cinnamic acid) and essential oil ( $\alpha$ -asarone and  $\beta$ -myrcene). The therapeutic properties of the rhizome are primarily due to the curcuminoids found in it [126]. Compounds like as mangiferin [(1,3,6,7)-Tetrahydroxy-2-[(2S,3R,4R,5S,6R)-3,4,5-trihydroxy-6-(hydroxymethyl)oxan-2-yl]-9H-xanthen-9-one] [127], several glycosides, alkaloids, flavanoids, steroids, and saponins, among other things, had been isolated from the rhizome extract [126,128,129].

They were well known for a wide range of biological activities, including antioxidant [130], antibacterial [131], antifungal [132], antiinflammatory [133], platelet aggregation inhibitory [134], antiallergic [135], enterokinase inhibitory [136], analgesic [137], antitubercular [138], brine-shrimp lethal [139], hypotriglyceridemic [140], biopesticidal [141], antitumor [142], and antiobesity and memory impairment properties [143]. According to reports, the essential oil extracted from the rhizome is high in pinene, ocimene, curcumene, and linalool. It has been reported that the chemical composition and bioactivities vary depending on the method of extraction [144].

Mango ginger appears to have high potential and has largely gone unexplored in terms of bioactive phytochemicals. The available literature on phytochemicals and bioactive divergent ingredients in

mango ginger may contribute to its disease-fighting abilities and use. Furthermore, it may provide scientific support for the bioactive properties of mango ginger rhizome.

Mango ginger's introduction into the sphere of nano technology was recently revealed. Chitosan-Tripolyphosphate nanoparticles were created in 2021 using an ethanolic extract of this spice [145].

### **Wild lemon leaves**

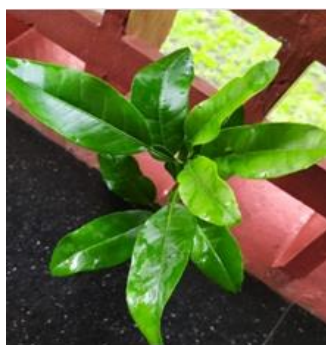


**Figure 2.3** Wild lemon leaves

Wild lemon (*Citrus pennivesiculata*) may be the less explored member from the Citrus species and is belonging to *Rutaceae* family and it known to posses almost all the features of the other members from the same family. The leaves of wild lemon (**Figure 2.3**) is an interesting bioresources having different kind of phytochemicals like acorbic acid, citric acid, alkaloids, steroids, flavonoids, phenols, cardiac glycosides, tannins and terpenoids [146].

The studies on this leaves are very few in literature, it exhibits antioxidant and antimicrobial activity in various solvent extracts.

Presence of these phytochemicals may be responsible for the medicinal value of this plant. Different extracts from leaves showed antibacterial and antifungal activity. The antibacterial activity might be due to the presence of active antimicrobial compounds in the plant. Plant based antimicrobials have enormous therapeutic potential as they can serve the purpose without any side effects that are often associated with synthetic antimicrobial compounds [146].

As previously said, the exploration of this species and, presumably, its materialisation has been overlooked in the literature.

### **Bilimbi fruit**



**Figure 2.4** Bilimbi fruits

Bilimbi (*Averrhoa bilimbi*) fruit (**Figure 2.4**) is a tropical fruit, which is primarily utilized in traditional medicinal systems to cure blood pressure, high levels of sugar in the blood and many infectious diseases. Tropical and subtropical countries like Malaysia, Myanmar, Indonesia, Thailand, Singapore, the Philippines, Sri Lanka, India,

Bangladesh, etc. are known for their abundance of the bilimbi (*Averrhoa bilimbi*). Kerala is well recognised for its adequate abundance in India, and the Kani tribal traditional healers in the Tholu hill region mostly use it for various therapeutic purposes [147].

The ability of this plant to operate as an antioxidant, antibacterial, antidiabetic, hypotensive, antiinflammatory, and hepatoprotective has been demonstrated through a variety of biological activities, demonstrating the excessive value this plant possesses as complementary and alternative medicine [147,148]. Although almost all plant components have substantial pharmacological effects, the majority of studies focus on the fruits and leaves [147].

Preliminary phytochemical analyses of the fruit extracts showed the presence of terpenes, coumarin, thiamine, niacin, flavonoids, tannins, bitter principles, essential oils, proteins, amino acids, carbohydrates, proteins, and flavonoids. The fruits are also a good source of oxalic acid and vitamin C [149,150]. The isolation of 2,4-dihydroxy-6-((4-methylpentyl)oxy) methyl benzaldehyde from the fruit extract has also been reported [147].

As per the reports, the bilimbi fruit extract also contains specific volatile substances. Aliphatic acids, alcohols, and aldehydes make up the majority of the volatiles. The main constituents included hexadecanoic acid, nonanoic acid, (Z)-9-octadecenoic acid, 2-furaldehyde, nonanal, (Z)-3-hexenol, octane tricosane, (E)-2-decenal, (Z)-9-pentacosene 2-furfural, and (Z)-9-tricosene. Several of the compounds were discovered to be esters, with butyl and hexyl

nicotinate having higher amounts than the rest [151,152]. There were minuscule amounts of the remaining chemicals. The fruit gets its distinctive fatty and green flavours from a group of C-9 chemicals called nonanal, nonanoic acid, and (E)-2-nonenal. It is also thought that the fruit's green tones are a result of the second-most prevalent chemical, (Z)-3-hexenol [152].

The bilimbi fruit is well recognised for its biological applications including antimicrobial activities; the aqueous and chloroform extracts the bilimbi fruits exerts a positive antibacterial activity against several microbes [153–155], antioxidant activities [156,157]. Apart from this it act as hepatoprotective agent [158], anticancer agent [159] and antithrombotic agent [160].

Aside from the above bioapplications, bilimbi fruit find application from the material science sector. Based on the literature it is used for the preparation various metal nanoparticles including gold and silver nanoparticles [161], zinc oxide nanoparticles [162] and lead oxide nanoparticles [163]. The direct materialisation of this amazing natural resource is left out of the literature, nevertheless.

### **Sweet flag**

Sweet flag (*Acorus calamus*) (**Figure 2.5**), a member of the *Acoraceae* family and commonly used alone or in conjunction with other herbs in Indian and Chinese traditional medicine, it has attracted a lot of interest and is thought to be beneficial [164]. The plant, which is native to India, Europe, Sri Lanka, Burma, Japan, China, Southern

Russia, Mongolia, and the Northern United States, is widely cultivated throughout many temperate and sub-temperate regions of the world [165,166]. The semi-aquatic and terrestrial habitat of the herbaceous perennial plant has creeping rhizomes. Rhizomes have a citrus fragrance, are heavily branching, pinkish or pale green in appearance, and have a bitter flavour [166].



**Figure 2.5** Sweet flag rhizomes

Many traditional and ethnomedicinal uses for the plant have been documented over a lengthy period of time. It has been used for thousands of years in various medical systems, including Ayurveda, Unani, Siddha, Chinese medicine, etc., to treat a wide range of conditions, including nervous disorders, appetite loss, bronchitis, chest pain, colic, cramps, diarrhoea, digestive disorders, flatulence, gas, indigestion, rheumatism, sedative, cough, fever, bronchitis, inflammation, depression, tumours and haemorrhoids [164,167]. This plant's rhizome has been given credit for a number of therapeutic potentials.

A number of active constituents from the rhizomes and essential oils of sweet flag have been isolated and characterized. Of the constituents, alpha-asarone (1,2,4-trimethoxy-5-[(E)-prop-1-enyl] benzene) and beta-asarone (1, 2, 4-trimethoxy-5-[(Z)-prop-1-enyl] benzene) are the predominant bioactive components. Aside from this, there are various important phytochemicals including glycosides (xanthone), volatile oil, sesquiterpenes, monoterpenes, flavonoids, steroids, saponins, lignin, tannins, mucilage, alkaloid and polyphenolic compounds [168,169]. Beside these, it also contains the other essential oil such as calameon, calamen, calamine, calamenol, calamenone, eugenol, camphene, pinene and asaronaldehyde, acorafuran [170]. Other compounds identified in the sweet flag rhizomes were 4-terpineol, 2-allyl-5-ethoxy-4-methoxyphenol, epieudesmin, lysidine, spathulenol, borneol, furylethyl ketone, nonanoic acid, 2,2,5,5-tetramethyl-3-hexanol, bornyl acetate, galgravin, retusin, (9E,12E,15E)-9,12,15-octadecatrien-1-ol, butyl butanoate, geranyl acetate, sakuranin, acetic acid, camphor, isoelemicin, a-ursolic acid, acetophenone, dehydroabiatic acid, isoeugenol methylether, apigenin 4,7-dimethyl ether, dehydrodiisoeugenol, linalool, elemicin, linolenic acid, n-heptanic acid, calamendiol, tannins, starches, mucin, soft gums and resins [164,171,172]

Various pharmacological activities of sweet flag rhizome has been reported, such as sedative, CNS depressant [173], anticonvulsant, memory enhancing [174], analgesic, antipyretic [175], antispasmodic [176], cardiovascular [177], hypolipidemic [178], immunosuppressive [179], antiinflammatory, antioxidant and neuroprotective [180],



antidiarrheal [181], antimicrobial [182], antifungal [183] anticancer [184,185] and antidiabetic [186].

Further to the pharmaceutical uses already described, this resource was successfully introduced to the field of nanomaterials. The synthesis of various metal nanoparticles using the extract's reducing capacity is the subject of a few papers in the literature. The extract was successfully used in the preparation of gold nanoparticles [187] and silver nanoparticles [188]. However, the direct materialisation of the resource was noticed to be lacking in the literature.

### **Long pepper**

Long pepper (*Piper longum*) (**Figure 2.6**) is a traditional medicinal plant that is a member of the *Piperaceae* family. It is indigenous to the Indo-Malaya region and is found throughout the tropical and subtropical world, including the Indian subcontinent, Sri Lanka, the Middle East, and North America. The fruits are primarily used as a culinary spice and preservative, but they are also a powerful remedy in various traditional medicinal systems for cold, bronchitis, cough, snakebite, and scorpion-sting, as well as a contraceptive [189].

There are numerous alkaloids and related substances in the fruit, with piperine being the most prevalent. Other alkaloids and related compounds include methyl piperine, piperonaline, piperettine, asarinine, pellitorine, piperundecalidine, piperlongumine, piperlonguminine, retrofractamide A, pergumidiene, brachystamide-B, a dimer of desmethoxyiplartine, N-isobutyl decadienamide, brachyamide-A, brachystine, pipericide, piperderidine, longamide, dehydropiperonaline piperidine, and tetrahydro piperine.

Recent studies reveals that the fruit is also comprised with 1-(3',4'-methylenedioxyphenyl)-1E-tetradecene, 3-(3',4'-methylenedioxyphenyl)-propenal, piperolic acid, 3',4'-di-hydroxy-biabol-1, 10-diene, eudesm-4(15)-ene-1beta, 6-alpha-diol, 7-epi-eudesm-4(15)-ene-1beta, 6beta-diol, guineesine, and 2E,4E-dienamide, (2E, 4E, 8E)-N-isobutylhenicosa-2,4,8-trienamide, tridecyl-dihydro-p-coumarate, eicosanyl-(E)-p-coumarate, and Z-12-octadecenoicglycerol-monoester [190,191].

In addition to the aforementioned components, the fruit is also said to contain lignans (a component of a class of plant compounds with estrogenic and anticancer properties) such as sesamin, pulviatilol, and fargesin. The fruit's essential oils are a complex blend. Caryophyllene, pentadecane, and bisabolone are the three main components, excluding the volatile piperine. Others include dihydrocarveol, vitamins A and E, thujone, terpinolene, zingiberene, p-cymene, p-methoxyacetophenone, and terpinolene [191].



**Figure 2.6** Long pepper fruits

It has many uses and is frequently used as a strong pharmacological agent. The pharmacological activity of long pepper

has been the subject of numerous investigations in the literature, including antimicrobial [192], antiplatelet [193], antidepressant [194], mosquito-larvicidal [195], antiinflammatory [196], antifungal [197], antifertility [198], antioxidant [199], anticancer [200], hepatoprotective [201], antihyperlipidaemic [202], immunomodulatory [203], agents.

In addition to the biological activities already stated, the reducing potential of the extract was employed for the extract-mediated synthesis of a variety of metal nanoparticles, including silver, copper, and nickel [204,205]. However the literature made a gap for the direct materialization of the fruit.

In conclusion, the literature analysis on green precursor derived CDs and natural resources raises the possibility of natural products materialisation in to an extremely appealing luminous particles. This process of value addition was found to be amazing, and it is exciting to examine the material side applications of some selected pharmaceutically relevant natural products as the only precursor without the usage of any hazardous chemicals or sophisticated and expensive instruments. The study of the exerting properties of natural product produced CDs and their fluorescence based applications are quite pleasing. The sensing applications against some selected pollutants by these CDs are also enhancing the interest. Based on these findings and understandings from the literature, the area for additional study was defined and worked on. The experiments and analyses carried out to attain the objectives are detailed in the following Chapters.

## 2.6 References

- [1] S.N. Baker, G.A. Baker, Luminescent Carbon Nanodots: Emergent Nanolights, *Angew. Chem. Int. Ed.* 49 (2010) 6726–6744. <https://doi.org/10.1002/anie.200906623>
- [2] S.Y. Lim, W. Shen, Z. Gao, Carbon quantum dots and their applications, *Chem. Soc. Rev.* 44 (2014) 362–381. <https://doi.org/10.1039/C4CS00269E>
- [3] H. Li, Z. Kang, Y. Liu, S.-T. Lee, Carbon nanodots: synthesis, properties and applications, *J. Mater. Chem.* 22 (2012) 24230–24253. <https://doi.org/10.1039/C2JM34690G>
- [4] S.C. Ray, A. Saha, N.R. Jana, R. Sarkar, Fluorescent Carbon Nanoparticles: Synthesis, Characterisation, and Bioimaging Application, *J. Phys. Chem. C.* 113 (2009) 18546–18551. <https://doi.org/10.1021/jp905912n>
- [5] M. Kurian, A. Paul, Recent trends in the use of green sources for carbon dot synthesis—A short review, *Carbon Trends.* 3 (2021) 100032. <https://doi.org/10.1016/j.cartre.2021.100032>
- [6] V. Manikandan, N.Y. Lee, Green synthesis of carbon quantum dots and their environmental applications, *Environ. Res.* 212 (2022) 113283. <https://doi.org/10.1016/j.envres.2022.113283>
- [7] W. Meng, X. Bai, B. Wang, Z. Liu, S. Lu, B. Yang, Biomass-Derived Carbon Dots and Their Applications, *Energy Environ. Mater.* 2 (2019) 172–192. <https://doi.org/10.1002/eem2.12038>
- [8] S. Zhao, M. Lan, X. Zhu, H. Xue, T.-W. Ng, X. Meng, C.-S. Lee, P. Wang, W. Zhang, Green Synthesis of Bifunctional Fluorescent Carbon Dots from Garlic for Cellular Imaging and Free Radical Scavenging, *ACS Appl. Mater. Interfaces.* 7 (2015) 17054–17060. <https://doi.org/10.1021/acsami.5b03228>
- [9] X. Feng, Y. Jiang, J. Zhao, M. Miao, S. Cao, J. Fang, L. Shi, Easy synthesis of photoluminescent N-doped carbon dots from winter melon for bioimaging, *RSC Adv.* 5 (2015) 31250–31254. <https://doi.org/10.1039/C5RA02271A>
- [10] A. Sachdev, P. Gopinath, Green synthesis of multifunctional carbon dots from coriander leaves and their potential application as

- antioxidants, sensors and bioimaging agents, *Analyst*. 140 (2015) 4260–4269. <https://doi.org/10.1039/C5AN00454C>
- [11] N. Wang, Y. Wang, T. Guo, T. Yang, M. Chen, J. Wang, Green preparation of carbon dots with papaya as carbon source for effective fluorescent sensing of Iron (III) and *Escherichia coli*, *Biosens. Bioelectron.* 85 (2016) 68–75. <https://doi.org/10.1016/j.bios.2016.04.089>
- [12] R. Bandi, B.R. Gangapuram, R. Dadigala, R. Eslavath, S.S. Singh, V. Guttena, Facile and green synthesis of fluorescent carbon dots from onion waste and their potential applications as sensor and multicolour imaging agents, *RSC Adv.* 6 (2016) 28633–28639. <https://doi.org/10.1039/C6RA01669C>
- [13] W. Lu, X. Qin, S. Liu, G. Chang, Y. Zhang, Y. Luo, A.M. Asiri, A.O. Al-Youbi, X. Sun, Economical, Green Synthesis of Fluorescent Carbon Nanoparticles and Their Use as Probes for Sensitive and Selective Detection of Mercury(II) Ions, *Anal. Chem.* 84 (2012) 5351–5357. <https://doi.org/10.1021/ac3007939>
- [14] S. Sahu, B. Behera, T.K. Maiti, S. Mohapatra, Simple one-step synthesis of highly luminescent carbon dots from orange juice: application as excellent bioimaging agents, *Chem. Commun.* 48 (2012) 8835–8837. <https://doi.org/10.1039/C2CC33796G>
- [15] C. Zhu, J. Zhai, S. Dong, Bifunctional fluorescent carbon nanodots: green synthesis via soy milk and application as metal-free electrocatalysts for oxygen reduction, *Chem. Commun.* 48 (2012) 9367–9369. <https://doi.org/10.1039/C2CC33844K>
- [16] B. De, N. Karak, A green and facile approach for the synthesis of water soluble fluorescent carbon dots from banana juice, *RSC Adv.* 3 (2013) 8286. <https://doi.org/10.1039/c3ra00088e>
- [17] J. Liao, Z. Cheng, L. Zhou, Nitrogen-Doping Enhanced Fluorescent Carbon Dots: Green Synthesis and Their Applications for Bioimaging and Label-Free Detection of Au<sup>3+</sup> Ions, *ACS Sustainable Chem. Eng.* 4 (2016) 3053–3061. <https://doi.org/10.1021/acssuschemeng.6b00018>
- [18] Y. Song, X. Yan, Z. Li, L. Qu, C. Zhu, R. Ye, S. Li, D. Du, Y. Lin, Highly photoluminescent carbon dots derived from linseed and their applications in cellular imaging and sensing, *J. Mater. Chem. B.* 6 (2018) 3181–3187. <https://doi.org/10.1039/C8TB00116B>

- [19] P. Song, L. Zhang, H. Long, M. Meng, T. Liu, Y. Yin, R. Xi, A multianalyte fluorescent carbon dots sensing system constructed based on specific recognition of Fe(III) ions, *RSC Adv.* 7 (2017) 28637–28646. <https://doi.org/10.1039/C7RA04122E>
- [20] G. Gedda, C.-Y. Lee, Y.-C. Lin, H. Wu, Green synthesis of carbon dots from prawn shells for highly selective and sensitive detection of copper ions, *Sens. Actuators, B.* 224 (2016) 396–403. <https://doi.org/10.1016/j.snb.2015.09.065>
- [21] A.-M. Alam, B.-Y. Park, Z.K. Ghouri, M. Park, H.-Y. Kim, Synthesis of carbon quantum dots from cabbage with down- and up-conversion photoluminescence properties: excellent imaging agent for biomedical applications, *Green Chem.* 17 (2015) 3791–3797. <https://doi.org/10.1039/C5GC00686D>
- [22] Y. Liu, Y. Zhao, Y. Zhang, One-step green synthesised fluorescent carbon nanodots from bamboo leaves for copper(II) ion detection, *Sens. Actuators, B.* 196 (2014) 647–652. <https://doi.org/10.1016/j.snb.2014.02.053>
- [23] X. Yang, Y. Zhuo, S. Zhu, Y. Luo, Y. Feng, Y. Dou, Novel and green synthesis of high-fluorescent carbon dots originated from honey for sensing and imaging, *Biosens. Bioelectron.* 60 (2014) 292–298. <https://doi.org/10.1016/j.bios.2014.04.046>
- [24] X. Qin, W. Lu, A.M. Asiri, A.O. Al-Youbi, X. Sun, Green, low-cost synthesis of photoluminescent carbon dots by hydrothermal treatment of willow bark and their application as an effective photocatalyst for fabricating Au nanoparticles–reduced graphene oxide nanocomposites for glucose detection, *Catal. Sci. Technol.* 3 (2013) 1027–1035. <https://doi.org/10.1039/C2CY20635H>
- [25] A. Tyagi, K.M. Tripathi, N. Singh, S. Choudhary, R.K. Gupta, Green synthesis of carbon quantum dots from lemon peel waste: applications in sensing and photocatalysis, *RSC Adv.* 6 (2016) 72423–72432. <https://doi.org/10.1039/C6RA10488F>
- [26] J. Wei, X. Zhang, Y. Sheng, J. Shen, P. Huang, S. Guo, J. Pan, B. Feng, Dual functional carbon dots derived from cornflour via a simple one-pot hydrothermal route, *Mater. Lett.* 123 (2014) 107–111. <https://doi.org/10.1016/j.matlet.2014.02.090>

- [27] W. Chen, D. Li, L. Tian, W. Xiang, T. Wang, W. Hu, Y. Hu, S. Chen, J. Chen, Z. Dai, Synthesis of graphene quantum dots from natural polymer starch for cell imaging, *Green Chem.* 20 (2018) 4438–4442. <https://doi.org/10.1039/C8GC02106F>
- [28] Q. Wang, X. Liu, L. Zhang, Y. Lv, Microwave-assisted synthesis of carbon nanodots through an eggshell membrane and their fluorescent application, *Analyst.* 137 (2012) 5392–5397. <https://doi.org/10.1039/C2AN36059D>
- [29] R. Liu, J. Zhang, M. Gao, Z. Li, J. Chen, D. Wu, P. Liu, A facile microwave-hydrothermal approach towards highly photoluminescent carbon dots from goose feathers, *RSC Adv.* 5 (2014) 4428–4433. <https://doi.org/10.1039/C4RA12077A>
- [30] R. Purbia, S. Paria, A simple turn on fluorescent sensor for the selective detection of thiamine using coconut water derived luminescent carbon dots, *Biosens. Bioelectron.* 79 (2016) 467–475. <https://doi.org/10.1016/j.bios.2015.12.087>
- [31] J. Feng, W.-J. Wang, X. Hai, Y.-L. Yu, J.-H. Wang, Green preparation of nitrogen-doped carbon dots derived from silkworm chrysalis for cell imaging, *J. Mater. Chem. B.* 4 (2016) 387–393. <https://doi.org/10.1039/C5TB01999K>
- [32] M. Si, J. Zhang, Y. He, Z. Yang, X. Yan, M. Liu, S. Zhuo, S. Wang, X. Min, C. Gao, L. Chai, Y. Shi, Synchronous and rapid preparation of lignin nanoparticles and carbon quantum dots from natural lignocellulose, *Green Chem.* 20 (2018) 3414–3419. <https://doi.org/10.1039/C8GC00744F>
- [33] V. Ramanan, S.K. Thiyagarajan, K. Raji, R. Suresh, R. Sekar, P. Ramamurthy, Outright Green Synthesis of Fluorescent Carbon Dots from Eutrophic Algal Blooms for In Vitro Imaging, *ACS Sustainable Chem. Eng.* 4 (2016) 4724–4731. <https://doi.org/10.1021/acssuschemeng.6b00935>
- [34] K. Raji, V. Ramanan, P. Ramamurthy, Facile and green synthesis of highly fluorescent nitrogen-doped carbon dots from jackfruit seeds and its applications towards the fluorimetric detection of Au<sup>3+</sup> ions in aqueous medium and in in vitro multicolor cell imaging, *New J. Chem.* 43 (2019) 11710–11719. <https://doi.org/10.1039/C9NJ02590A>

- [35] C. D'Angelis do E. S. Barbosa, J.R. Corrêa, G.A. Medeiros, G. Barreto, K.G. Magalhães, A.L. de Oliveira, J. Spencer, M.O. Rodrigues, B.A.D. Neto, Carbon Dots (C-dots) from Cow Manure with Impressive Subcellular Selectivity Tuned by Simple Chemical Modification, *Chem. Eur. J.* 21 (2015) 5055–5060. <https://doi.org/10.1002/chem.201406330>
- [36] Z. Wang, J. Yu, X. Zhang, N. Li, B. Liu, Y. Li, Y. Wang, W. Wang, Y. Li, L. Zhang, S. Dissanayake, S.L. Suib, L. Sun, Large-Scale and Controllable Synthesis of Graphene Quantum Dots from Rice Husk Biomass: A Comprehensive Utilization Strategy, *ACS Appl. Mater. Interfaces.* 8 (2016) 1434–1439. <https://doi.org/10.1021/acsami.5b10660>
- [37] J.B. Essner, C.H. Laber, S. Ravula, L. Polo-Parada, G.A. Baker, Peedots: biocompatible fluorescent carbon dots derived from the upcycling of urine, *Green Chem.* 18 (2015) 243–250. <https://doi.org/10.1039/C5GC02032H>
- [38] X. Teng, C. Ma, C. Ge, M. Yan, J. Yang, Y. Zhang, P.C. Morais, H. Bi, Green synthesis of nitrogen-doped carbon dots from konjac flour with “off-on” fluorescence by  $\text{Fe}^{3+}$  and L-lysine for bioimaging, *J. Mater. Chem. B.* 2 (2014) 4631–4639. <https://doi.org/10.1039/C4TB00368C>
- [39] M. Xue, Z. Zhan, M. Zou, L. Zhang, S. Zhao, Green synthesis of stable and biocompatible fluorescent carbon dots from peanut shells for multicolor living cell imaging, *New J. Chem.* 40 (2016) 1698–1703. <https://doi.org/10.1039/C5NJ02181B>
- [40] M. Batoool, H.M. Junaid, S. Tabassum, F. Kanwal, K. Abid, Z. Fatima, A.T. Shah, Metal Ion Detection by Carbon Dots—A Review, *Critical Reviews in Analytical Chemistry.* (2020) 1–12. <https://doi.org/10.1080/10408347.2020.1824117>
- [41] G. Jian-feng, H. Chang-jun, Y. Mei, H. Dan-qun, L. Jun-jie, F. Huan-bao, L. Hui-bo, Y. Ping, Colorimetric sensing of chromium(VI) ions in aqueous solution based on the leaching of protein-stabled gold nanoparticles, *Anal. Methods.* 8 (2016) 5526–5532. <https://doi.org/10.1039/C6AY01200K>
- [42] R. Siavash Moakhar, G.K.L. Goh, A. Dolati, M. Ghorbani, Sunlight-driven photoelectrochemical sensor for direct determination of hexavalent chromium based on Au decorated rutile  $\text{TiO}_2$  nanorods, *Appl. Catal., B.* 201 (2017) 411–418. <https://doi.org/10.1016/j.apcatb.2016.08.026>



- [43] W. Zhou, B.-C. Yin, B.-C. Ye, Highly sensitive surface-enhanced Raman scattering detection of hexavalent chromium based on hollow sea urchin-like TiO<sub>2</sub>@Ag nanoparticle substrate, *Biosens. Bioelectron.* 87 (2017) 187–194. <https://doi.org/10.1016/j.bios.2016.08.036>
- [44] G.-Z. Zhong, Z.-B. Hu, X.-J. Tu, X.-S. Chai, G. Chen, Determination of hexavalent chromium in solid waste hypochlorite treated leachates by headspace gas chromatography, *Microchem. J.* 153 (2020) 104494. <https://doi.org/10.1016/j.microc.2019.104494>
- [45] L.E. Korshoj, A.J. Zaitouna, R.Y. Lai, Methylene Blue-Mediated Electrocatalytic Detection of Hexavalent Chromium, *Anal. Chem.* 87 (2015) 2560–2564. <https://doi.org/10.1021/acs.analchem.5b00197>
- [46] D. Spanu, D. Monticelli, G. Binda, C. Dossi, L. Rampazzi, S. Recchia, One-minute highly selective Cr(VI) determination at ultra-trace levels: An ICP-MS method based on the on-line trapping of Cr(III), *J. Hazard. Mater.* 412 (2021) 125280. <https://doi.org/10.1016/j.jhazmat.2021.125280>
- [47] H. Zhang, Y. Huang, Z. Hu, C. Tong, Z. Zhang, S. Hu, Carbon dots codoped with nitrogen and sulfur are viable fluorescent probes for chromium(VI), *Microchim. Acta.* 184 (2017) 1547–1553. <https://doi.org/10.1007/s00604-017-2132-4>
- [48] D. Tai, C. Liu, J. Liu, Facile synthesis of fluorescent carbon dots from shrimp shells and using the carbon dots to detect chromium(VI), *Spectrosc. Lett.* 52 (2019) 194–199. <https://doi.org/10.1080/00387010.2019.1607879>
- [49] L. Wang, B. Qian, H. Chen, Y. Liu, A. Liang, A novel terbium composite nanoparticles: Preparation and selective fluorescence determination of chromium(VI), *J. Lumin.* 128 (2008) 1952–1956. <https://doi.org/10.1016/j.jlumin.2008.06.005>
- [50] Y.-S. Lin, T.-C. Chiu, C.-C. Hu, Fluorescence-tunable copper nanoclusters and their application in hexavalent chromium sensing, *RSC Adv.* 9 (2019) 9228–9234. <https://doi.org/10.1039/C9RA00916G>
- [51] L.M.T. Phan, S.H. Baek, T.P. Nguyen, K.Y. Park, S. Ha, R. Rafique, S.K. Kailasa, T.J. Park, Synthesis of fluorescent silicon quantum dots for ultra-rapid and selective sensing of Cr(VI) ion and biomonitoring of cancer cells, *Materials Science and Engineering: C.* 93 (2018) 429–436. <https://doi.org/10.1016/j.msec.2018.08.024>

- [52] H. Huang, J.-J. Lv, D.-L. Zhou, N. Bao, Y. Xu, A.-J. Wang, J.-J. Feng, One-pot green synthesis of nitrogen-doped carbon nanoparticles as fluorescent probes for mercury ions, *RSC Adv.* 3 (2013) 21691–21696. <https://doi.org/10.1039/C3RA43452D>
- [53] Y. Guo, L. Zhang, F. Cao, Y. Leng, Thermal treatment of hair for the synthesis of sustainable carbon quantum dots and the applications for sensing Hg<sup>2+</sup>, *Sci Rep.* 6 (2016) 35795. <https://doi.org/10.1038/srep35795>
- [54] X. Qin, W. Lu, A.M. Asiri, A.O. Al-Youbi, X. Sun, Microwave-assisted rapid green synthesis of photoluminescent carbon nanodots from flour and their applications for sensitive and selective detection of mercury(II) ions, *Sens. Actuators, B.* 184 (2013) 156–162. <https://doi.org/10.1016/j.snb.2013.04.079>
- [55] C. Wang, D. Sun, K. Zhuo, H. Zhang, J. Wang, Simple and green synthesis of nitrogen-, sulfur-, and phosphorus-co-doped carbon dots with tunable luminescence properties and sensing application, *RSC Adv.* 4 (2014) 54060–54065. <https://doi.org/10.1039/C4RA10885J>
- [56] J. Yu, N. Song, Y.-K. Zhang, S.-X. Zhong, A.-J. Wang, J. Chen, Green preparation of carbon dots by Jinhua bergamot for sensitive and selective fluorescent detection of Hg<sup>2+</sup> and Fe<sup>3+</sup>, *Sens. Actuators, B.* 214 (2015) 29–35. <https://doi.org/10.1016/j.snb.2015.03.006>
- [57] Z. Li, Y. Ni, S. Kokot, A new fluorescent nitrogen-doped carbon dot system modified by the fluorophore-labeled ssDNA for the analysis of 6-mercaptopurine and Hg (II), *Biosens. Bioelectron.* 74 (2015) 91–97. <https://doi.org/10.1016/j.bios.2015.06.014>
- [58] D. Gu, S. Shang, Q. Yu, J. Shen, Green synthesis of nitrogen-doped carbon dots from lotus root for Hg(II) ions detection and cell imaging, *Appl. Surf. Sci.* 390 (2016) 38–42. <https://doi.org/10.1016/j.apsusc.2016.08.012>
- [59] J. Zhao, M. Huang, L. Zhang, M. Zou, D. Chen, Y. Huang, S. Zhao, Unique Approach To Develop Carbon Dot-Based Nanohybrid Near-Infrared Ratiometric Fluorescent Sensor for the Detection of Mercury Ions, *Anal. Chem.* 89 (2017) 8044–8049. <https://doi.org/10.1021/acs.analchem.7b01443>
- [60] S. Xu, Y. Liu, H. Yang, K. Zhao, J. Li, A. Deng, Fluorescent nitrogen and sulfur co-doped carbon dots from casein and their applications for

- sensitive detection of Hg<sup>2+</sup> and biothiols and cellular imaging, *Anal. Chim. Acta.* 964 (2017) 150–160.  
<https://doi.org/10.1016/j.aca.2017.01.037>
- [61] S.A.A. Vandarkuzhali, S. Natarajan, S. Jeyabalan, G. Sivaraman, S. Singaravadivel, S. Muthusubramanian, B. Viswanathan, Pineapple Peel-Derived Carbon Dots: Applications as Sensor, Molecular Keypad Lock, and Memory Device, *ACS Omega.* 3 (2018) 12584–12592.  
<https://doi.org/10.1021/acsomega.8b01146>
- [62] D. Bano, V. Kumar, V.K. Singh, S.H. Hasan, Green synthesis of fluorescent carbon quantum dots for the detection of mercury(II) and glutathione, *New J. Chem.* 42 (2018) 5814–5821.  
<https://doi.org/10.1039/C8NJ00432C>
- [63] Z. Liu, W. Jin, F. Wang, T. Li, J. Nie, W. Xiao, Q. Zhang, Y. Zhang, Ratiometric fluorescent sensing of Pb<sup>2+</sup> and Hg<sup>2+</sup> with two types of carbon dot nanohybrids synthesised from the same biomass, *Sens. Actuators, B.* 296 (2019) 126698.  
<https://doi.org/10.1016/j.snb.2019.126698>
- [64] P.B. Tchounwou, C.G. Yedjou, A.K. Patlolla, D.J. Sutton, Heavy Metal Toxicity and the Environment, in: A. Luch (Ed.), *Molecular, Clinical and Environmental Toxicology: Volume 3: Environmental Toxicology*, Springer, Basel, 2012: pp. 133–164. [https://doi.org/10.1007/978-3-7643-8340-4\\_6](https://doi.org/10.1007/978-3-7643-8340-4_6)
- [65] S.D. Torres Landa, N.K. Reddy Bogireddy, I. Kaur, V. Batra, V. Agarwal, Heavy metal ion detection using green precursor derived carbon dots, *IScience.* 25 (2022) 103816.  
<https://doi.org/10.1016/j.isci.2022.103816>
- [66] H. Abadin, A. Ashizawa, Y.-W. Stevens, F. Lladós, G. Diamond, G. Sage, M. Citra, A. Quinones, S.J. Bosch, S.G. Swarts, *Toxicological Profile for Lead*, Agency for Toxic Substances and Disease Registry (US), Atlanta (GA), 2007.  
<http://www.ncbi.nlm.nih.gov/books/NBK158766/>
- [67] Y.-Y. Chen, H.-T. Chang, Y.-C. Shiang, Y.-L. Hung, C.-K. Chiang, C.-C. Huang, Colorimetric Assay for Lead Ions Based on the Leaching of Gold Nanoparticles, *Anal. Chem.* 81 (2009) 9433–9439.  
<https://doi.org/10.1021/ac9018268>

- [68] A. Gupta, N.C. Verma, S. Khan, S. Tiwari, A. Chaudhary, C.K. Nandi, Paper strip based and live cell ultrasensitive lead sensor using carbon dots synthesised from biological media, *Sens. Actuators, B.* 232 (2016) 107–114. <https://doi.org/10.1016/j.snb.2016.03.110>
- [69] C. Hou, Y. Xiong, N. Fu, C.C. Jacquot, T.C. Squier, H. Cao, Turn-on ratiometric fluorescent sensor for Pb<sup>2+</sup> detection, *Tetrahedron Lett.* 52 (2011) 2692–2696. <https://doi.org/10.1016/j.tetlet.2011.03.075>
- [70] A. Kumar, A.R. Chowdhuri, D. Laha, T.K. Mahto, P. Karmakar, S.K. Sahu, Green synthesis of carbon dots from *Ocimum sanctum* for effective fluorescent sensing of Pb<sup>2+</sup> ions and live cell imaging, *Sens. Actuators, B.* 242 (2017) 679–686. <https://doi.org/10.1016/j.snb.2016.11.109>
- [71] R. Bandi, R. Dadigala, B.R. Gangapuram, V. Guttena, Green synthesis of highly fluorescent nitrogen – Doped carbon dots from *Lantana camara* berries for effective detection of lead(II) and bioimaging, *J. Photochem. Photobiol., B.* 178 (2018) 330–338. <https://doi.org/10.1016/j.jphotobiol.2017.11.010>
- [72] N. Johri, G. Jacquillet, R. Unwin, Heavy metal poisoning: the effects of cadmium on the kidney, *Biometals.* 23 (2010) 783–792. <https://doi.org/10.1007/s10534-010-9328-y>
- [73] S.C. Pandey, A. Kumar, S.K. Sahu, Single Step Green Synthesis of Carbon Dots from *Murraya koenigii* leaves; A Unique Turn-off Fluorescent contrivance for Selective Sensing of Cd (II) ion, *J. Photochem. Photobiol., A.* 400 (2020) 112620. <https://doi.org/10.1016/j.jphotochem.2020.112620>
- [74] P. Chauhan, S. Dogra, S. Chaudhary, R. Kumar, Usage of coconut coir for sustainable production of high-valued carbon dots with discriminatory sensing aptitude toward metal ions, *Mater. Today Chem.* 16 (2020) 100247. <https://doi.org/10.1016/j.mtchem.2020.100247>
- [75] Sariga, M.K. Ayilliath Kolaprath, L. Benny, A. Varghese, A facile, green synthesis of carbon quantum dots from *Polyalthia longifolia* and its application for the selective detection of cadmium, *Dyes Pigm.* 210 (2023) 111048. <https://doi.org/10.1016/j.dyepig.2022.111048>
- [76] S. Bhatt, M. Bhatt, A. Kumar, G. Vyas, T. Gajaria, P. Paul, Green route for synthesis of multifunctional fluorescent carbon dots from *Tulsi* leaves and its application as Cr (VI) sensors, bioimaging and patterning

- agents, *Colloids and Surfaces B: Biointerfaces*. 167 (2018) 126.  
<https://doi.org/10.1016/j.colsurfb.2018.04.008>
- [77] S. Feng, Z. Gao, H. Liu, J. Huang, X. Li, Y. Yang, Feasibility of detection valence speciation of Cr(III) and Cr(VI) in environmental samples by spectrofluorimetric method with fluorescent carbon quantum dots, *Spectrochim. Acta, Part A*. 212 (2019) 286–292.  
<https://doi.org/10.1016/j.saa.2018.12.055>
- [78] K. Srinivasan, K. Subramanian, K. Murugan, K. Dinakaran, Sensitive fluorescence detection of mercury(II) in aqueous solution by the fluorescence quenching effect of MoS<sub>2</sub> with DNA functionalized carbon dots, *Analyst*. 141 (2016) 6344–6352.  
<https://doi.org/10.1039/C6AN00879H>
- [79] V. Roshni, D. Ottor, Synthesis of carbon nanoparticles using one step green approach and their application as mercuric ion sensor, *J. Lumin.* 161 (2015) 117–122. <https://doi.org/10.1016/j.jlumin.2014.12.048>
- [80] M.L. Desai, S. Jha, H. Basu, R.K. Singhal, T.-J. Park, S.K. Kailasa, Acid Oxidation of Muskmelon Fruit for the Fabrication of Carbon Dots with Specific Emission Colors for Recognition of Hg<sup>2+</sup> Ions and Cell Imaging, *ACS Omega*. 4 (2019) 19332–19340.  
<https://doi.org/10.1021/acsomega.9b02730>
- [81] J. Xu, X. Jie, F. Xie, H. Yang, W. Wei, Z. Xia, Flavonoid moiety-incorporated carbon dots for ultrasensitive and highly selective fluorescence detection and removal of Pb<sup>2+</sup>, *Nano Res.* 11 (2018) 3648–3657. <https://doi.org/10.1007/s12274-017-1931-6>
- [82] V.A. Ansi, N.K. Renuka, Table sugar derived Carbon dot – a naked eye sensor for toxic Pb<sup>2+</sup> ions, *Sens. Actuators, B*. 264 (2018) 67–75.  
<https://doi.org/10.1016/j.snb.2018.02.167>
- [83] Z.-Y. Huang, W.-Z. Wu, Z.-X. Li, Y. Wu, C.-B. Wu, J. Gao, J. Guo, Y. Chen, Y. Hu, C. Huang, Solvothermal production of tea residue derived carbon dots by the pretreatment of choline chloride/urea and its application for cadmium detection, *Ind. Crops Prod.* 184 (2022) 115085. <https://doi.org/10.1016/j.indcrop.2022.115085>
- [84] C. Sakaew, P. Sricharoen, N. Limchoowong, P. Nuengmatcha, C. Kukusamude, S. Kongsri, S. Chanthai, Green and facile synthesis of water-soluble carbon dots from ethanolic shallot extract for chromium

- ion sensing in milk, fruit juices, and wastewater samples, *RSC Adv.* 10 (2020) 20638–20645. <https://doi.org/10.1039/D0RA03101A>
- [85] G. Hu, L. Ge, Y. Li, M. Mukhtar, B. Shen, D. Yang, J. Li, Carbon dots derived from flax straw for highly sensitive and selective detections of cobalt, chromium, and ascorbic acid, *J. Colloid Interface Sci.* 579 (2020) 96–108. <https://doi.org/10.1016/j.jcis.2020.06.034>
- [86] R. V. S. Misra, M.K. Santra, D. Ootoor, One pot green synthesis of C-dots from groundnuts and its application as Cr(VI) sensor and in vitro bioimaging agent, *J. Photochem. Photobiol., A.* 373 (2019) 28–36. <https://doi.org/10.1016/j.jphotochem.2018.12.028>
- [87] C. Wang, J. Xu, R. Zhang, W. Zhao, Facile and low-energy-consumption synthesis of dual-functional carbon dots from *Cornus walteri* leaves for detection of p-nitrophenol and photocatalytic degradation of dyes, *Colloids Surf., A.* 640 (2022) 128351. <https://doi.org/10.1016/j.colsurfa.2022.128351>
- [88] A. Chatzimarkou, T.G. Chatzimitakos, A. Kasouni, L. Sygellou, A. Avgeropoulos, C.D. Stalikas, Selective FRET-based sensing of 4-nitrophenol and cell imaging capitalizing on the fluorescent properties of carbon nanodots from apple seeds, *Sens. Actuators, B.* 258 (2018) 1152–1160. <https://doi.org/10.1016/j.snb.2017.11.182>
- [89] H. Soni, P.S. Pamidimukkala, Green synthesis of N, S co-doped carbon quantum dots from triflic acid treated palm shell waste and their application in nitrophenol sensing, *Mater. Res. Bull.* 108 (2018) 250–254. <https://doi.org/10.1016/j.materresbull.2018.08.033>
- [90] M.K. Bera, S. Mohapatra, Ultrasensitive detection of glyphosate through effective photoelectron transfer between CdTe and chitosan derived carbon dot, *Colloids Surf., A.* 596 (2020) 124710. <https://doi.org/10.1016/j.colsurfa.2020.124710>
- [91] M. Zheng, C. Wang, Y. Wang, W. Wei, S. Ma, X. Sun, J. He, Green synthesis of carbon dots functionalized silver nanoparticles for the colorimetric detection of phoxim, *Talanta.* 185 (2018) 309–315. <https://doi.org/10.1016/j.talanta.2018.03.066>
- [92] J. Hou, X. Wang, S. Lan, C. Zhang, C. Hou, Q. He, D. Huo, A turn-on fluorescent sensor based on carbon dots from *Sophora japonica* leaves for the detection of glyphosate, *Anal. Methods.* 12 (2020) 4130–4138. <https://doi.org/10.1039/D0AY01241F>

- [93] H. Liu, J. Ding, K. Zhang, L. Ding, Construction of biomass carbon dots based fluorescence sensors and their applications in chemical and biological analysis, *TrAC, Trends Anal. Chem.* 118 (2019) 315–337. <https://doi.org/10.1016/j.trac.2019.05.051>
- [94] Y. Feng, D. Zhong, H. Miao, X. Yang, Carbon dots derived from rose flowers for tetracycline sensing, *Talanta*. 140 (2015) 128–133. <https://doi.org/10.1016/j.talanta.2015.03.038>
- [95] H. Miao, Y. Wang, X. Yang, Carbon dots derived from tobacco for visually distinguishing and detecting three kinds of tetracyclines, *Nanoscale*. 10 (2018) 8139–8145. <https://doi.org/10.1039/C8NR02405G>
- [96] F. Guo, Z. Zhu, Z. Zheng, Y. Jin, X. Di, Z. Xu, H. Guan, Facile synthesis of highly efficient fluorescent carbon dots for tetracycline detection, *Environ. Sci. Pollut. Res.* 27 (2020) 4520–4527. <https://doi.org/10.1007/s11356-019-06779-3>
- [97] S. Anmei, Z. Qingmei, C. Yuye, W. Yilin, Preparation of carbon quantum dots from cigarette filters and its application for fluorescence detection of Sudan I, *Anal. Chim. Acta.* 1023 (2018) 115–120. <https://doi.org/10.1016/j.aca.2018.03.024>
- [98] H. Xu, X. Yang, G. Li, C. Zhao, X. Liao, Green Synthesis of Fluorescent Carbon Dots for Selective Detection of Tartrazine in Food Samples, *J. Agric. Food Chem.* 63 (2015) 6707–6714. <https://doi.org/10.1021/acs.jafc.5b02319>
- [99] M. Ghereghlou, A.A. Esmaili, M. Darroudi, Green Synthesis of Fluorescent Carbon Dots from *Elaeagnus angustifolia* and its Application as Tartrazine Sensor, *J Fluoresc.* 31 (2021) 185–193. <https://doi.org/10.1007/s10895-020-02645-5>
- [100] Y. Qu, L. Yu, B. Zhu, F. Chai, Z. Su, Green synthesis of carbon dots by celery leaves for use as fluorescent paper sensors for the detection of nitrophenols, *New J. Chem.* 44 (2020) 1500–1507. <https://doi.org/10.1039/C9NJ05285B>
- [101] Q. Zhang, J. Liang, L. Zhao, Y. Wang, Y. Zheng, Y. Wu, L. Jiang, Synthesis of Novel Fluorescent Carbon Quantum Dots From *Rosa roxburghii* for Rapid and Highly Selective Detection of *o*-nitrophenol and Cellular Imaging, *Front. Chem.* 8 (2020) <https://www.frontiersin.org/articles/10.3389/fchem.2020.00665>

- [102] H. Wang, L. Zhang, X. Guo, W. Dong, R. Wang, S. Shuang, X. Gong, C. Dong, Comparative study of Cl,N-Cdots and N-Cdots and application for trinitrophenol and ClO<sup>-</sup> sensor and cell-imaging, *Anal. Chim. Acta.* 1091 (2019) 76–87.  
<https://doi.org/10.1016/j.aca.2019.09.019>
- [103] H. Liu, J. Ding, L. Chen, L. Ding, A novel fluorescence assay based on self-doping biomass carbon dots for rapid detection of dimethoate, *J. Photochem. Photobiol., A.* 400 (2020) 112724.  
<https://doi.org/10.1016/j.jphotochem.2020.112724>
- [104] W.-K. Li, J.-T. Feng, Z.-Q. Ma, Nitrogen, sulfur, boron and flavonoid moiety co-incorporated carbon dots for sensitive fluorescence detection of pesticides, *Carbon.* 161 (2020) 685–693.  
<https://doi.org/10.1016/j.carbon.2020.01.098>
- [105] J. Hou, G. Dong, Z. Tian, J. Lu, Q. Wang, S. Ai, M. Wang, A sensitive fluorescent sensor for selective determination of dichlorvos based on the recovered fluorescence of carbon dots-Cu(II) system, *Food Chem.* 202 (2016) 81–87. <https://doi.org/10.1016/j.foodchem.2015.11.134>
- [106] S. Chandra, D. Bano, K. Sahoo, D. Kumar, V. Kumar, P. Kumar Yadav, S. Hadi Hasan, Synthesis of fluorescent carbon quantum dots from *Jatropha* fruits and their application in fluorometric sensor for the detection of chlorpyrifos, *Microchem. J.* 172 (2022) 106953.  
<https://doi.org/10.1016/j.microc.2021.106953>
- [107] K. Wang, Q. Ji, J. Xu, H. Li, D. Zhang, X. Liu, Y. Wu, H. Fan, Highly Sensitive and Selective Detection of Amoxicillin Using Carbon Quantum Dots Derived from Beet, *J Fluoresc.* 28 (2018) 759–765.  
<https://doi.org/10.1007/s10895-018-2237-0>
- [108] J. Zhu, H. Chu, J. Shen, C. Wang, Y. Wei, Green preparation of carbon dots from plum as a ratiometric fluorescent probe for detection of doxorubicin, *Opt. Mater.* 114 (2021) 110941.  
<https://doi.org/10.1016/j.optmat.2021.110941>
- [109] H. Qi, M. Teng, M. Liu, S. Liu, J. Li, H. Yu, C. Teng, Z. Huang, H. Liu, Q. Shao, A. Umar, T. Ding, Q. Gao, Z. Guo, Biomass-derived nitrogen-doped carbon quantum dots: highly selective fluorescent probe for detecting Fe<sup>3+</sup> ions and tetracyclines, *J. Colloid Interface Sci.* 539 (2019) 332–341. <https://doi.org/10.1016/j.jcis.2018.12.047>



- [110] H. Zhang, Q. Zhou, X. Han, M. Li, J. Yuan, R. Wei, X. Zhang, M. Wu, W. Zhao, Nitrogen-doped carbon dots derived from hawthorn for the rapid determination of chlortetracycline in pork samples, *Spectrochim. Acta, Part A*. 255 (2021) 119736.  
<https://doi.org/10.1016/j.saa.2021.119736>
- [111] G. Huang, X. Chen, C. Wang, H. Zheng, Z. Huang, D. Chen, H. Xie, Photoluminescent carbon dots derived from sugarcane molasses: synthesis, properties, and applications, *RSC Adv.* 7 (2017) 47840–47847. <https://doi.org/10.1039/C7RA09002A>
- [112] D. Shukla, F.P. Pandey, P. Kumari, N. Basu, M.K. Tiwari, J. Lahiri, R.N. Kharwar, A.S. Parmar, Label-Free Fluorometric Detection of Adulterant Malachite Green Using Carbon Dots Derived from the Medicinal Plant Source *Ocimum tenuiflorum*, *ChemistrySelect.* 4 (2019) 4839–4847. <https://doi.org/10.1002/slct.201900530>
- [113] A. Vijeata, S. Chaudhary, G.R. Chaudhary, Fluorescent carbon dots from Indian Bael patra as effective sensing tool to detect perilous food colorant, *Food Chem.* 373 (2022) 131492.  
<https://doi.org/10.1016/j.foodchem.2021.131492>
- [114] T. Chatzimitakos, A. Kasouni, L. Sygellou, A. Avgeropoulos, A. Troganis, C. Stalikas, Two of a kind but different: Luminescent carbon quantum dots from Citrus peels for iron and tartrazine sensing and cell imaging, *Talanta.* 175 (2017) 305–312.  
<https://doi.org/10.1016/j.talanta.2017.07.053>
- [115] A. Chunduri, A. Kurdekar, S. Patnaik, B. Dev, T. Rattan, V. Kamiseti, Carbon Quantum Dots from Coconut Husk: Evaluation for Antioxidant and Cytotoxic Activity, *Mater. Focus.* 5 (2016) 55–61.  
<https://doi.org/10.1166/mat.2016.1289>
- [116] S. Rodríguez-Varillas, T. Fontanil, Á.J. Obaya, A. Fernández-González, C. Murru, R. Badía-Laíño, Biocompatibility and Antioxidant Capabilities of Carbon Dots Obtained from Tomato (*Solanum lycopersicum*), *Appl. Sci.* 12 (2022) 773.  
<https://doi.org/10.3390/app12020773>
- [117] S. Roy, P. Ezati, J.-W. Rhim, R. Molaei, Preparation of turmeric-derived sulfur-functionalized carbon dots: antibacterial and antioxidant activity, *J Mater Sci.* 57 (2022) 2941–2952.  
<https://doi.org/10.1007/s10853-021-06804-2>

- [118] D. Bhattacharya, V. Kumar, G. Packirisamy, Biocompatible carbon nanodots from red onion peels for anti-oxidative and bioimaging applications, *Mater. Express*. 11 (2021) 1958–1965. <https://doi.org/10.1166/mex.2021.2101>
- [119] Y. Guo, T. Li, L. Xie, X. Tong, C. Tang, S. Shi, Red pitaya peels-based carbon dots for real-time fluorometric and colorimetric assay of Au<sup>3+</sup>, cellular imaging, and antioxidant activity., *Anal. Bioanal. Chem.* 413 (2021) 935–944. <https://doi.org/10.1007/s00216-020-03049-x>
- [120] S. Rajamanikandan, M. Biruntha, G. Ramalingam, Blue Emissive Carbon Quantum Dots (CQDs) from Biowaste Peels and Its Antioxidant Activity, *J Clust Sci.* 33 (2022) 1045–1053. <https://doi.org/10.1007/s10876-021-02029-0>
- [121] Y.-Y. Chen, W.-P. Jiang, H.-L. Chen, H.-C. Huang, G.-J. Huang, H.-M. Chiang, C.-C. Chang, C.-L. Huang, T.-Y. Juang, Cytotoxicity and cell imaging of six types of carbon nanodots prepared through carbonization and hydrothermal processing of natural plant materials, *RSC Adv.* 11 (2021) 16661–16674. <https://doi.org/10.1039/D1RA01318A>
- [122] S. Mishra, K. das, S. Chatterjee, P. Sahoo, S. Kundu, M. Pal, A. Bhaumik, C.K. Ghosh, Facile and Green Synthesis of Novel Fluorescent Carbon Quantum Dots and Their Silver Heterostructure: An In Vitro Anticancer Activity and Imaging on Colorectal Carcinoma, *ACS Omega.* 8 (2023) 4566–4577. <https://doi.org/10.1021/acsomega.2c04964>
- [123] E. Arkan, A. Barati, M. Rahmanpanah, L. Hosseinzadeh, S. Moradi, M. Hajialyani, Green Synthesis of Carbon Dots Derived from Walnut Oil and an Investigation of Their Cytotoxic and Apoptogenic Activities toward Cancer Cells, *Adv Pharm Bull.* 8 (2018) 149–155. <https://doi.org/10.15171/apb.2018.018>
- [124] A. Paul, M. Kurian, Facile synthesis of nitrogen doped carbon dots from waste biomass: Potential optical and biomedical applications, *Cleaner Engineering and Technology.* 3 (2021) 100103. <https://doi.org/10.1016/j.clet.2021.100103>
- [125] B. Sasikumar, Genetic resources of Curcuma: diversity, characterisation and utilization, *Plant Genetic Resources.* 3 (2005) 230–251. <https://doi.org/10.1079/PGR200574>

- [126] M. R, R. Kavitha, Phytochemical and pharmacological properties of *Curcuma amada*: A Review, *Int. J. Res. Pharm. Sci.* 11 (2020) 3546–3555. <https://doi.org/10.26452/ijrps.v11i3.2510>
- [127] K. Padmapriya, A. Dutta, S. Chaudhuri, D. Dutta, Microwave assisted extraction of mangiferin from *Curcuma amada*, *3 Biotech.* 2 (2012) 27–30. <https://doi.org/10.1007/s13205-011-0023-7>
- [128] D. Prema, M. Kamaraj, S. Achiraman, R. Udayakumar, In vitro antioxidant and cytotoxicity studies of *Curcuma amada* Roxb. (Mango ginger), *International Journal of Scientific and Research Publications.* 4 (2014). <https://www.ijsrp.org/research-paper-0414/ijsrp-p2893.pdf>
- [129] T.S. Singh, I.T. Phucho, T.B. Singh, Phytochemical Evaluation, Determination of Total Terpenoid Content On The Rhizome Of *Curcuma Amada*, *World J. Pharm. Res.* 4 (2015) 2286–2294. <https://www.semanticscholar.org/paper/8bf0a7ce0c484491a1621ab3435cc9523a4ac962>
- [130] D. Prakash, S. Suri, G. Upadhyay, B.N. Singh, Total phenol, antioxidant and free radical scavenging activities of some medicinal plants, *Int. J. Food Sci. Nutr.* 58 (2007) 18–28. <https://doi.org/10.1080/09637480601093269>
- [131] H.Chandarana, S. Baluja, S. Chanda, Comparison of Antibacterial Activities of Selected Species of Zingiberaceae Family and Some Synthetic Compounds, *Turk. J. Biol.* 29 (2005) 83–97. <https://journals.tubitak.gov.tr/biology/vol29/iss2/2>
- [132] G. Singh, O.P. Singh, S. Maurya, Chemical and biocidal investigations on essential oils of some Indian *Curcuma* species, *Prog. Cryst. Growth Charact. Mater.* 45 (2002) 75–81. [https://doi.org/10.1016/S0960-8974\(02\)00030-X](https://doi.org/10.1016/S0960-8974(02)00030-X)
- [133] A.M. Mujumdar, D.G. Naik, C.N. Dandge, H.M. Puntambekar, Antiinflammatory activity of *Curcuma amada* Roxb. In albino rats, *Indian J. Pharmacol.* 32 (2000) 375. <https://www.ijp-online.com/article.asp?issn=02537613;year=2000;volume=32;issue=6;page=375;epage=377;aulast=Mujumdar;type=0>
- [134] R.S. Policegoudra, K. Rehna, L. Jaganmohan Rao, S.M. Aradhya, Antimicrobial, antioxidant, cytotoxicity and platelet aggregation inhibitory activity of a novel molecule isolated and characterized from

- mango ginger (*Curcuma amada* Roxb.) rhizome, *J Biosci.* 35 (2010) 231–240. <https://doi.org/10.1007/s12038-010-0027-1>
- [135] R.S. Policegoudra, S.M. Aradhya, L. Singh, Mango ginger (*Curcuma amada* Roxb.) – A promising spice for phytochemicals and biological activities, *J Biosci.* 36 (2011) 739–748. <https://doi.org/10.1007/s12038-011-9106-1>
- [136] P.G. Bhat, R.T. Jacob, T.N. Pattabiraman, Enzyme inhibitors from plants: Enterokinase inhibitors in tubers and seeds, *J Biosci.* 3 (1981) 371–377. <https://doi.org/10.1007/BF02702624>
- [137] A.M. Mujumdar, D.G. Naik, A.V. Misar, H.M. Puntambekar, C.N. Dandge, CNS Depressant and Analgesic Activity of a Fraction Isolated from an Ethanol Extract of *Curcuma amada* Rhizomes, *Pharma. Biol.* 42 (2004) 542–546. <https://doi.org/10.3109/13880200490893429>
- [138] S. Singh, J.K. Kumar, D. Saikia, K. Shanker, J.P. Thakur, A.S. Negi, S. Banerjee, A bioactive labdane diterpenoid from *Curcuma amada* and its semisynthetic analogues as antitubercular agents, *Eur. J. Med. Chem.* 45 (2010) 4379–4382. <https://doi.org/10.1016/j.ejmech.2010.06.006>
- [139] A.V. Krishnaraju, T.V.N. Rao, D. Sundararaju, M. Vanisree, H.-S. Tsay, G.V. Subbaraju, Biological Screening of Medicinal Plants Collected from Eastern Ghats of India Using *Artemia salina* (Brine Shrimp Test), *Int. J. Appl. Sci. Eng.* 4 (2006) 115–125. [https://doi.org/10.6703/IJASE.2006.4\(2\).115](https://doi.org/10.6703/IJASE.2006.4(2).115)
- [140] M.R. Srinivasan, N. Chandrasekhara, Effect of mango ginger [*Curcuma amada* Roxb.] on triton WR-1339 induced-hyperlipidemia and plasma lipases activity in the rat, *Nutr. Res.* 13 (1993) 1183–1190. [https://doi.org/10.1016/S0271-5317\(05\)80742-0](https://doi.org/10.1016/S0271-5317(05)80742-0)
- [141] D. Singh, A.K. Singh, Repellent and Insecticidal Properties of Essential Oils Against Housefly, *Musca Domestica* L., *Int J Trop Insect Sci.* 12 (1991) 487–491. <https://doi.org/10.1017/S1742758400011401>
- [142] C. Ramachandran, I.V. Lollett, E. Escalon, K.-W. Quirin, S.J. Melnick, Anticancer Potential and Mechanism of Action of Mango Ginger (*Curcuma amada* Roxb.) Supercritical CO<sub>2</sub> Extract in Human Glioblastoma Cells, *J Evid Based Complementary Altern Med.* 20 (2015) 109–119. <https://doi.org/10.1177/2156587214563731>

- [143] L.S. Nissankara Rao, E.K. Kilari, P.K. Kola, Protective effect of Curcuma amada acetone extract against high-fat and high-sugar diet-induced obesity and memory impairment, *Nutr. Neurosci.* 24 (2021) 212–225. <https://doi.org/10.1080/1028415X.2019.1616436>
- [144] A. Narayanankutty, A. Sasidharan, J.T. Job, R. Rajagopal, A. Alfarhan, Y.O. Kim, H.-J. Kim, Mango ginger (*Curcuma amada* Roxb.) rhizome essential oils as source of environmental friendly biocides: Comparison of the chemical composition, antibacterial, insecticidal and larvicidal properties of essential oils extracted by different methods, *Environ. Res.* 202 (2021) 111718. <https://doi.org/10.1016/j.envres.2021.111718>
- [145] B. Muchtaromah, D. Wahyudi, M. Ahmad, A. Ansori, R. Annisa, L. Hanifah, Chitosan-Tripolyphosphate Nanoparticles of Mango Ginger (*Curcuma mangga*) Extract: Phytochemical Screening, Formulation, Characterisation, and Antioxidant Activity, *Pharmacogn. J.* 13 (2021) 1065–1071. <https://doi.org/10.5530/pj.2021.13.138>
- [146] S. Menon K, Phytochemical analysis, antioxidant and antimicrobial potential of *Citrus medica* and *Citrus pennivesiculata*, 2020. [https://www.researchgate.net/publication/344364895\\_Phytochemical\\_analysis\\_antioxidant\\_and\\_antimicrobial\\_potential\\_of\\_Citrus\\_medica\\_and\\_Citrus\\_pennivesiculata](https://www.researchgate.net/publication/344364895_Phytochemical_analysis_antioxidant_and_antimicrobial_potential_of_Citrus_medica_and_Citrus_pennivesiculata)
- [147] M. Garg, S.K. Chaudhary, S. Kumari, A. Goyal, Phytochemical, Biological and Traditional Claims on *Averrhoa bilimbi*: An Overview, *Indian J. Pharm. Sci.* 84 (2022) 532–542. <https://doi.org/10.36468/pharmaceutical-sciences.947>
- [148] A.M. Alhassan, Q.U. Ahmed, *Averrhoa bilimbi* Linn.: A review of its ethnomedicinal uses, phytochemistry, and pharmacology, *J. Pharm. BioAllied Sci.* 8 (2016) 265. <https://doi.org/10.4103/0975-7406.199342>
- [149] M. Hasanuzzaman, M.R. Ali, M. Hossain, S. Kuri, M.S. Islam, Evaluation of total phenolic content, free radical scavenging activity and phytochemical screening of different extracts of *Averrhoa bilimbi* (fruits), *Int. Curr. Pharm. J.* 2 (2013) 92–96. <https://doi.org/10.3329/icpj.v2i4.14058>
- [150] A.G. Patil, S.P. Koli, D.A. Patil, Pharmacognostical standardization and HPTLC fingerprint of *Averrhoa bilimbi* (L.) fruits, *J. Pharm. Res.* 6 (2013) 145–150. <https://doi.org/10.1016/j.jopr.2012.11.030>

- [151] K.C. Wong, S.N. Wong, Volatile Constituents of *Averrhoa bilimbi* L. Fruit, *J. Essent. Oil Res.* 7 (1995) 691–693.  
<https://doi.org/10.1080/10412905.1995.9700533>
- [152] J.A. Pino, R. Marbot, A. Bello, Volatile Components of *Averrhoa bilimbi* L. Fruit Grown in Cuba, *J. Essent. Oil Res.* 16 (2004) 241–242.  
<https://doi.org/10.1080/10412905.2004.9698710>
- [153] Z.A. Zakaria, H. Zaiton, E.F.P. Henie, A.M. Jais, E.N.H. Zainuddin, In vitro antibacterial activity of *Averrhoa bilimbi* L. leaves and fruits extracts, *Int J Trop Med.* 2 (2007) 96–100.  
[https://www.researchgate.net/publication/285678620\\_In\\_vitro\\_antibacterial\\_activity\\_of\\_Averrhoa\\_bilimbi\\_L\\_leaves\\_and\\_fruits\\_extract](https://www.researchgate.net/publication/285678620_In_vitro_antibacterial_activity_of_Averrhoa_bilimbi_L_leaves_and_fruits_extract)
- [154] S. Mohamad, N.M. Zin, H.A. Wahab, P. Ibrahim, S.F. Sulaiman, A.S.M. Zahariluddin, S.S.Md. Noor, Antituberculosis potential of some ethnobotanically selected Malaysian plants, *J. Ethnopharmacol.* 133 (2011) 1021–1026. <https://doi.org/10.1016/j.jep.2010.11.037>
- [155] M.N. Wan Norhana, M.N.A. A., S.E. Poole, H.C. Deeth, G.A. Dykes, Effects of bilimbi (*Averrhoa bilimbi* L.) and tamarind (*Tamarindus indica* L.) juice on *Listeria monocytogenes* Scott A and *Salmonella Typhimurium* ATCC 14028 and the sensory properties of raw shrimps, *Int. J. Food Microbiol.* 136 (2009) 88–94.  
<https://doi.org/10.1016/j.ijfoodmicro.2009.09.011>
- [156] F. Abas, N.H. Lajis, D.A. Israf, S. Khozirah, Y. Umi Kalsom, Antioxidant and nitric oxide inhibition activities of selected Malay traditional vegetables, *F.* 95 (2006) 566–573.  
<https://doi.org/10.1016/j.foodchem.2005.01.034>
- [157] S. Sabiha, S. Chowdhury, G.M. Uddin, N. Mumtahana, M. Hossain, R. Hasan, In vitro antioxidant and cytotoxic potential of hydromethanolic extract of *Averrhoa bilimbi* L. fruits, *J. Pharm. Sci. Res.* 3 (2012) 2263–2268.  
[https://www.researchgate.net/publication/236635051\\_Invitro\\_antioxidant\\_and\\_cytotoxic\\_potential\\_of\\_hydromethanolic\\_extract\\_of\\_Averrhoa\\_bilimbi\\_L\\_fruits](https://www.researchgate.net/publication/236635051_Invitro_antioxidant_and_cytotoxic_potential_of_hydromethanolic_extract_of_Averrhoa_bilimbi_L_fruits)
- [158] S.N. Thamizh, P.S. Santhi, Y.R. Sanjayakumar, T.N. Venugopalan, K.G. Vasanthakumar, G.K. Swamy, Hepatoprotective activity of *Averrhoa bilimbi* fruit in acetaminophen induced hepatotoxicity in Wistar albino rats., *J. Chem. Pharm. Res.* 7 (2015) 535–540.  
<https://www.semanticscholar.org/paper/Hepatoprotective-activity->

of-Averrhoa-bilimbi-fruit-  
Selvam/f2355f8336212f5d3e498bd60114d64d6b86c864

- [159] M.R. Ali, M. Hossain, J.F. Runa, M. Hasanuzzaman, Preliminary cytotoxic activity of different extracts of *Averrhoa bilimbi* (fruits), *Int. Curr. Pharm. J.* 2 (2013) 83–84. <https://doi.org/10.3329/icpj.v2i3.13634>
- [160] A. Ramjan, M. Hossain, J.F. Runa, H. Md, I. Mahmodul, Evaluation of thrombolytic potential of three medicinal plants available in Bangladesh, as a potent source of thrombolytic compounds, *Avicenna J Phytomed.* 4 (2014) 430–436. <https://www.ncbi.nlm.nih.gov/pmc/articles/PMC4224957/>
- [161] R.S.R. Isaac, G. Sakthivel, C. Murthy, Green Synthesis of Gold and Silver Nanoparticles Using *Averrhoa bilimbi* Fruit Extract, *J. Nanotechnol.* 2013 (2013) e906592. <https://doi.org/10.1155/2013/906592>
- [162] R. Ramanarayanan, N.M. Bhabhina, M.V. Dharsana, C.V. Nivedita, S. Sindhu, Green synthesis of zinc oxide nanoparticles using extract of *Averrhoa bilimbi*(L) and their photoelectrode applications, *Mater. Today: Proc.* 5 (2018) 16472–16477. <https://doi.org/10.1016/j.matpr.2018.05.150>
- [163] T. Sutjaritvorakul, S. Chutipaijit, Biological synthesis and characterisation of lead oxide nanoparticles using *Averrhoa bilimbi* Linn. aqueous extract, *AIP Conf. Proc.* 2279 (2020) 130001. <https://doi.org/10.1063/5.0026158>
- [164] S.B. Rajput, M.B. Tonge, S.M. Karuppayil, An overview on traditional uses and pharmacological profile of *Acorus calamus* Linn. (Sweet flag) and other *Acorus* species, *Phytomedicine.* 21 (2014) 268–276. <https://doi.org/10.1016/j.phymed.2013.09.020>
- [165] R.V. Bhagwat, D.B. Boralkar, R.D. Chavhan, Remediation capabilities of pilot-scale wetlands planted with *Typha aungstifolia* and *Acorus calamus* to treat landfill leachate, *J Ecology Environ.* 42 (2018) 23. <https://doi.org/10.1186/s41610-018-0085-0>
- [166] B.K. Das, A.V. Swamy, B.C. Koti, P.C. Gadad, Experimental evidence for use of *Acorus calamus* (asarone) for cancer chemoprevention, *Heliyon.* 5 (2019) e01585. <https://doi.org/10.1016/j.heliyon.2019.e01585>

- [167] K.R. Kirtikar, B.D. Basu, *Indian Medicinal Plants.*, Indian Medicinal Plants. (1918).  
[https://www.scirp.org/\(S\(i43dyn45teexjx455qlt3d2q\)\)/reference/ReferencesPapers.aspx?ReferenceID=1712751](https://www.scirp.org/(S(i43dyn45teexjx455qlt3d2q))/reference/ReferencesPapers.aspx?ReferenceID=1712751)
- [168] R. Singh, P. Sharma, R. Malviya, Pharmacological Properties and Ayurvedic Value of Indian Buch Plant (*Acorus calamus*): A Short Review, *J. Biol. Res.* 5 (2011) 145–154. <https://www.researchgate.net/publication/235989568>
- [169] A. Muthuraman, N. Singh, Acute and sub-acute oral toxicity profile of *Acorus calamus* (Sweet flag) in rodents, *Asian Pac. J. Trop. Biomed.* 2 (2012) S1017–S1023. [https://doi.org/10.1016/S2221-1691\(12\)60354-2](https://doi.org/10.1016/S2221-1691(12)60354-2)
- [170] V. Pandey, N. Jose, H. Subhash, CNS Activity of Methanol and Acetone Extracts of *Acorus calamus* Leaves in Mice, *J. Pharmacol. Toxicol.* 4 (n.d.) 79–86. <https://doi.org/10.3923/jpt.2009.79.86>
- [171] D.B. R, K. Rajamani, K. Kumanan, *Acorus calamus*: An overview, *J. Med. Plants Res.* 4 (2010).
- [172] T.J. Motley, The ethnobotany of sweet flag, *acorus Calamus* (Araceae), *Econ Bot.* 48 (1994) 397–412. <https://doi.org/10.1007/BF02862235>
- [173] P.K. Mukherjee, V. Kumar, M. Mal, P.J. Houghton, In vitro Acetylcholinesterase Inhibitory Activity of the Essential Oil from *Acorus calamus* and its Main Constituents, *Planta Med.* 73 (2007) 283–285. <https://doi.org/10.1055/s-2007-967114>
- [174] S. Halder, U. Anand, S. Nandy, P. Oleksak, S. Qusti, E.M. Alshammari, G. El-Saber Batiha, E.P. Koshy, A. Dey, Herbal drugs and natural bioactive products as potential therapeutics: A review on pro-cognitives and brain boosters perspectives, *Saudi Pharm J.* 29 (2021) 879–907. <https://doi.org/10.1016/j.jsps.2021.07.003>
- [175] A. Daniel, R. Ambalavanan, E.P. Sabina, S. Devi, Evaluation of analgesic, antipyretic and ulcerogenic activities of *Acorus calamus* rhizome extract in Swiss Aalbino mice, *Res. J. Pharm., Biol. Chem. Sci.* 5 (2014) 503–507. <https://www.researchgate.net/publication/289189637>
- [176] B.C. Bose, R. Vijayvargiya, A.Q. Saifi, S.K. Sharma, Some Aspects of Chemical and Pharmacological Studies of *Acorus calamus* Linn. \*\*Received June 15, 1959, from the Department of Pharmacology, M. G. M. Medical College, Indore, India., *J. Am.*



- Pharm. Assoc., Sci. Ed. 49 (1960) 32–34.  
<https://doi.org/10.1002/jps.3030490110>
- [177] A.J. Shah, A.H. Gilani, Aqueous-methanolic extract of sweet flag (*Acorus calamus*) possesses cardiac depressant and endothelial-derived hyperpolarizing factor-mediated coronary vasodilator effects, *J Nat Med.* 66 (2012) 119–126. <https://doi.org/10.1007/s11418-011-0561-7>
- [178] R.S. Parab, S.A. Mengi, Hypolipidemic activity of *Acorus calamus* L. in rats, *Fitoterapia.* 73 (2002) 451–455. [https://doi.org/10.1016/S0367-326X\(02\)00174-0](https://doi.org/10.1016/S0367-326X(02)00174-0)
- [179] S. Mehrotra, K.P. Mishra, R. Maurya, R.C. Srimal, V.S. Yadav, R. Pandey, V.K. Singh, Anticellular and immunosuppressive properties of ethanolic extract of *Acorus calamus* rhizome, *Int. Immunopharmacol.* 3 (2003) 53–61. [https://doi.org/10.1016/S1567-5769\(02\)00212-6](https://doi.org/10.1016/S1567-5769(02)00212-6)
- [180] P.K. Shukla, V.K. Khanna, M.M. Ali, R. Maurya, M.Y. Khan, R.C. Srimal, Neuroprotective effect of *Acorus calamus* against middle cerebral artery occlusion–induced ischaemia in rat, *Hum Exp Toxicol.* 25 (2006) 187–194.  
<https://doi.org/10.1191/0960327106ht613oa>
- [181] F.G. Shoba, M. Thomas, Study of antidiarrhoeal activity of four medicinal plants in castor-oil induced diarrhoea, *J. Ethnopharmacol.* 76 (2001) 73–76. [https://doi.org/10.1016/S0378-8741\(00\)00379-2](https://doi.org/10.1016/S0378-8741(00)00379-2)
- [182] P. Souwalak, P. Nongyao, R. Vatcharin, O. Metta, Antimicrobial activities of the crude methanol extract of *Acorus calamus* Linn, *Songklanakarin J. Sci. Technol.* 26 (2005). <https://www.thaiscience.info/journals/Article/SONG/10986964.pdf>
- [183] S.B. Rajput, S.M. Karuppaiyl,  $\beta$ -Asarone, an active principle of *Acorus calamus* rhizome, inhibits morphogenesis, biofilm formation and ergosterol biosynthesis in *Candida albicans*, *Phytomedicine.* 20 (2013) 139–142. <https://doi.org/10.1016/j.phymed.2012.09.029>
- [184] J.S. Bains, V. Dhuna, J. Singh, S.S. Kamboj, K.K. Nijjar, J.N. Agrewala, Novel lectins from rhizomes of two *Acorus* species with mitogenic activity and inhibitory potential towards murine cancer cell lines, *Int. Immunopharmacol.* 5 (2005) 1470–1478.  
<https://doi.org/10.1016/j.intimp.2005.04.004>

- [185] S. Gaidhani, G. Lavekar, A.S. Juvekar, S. Sen, A. Singh, S. Kumari, In-vitro anticancer activity of standard extracts used in ayurveda, *Pharmacogn. Mag.* 5 (2009) 425–429. [https://www.researchgate.net/publication/288520102\\_In-vitro\\_anticancer\\_activity\\_of\\_standard\\_extract\\_used\\_in\\_ayurveda](https://www.researchgate.net/publication/288520102_In-vitro_anticancer_activity_of_standard_extract_used_in_ayurveda)
- [186] H.-S. Wu, D.-F. Zhu, C.-X. Zhou, C.-R. Feng, Y.-J. Lou, B. Yang, Q.-J. He, Insulin sensitizing activity of ethyl acetate fraction of *Acorus calamus* L. in vitro and in vivo, *J Ethnopharmacol.* 123 (2009) 288–292. <https://doi.org/10.1016/j.jep.2009.03.004>
- [187] RM. Ganesan, H. Gurumallesh Prabu, Synthesis of gold nanoparticles using herbal *Acorus calamus* rhizome extract and coating on cotton fabric for antibacterial and UV blocking applications, *Arabian J. Chem.* 12 (2019) 2166–2174. <https://doi.org/10.1016/j.arabjc.2014.12.017>
- [188] C. Sudhakar, K. Selvam, M. Govarthanam, B. Senthilkumar, A. Sengottaiyan, M. Stalin, T. Selvankumar, *Acorus calamus* rhizome extract mediated biosynthesis of silver nanoparticles and their bactericidal activity against human pathogens, *J. Genet. Eng. Biotechnol.* 13 (2015) 93–99. <https://doi.org/10.1016/j.jgeb.2015.10.003>
- [189] P. Biswas, M. Ghorai, T. Mishra, A.V. Gopalakrishnan, D. Roy, A.B. Mane, A. Mundhra, N. Das, V.M. Mohture, M.T. Patil, Md.H. Rahman, N.K. Jha, G.E.-S. Batiha, S.C. Saha, M.S. Shekhawat, Radha, M. Kumar, D.K. Pandey, A. Dey, *Piper longum* L.: A comprehensive review on traditional uses, phytochemistry, pharmacology, and health-promoting activities, *Phytother. Res.* 36 (2022) 4425–4476. <https://doi.org/10.1002/ptr.7649>
- [190] K.R. Kirtikar, B.D. Basu, *Indian Medicinal Plants.*, Indian Medicinal Plants. (1918). <https://www.cabdirect.org/cabdirect/abstract/19202900465>.
- [191] S. Kumar, J. Kamboj, Suman, S. Sharma, Overview for Various Aspects of the Health Benefits of *Piper Longum* Linn. Fruit, *JAMS.* 4 (2011) 134–140. [https://doi.org/10.1016/S2005-2901\(11\)60020-4](https://doi.org/10.1016/S2005-2901(11)60020-4)
- [192] P. Srinivasa Reddy, K. Jamil, P. Madhusudhan, G. Anjani, B. Das, Antibacterial Activity of Isolates from *Piper longum* and *Taxus baccata*, *Pharm. Biol.* 39 (2001) 236–238. <https://doi.org/10.1076/phbi.39.3.236.5926>

- [193] M. Iwashita, M. Saito, Y. Yamaguchi, R. Takagaki, N. Nakahata, Inhibitory Effect of Ethanol Extract of *Piper longum* L. on Rabbit Platelet Aggregation through Antagonizing Thromboxane A<sub>2</sub> Receptor, *Biol. Pharm. Bull.* 30 (2007) 1221–1225. <https://doi.org/10.1248/bpb.30.1221>
- [194] S.A. Lee, J.S. Hwang, X.H. Han, C. Lee, M.H. Lee, S.G. Choe, S.S. Hong, D. Lee, M.K. Lee, B.Y. Hwang, Methylpiperate derivatives from *Piper longum* and their inhibition of monoamine oxidase, *Arch. Pharm. Res.* 31 (2008) 679–683. <https://doi.org/10.1007/s12272-001-1212-7>
- [195] Y.-C. Yang, S.-G. Lee, H.-K. Lee, M.-K. Kim, S.-H. Lee, H.-S. Lee, A Piperidine Amide Extracted from *Piper longum* L. Fruit Shows Activity against *Aedes aegypti* Mosquito Larvae, *J. Agric. Food Chem.* 50 (2002) 3765–3767. <https://doi.org/10.1021/jf0111708f>
- [196] S. Kumar, P. Arya, C. Mukherjee, B.K. Singh, N. Singh, V.S. Parmar, A.K. Prasad, B. Ghosh, Novel Aromatic Ester from *Piper longum* and Its Analogues Inhibit Expression of Cell Adhesion Molecules on Endothelial Cells, *Biochemistry.* 44 (2005) 15944–15952. <https://doi.org/10.1021/bi050941u>
- [197] S.-E. Lee, B.-S. Park, M.-K. Kim, W.-S. Choi, H.-T. Kim, K.-Y. Cho, S.-G. Lee, H.-S. Lee, Fungicidal activity of piperonaline, a piperidine alkaloid derived from long pepper, *Piper longum* L., against phytopathogenic fungi, *Crop Prot.* 20 (2001) 523–528. [https://doi.org/10.1016/S0261-2194\(00\)00172-1](https://doi.org/10.1016/S0261-2194(00)00172-1)
- [198] V. Lakshmi, R. Kumar, S.K. Agarwal, J.D. Dhar, Antifertility activity of *Piper longum* Linn. in female rats, *Nat. Prod. Res.* 20 (2006) 235–239. <https://doi.org/10.1080/14786410500045465>
- [199] K.S. Natarajan, M. Narasimhan, K.R. Shanmugasundaram, E.R.B. Shanmugasundaram, Antioxidant activity of a salt–spice–herbal mixture against free radical induction, *J. Ethnopharmacol.* 105 (2006) 76–83. <https://doi.org/10.1016/j.jep.2005.09.043>
- [200] C.R. Pradeep, G. Kuttan, Effect of piperine on the inhibition of lung metastasis induced B16F-10 melanoma cells in mice, *Clin Exp Metastasis.* 19 (2002) 703–708. <https://doi.org/10.1023/A:1021398601388>

- [201] I.B. Koul, A. Kapil, Evaluation of the Liver Protective Potential of Piperine, an Active Principle of Black and Long Peppers, *Planta Med.* 59 (1993) 413–417. <https://doi.org/10.1055/s-2006-959721>
- [202] Z. Jin, G. Borjihan, R. Zhao, Z. Sun, G.B. Hammond, T. Uryu, Antihyperlipidemic Compounds from the Fruit of *Piper longum* L., *Phytother. Res.* 23 (2009) 1194–1196. <https://doi.org/10.1002/ptr.2630>
- [203] D.M. Tripathi, N. Gupta, V. Lakshmi, K.C. Saxena, A.K. Agrawal, Anti-giardial and immunostimulatory effect of *Piper longum* on giardiasis due to *Giardia lamblia* †, *Phytother. Res.* 13 (1999) 561–565. [https://doi.org/10.1002/\(SICI\)1099-1573\(199911\)13:7<561::AID-PTR479>3.0.CO;2-W](https://doi.org/10.1002/(SICI)1099-1573(199911)13:7<561::AID-PTR479>3.0.CO;2-W)
- [204] N. Jamila, N. Khan, A. Bibi, A. Haider, S. Noor Khan, A. Atlas, U. Nishan, A. Minhaz, F. Javed, A. Bibi, Piper longum catkin extract mediated synthesis of Ag, Cu, and Ni nanoparticles and their applications as biological and environmental remediation agents, *Arabian Journal of Chemistry.* 13 (2020) 6425–6436. <https://doi.org/10.1016/j.arabjc.2020.06.001>
- [205] T. Imtiaz, P. Ranganathan, S. B, S. Palati, Green synthesis and Characterisation of Silver Nanoparticles Synthesised Using *Piper longum* and its Antioxidant Activity, *J. Pharm. Res. Int.* 33 (2021) 342–352. <https://doi.org/10.9734/JPRI/2021/v33i51A33501>

# Chapter 3

## MATERIALS, INSTRUMENTS AND METHODS



---

This chapter list the materials, chemicals, and characterisation instruments used in the study. The common methods employed are also briefly outlined.



### **3.1 Introduction**

In this study, fluorescent CDs were prepared from five different natural sources and successfully used for fluorescence sensing and biological applications. The performance of CDs is heavily dependent on their physiochemical properties, which are investigated using various methods. The current chapter describes the materials used, various analytical instruments used for the characterisation of CDs, and some common methods being used in synthesis, fluorescence sensing, fluorescence quantum yield determination, fluorescence life time measurements, real sample analysis, antioxidant activity and *in vitro* cytotoxicity analysis.

### **3.2 Materials used**

#### **3.2.1 Plant sources**

All the precursors for CDs synthesis were collected locally and scientifically verified by an authorized taxonomist.

1. Mangoginger rhizomes (*Cucuma amada*) - Collected from garden in the month of July
2. Lemon leaves (*Citrus pennivesiculata*) - Collected from garden in the month of August
3. Bilimbi fruit (*Averrhoa bilimbi*) - Collected from garden in the month of June

4. Long pepper (*Acorus calamus*) - Collected from Kottakkal Arya Vaidya Sala
5. Sweet flag (*Piper longum*) - Collected from Kottakkal Arya Vaidya Sala

### 3.2.2 Chemicals

All the chemicals were of analytical grade and used without further purification. Distilled water was used for all the purposes throughout the whole work. Real samples for the analysis were collected locally. The important chemicals used for the work is given below (**Table 3.1**).

**Table 3.1** List of chemicals used

Chemicals	Suppliers/Manufacturers
Acetone	NICE Chemicals Pvt. Ltd. India
Acid red	APEE Chem, India
Alanine	NICE Chemicals Pvt. Ltd. India
Aluminium sulphate	Merck Specialities Pvt. Ltd. India
Anthracene	Merck Specialities Pvt. Ltd. India
Ascorbic acid	NICE Chemicals Pvt. Ltd. India
Aspartic acid	NICE Chemicals Pvt. Ltd. India
Cadmium chloride	Merck Specialities Pvt. Ltd. India
Cadmium nitrate	Merck Specialities Pvt. Ltd. India
Calcium chloride	Merck Specialities Pvt. Ltd. India
Chlorpyrifos	Merck Specialities Pvt. Ltd. India
Chlorotetracycline	HiMedia Laboratories Pvt. Ltd, India
Chromium chloride	Merck Specialities Pvt. Ltd. India



Cobalt nitrate	Merck Specialities Pvt. Ltd. India
Copper sulphate pentahydrate	Merck Specialities Pvt. Ltd. India
Dialysis membrane	HiMedia Laboratories Pvt. Ltd. India
Dichlorvos	Merck Specialities Pvt. Ltd. India
Diethylthiocarbamate	Merck Specialities Pvt. Ltd. India
DPPH	Sisco Research laboratories Pvt. Ltd. India
Ethanol	NICE Chemicals Pvt. Ltd. India
Ferric chloride	Merck Specialities Pvt. Ltd. India
Ferrous sulphate	Merck Specialities Pvt. Ltd. India
Florfenicol	Merck Specialities Pvt. Ltd. India
Glucose	Merck Specialities Pvt. Ltd. India
Glyphosate	HiMedia Laboratories Pvt. Ltd. India
Lead nitrate	Merck Specialities Pvt. Ltd. India
Leucine	NICE Chemicals Pvt. Ltd. India
Magnesium sulphate	Merck Specialities Pvt. Ltd. India
Malathion	Merck Specialities Pvt. Ltd. India
Manganese chloride	Merck Specialities Pvt. Ltd. India
Mercuric chloride	Merck Specialities Pvt. Ltd. India
Methyl red	APEE Chem, India
Nickel nitrate	Merck Specialities Pvt. Ltd. India
Oxytetracycline hydrochloride	Sisco Research laboratories Pvt. Ltd. India
Phenol	NICE Chemicals Pvt. Ltd. India
Phenyl alanine	NICE Chemicals Pvt. Ltd. India
Potassium chloride	NICE Chemicals Pvt. Ltd. India
Potassium cyanide	NICE Chemicals Pvt. Ltd. India
Potassium dichromate	Merck Specialities Pvt. Ltd. India

Pottasium bromide	Merck Specialities Pvt. Ltd. India
Pottasium iodide	NICE Chemicals Pvt. Ltd. India
Quinalphos	Merck Specialities Pvt. Ltd. India
Quinine sulphate	Loba Chemie Pvt. Ltd. India
Resorcinol	NICE Chemicals Pvt. Ltd. India
Silver nitrate	NICE Chemicals Pvt. Ltd. India
Sodium carbonate	NICE Chemicals Pvt. Ltd. India
Sodium chloride	NICE Chemicals Pvt. Ltd. India
Streptomycin	HiMedia Laboratories Pvt. Ltd, India
Sudan I	APEE Chem, India
Sudan II	APEE Chem, India
Sudan III	APEE Chem, India
Sudan IV	APEE Chem, India
Sulfamerazine	HiMedia Laboratories Pvt. Ltd, India
Tetracycline hydrochloride	Sisco Research laboratories Pvt. Ltd. India
Urea	NICE Chemicals Pvt. Ltd. India
Valine	NICE Chemicals Pvt. Ltd. India
Zinc acetate	Merck Specialities Pvt. Ltd. India
Zinc chloride	Merck Specialities Pvt. Ltd. India
2-methylphenol	NICE Chemicals Pvt. Ltd. India
2-nitrophenol	NICE Chemicals Pvt. Ltd. India
3-methylphenol	NICE Chemicals Pvt. Ltd. India
3-nitrophenol	NICE Chemicals Pvt. Ltd. India
4-chlorophenol	NICE Chemicals Pvt. Ltd. India
4-methylphenol	NICE Chemicals Pvt. Ltd. India
4-nitrophenol	Merck Specialities Pvt. Ltd. India

### **3.3 Instruments**

Various spectroscopic and microscopic techniques were used to characterize the prepared carbon dots in the present investigation and some of them also used for the application studies. Brief descriptions of the used instruments are given below.

#### **3.3.1. Transmission electron microscope**

Transmission electron microscopy (TEM) analysis have been considered as the primary technique for the carbon dots, by providing relevant information up on morphology, size distribution and crystalline organization of the particles. Since TEM have high resolution of  $\sim 0.1\text{-}0.2$  nm, particles can be amplified millions of time and can be used for revealing the ultra structure of the particles in the samples [1]. Transmission electron microscope is a type of electron microscope which is used in the TEM analysis. In the present work, TEM images and selected area electron diffraction (SAED) pattern of the samples were captured through JEOL JEM 2100 transmission electron microscope, with point resolution of 0.23 nm and lattice resolution of 0.14 nm with 200 kV of accelerating voltage using LaB6 electron gun.

#### **3.3.2. Raman microscope**

Raman spectra of the samples were used to identify the defects present in the samples and roughly gives the idea of extend of graphitisation and crystalline nature of the materials [2,3]. Raman spectra of CDs in the present work were recorded by confocal WiTec

alpha 300RA Raman Microscope, with 532 nm DPSS laser, maximum power of 70 mW.

### **3.3.3. Fourier transform infrared spectrometer**

Fourier transform infrared spectroscopy (FTIR) analysis was used for the identification of surface functionalities associated with the CDs. The FTIR spectra of all the samples in this study were obtained using a PerkinElmer Fourier transform infrared spectrum instrument with KBr pellet as a background and an average scan rate of 64 scans in the 400 to 4000  $\text{cm}^{-1}$  range.

### **3.3.4. X-ray diffractometer**

The crystalline/amorphous nature of the CDs can also be revealed by X-ray diffraction (XRD) analysis. The XRD pattern of the selected CDs were obtained from PANalytical X'pert3Powder X-ray diffractometer using  $\text{CuK}\alpha$  radiation with wavelength of 0.15406 nm.

### **3.3.5 Dynamic light scattering instrument**

Dynamic light scattering (DLS) analysis of CDs was performed in order to determine the sample's average hydrodynamic diameter. DLS analysis of selected CDs was performed using Malvern Panalytical Zetasizer 7.13 instrument.

### **3.3.6 UV-Vis spectrophotometer**

UV-Vis spectroscopy technique is used to explore the optical properties of CDs. All the absorption studies of CDs were carried out

using PerkinElmer UV-Vis spectrophotometer (Scan lambda 850) in the scan range of 200-800 nm.

### **3.3.7. Fluorescence spectrophotometer**

The luminescence behavioural studies and sensing applications of all the CDs were executed with the fluorescence spectrophotometer. In the present investigation, three different fluorescence spectrophotometers were used for fluorescence-based analysis of CDs. And they were (i) PerkinElmer FL-6500 fluorescence spectrometer with a pulse Xenon lamp as an excitation source; (ii) Horiba Fluorolog 3 TCSPC instrument with a steady state excitation source of 450 W Xenon arc lamp; (iii) Hitachi F-4600 fluorescence spectrophotometer with a 150 W Xenon lamp as an excitation source. All the instruments having the scan range from 200- 800 nm.

## **3.4 Methods**

### **3.4.1 Synthesis of CDs**

Microwave assisted pyrolysis was selected as the synthetic method for the preparation of all the CDs systems in the present work and were carried out using a domestic microwave oven (Haier (HIL2001MFPH) 20 L, 700 W) as microwave source. Definite amount of the precursor was weighed out and crushed or powdered depending up on the nature, the crushed or powdered precursor was magnetically stirred with hot distilled water and centrifuged. The obtained solution subjected to microwave irradiation of appropriate watts and time. The dry residue after microwave irradiation again magnetically stirred with

distilled water, centrifuged and filtered. The obtained solution was stored at 4 °C. Detailed procedure is included in relevant chapters, under the Experimental part.

### 3.4.2 Sensing studies

All the prepared CDs were employed as a fluorescent sensor against different species including aquatic pollutants and food adulterants. In each case the fluorescence sensing method is almost similar and the method of analysis is as follows: A fixed concentration of quencher solution was introduced to the system using a micropipette and the emission spectra were recorded after the incubation time. Following that, the procedure was repeated with varying concentrations of quenching species solution in stepwise fashion, and the corresponding emission spectra were recorded at the same excitation wavelength. The procedure is detailed in the relevant chapters under the Experimental part.

### 3.4.3 Fluorescence quantum yield determination

Fluorescence quantum yield of the prepared systems were determined through standard method using quinine sulphate in 0.1 M H<sub>2</sub>SO<sub>4</sub> (with quantum yield of 54 %) as reference standard, using equation (1)

$$Q_{\text{CDS}} = Q_{\text{S}} \frac{M_{\text{CDS}}}{M_{\text{S}}} \frac{\eta_{\text{CDS}}^2}{\eta_{\text{S}}^2} \quad (1)$$

Where,  $Q_{\text{CDs}}$  and  $Q_{\text{S}}$  indicates quantum yield of CDs and standard reference, respectively.  $M_{\text{CDs}}$  and  $M_{\text{S}}$  represent the slope obtained from the linear curve from the graph drawn by integrated fluorescence intensity and UV-Vis absorbance of CDs and reference standard, respectively and  $\eta$  stand for the refractive index of the solvents.

#### 3.4.4 XRD interlayer spacing calculations

The XRD pattern of the CDs is used for the crystalline character evaluation of the systems. The interlayer spacing ( $d$ ) value is determined by Bragg's equation (equation 2).

$$n\lambda = 2d \sin \theta \quad (2)$$

Where,  $\lambda$  is the wavelength;  $n$  is the order of diffraction;  $d$  is the interlayer spacing and  $\theta$  is the incident angle.

#### 3.4.5 Fluorescence lifetime measurements

Fluorescence lifetime of bare CDs and CDs with analyte species plays an important role in the study of sensing mechanism of the CDs. The average fluorescence lifetimes of the samples were determined from the decay profile of CDs by applying multi exponential fit to the curve. The average lifetime values of each CDs and CDs with analyte were calculated by the following equation [4].

$$\tau_{\text{avg}} = \frac{\sum \tau_i \times B_i}{\sum B_i} \quad (3)$$

Where,  $\tau_{\text{avg}}$  is the average lifetime of the sample,  $\tau_i$  is the decay time components and  $B_i$  is the relative amplitude of the corresponding time and both were obtained from the exponential fit data.

For the case of three exponential fit the equation (2) can be written as follows.

$$\tau_{\text{avg}} = \frac{(\tau_1 \times B_1) + (\tau_2 \times B_2) + (\tau_3 \times B_3)}{B_1 + B_2 + B_3} \quad (4)$$

### 3.4.6 Real sample analysis

The real sample analysis was carried out using all the prepared CDs with corresponding analyte (quenching species). Standard addition method through spiking was adopted for the real analysis. The common procedure for the real analysis is as follows; different standard solution of analyte species was prepared. Finite amount of this standard solution was added to pre-treated real samples. Later on, the above solution was mixed with finite volume of CDs solution, after the time of incubation, fluorescence of the mixture was monitored. Subsequently, definite amount of analyte solutions were added to the mixture and fluorescence spectrum was recorded in each addition [5]. The concentration of analyte in the whole of the solution was determined using dilution formula. Detailed procedure is included in relevant chapters.

The recovery % and error % of the analysis was calculated from the obtained results using the following equations (4) and (5)



$$\text{Recovery \%} = \frac{\text{Found amount of analyte}}{\text{Added amount of analyte}} \times 100 \quad (5)$$

$$\text{Error \%} = \frac{(\text{Added amount of analyte}) - (\text{Found amount of analyte})}{\text{Added amount of analyte}} \times 100 \quad (6)$$

### 3.4.7 Antioxidant activity- DPPH scavenging assay

Antioxidant potential of the prepared CDs were measured by 1,1-diphenyl-2-(2,4,6-trinitrophenyl)hydrazine (DPPH) free radical assay with some sort of modifications [6]. For DPPH scavenging assay, different concentrations of CDs solutions were added to finite amount of 0.005% DPPH solution in ethanol. After shaking and standing in dark for 30 minutes, scavenging activity was determined by measuring absorbance at 520 nm using UV-Vis spectrophotometer. Same procedure was used to determine the DPPH scavenging activity of ascorbic acid taken as standard. Detailed procedure is included in Chapter 9. The % of radical scavenging activity (S %) of the sample was calculated from the decrease in absorbance at 520 nm, it is calculated using the following equation.

$$S \% = \frac{A_{\text{control}} - A_{\text{sample}}}{A_{\text{control}}} \quad (7)$$

Where,  $A_{\text{control}}$  and  $A_{\text{sample}}$  are the absorbance of the blank and absorbance of the test sample, respectively.

### 3.4.8 *In vitro* cytotoxic activity – Trypan blue exclusion method

*In vitro* cytotoxicity of the prepared CDs and corresponding extracts was carried out by the standard Trypan blue exclusion method by using Dalton's lymphoma ascites (DLA) cell lines as model. In brief, the tumour cells aspirated from the peritoneal cavity of tumour bearing mice were with phosphate buffered cell line (PBS). And the cell lines were mixed with different concentration of CDs. These assay mixture were incubated for 3 hour at 37 °C. After the incubation time, the cell suspension was mixed with trypan blue solution and kept for 2-3 minutes and loaded on a haemocytometer. Dead cells take up the blue colour of typan blue while live cells do not take up the dye. Simultaneously a control was also performed with excluding the sample solutions. The numbers of stained and unstained cells were counted separately; detailed procedure is included in Chapter 9. The % of cytotoxicity was calculated using the equation (8) [7].

$$\% \text{ of cytotoxicity} = \frac{\text{Number of dead cells}}{(\text{Number of dead cells}) + (\text{Number of live cells})} \times 100 \quad (8)$$

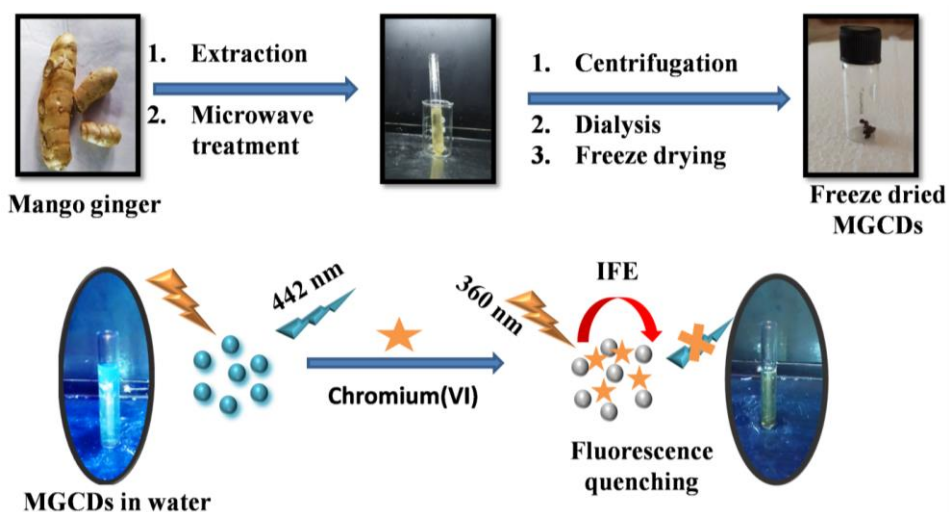
### 3.5 References

- [1] P. Zuo, X. Lu, Z. Sun, Y. Guo, H. He, A review on syntheses, properties, characterisation and bioanalytical applications of fluorescent carbon dots, *Microchim Acta*. 183 (2016) 519–542. <https://doi.org/10.1007/s00604-015-1705-3>
- [2] A.C. Ferrari, J. Robertson, Interpretation of Raman spectra of disordered and amorphous carbon, *Phys. Rev. B*. 61 (2000) 14095–14107. <https://doi.org/10.1103/PhysRevB.61.14095>
- [3] A.C. Ferrari, D.M. Basko, Raman spectroscopy as a versatile tool for studying the properties of graphene, *Nature Nanotech.* 8 (2013) 235–246. <https://doi.org/10.1038/nnano.2013.46>
- [4] J.R. Lakowicz, Measurement of Fluorescence Lifetimes, in: J.R. Lakowicz (Ed.), *Principles of Fluorescence Spectroscopy*, Springer US, Boston, MA, 1983: pp. 51–93. [https://doi.org/10.1007/978-1-4615-7658-7\\_3](https://doi.org/10.1007/978-1-4615-7658-7_3)
- [5] B.E.H. Saxberg, B.R. Kowalski, Generalized standard addition method, *Anal. Chem.* 51 (1979) 1031–1038. <https://doi.org/10.1021/ac50043a059>
- [6] J. Shen, S. Shang, X. Chen, D. Wang, Y. Cai, Highly fluorescent N, S-co-doped carbon dots and their potential applications as antioxidants and sensitive probes for Cr (VI) detection, *Sens. Actuators, B*. 248 (2017) 92–100. <https://doi.org/10.1016/j.snb.2017.03.123>
- [7] W. Strober, Trypan Blue Exclusion Test of Cell Viability, *Curr. Protoc. Immunol.* 111 (2015) A3.B.1-A3.B.3. <https://doi.org/10.1002/0471142735.ima03bs111>



# Chapter 4

## MANGO GINGER DERIVED CARBON DOTS



This work is published in Spectroscopy Letters

P. Venugopalan and N. Vidya, Green synthesis of mango ginger (*Curcuma amada*) derived fluorescent carbon dots—a potent label-free probe for hexavalent chromium sensing in water, *Spectroscopy Letters*, 55 (2022) 373–388

<https://doi.org/10.1080/00387010.2022.2082483>



## 4.1 Introduction

As discussed in Chapter 2, mango ginger (*Curcuma amada*) is a unique spice from the *Zingiberaceae* family. It has morphological similarities to ginger, but when crushed, it emits a raw mango aroma. Its pharmacological properties are well documented in the literature, and the *Ayurvedic* medicinal system places a high value on this species [1,2]. Even though the biological and pharmacological studies of this spice were found to be very impressive, its materialization studies based on its transformation in to nanomaterials are limited in literature.

The present work describes about the synthesis, characterisation and application of CDs derived from the aqueous extract of mango ginger rhizomes, by the aid of microwave energy. It was chosen for a variety of reasons, including its ease of availability, environmental friendliness, and low cost. As per the literature, it contains a high concentration of water soluble phenolic acids, as well as several other chemical constituents that make it suitable for the use as a precursor in the synthesis of CDs [1]. These phenolic acids are expected to carry a vital role in the formation of CDs. The as prepared system is designated as MGCDs. The characterisation of the developed system was carried out using different instrumental methods such as TEM, Raman and FTIR. The fluorescent behaviour and other optical properties were explored using UV-Vis and fluorescence spectrophotometer.

The selective and specific interactions of several metal ions with CDs, leading to the fluorescence alteration are well established in

the literature. This specific metal ion interaction is highly dependent on the nature of CDs. Therefore, the interaction of MGCDs with various metal ions was investigated by monitoring the changes in fluorescence. According to the findings, chromium(VI) had the greatest quenching in the native fluorescence of MGCDs. As a result, additional research on chromium(VI) was conducted.

Chromium (Cr) has acquired great economical importance on account of its numerous industrial and agricultural applications. Several chromium compounds are used in leather tanning, manufacturing of steel, magnetic tape, dyes, pigments, pesticides and also find application as an industrial catalyst/oxidizing agent [3]. The expansive usage of this metal leads to the chromium contamination adversely effects the environmental system [4]. Out of two common oxidation states of chromium, trivalent chromium is an essential trace element in humans and animals, while hexavalent chromium (chromium(VI)) compounds are responsible for the acute and chronic toxicity of chromium [5]. International Agency for Research on Cancer ranked it as No.1 carcinogen and exposure to air contaminated with chromium(VI) and ingestion causes severe health issues including respiratory illness, ocular damages, and chronic and allergic bronchitis pulmonary tuberculosis [6]. According to WHO, the allowed level of chromium(VI) in drinking water should be below 50  $\mu\text{g/L}$  [7]. Consequently it is essential to monitor the chromium(VI) especially in water bodies since most of the industrial effluents are directly let in to rivers.



The observed quenching in fluorescence of MGCDs were explored in detail and developed as a fluorescent probe for the sensing of chromium(VI) in real water samples with acceptable level of detection and satisfactory level of statistical parameters. The experimental procedures and results are discussed in the following sections.

## **4.2 Experimental**

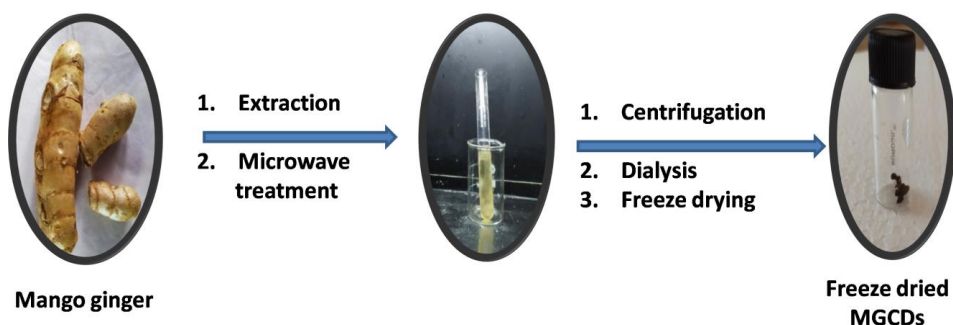
### **4.2.1 Synthesis of MGCDs**

Microwave pyrolysis of aqueous extract of mango ginger rhizomes was used for the synthesis of MGCDs. The complete procedure of preparation is outlined below.

Mango gingers rhizomes were well cleaned using distilled water. 10 g of these rhizomes were peeled, cut in to small pieces and crushed using mortar and pestle. The pasty portion was added to 30 mL lukewarm distilled water and stirred with the aid of magnetic stirrer for 30 minutes. The obtained solution filtered and placed in a domestic microwave oven for 20 minutes at 695 W with intermittent cooling in every 5 minutes. To the dry residue as obtained, 30 mL of distilled water was added and filtered after 5 min of magnetic stirring, resultant brown solution subjected to centrifugation for 10 minutes at 1500 rpm to remove large particles. The supernatant yellow - brown solution was then dialyzed against distilled water for 48 hrs through a dialysis membrane having molecular weight cut off 3000 Da.

The MGCDs so obtained were freeze dried and stored at 4 °C.

The scheme of preparation is depicted in **Scheme 4.1**. Formation of CDs was preliminarily confirmed by the fluorescence under UV light. MGCDs give cyan blue fluorescence on irradiation with UV light.



**Scheme 4.1** Synthetic route of MGCDs

#### 4.2.2 Sensing of chromium(VI)

Sensing of chromium(VI) by MGCDs was carried out at the excitation wavelength of 360 nm. The procedure adopted for the analysis is as follows: 2 mL of the MGCDs solution were taken in the cuvette and fluorescence spectra recorded and then a fixed concentration of chromium(VI) solution was introduced to the system with the help of a micropipette and recorded the emission spectra after an incubation of one minute of time. Subsequently, the procedure is repeated with varying concentration of chromium(VI) solution in stepwise and the corresponding emission spectra were recorded at the same excitation wavelength.

The same procedure was followed for the selectivity studies, in which 100  $\mu\text{L}$  of 1 mM solutions of various ions ( $\text{K}^+$ ,  $\text{Zn}^{2+}$ ,  $\text{Na}^+$ ,  $\text{Mn}^{2+}$ ,

$\text{Ag}^+$ ,  $\text{Cd}^{2+}$ ,  $\text{Mg}^{2+}$ ,  $\text{Pb}^{2+}$ ,  $\text{Ca}^{2+}$ ,  $\text{Al}^{3+}$ ,  $\text{Co}^{2+}$ ,  $\text{Hg}^{2+}$ ,  $\text{Cr}^{3+}$ ,  $\text{Ni}^{2+}$ ,  $\text{Cu}^{2+}$ ,  $\text{Fe}^{3+}$  and chromium(VI) to the MGCDs solution and fluorescence was monitored as the same as above.

#### **4.2.3 Real water analysis**

Sensing of chromium(VI) in real water samples was carried out using the standard addition method through spiking process. Laboratory tap water and nearby bore well water was opted as real water samples and all fluorescence measurements were performed under the same experimental conditions as above. The procedure for the analysis is as follows; water samples collected from the tap and bore well were filtered and centrifuged at 1500 rpm for 20 minutes to remove dust and impurities, if any. Then the samples were spiked with different standard solutions of chromium(VI). Afterwards, the fluorescence spectra of MGCDs along with this spiked water samples were recorded. The spiking process used for the analysis is as follows; 10  $\mu\text{L}$  of standard chromium(VI) solution was added to 1 mL of water sample, then it is mixed with 1 mL of MGCDs solution, after one minute of incubation time, the fluorescence spectrum was recorded. Subsequently different amount of chromium(VI) solution was added to the same mixture and intensity of emission was carefully monitored in each case.

### **4.3 Results and discussion**

#### **4.3.1 Formation of MGCDs**

CDs were prepared by the microwave pyrolysis of mango ginger extract which is found to consist of several carbohydrates along

with different types of phenolic acids like gallic acid, syringic acid, etc. The exact mechanism of carbon dots formation from organic compounds is still ambiguous [8]. The proposed mechanism belongs to the bottom-up strategy, which includes pyrolysis of smaller molecules to form products having nano dimensions through various steps like condensation, polymerisation, carbonization and nuclear burst to form the final products. The carbohydrates in the present extract solution undergo hydrolysis, dehydration and decomposition in presence of phenolic acids by the aid of microwave heating to form simple molecules (generally furfural derivatives). These molecules up on self-condensation and reactions with other reactive molecules in the system resulting variety of polymeric products and the above polymeric products finally undergoes condensation or aromatisation to form carbon clusters, which up on nuclear burst gives out the water soluble fluorescent CDs. All these reactions taking place by the use of microwave energy in a short period of time [8–10].

#### **4.3.2 Characterisation of MGCDs**

Characterisation is an important part of the study since it gives the idea about morphology and functionalities associated with MGCDs. Different techniques such as TEM, Raman and FTIR used for the material characterisation purpose. The details of the instruments used are explained in Chapter 3.

##### **TEM analysis**

The transmission electron microscopy (TEM) analysis is the primary analytical technique used to characterise the morphology and

the size of MGCDs. The results shown in **Figure 4.1** reveal that, MGCDs having nearly spherical nature and the corresponding histogram indicates that the size distribution is ranges from 3.6 nm to 9.7 nm. The lattice fringes in the high resolution TEM image of MGCDs are not very clear and this observation indicates the poor crystalline nature of MGCDs. Similarly, The selected area electron diffraction (SAED) pattern of MGCDs is found to be fade and is exclusive of bright spots which also imply poor crystallisation of the sample [11].

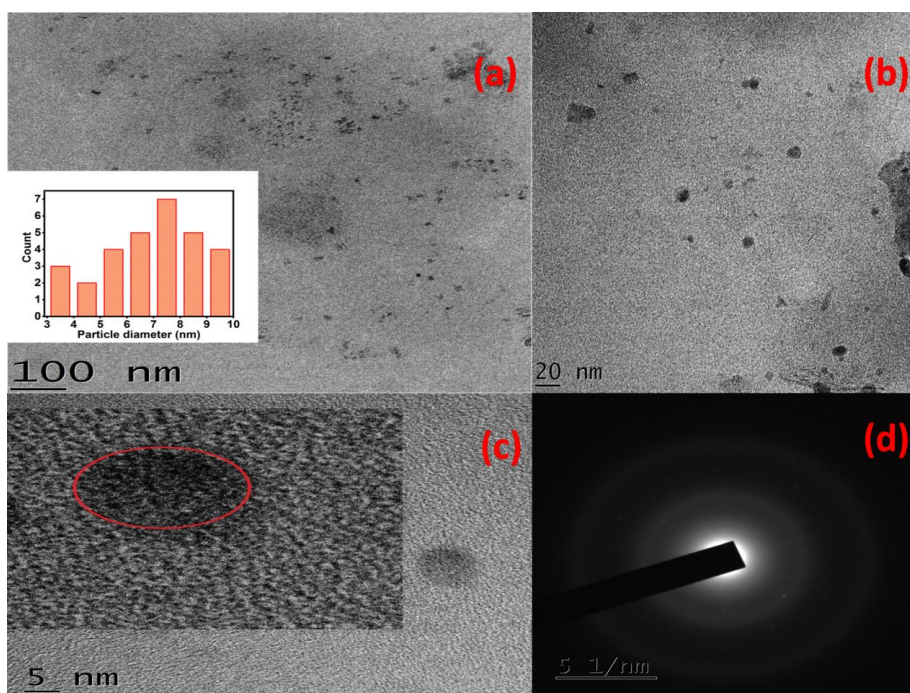


**Figure 4.1:** (a, b and c): TEM images of MGCDs at different magnifications (inset showing the particle size distribution histogram (n=30)); (d): SAED pattern of MGCDs

### Raman and FTIR spectral analysis

The Raman spectrum of MGCDs (**Figure 4.2**) displays two broad peaks at 1349 and 1560  $\text{cm}^{-1}$  indicating D band and G band respectively. The D band corresponds to the vibration of carbon atoms with dangling bonds in the termination plane of disordered graphite or glassy carbon. The G band associated with the  $E_{2g}$  mode and is related to the vibration of  $sp^2$  bonded carbon atoms in a two dimensional hexagonal lattice. Besides, the broad nature of D and G bands are in agreement with the poor crystalline and lesser graphitization nature of MGCDs [12].

Fourier transform infrared spectrum (FTIR) (**Figure 4.3**) was used to identify the surface functional groups present in the MGCDs. Broad band at 3257  $\text{cm}^{-1}$  attributed to the O–H stretching vibration, and the one at 1450  $\text{cm}^{-1}$  belongs to the C=C stretching of polycyclic aromatic hydrocarbons and it appears to be small due to less polar nature of the bond and a peak at 1279  $\text{cm}^{-1}$  and a medium band at 1036  $\text{cm}^{-1}$  assigned to the C–O stretching vibrations. In addition peaks at 1587  $\text{cm}^{-1}$  and 1400  $\text{cm}^{-1}$  is due to the asymmetric and symmetric stretching vibration of  $\text{COO}^-$  [13]. Moreover a band at 2925  $\text{cm}^{-1}$  was ascribed to the C–H stretching vibration and a small band at 776  $\text{cm}^{-1}$  arises due to C–H bending vibration [14]. These results imply that the surface of MGCDs consist of C=C, C–O, -OH, and –COOH groups [5]. As a whole the FTIR spectrum reveals that the surface of MGCDs is enriched with hydrophilic groups like hydroxyl and carboxyl. These

functionalities increase the solubility and stability of the system in aqueous medium.

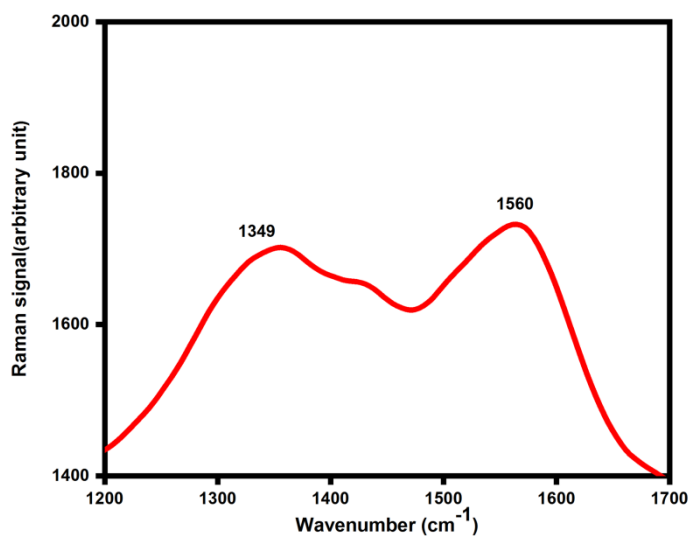


**Figure 4.2:** Raman spectrum of MGCDs

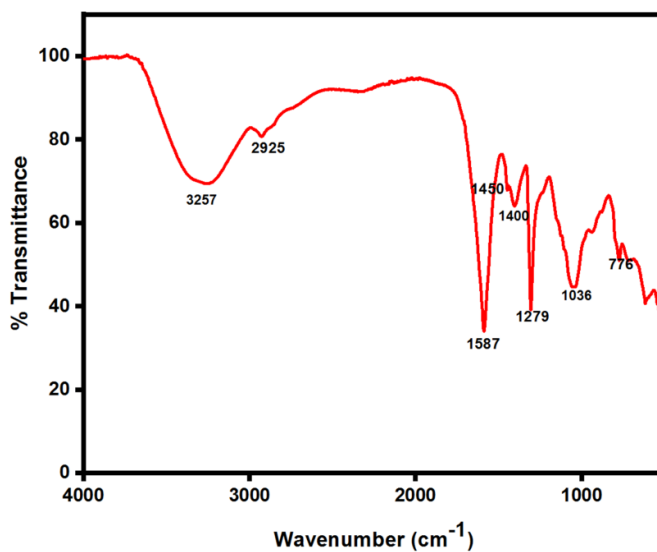


**Figure 4.3:** FTIR spectrum of MGCDs

### UV-Vis spectral analysis

The UV-Vis spectroscopy analysis was used to explore the optical properties of MGCDs. The UV-Vis absorption spectrum of MGCDs was recorded, and is displayed in **Figure 4.4**. The spectrum exhibit two peaks, the one peak at 203 nm and another at 280 nm. The first one corresponds to  $\pi - \pi^*$  transition of C=C bonds and the latter one is attributed to  $n - \pi^*$  transition of C = O bonds present in the surface of MGCDs [15].

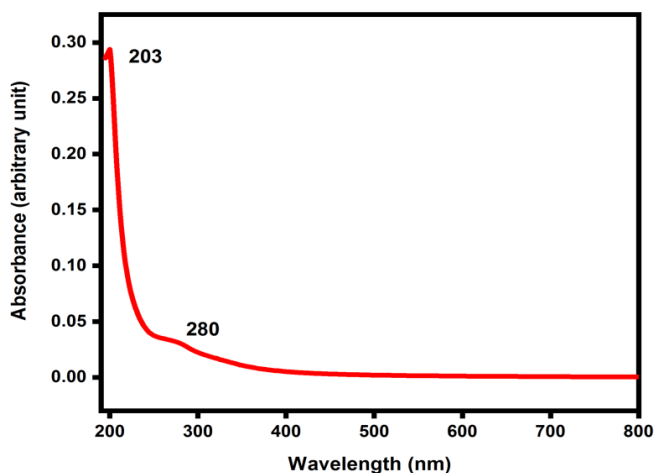


**Figure 4.4:** UV-Vis absorbance spectrum of MGCDs

### Fluorescence spectral analysis

Similar to UV-Vis spectroscopy analysis, optical features of MGCDs are investigated through fluorescence spectrum analysis. Fluorescence spectrum of MGCDs was recorded and the corresponding spectrum is depicted in **Figure 4.5** showing emission maxima at 442 nm when excitation wavelength of 360 nm was applied and the scan range was from 370 nm to 600 nm.



The excitation dependent emission behaviour of the system was revealed from the excitation dependence studies. The studies were conducted from 310 nm to 410 nm with 10 nm interval and the resulting spectra are shown in **Figure 4.6**. Such a behaviour of the MGCDs may attribute to the presence of different sized particles (polydispersity) and different surface functional groups each contributes different surface states in MGCDs [16]. The system shows maximum intensity at 442 nm when it excited at a wavelength of 360 nm and these values selected as the emission and excitation wavelength of MGCDs respectively for further studies.

MGCDs exhibits strong cyan blue fluorescence under UV light of 365 nm and the photographs are shown in **Figure 4.7** along with the excitation and emission graphs. **Figure 4.8** shows the photographs of filter paper under day light and UV light written with the MGCDs solution.

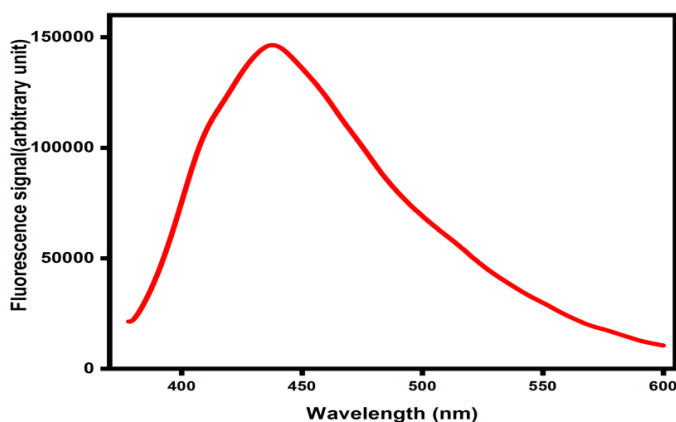


**Figure 4.5:** Fluorescence spectrum of MGCDs

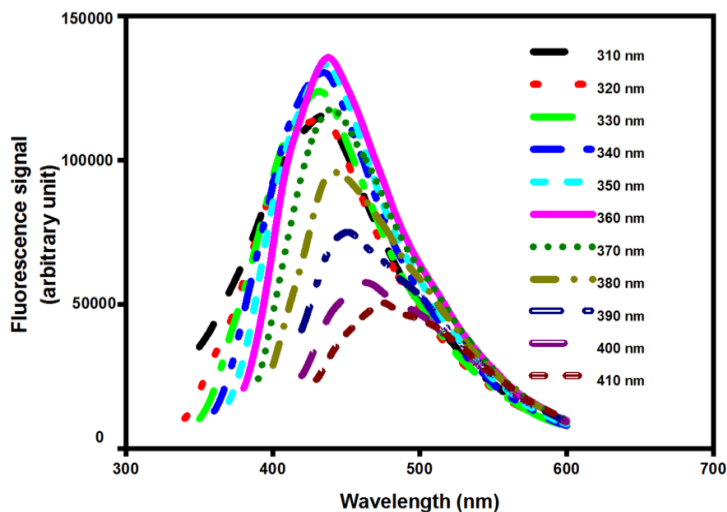


**Figure 4.6:** Fluorescence excitation dependent emission spectra of MGCDs

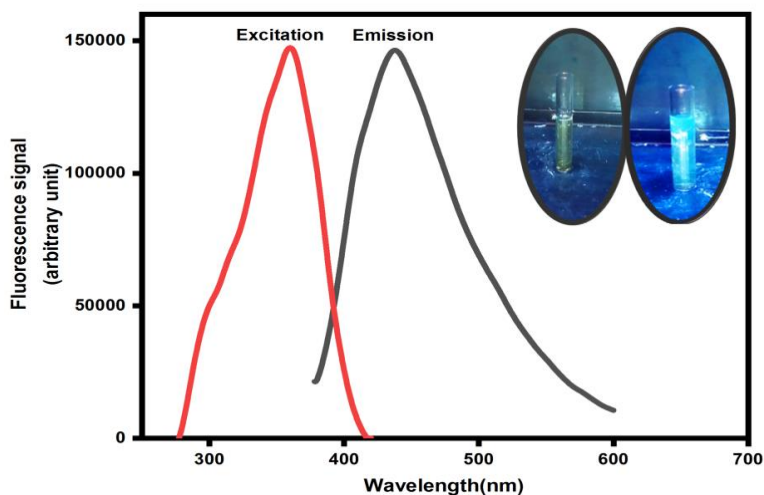


**Figure 4.7:** Excitation and emission spectra of MGCDs (inset showing photographs of MGCDs under normal light and UV light, displays fluorescence.)



**Figure 4.8:** Photographs of filter paper written using MGCDs solution under day light and UV light

#### **4.3.3 Fluorescence quantum yield and fluorescence stability of MGCDs**

Quantum yield (QY) of the MGCDs in water was determined through the standard method as explained in Chapter 3, using quinine sulphate (54 % in 0.1 M  $\text{H}_2\text{SO}_4$ ) as standard reference and the value of QY was found to be 3.87 %.

The stability of the prepared system in freeze dried state was found to be up to twelve months of time when stored at  $4^\circ\text{C}$ , while in solution state the stability was reduced to three months of time afterwards the fluorescence was decreased gradually. This decay of fluorescence over time may be due to the increase of particle size through aggregation [17]. However stability of MGCDs solution was found to be less when it placed in open atmosphere and some sort of fungal infections were noticed after few days when it placed in open air.

Moreover, the influence of ionic concentration in the fluorescence intensity of MGCDs was studied by adding different concentration of KCl solution (1mM to 10 mM) to the system. The spectra were recorded at each addition of KCl and fluorescence intensity was carefully monitored. The resulting plot of fluorescence intensity with concentration of KCl is displayed in **Figure 4.9**. The fluorescence of the system almost unaltered in the whole range. This in turn implies that the particles not aggregate at this range of ionic strength, since such aggregation definitely reduce the fluorescence and was missing here.

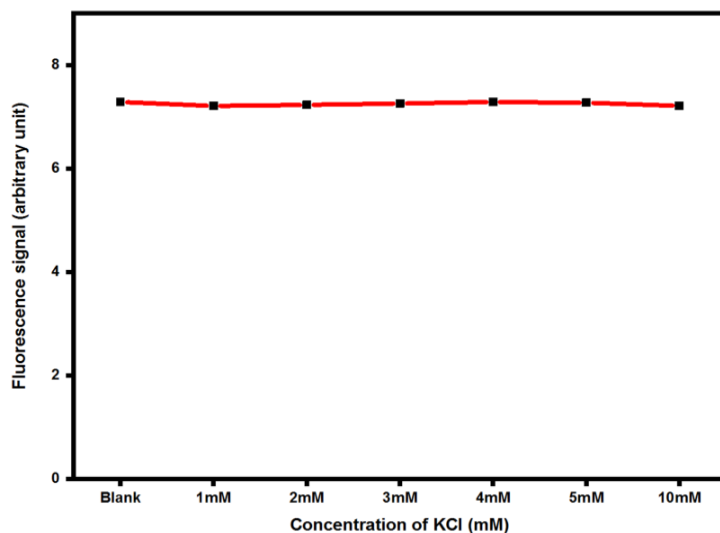


**Figure 4.9:** Variation of fluorescence of MGCDs with different concentration of KCl

#### 4.3.4 Selectivity studies

Several fluorescent investigations were carried out to examine the potential of the system as a fluorescent sensing probe due to its conspicuous fluorescence characteristics. In order to identify the selective quencher that efficiently reduces the natural fluorescence of MGCDs, the selectivity investigation was carried out. The study was conducted by the fluorescence measurements of the MGCDs in presence of different metal ions; those are commonly found in water as pollutant. The relative fluorescence intensities were examined by adding 100  $\mu\text{L}$  of 1 mM solutions of various ions ( $\text{K}^+$ ,  $\text{Zn}^{2+}$ ,  $\text{Na}^+$ ,  $\text{Mn}^{2+}$ ,  $\text{Ag}^+$ ,  $\text{Cd}^{2+}$ ,  $\text{Mg}^{2+}$ ,  $\text{Pb}^{2+}$ ,  $\text{Ca}^{2+}$ ,  $\text{Al}^{3+}$ ,  $\text{Co}^{2+}$ ,  $\text{Hg}^{2+}$ ,  $\text{Cr}^{3+}$ ,  $\text{Ni}^{2+}$ ,  $\text{Cu}^{2+}$ ,  $\text{Fe}^{3+}$  and chromium(VI) to the working solution.

The results of selectivity investigations are given in **Figure 4.10**. It is very clear that chromium(VI) exhibiting highest degree of fluorescence quenching efficiency among the various metal ions. However, small quenching was observed for  $\text{Fe}^{3+}$  is may be due to the interaction of this metal with the surface functionalities of carbon dots resulting fluorescence quenching. All the metal ions are likely to have some sort of interactions with the surface hydroxyl and carboxyl groups. According to previous reports in this area,  $\text{Fe}^{3+}$  exhibits greater tendency to interact with the surface hydroxyl and carboxyl functionalities of carbon dots [18]. Although chromium(VI) exerts superior quenching efficiency, such superiority was not observed even with  $\text{Cr}^{3+}$  ions. At the same time, rest of the metal ions shows slight quenching effect and can be negligible. It indicates the strong selectivity of the fluorescent probe to the chromium(VI) detection.

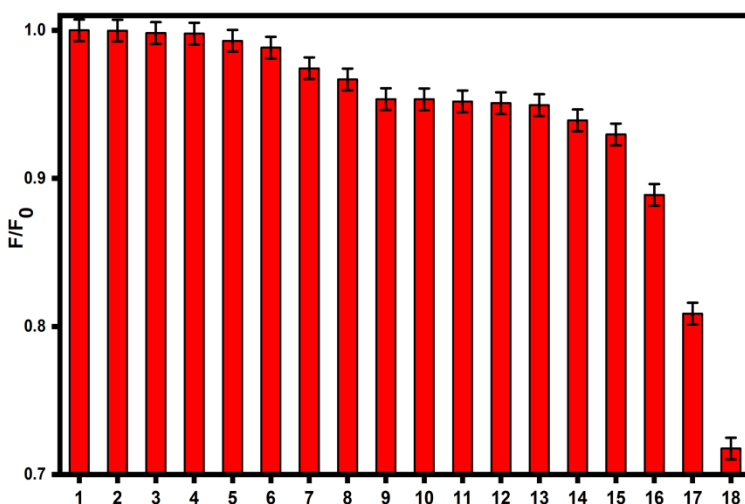


**Figure 4.10:** Relative fluorescence intensity of MGCDs in presence of different metal ions (100  $\mu$ L of 1 mM concentration) ( from 1 to 18: blank, K<sup>+</sup>, Zn<sup>2+</sup>, Na<sup>+</sup>, Mn<sup>2+</sup>, Ag<sup>+</sup>, Cd<sup>2+</sup>, Mg<sup>2+</sup>, Pb<sup>2+</sup>, Ca<sup>2+</sup>, Al<sup>3+</sup>, Co<sup>2+</sup>, Hg<sup>2+</sup>, Cr<sup>3+</sup>, Ni<sup>2+</sup>, Cu<sup>2+</sup>, Fe<sup>3+</sup> and chromium(VI))

#### 4.3.5 Sensing studies with chromium(VI)

The selectivity results show that chromium (VI) may strongly quench the fluorescence of MGCDs; hence more sensing studies using the quencher were carried out.

The studies were conducted by adding different concentration of chromium(VI) (0 – 73.33  $\mu$ M ) solution to the working system. It is observed that, as the concentration of chromium(VI) increases the fluorescence intensity of MGCDs found to be decreased gradually and is clear from the **Figure 4.11**.

The sensitivity and relationship of the concentration of chromium(VI) with fluorescence of the system was obtained from the plot of fluorescence quenching ratio ((F<sub>0</sub> – F)/F<sub>0</sub>) with concentration of

chromium(VI) and is given in **Figure 4.12**, where  $F_0$  and  $F$  are the fluorescence intensity of the system without and with the presence quenching moiety. It shows that the linear response of the system towards the concentration of the quenching species was maintained in the range of  $0 \mu\text{M} - 33.33 \mu\text{M}$  with correlation coefficient  $R^2$  of 0.9988. The limit of detection (LOD) was estimated to be  $84 \text{ nM}$  based on  $3\sigma/\text{slope}$  method, where  $\sigma$  is the standard deviation of the measurements.

LOD value as well as the linear range obtained for the system found to be comparable with the previously reported systems and are listed in **Table 4.1**. It can be found that the present study exhibits higher sensitivity, lower limit of detection and a moderate range of linear response. Therefore the as prepared system can be employed for monitoring chromium(VI) concentration in real water samples.

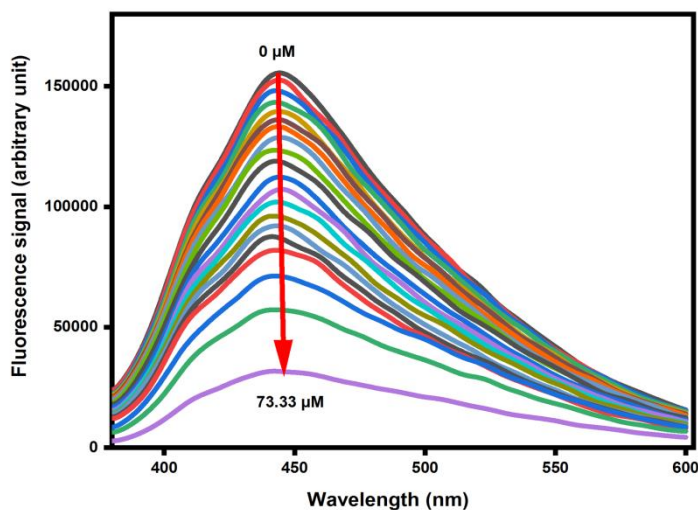


**Figure 4.11:** Steady decrease of fluorescence intensity on increasing the concentration of chromium(VI) from  $0 \mu\text{M}$  to  $73.33 \mu\text{M}$

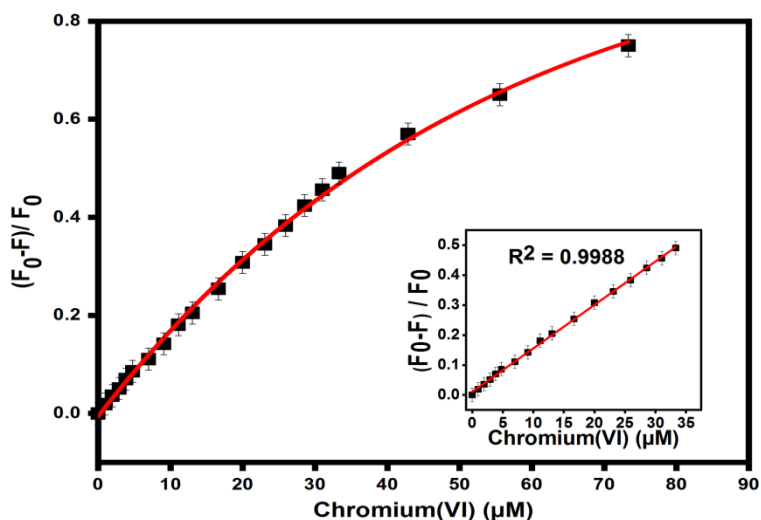


**Figure 4.12:** Plot of  $(F_0 - F)/F_0$  with different concentration of chromium(VI) (inset showing linear response of  $(F_0 - F)/F_0$  with increasing concentration of chromium(VI))

#### 4.3.6 Determination of chromium(VI) in environmental water samples

The practicability of the MGCDs as fluorescent probe was investigated by applying the system to detect chromium(VI) in real water samples by standard addition method. Results are shown in **Table 4.2**. Chromium(VI) recovery in these samples ranged from 95.07 % to 102.70 % with relative error between 0.24 % to 4.92 %, indicating good level of accuracy and precision in the method ( The recovery and error percentages were found out using standard equations and is given in Chapter 3).



**Table 4.1:** Comparison of different CDs based fluorescent sensors for chromium(VI)

Sensing probe for chromium(VI)	LOD ( $\mu\text{M}$ )	Linear range ( $\mu\text{M}$ )	Reference
CDs synthesised from citric acid and thiourea	0.2	1 – 10	[19]
CDs derived from shrimp cells	0.1	0 – 70	[20]
CDs synthesised from ammonium citrate and cysteamine hydrochloride	0.11	0.35 – 126	[21]
CDs synthesised from shallots	3.5	20 – 100	[22]
CDs derived from tulsi leaves	0.086	1.6 – 50	[23]
CDs derived from lemon peel waste	0.073	2.5 – 50	[24]
CDs derived from flax straw	0.19	0.5 – 80	[25]
CDs synthesised from citric acid and glycine	4.16	5 – 200	[26]
CDs synthesised from citric acid and reduced glutathione	0.57	1.92 – 230	[27]
CDs derived from mango ginger	0.084	0 – 31.3	This work

**Table 4.2:** Detection of chromium(VI) in different water samples

Water sample	Added chromium(VI) ( $\mu\text{M}$ )	Found ( $\mu\text{M}$ )	Error %	Recovery (%)
Tap water	0	NF <sup>a</sup>	-	-
	2.03	1.93	4.92	95.07
	4.05	3.87	4.44	95.55
	5.92	5.88	0.68	99.32
Bore well water	0	NF <sup>a</sup>	-	-
	2.03	1.94	4.43	95.56
	4.05	4.04	0.24	99.75
	5.92	6.08	2.70	102.70

a: Not Found

### 4.3.7 Mechanism of quenching

The mechanism behind the quenching of native fluorescence of MGCDs by chromium(VI) was investigated. Generally fluorescence quenching mechanisms are of five types; dynamic quenching mechanism, static quenching mechanism, inner filter effect, Förster resonance energy transfer (FRET) and photo induced electron transfer (PET) [28].

In order to acquire insight of fluorescence quenching mechanism, firstly the fluorescence decay spectra of the MGCDs and MGCDs with chromium(VI) were recorded since it can eliminate several mechanism from the above list, and are given in (**Figure 4.13**). The average lifetime of MGCDs and MGCDs+chromium(VI) were calculated by the standard formula and is explained in Chapter 3, and the values were found to be 2.18 ns and 2.14 ns respectively. This small change indicates that there was no remarkable electron transfer between MGCDs and chromium(VI). Since the resonance electron transfer (RET) between donor and acceptor significantly changes the average life time fluorescence of donor. So the chance of dynamic quenching, FRET and PET can be excluded [15,28]. Then the further investigation is focussed on the rest of two mechanisms that is static quenching and inner filter effect.

In order to explore the quenching mechanism in detail, the UV-Vis spectra of chromium(VI), MGCDs and MGCDs with chromium(VI) were studied. The UV-Vis spectrum of MGCDs with chromium(VI) matches with summed UV-Vis absorption spectrum of

MGCDs and chromium(VI) as shown in **Figure 4.14**, it is clear that there was neither absorption changes nor extra peaks formed in the system when quencher was mixed with the MGCDs, indicates there was no new compound formed on mixing, therefore the quenching was not attributed to static quenching process [29].

Then the UV-Vis spectra of chromium(VI) (100  $\mu\text{M}$ ) was recorded and compared it with the fluorescence excitation and emission spectra of MGCDs. Surprisingly, it was found that the absorption spectrum of chromium(VI) overlapping with the fluorescent spectra of our system of study. This observation strengthens the chance for quenching of fluorescence through inner filter effect (IFE). **Figure 4.15** shows that chromium(VI) had a broad absorption at 258 nm and 358 nm while MGCDs shows a broad excitation at 360 nm with an emission wavelength 442 nm. This effective overlap of excitation spectrum of the system with absorbance spectrum of chromium(VI) indicates that chromium(VI) can effectively shield the excitation light for MGCDs and leads to the quenching of fluorescence [5,7,15]. For further clarification the absorbance spectra of other metal ions including  $\text{Cr}^{3+}$  were also recorded; no one shows such spectral overlap with the present system excitation spectra.

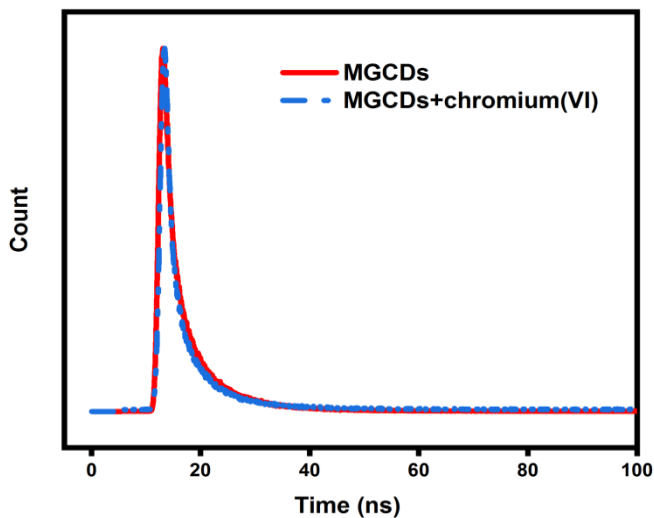


**Figure 4.13:** Fluorescent decay profile of MGCDs and MGCDs + chromium(VI)

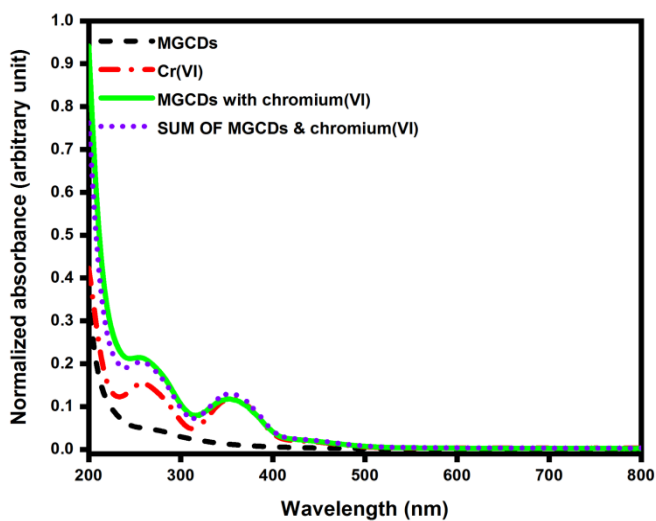


**Figure 4.14:** UV-Vis spectra of chromium(VI), MGCDs, MGCDs with chromium, and summed UV-Vis absorption spectrum of MGCDs and chromium(VI)

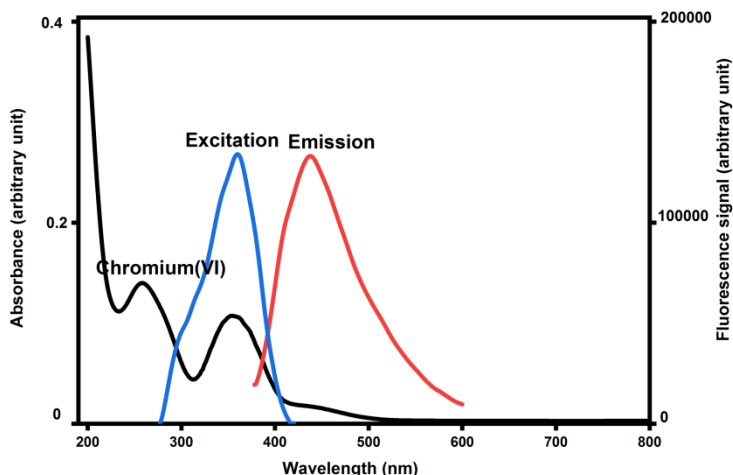


**Figure 4.15:** Spectral overlap between absorption band of chromium(VI) with excitation band of MGCDs and emission band of MGCDs

From the above studies, it is concluded that the probable mechanism for quenching is IFE and the fast response and higher selectivity and sensitivity, exponential decrease of fluorescence intensity were also are in line with IFE mechanism [30].

So as to prove this, two equations were used to calculate the corrected fluorescence intensity ( $F_{\text{corr}}$ ) of MGCDs. The first equation used to manifest the mechanism was the Lackowicz equation. It is the simplest method for IFE correction of fluorescence so can be used to find  $F_{\text{corr}}$  and is depicted as equation (1).

$$F_{\text{corr}} = F_{\text{obsd}} \times 10^{(A_{\text{ex}} + A_{\text{em}})/2} \quad (1)$$

Where  $F_{\text{obsd}}$  is the observed fluorescence intensity with IFE,  $F_{\text{corr}}$  is the fluorescence intensity after removing IFE from  $F_{\text{obsd}}$  and

$A_{\text{ex}}$  ( $\lambda= 360$  nm) and  $A_{\text{em}}$  ( $\lambda= 442$  nm) are the absorbance of system at excitation and emission wavelength of fluorophore, respectively [31].

In addition to above equation, Parker equation was also used to calculate  $F_{\text{corr}}$  and is shown in equation (2), because the former equation is an approximation equation and does not consider geometry parameters of the cuvette and these factors are included in Parker equation and is more advanced.

$$F_{\text{corr}} = F_{\text{obsd}} \times \frac{2.3d A_{\text{ex}}}{1-10^{-dA_{\text{ex}}}} \times 10^{gA_{\text{ex}}} \times \frac{2.3s A_{\text{em}}}{1-10^{-sA_{\text{em}}}} \quad (2)$$

Where  $F_{\text{obsd}}$  is the measured maximum fluorescence intensity and  $F_{\text{corr}}$  is the corrected maximum fluorescent intensity after removing the IFE from  $F_{\text{obsd}}$ ,  $d$  is the pathlength of cuvette cell,  $s$  is the width or thickness of excitation beam,  $g$  is the distance between the edges of excitation beam to the cuvette edge along the direction of fluorescence detection,  $A_{\text{ex}}$  and  $A_{\text{em}}$  are the absorbance at excitation and emission wavelength respectively.

There are two factors which used determine the role of IFE in the quenching mechanism. The first one is the fluorescent suppression efficiency (E) which is the parameter indicates the reduction of fluorescence intensity by the addition of different concentration of chromium(VI), and the second one is the correction factor (CF) which is the ratio of  $F_{\text{corr}}$  to  $F_{\text{obsd}}$ .

$E_{\text{obsd}}$  and  $E_{\text{corr}}$  are the fluorescent suppression efficiency with and without taking IFE to consideration and  $F_{\text{obsd}, 0}$  and  $F_{\text{corr}, 0}$  are the

observed and corrected fluorescence intensity at zero concentration of quenching species. All the parameters were calculated using the equations (3), (4) and (5) [29].

$$E_{\text{obsd}} = 1 - \frac{F_{\text{obsd}}}{F_{\text{obsd},0}} \quad (3)$$

$$E_{\text{corr}} = 1 - \frac{F_{\text{corr}}}{F_{\text{corr},0}} \quad (4)$$

$$CF = 1 - \frac{F_{\text{corr}}}{F_{\text{obsd}}} \quad (5)$$

From the value of CF and difference between fluorescent suppressed efficiencies ( $E_{\text{obsd}} - E_{\text{corr}}$ ), the effect of IFE in quenching mechanism can be evaluated. CF and  $E_{\text{obsd}} - E_{\text{corr}}$  values obtained from two methods were found to be increased gently with increasing concentration of chromium(VI), implies that the IFE was continuously intensified as concentration of chromium(VI) increases, the suppressed fluorescence efficiency due to IFE ( $E_{\text{obsd}}$ ) always dominates and contributes effectively to the quenching and increases with concentration of quenching species, indicates that fluorescence quenching of MGCDs with chromium(VI) is mainly due to IFE [32]. All the values were calculated by both Lackowicz and Parker equations and are tabulated in **Table 4.3** and **Table 4.4**, respectively ( $s = 0.1$  cm,  $g = 0.4$  cm,  $d = 1.0$  cm).

Based on the above results, chromium(VI) sensing mechanism by the MGCDs nanoprobe through fluorescence quenching can be strongly attributed to IFE mechanism.

**Table 4.3:** Parameters used to calculate inner filter effect (IFE) of chromium(VI) on fluorescence of MGCDs based on Lackowicz equation

Chromium(VI) $\mu\text{M}$	$A_{\text{ex}}$	$A_{\text{em}}$	$F_{\text{obsd}}$	$F_{\text{corr}}$	$E_{\text{obsd}}$	$E_{\text{corr}}$	$\text{CF}^{\text{a}}$	$\frac{E_{\text{obsd}}}{E_{\text{corr}}}$
0	0.0245	0.0014	1555	1602	0	0	1.0277	0
4.76	0.0412	0.0049	1361	1435	0.1248	0.1042	1.0514	0.0205
9.09	0.0601	0.0083	1287	1392	0.1723	0.1310	1.0777	0.0412
16.66	0.1026	0.0119	1122	1280	0.2784	0.2009	1.1346	0.0775
20	0.1271	0.0154	1071	1262	0.3112	0.2122	1.1783	0.0990

**Table 4.4:** Parameters used to calculate inner filter effect (IFE) of chromium(VI) on fluorescence of MGCDs based on Parker equation

Chromium(VI) $\mu\text{M}$	$A_{\text{ex}}$	$A_{\text{em}}$	$F_{\text{obsd}}$	$F_{\text{corr}}$	$E_{\text{obsd}}$	$E_{\text{corr}}$	$\text{CF}^{\text{a}}$	$\frac{E_{\text{obsd}}}{E_{\text{corr}}}$
0	0.0245	0.0014	1555	1598	0	0	1.0277	0
4.76	0.0412	0.0049	1361	1431	0.1248	0.1045	1.0514	0.0203
9.09	0.0601	0.0083	1287	1387	0.1723	0.1320	1.0777	0.0403
16.66	0.1026	0.0119	1122	1273	0.2784	0.2034	1.1346	0.0750
20	0.1271	0.0154	1071	1252	0.3112	0.2165	1.1690	0.0947

#### 4.4 Conclusions

In summary an agro-biomass derived CDs were synthesised from mango ginger rhizomes through a completely greener route by one step microwave pyrolysis method, devoid of any other chemicals,



it was characterised by different methods. The excellent fluorescent property of prepared CDs is explored for the sensing applications. The studies clearly revealed that the prepared MGCDs can be executed as a selective, sensitive and rapid label free chromium(VI) sensor in water without any modifications. The sensing is based on fluorescence quenching through inner filter effect (IFE), with limit of detection in nanomolar range (84 nM) and maintained a linear response from 0  $\mu$ M – 33.33  $\mu$ M. This selectivity of MGCDs towards chromium(VI) is mainly due to the spectral overlap of excitation band of prepared nanoprobe with the UV-Vis absorption band of chromium(VI) in aqueous medium.

The sensing procedure illustrated in this work is simple, rapid and economical. Moreover it is highly environmentally benign one because no harsh chemicals were used in the entire processes, making it more impressive and more eco-friendly. Lower limits of detection, moderate linear range of detection, higher selectivity as well as sensitivity and fast responses are some salient features of this piece of work when compared to similar works reported in the literature. The present system is also successfully employed for sensing of chromium(VI) in real water samples with good recoveries.

## 4.5 References

- [1] R.S. Policegoudra, S.M. Aradhya, L. Singh, Mango ginger (*Curcuma amada* Roxb.) – A promising spice for phytochemicals and biological activities, *J Biosci.* 36 (2011) 739–748. <https://doi.org/10.1007/s12038-011-9106-1>
- [2] B. Sasikumar, Genetic resources of *Curcuma*: diversity, characterisation and utilization, *Plant Genetic Resources.* 3 (2005) 230–251. <https://doi.org/10.1079/PGR200574>
- [3] F. Baruthio, Toxic effects of chromium and its compounds, *Biol Trace Elem Res.* 32 (1992) 145–153. <https://doi.org/10.1007/BF02784599>
- [4] S. Prasad, K.K. Yadav, S. Kumar, N. Gupta, M.M.S. Cabral-Pinto, S. Rezania, N. Radwan, J. Alam, Chromium contamination and effect on environmental health and its remediation: A sustainable approaches, *J. Environ. Manage.* 285 (2021) 112174. <https://doi.org/10.1016/j.jenvman.2021.112174>
- [5] S. Zhang, L. Jin, J. Liu, Q. Wang, L. Jiao, A label-free yellow-emissive carbon dot-based nanosensor for sensitive and selective ratiometric detection of chromium (VI) in environmental water samples, *Mater. Chem. Phys.* 248 (2020) 122912. <https://doi.org/10.1016/j.matchemphys.2020.122912>
- [6] N.A. Azeez, S.S. Dash, S.N. Gummadi, V.S. Deepa, Nano-remediation of toxic heavy metal contamination: Hexavalent chromium [Cr(VI)], *Chemosphere.* 266 (2021) 129204. <https://doi.org/10.1016/j.chemosphere.2020.129204>
- [7] M. Zheng, Z. Xie, D. Qu, D. Li, P. Du, X. Jing, Z. Sun, On–Off–On Fluorescent Carbon Dot Nanosensor for Recognition of Chromium(VI) and Ascorbic Acid Based on the Inner Filter Effect, *ACS Appl. Mater. Interfaces.* 5 (2013) 13242–13247. <https://doi.org/10.1021/am4042355>
- [8] M.L. Liu, B.B. Chen, C.M. Li, C.Z. Huang, Carbon dots: synthesis, formation mechanism, fluorescence origin and sensing applications, *Green Chem.* 21 (2019) 449–471. <https://doi.org/10.1039/C8GC02736F>
- [9] B. De, N. Karak, A green and facile approach for the synthesis of water soluble fluorescent carbon dots from banana juice, *RSC Adv.* 3 (2013) 8286. <https://doi.org/10.1039/c3ra00088e>

- [10] R. Atchudan, T.N.J.I. Edison, D. Chakradhar, S. Perumal, J.-J. Shim, Y.R. Lee, Facile green synthesis of nitrogen-doped carbon dots using *Chionanthus retusus* fruit extract and investigation of their suitability for metal ion sensing and biological applications, *Sens. Actuators, B.* 246 (2017) 497–509. <https://doi.org/10.1016/j.snb.2017.02.119>
- [11] A. Pal, M. Palashuddin Sk, A. Chattopadhyay, Recent advances in crystalline carbon dots for superior application potential, *Mater. Adv.* 1 (2020) 525–553. <https://doi.org/10.1039/D0MA00108B>
- [12] V. Ramanan, S.K. Thiyagarajan, K. Raji, R. Suresh, R. Sekar, P. Ramamurthy, Outright Green Synthesis of Fluorescent Carbon Dots from Eutrophic Algal Blooms for In Vitro Imaging, *ACS Sustainable Chem. Eng.* 4 (2016) 4724–4731. <https://doi.org/10.1021/acssuschemeng.6b00935>.
- [13] H. Xu, X. Yang, G. Li, C. Zhao, X. Liao, Green Synthesis of Fluorescent Carbon Dots for Selective Detection of Tartrazine in Food Samples, *J. Agric. Food Chem.* 63 (2015) 6707–6714. <https://doi.org/10.1021/acs.jafc.5b02319>
- [14] P. Murugesan, J.A. Moses, C. Anandharamakrishnan, One step synthesis of fluorescent carbon dots from neera for the detection of silver ions, *Spectrosc. Lett.* 53 (2020) 407–415. <https://doi.org/10.1080/00387010.2020.1764589>
- [15] M. Wang, R. Shi, M. Gao, K. Zhang, L. Deng, Q. Fu, L. Wang, D. Gao, Sensitivity fluorescent switching sensor for Cr (VI) and ascorbic acid detection based on orange peels-derived carbon dots modified with EDTA, *Food Chem.* 318 (2020) 126506. <https://doi.org/10.1016/j.foodchem.2020.126506>
- [16] J. Peng, W. Gao, B.K. Gupta, Z. Liu, R. Romero-Aburto, L. Ge, L. Song, L.B. Alemany, X. Zhan, G. Gao, S.A. Vithayathil, B.A. Kaiparettu, A.A. Marti, T. Hayashi, J.-J. Zhu, P.M. Ajayan, Graphene Quantum Dots Derived from Carbon Fibers, *Nano Lett.* 12 (2012) 844–849. <https://doi.org/10.1021/nl2038979>
- [17] N. Javed, D.M. O’Carroll, Long-term effects of impurities on the particle size and optical emission of carbon dots, *Nanoscale Adv.* 3 (2021) 182–189. <https://doi.org/10.1039/D0NA00479K>
- [18] M. Batool, H.M. Junaid, S. Tabassum, F. Kanwal, K. Abid, Z. Fatima, A.T. Shah, Metal Ion Detection by Carbon Dots—A Review, *Critical*

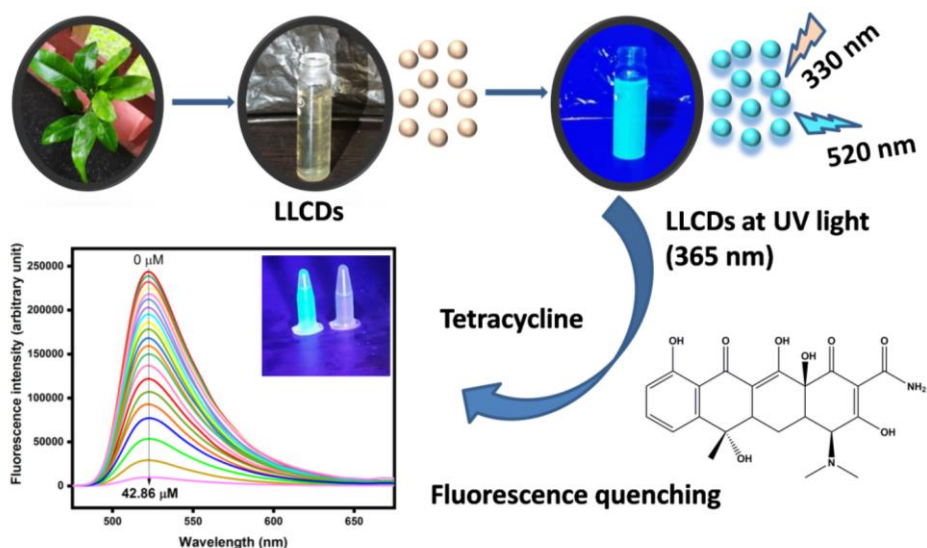
- Reviews in Analytical Chemistry. (2020) 1–12.  
<https://doi.org/10.1080/10408347.2020.1824117>
- [19] H. Zhang, Y. Huang, Z. Hu, C. Tong, Z. Zhang, S. Hu, Carbon dots codoped with nitrogen and sulfur are viable fluorescent probes for chromium(VI), *Microchim. Acta.* 184 (2017) 1547–1553.  
<https://doi.org/10.1007/s00604-017-2132-4>
- [20] D. Tai, C. Liu, J. Liu, Facile synthesis of fluorescent carbon dots from shrimp shells and using the carbon dots to detect chromium(VI), *Spectrosc. Lett.* 52 (2019) 194–199.  
<https://doi.org/10.1080/00387010.2019.1607879>
- [21] H. Yang, L. He, Y. Long, H. Li, S. Pan, H. Liu, X. Hu, Fluorescent carbon dots synthesised by microwave-assisted pyrolysis for chromium(VI) and ascorbic acid sensing and logic gate operation, *Spectrochim. Acta, Part A.* 205 (2018) 12–20.  
<https://doi.org/10.1016/j.saa.2018.07.015>
- [22] C. Sakaew, P. Sricharoen, N. Limchoowong, P. Nuengmatcha, C. Kukulamude, S. Kongsri, S. Chanthai, Green and facile synthesis of water-soluble carbon dots from ethanolic shallot extract for chromium ion sensing in milk, fruit juices, and wastewater samples, *RSC Adv.* 10 (2020) 20638–20645. <https://doi.org/10.1039/D0RA03101A>
- [23] S. Bhatt, M. Bhatt, A. Kumar, G. Vyas, T. Gajaria, P. Paul, Green route for synthesis of multifunctional fluorescent carbon dots from Tulsi leaves and its application as Cr (VI) sensors, bio-imaging and patterning agents, *Colloids and Surfaces B: Biointerfaces.* 167 (2018) 126. <https://doi.org/10.1016/j.colsurfb.2018.04.008>
- [24] A. Tyagi, K.M. Tripathi, N. Singh, S. Choudhary, R.K. Gupta, Green synthesis of carbon quantum dots from lemon peel waste: applications in sensing and photocatalysis, *RSC Adv.* 6 (2016) 72423–72432.  
<https://doi.org/10.1039/C6RA10488F>
- [25] G. Hu, L. Ge, Y. Li, M. Mukhtar, B. Shen, D. Yang, J. Li, Carbon dots derived from flax straw for highly sensitive and selective detections of cobalt, chromium, and ascorbic acid, *J. Colloid Interface Sci.* 579 (2020) 96–108. <https://doi.org/10.1016/j.jcis.2020.06.034>
- [26] H. Wang, S. Liu, Y. Xie, J. Bi, Y. Li, Y. Song, S. Cheng, D. Li, M. Tan, Facile one-step synthesis of highly luminescent N-doped carbon dots as an efficient fluorescent probe for chromium( VI ) detection based on the

- inner filter effect, *New J. Chem.* 42 (2018) 3729–3735.  
<https://doi.org/10.1039/C8NJ00216A>
- [27] R. Vaz, J. Bettini, J.G.F. Júnior, E.D.S. Lima, W.G. Botero, J.C.C. Santos, M.A. Schiavon, High luminescent carbon dots as an eco-friendly fluorescence sensor for Cr(VI) determination in water and soil samples, *J. Photochem. Photobiol., A* 346 (2017) 502–511.  
<https://doi.org/10.1016/j.jphotochem.2017.06.047>
- [28] F. Zu, F. Yan, Z. Bai, J. Xu, Y. Wang, Y. Huang, X. Zhou, The quenching of the fluorescence of carbon dots: A review on mechanisms and applications, *Microchim. Acta.* 184 (2017) 1899–1914.  
<https://doi.org/10.1007/s00604-017-2318-9>
- [29] Y. Qiu, D. Gao, H. Yin, K. Zhang, J. Zeng, L. Wang, L. Xia, K. Zhou, Z. Xia, Q. Fu, Facile, green and energy-efficient preparation of fluorescent carbon dots from processed traditional Chinese medicine and their applications for on-site semi-quantitative visual detection of Cr(VI), *Sens. Actuators, B* 324 (2020) 128722.  
<https://doi.org/10.1016/j.snb.2020.128722>
- [30] P. Li, Y. Hong, H. Feng, S.F.Y. Li, An efficient “off-on” carbon nanoparticle-based fluorescent sensor for recognition of chromium(VI) and ascorbic acid based on the inner filter effect, *J. Mater. Chem. B* 5 (2017) 2979–2988. <https://doi.org/10.1039/C7TB00017K>
- [31] S. Kumar Panigrahi, A. Kumar Mishra, Inner filter effect in fluorescence spectroscopy: As a problem and as a solution, *J. Photochem. Photobiol., C* 41 (2019) 100318.  
<https://doi.org/10.1016/j.jphotochemrev.2019.100318>
- [32] F. Yan, Z. Sun, T. Ma, X. Sun, J. Xu, R. Wang, L. Chen, Ratiometric fluorescent nanoprobe based on Resonance Rayleigh Scattering and inner filter effect for detecting alizarin red and Pb<sup>2+</sup>, *Spectrochim. Acta, Part A* 228 (2020) 117843.  
<https://doi.org/10.1016/j.saa.2019.117843>



# Chapter 5

## WILD LEMON LEAVES DERIVED CARBON DOTS



*This work is published in Spectrochimica Acta Part A: Molecular and Biomolecular Spectroscopy.*

P. Venugopalan and N. **Vidya**, Microwave-assisted green synthesis of carbondots derived from wild lemon (*Citrus pennivesiculata*) leaves as a fluorescent probe for tetracycline sensing in water, *Spectrochimica Acta Part A: Molecular and Biomolecular Spectroscopy*, 286(2023),122024.

<https://doi.org/10.1016/j.saa.2022.122024>





## 5.1 Introduction

As discussed in Chapter 2, natural products based carbon dots recently received commendable importance than the other organic precursor based systems. It is basically owing to its nontoxicity, renewability, bioavailability, low-cost and greener nature[1,2]. In the present work, a partially biowaste material, wild lemon (*Citrus pennivesiculata*) leaves were used as precursor for the synthesis of CDs.

It is well established that lemon fruit can be successfully used for CDs synthesis [3]. By literature, the leaves of lemon and lemon shares major of its constituents and possessing variety of medicinal values [4], hence the materialization of this partially wasting highly available precursor through completely greener and facile method, imparting value addition to the precursor.

The present chapter dealing with the synthesis, characterisation and application of CDs derived from this partially biowaste material through microwave heating as the method of preparation. The as prepared system is designated as LLCs and was characterised by transmission electron microscopy, fluorescent, UV-Vis absorption, Fourier transform infrared and Raman spectroscopic techniques.

From the selectivity studies of LLCs with different metal ions, anions, biomolecules, and antibiotics, a significant quenching in the native fluorescence of LLCs was observed

with tetracycline antibiotic. Based on this observation further studies was conducted with tetracycline.

Tetracycline has been considered as the most widely used antibiotics; it belongs to broad-spectrum antibiotics and acts effectively against both Gram-positive as well as Gram-negative bacteria. Nevertheless, tetracycline absorption is comparatively difficult for animal metabolism. So most them are excreted to the nature as in the form of parental compound [5,6]. The unrestrained uses of tetracycline and its releases to the nature constitute major threat to environmental system. The tetracycline excretion created by human as well as animals primarily pollutes the water bodies, since most of such wastes finally reach to the water system. Use as growth promoter in the farming fields extremely enlarges the issue and the water sources near these farms are highly affected. In spite of the fact that tetracycline is not easily causes chronic toxicity in typical circumstances, durable exposure to the tetracycline contaminated water has been leads to acute toxicity in non-targeted beings [5]. These antibiotic residues are heavily toxics to microbes and it can accumulate in the different organs of the body and leads to several diseases like, allergies, gastrointestinal diseases, nephrotoxicity and severe reactions in central nervous system and blood [7]. Hence, trace level detection of tetracycline in water system is reckoned with significant importance for the protection of health and environment.

Based on the selective interaction of tetracycline with LLCs, a simple and cost effective analytical method was proposed to detect tetracycline in water with satisfactory parameters. The mechanism of quenching was also investigated through various experiments. Furthermore, the same method has been practically applied for tetracycline detection in natural water resources with acceptable recoveries. The next sections address the experimental approaches and results.

## **5.2 Experimental**

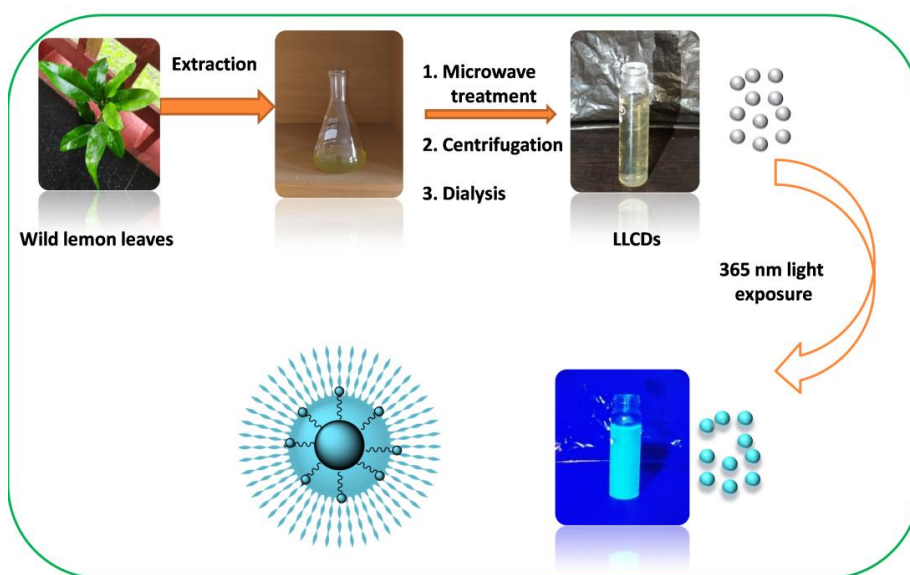
### **5.2.1 Synthesis of LLCs**

LLCs were prepared by a facile, one step microwave pyrolysis method with aqueous extract of wild lemon leaves as precursor. The entire preparation process is described below.

About 30 g of cleaned wild lemon leaves were crushed with domestic grinder and then by mortar and pestle, it was transferred to a beaker with 30 mL hot water and subjected to stirring by the aid of magnetic stirrer for 30 minutes of time. After filtration and centrifugation of 10 minutes, 30 mL of the supernatant solution was exposed to microwave irradiation for 20 minutes at 500 W with periodic cooling in each 5 minutes. The resulting dried residue was magnetically stirred for 5 minutes with 30 mL of distilled water and filtered off. Afterwards, the as obtained solution was centrifuged at 1500 rpm for 20 minutes. The clear pale yellow coloured supernatant liquid

was then subjected to dialysis against distilled water for 48 hours by a dialysis membrane with molecular cut off 3 KDa.

The solution emitting bright greenish blue fluorescence under UV light denotes the formation of CDs. The obtained solution was stored at 4 °C. The preparation of LLCs is depicted in **Scheme 5.1**.



**Scheme 5.1:** Synthesis of LLCs

### 5.2.2 Detection of tetracycline

Fluorescence behaviour of the CDs was studied by recording the fluorescence spectra at excitation of 330 nm, with emission maxima centred at 520 nm. The procedure for the quenching studies on LLCs with tetracycline is as follows: 2 mL of the LLCs solution was introduced in to the quartz

cuvette, fluorescence spectrum was recorded at an excitation of 330 nm. Afterwards a definite amount of tetracycline solution was added by the aid of micropipette, after an incubation of 2 minutes the corresponding fluorescence spectrum was recorded. The same procedure was repeated with different concentration of tetracycline solution in ascending manner and fluorescence spectra were recorded in every time at the same excitation wavelength.

The selectivity studies on the system were carried out by introducing 100  $\mu\text{L}$  of 1 mM solutions of different foreign substances including biomolecules (urea, glucose, ascorbic acid, alanine, phenyl alanine, aspartic acid, leucine, valine), anions ( $\text{Cl}^-$ ,  $\text{SO}_4^{2-}$ ,  $\text{NO}_3^-$ ,  $\text{CN}^-$ ,  $\text{Br}^-$ ,  $\text{I}^-$ ,  $\text{CO}_3^{2-}$ ), metal ions ( $\text{K}^+$ ,  $\text{Zn}^{2+}$ ,  $\text{Na}^+$ ,  $\text{Mn}^{2+}$ ,  $\text{Cd}^{2+}$ ,  $\text{Ca}^{2+}$ ,  $\text{Pb}^{2+}$ ,  $\text{Co}^{2+}$ ,  $\text{Hg}^{2+}$ ,  $\text{Cu}^{2+}$ ,  $\text{Fe}^{3+}$ ) and antibiotics (florfenicol, streptomycin and sulfamerazine) in absence and presence of tetracycline to 2 mL of LLCs. The selectivity investigations also follow the same procedure of quenching studies. The corresponding effect on fluorescence behaviour was monitored by recording the spectra at an excitation wavelength of 330 nm.

### **5.2.3 Environmental water analysis**

Water samples were collected from the river and pond, filtered to remove impurities and followed by centrifugation at 1500 rpm for 20 minutes of time. To detect the tetracycline in real samples, pre-treated water samples were spiked with

different concentration of standard tetracycline solutions and were introduced to LLCs solution. Briefly 10  $\mu\text{L}$  of standard tetracycline solution (498, 998, 1454  $\mu\text{M}$ ) was primarily added to 1 mL of pre-treated water sample and then mixed with 1 mL of the probe solution and after incubation of 2 minutes the fluorescence spectrum of the probe with spiked sample was recorded, again 10  $\mu\text{L}$  of tetracycline solution was added to the same solution and fluorescence was monitored the process was continued till the total volume of added tetracycline was about 100  $\mu\text{L}$ . The same procedure was followed for all the three different concentrations of tetracycline in each environmental sample. The fluorescence spectra of the probe with tetracycline spiked water samples were recorded using the same instrument and conditions as above.

## **5.3 Results and discussions**

### **5.3.1 Formation of LLCs**

LLCs were synthesised by the microwave heating of the green wild lemon leaves. The water extract of the leaves contains plenty of acids and several carbohydrates [4]. The exact formation mechanism of carbon dots from organic compounds is still obscure in nature. As per the proposed mechanism, the microwave irradiation initiates the bottom-up synthesis of carbon nano materials from the small molecules present in the extract. In short, the microwave irradiation enables the carbohydrates in the extract to go through a variety of chemical processes like

hydrolysis, dehydration, and decomposition. The polyphenolic acids included in the extract, especially the precursor is enriched with ascorbic and citric acids promote these processes. The above reactions generally result in the formation of furfural derivatives, which then go through a series of reactions, including self-condensation and reactions with other reactive molecules in the system, which result in the formation of various products, some of which may go through a polymerisation reaction. Condensation and aromatisation of these polymerised products leads to the formation of carbon clusters, which are then converted into fluorescent CDs by the cluster's nuclear explosion. All processes are accelerated by microwave radiation in a short amount of time. The acidic groups, and other functional groups present in the precursor plays an important role in the formation process [8,9].

### **5.3.2 Characterisation**

The chemical as well as optical properties of the LLCs were explored using the following analysis.

#### **TEM and DLS analysis**

TEM images were directly utilised to detect the morphology and particle size of the LLCs. As seen in **Figure 5.1** they possess almost spherical character and the average size and particle size distribution of the prepared LLCs was determined through the dynamic light scattering (DLS) analysis

and it was about 4.08 nm and 1.62 nm to 8.16 nm, respectively. The corresponding curve was displayed in **Figure 5.1(d)**. The crystallographic nature of the LLCs was primarily confirmed from the SAED pattern. Since the SAED pattern having neither clear design nor bright spots, implies that the prepared LLCs having very poor crystalline nature or it is nearly amorphous [10].

### **Raman and FTIR spectral analysis**

Raman spectrum of the LLCs displayed in **Figure 5.2**, exhibits two strong peaks. The band at  $1339\text{ cm}^{-1}$  representing the D band whereas band at  $1572\text{ cm}^{-1}$  was attributed to G band. Both the bands are found to be broader and this broad nature also supports the poor crystalline as well as lesser graphitization nature of the prepared LLCs [11].

FTIR spectrum was used to reveal the surface functionalities associated with the prepared LLCs. As seen in **Figure 5.3**, a strong broad band centred at  $3274\text{ cm}^{-1}$  is ascribed to O-H stretching vibrations and small bands at  $2918\text{ cm}^{-1}$ ,  $2825\text{ cm}^{-1}$  representing C-H stretching where as one at  $925\text{ cm}^{-1}$  attributed to C-H bending vibrations [12]. A shoulder peak at  $1632\text{ cm}^{-1}$  could be ascribed to C=C stretching vibration, and band at  $1051\text{ cm}^{-1}$  assigned to C-O stretching vibrations of carboxylic as well as alcoholic functionalities. In addition, bands at  $1556\text{ cm}^{-1}$  and  $1401\text{ cm}^{-1}$  was arises due to symmetric and asymmetric stretching vibrations associated with  $\text{COO}^-$  [13]. The



above results implies that LLCs surface contains mainly  $\text{-OH}$ ,  $\text{-COOH}$ ,  $\text{C-O}$  and  $\text{C=C}$  functionalities [14]. Thus the FTIR spectrum disclose that LLCs surface consists of hydroxyl and carboxyl groups and being hydrophilic these groups also contributes toward the water solubility and stability of the system in water.

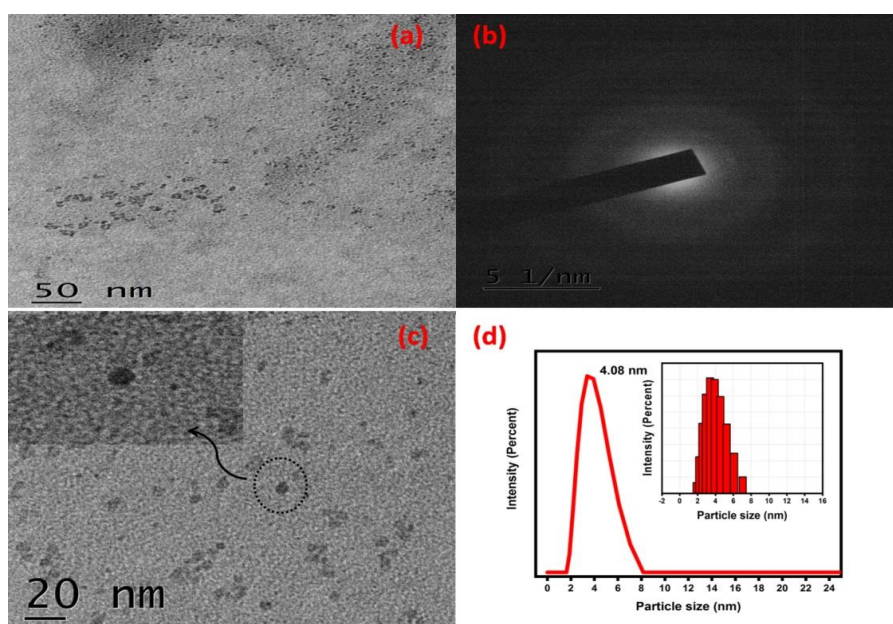


**Figure 5.1:** (a): Transmission electron microscopy (TEM) image of LLCs; (b) : The selected area electron diffraction (SAED) pattern; (c): TEM image at lower scale; (d): Dynamic light scattering size distribution curve of LLCs

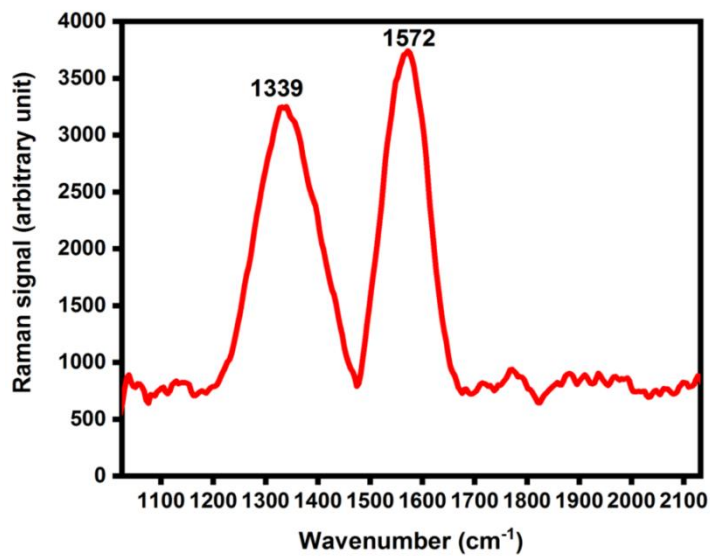


**Figure 5.2:** Raman spectrum of LLCs

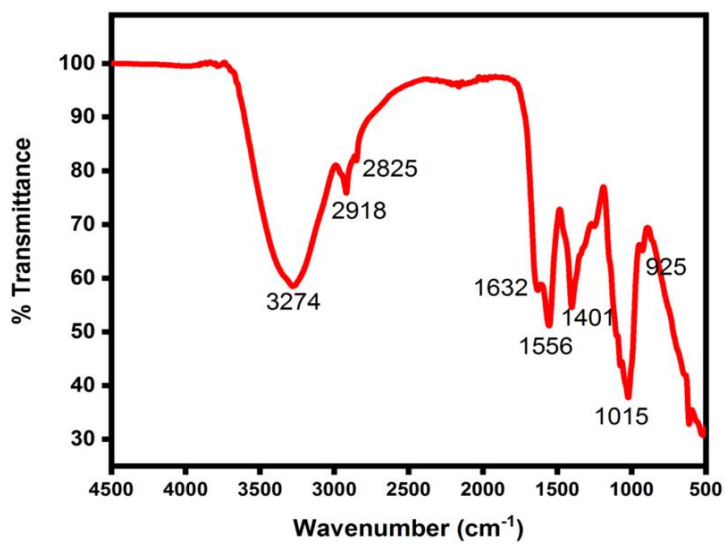


**Figure 5.3:** FTIR spectrum of LLCs

### UV-Vis spectral analysis

The UV-Vis spectrum of the LLCs (Figure 5.4) has three shoulders at 207, 268, and 315 nm. The first two peaks were ascribed to  $\pi$ - $\pi^*$  transitions of C=C bonds whereas the third one assigned to n- $\pi^*$  transition of C=O bonds present at the surface of LLCs [15]. Multi absorption transition modes may be the reason for the weak and asymmetric shoulder peaks [16].

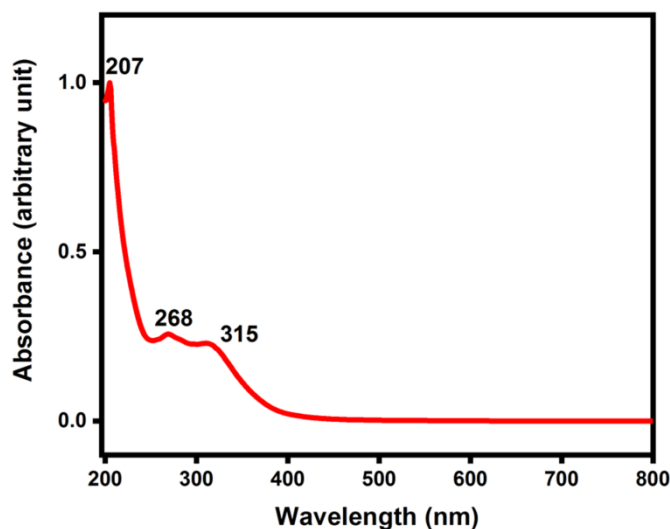


**Figure 5.4:** UV-Vis absorbance spectrum of LLCs

### Fluorescence spectral analysis

The fluorescence spectrum of the LLCs is shown in Figure 5.5, exhibiting emission maxima centred at 520 nm when excited at 330 nm. The present system shows excitation dependent fluorescence behaviour and it was evaluated by monitoring fluorescence spectra of the LLCs recorded at different excitation wavelength (300 – 410 nm). The results of

the same were depicted in **Figure 5.6**. The variation in the intensity and emission maxima of the LLCs, when excited at different wavelength may ascribed to polydispersity and surface functionalities of LLCs [17]. From the excitation dependence study it is clear that the system possessing highest intensity when excited at 330 nm and its emission spectra was centred at 520 nm and these values are opted as excitation and emission wavelength of the LLCs, respectively. The corresponding excitation and emission peaks were shown in **Figure 5.7**.

The prepared LLCs showing bright greenish blue fluorescence in UV lamp of 365 nm, and is given in the inset of **Figure 5.5**.

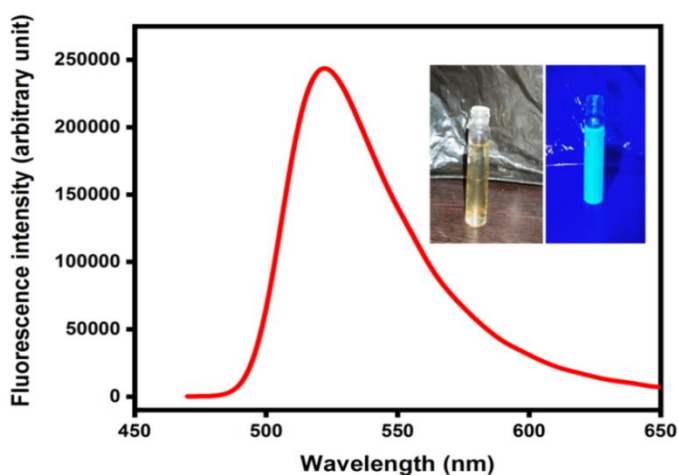


**Figure 5.5:** Fluorescence spectrum of LLCs (inset shows photographs of LLCs solution under normal light (left) and UV light (right))

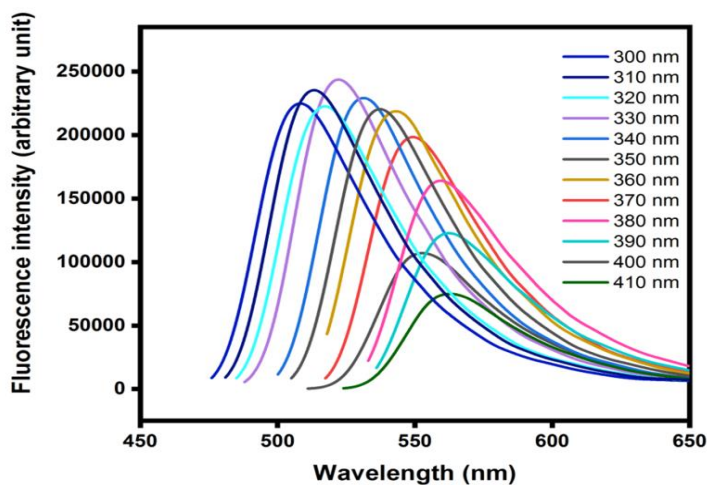


**Figure 5.6:** Excitation dependent spectra of LLCs

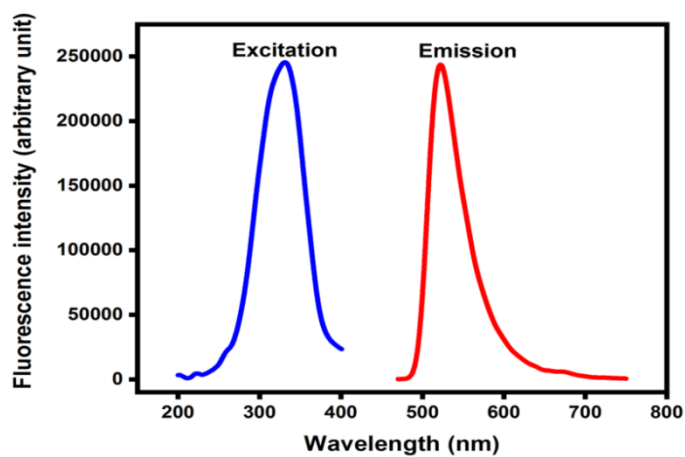


**Figure 5.7:** Excitation and emission spectra of LLCs

### 5.3.3 Fluorescence quantum yield and fluorescence stability of LLCs

The fluorescence quantum yield (QY) of LLCs was found to be about 7.2 % as calculated by the standard method

with quinine sulphate in 0.1 M H<sub>2</sub>SO<sub>4</sub> with 54% quantum yield as standard. The method of calculation of QY was given in Chapter 3.

The effect of storage time and conditions on fluorescence stability of prepared system was studied. **Figure 5.8** shows the normalized fluorescence intensity of the system vs. time of storage (sample was stored at 4 °C). The system has only infinitesimal changes even after 10 weeks of time, revealing that, it exhibits strong resistance against photo bleaching. The intensity of the LLCs were gradually declined as it was stored at above 25 °C, however it is stable up to one week. The instability at this temperature may attributed to increased tendency for aggregation of particles, leads to particle size increment [18].

Moreover, the system was subjected to continuous UV irradiation to study fluorescence stability under UV light of 365 nm lamp inside the UV cabinet, and it was stable up to 2 hours after that the fluorescence intensity was slowly reduced.

The fluorescence stability of as prepared LLCs was also investigated in variable ionic strength. The fluorescence intensity of the LLCs almost same in different concentration of KCl and is shown in **Figure 5.9**, indicates that the system was stable at higher ionic strength, and thus ensure that it can be applicable in distinct ionic conditions. The obtained results suggested that, the system exhibits admirable fluorescent stability.

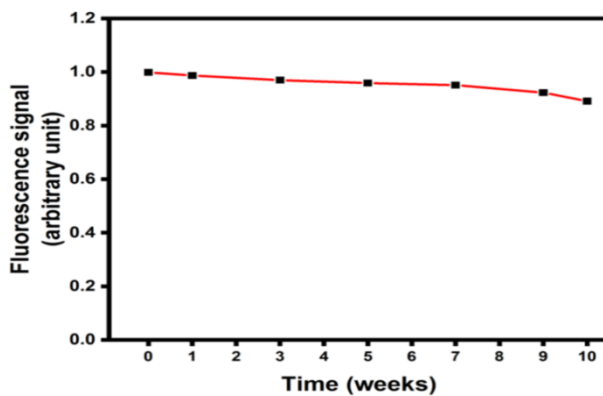


**Figure 5.8:** Variation fluorescence intensity of LLCs with storage time

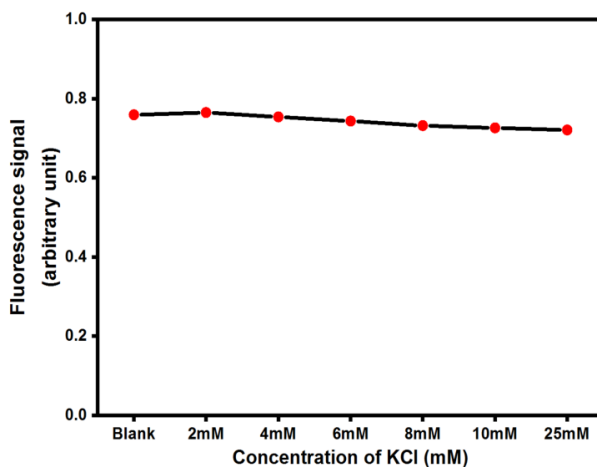


**Figure 5.9:** Variation of fluorescence intensity with ionic strength (with different concentration of KCl)

### 5.3.4 Selectivity studies

In virtue of superior fluorescent behaviour of the prepared system, it was tested whether it can be applied as a fluorescent probe or not. To study the selectivity of the LLCs, several biomolecules, anions, metal ions and some of the antibiotics which are widely used in aquaculture and veterinary farms

including tetracycline were used for this purpose. The results of the selectivity study reveals that the native fluorescence of the present system significantly reduced by the addition of tetracycline antibiotics. Interference studies were also conducted to ensure this selectivity with tetracycline.

Relative fluorescence response of LLCs in presence and absence of tetracycline with these substances was given in **Figure 5.10**. It clearly reveals that the fluorescence of the LLCs get reduced predominantly by the addition of tetracycline. However  $\text{Fe}^{3+}$  and  $\text{Cu}^{2+}$  exerts small quenching behaviour and is may be attributed to the interaction of these metal ions with the surface functionalities of CDs and this quenching percentage is very small as compared with that of tetracycline [19]. By the addition of  $\text{Fe}^{3+}$  and  $\text{Cu}^{2+}$  about 19 % and 12 % reduction in the native fluorescence of the probe was observed, similarly florfenicol and streptomycin causes about 19 % reduction in fluorescence and this may be due to the hydrogen bond formation with the surface functionalities [20]. But the same time it is about 40 % in the case of tetracycline. All others exert minute and negligible quenching effect. Even though, none of these substances exerts significant interference in tetracycline detection and is clear from the interference studies.

### **5.3.5 Sensing studies with tetracycline**

Since the fluorescence of LLCs selectively quenched by the addition tetracycline, further sensing studies with tetracycline were carried out.



In addition to the above mentioned moieties, other antibiotics belongs to tetracycline class were also tested and all were shows similar quenching effects (**Figure 5.11**). Therefore, tetracycline was opted as a representative of the tetracycline antibiotic family.

The sensitivity of the system towards tetracycline was studied by recording the fluorescence spectra of LLCs with different concentration of tetracycline solution (0- 42.86  $\mu\text{M}$ ). The spectra showing quenching of fluorescence by addition of tetracycline was displayed in **Figure 5.12**, the inset of the same figure representing the LLCs solution before and after the addition of tetracycline, the fluorescence quenching is very clear from the photographs.

Moreover, the fluorescence quantum yield of the LLCs solution with tetracycline was also determined by the same method as used for quantum yield calculation and is found to be 2.5 % by using quinine sulphate as reference standard solution. The decrease of fluorescence quantum yield of LLCs from 7.2 % to 2.5 % by the addition of 42.86  $\mu\text{M}$  of tetracycline solution, indicate the formation of non-fluorescent species within the system.

To study the relationship between fluorescence intensity signals with concentration of quencher, a plot of  $F_0/F$  with concentration of tetracycline in  $\mu\text{M}$  was plotted and was shown in **Figure 5.13**, where  $F_0$  and  $F$  are the fluorescence intensity of LLCs and LLCs with tetracycline, respectively. It reveals that

the  $F_0/F$  ratio was proportionally increased with increasing concentrations of tetracycline. This curve is found to be linear from 0 to 27.27  $\mu\text{M}$  of tetracycline with  $R^2=0.9979$ .

The limit of detection (LOD) of the probe was calculated from the linear part of the plot by considering  $S/N$  ratio as 3 by using the equation  $3\sigma / \kappa$ , where  $\sigma$  is the standard deviation of the measurements and  $\kappa$  is the slope obtained from the linear equation ( $F_0/F = 0.07242 C_{\text{TC}} + 0.9664$ ) and it was about 0.42  $\mu\text{M}$ . These parameters were found to be comparable with recent reports, and some of the very recent works are tabulated in **Table 5.1**.

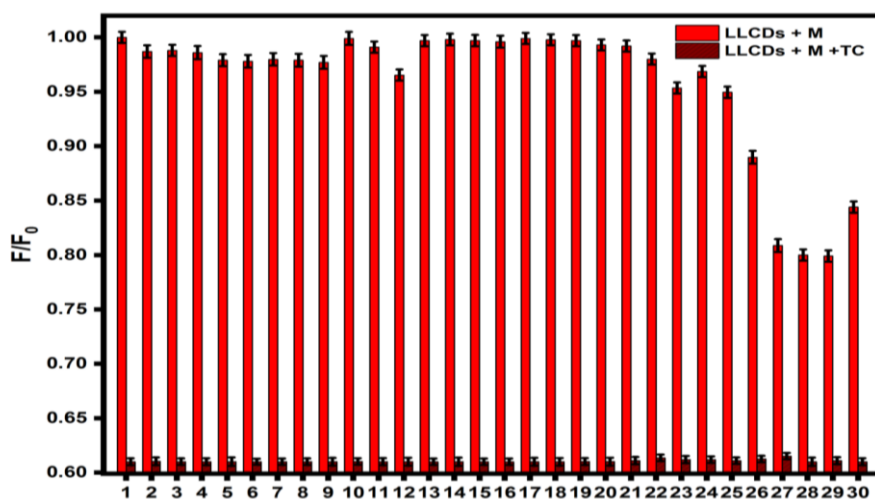


**Figure 5.10:** Relative fluorescence intensity of LLCs in absence and presence of tetracycline with different foreign substances (from 1 to 30: LLCs, urea, glucose, ascorbic acid, alanine, phenyl alanine, aspartic acid, leucine, valine,  $\text{Cl}^-$ ,  $\text{SO}_4^{2-}$ ,  $\text{NO}_3^-$ ,  $\text{CN}^-$ ,  $\text{Br}^-$ ,  $\text{I}^-$ ,  $\text{CO}_3^{2-}$ ,  $\text{K}^+$ ,  $\text{Zn}^{2+}$ ,  $\text{Na}^+$ ,  $\text{Mn}^{2+}$ ,  $\text{Cd}^{2+}$ ,  $\text{Ca}^{2+}$ ,  $\text{Pb}^{2+}$ ,  $\text{Co}^{2+}$ ,  $\text{Hg}^{2+}$ ,  $\text{Cu}^{2+}$ ,  $\text{Fe}^{3+}$ , florfenicol, streptomycin and sulfamerazine)

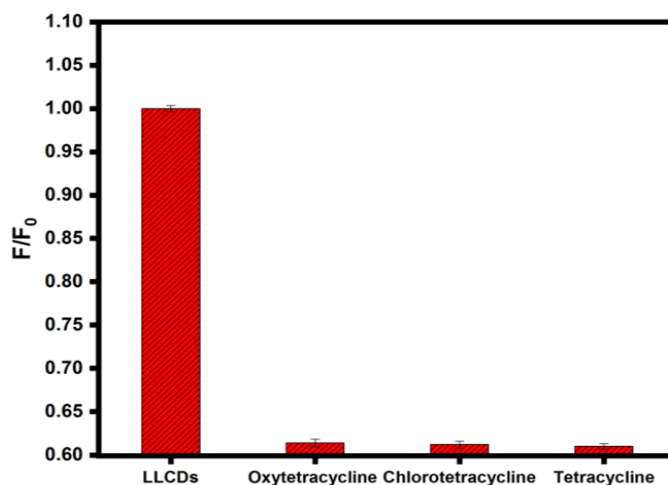


**Figure 5.11:** Relative fluorescence response of LLCs with different tetracycline antibiotics (oxytetracycline, chlorotetracycline and tetracycline)

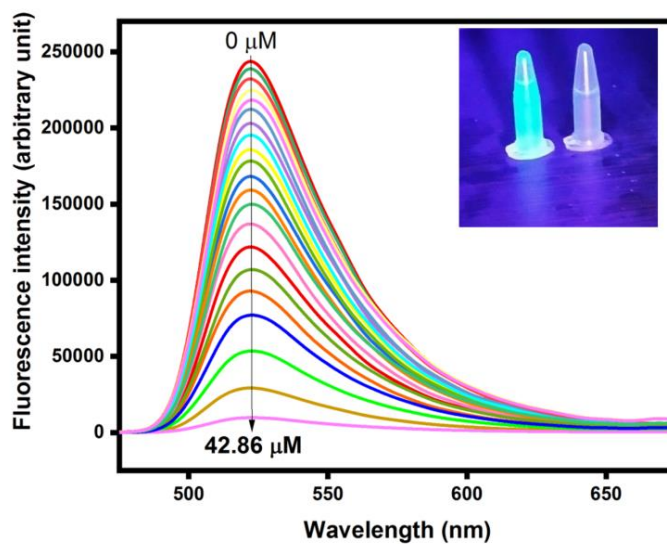


**Figure 5.12:** Steady decrease of fluorescence intensity with increasing concentration of LLCs (inset displays photographs of LLCs before (left) and after (right) the addition of tetracycline)

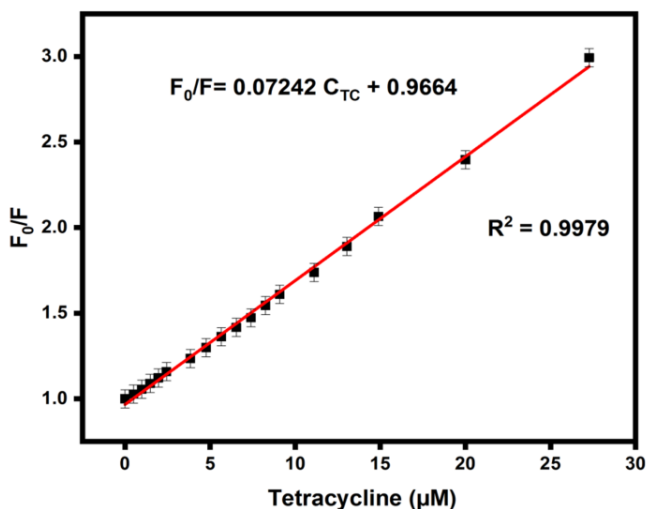


**Figure 5.13:** Plot of relative fluorescence  $F_0/F$  intensity with tetracycline solution

**Table 5.1:** Comparison of different CDs based sensors for tetracycline detection

Sensing probe for the detection of tetracycline	LOD ( $\mu\text{M}$ )	Linear range ( $\mu\text{M}$ )	Reference
CDs from resazurin and urea	0.0385	3–40	[21]
CDs from egg white	0.0323	0.1–200	[22]
CDs from red beet pigment	0.36	0.5–30	[23]
CDs from citric acid and D-penicillamine	0.072	0.2–70	[24]
CDs from pomelo peel	0.045	0–100	[25]
CDs from Glutathione and citric acid	0.56	1.88–60	[26]
CDs from wild lemon leaves	0.42	0–27.27	This work

On the basis of above study results, the present system can be employed as magnificent candidate for detection of tetracycline in environmental water samples.

### **5.3.6 Determination of tetracycline in environmental water samples**

With regard to the tetracycline activated fluorescence quenching, LLCs were successfully applied to detect tetracycline in real water samples. River water from Nila river and nearby pond water was selected as the environmental samples for the analysis. The real water analysis follows standard addition method. Fluorescence spectra of the water samples were recorded after the pre-treatment without tetracycline, then the samples were spiked with different concentration of tetracycline in  $\mu\text{M}$ . Afterwards the fluorescence spectra of the samples with LLCs nanoprobe were recorded, and fluorescence intensity in each measurement was carefully monitored. Results from the analysis are given in **Table 5.2** and the recovery and error % of the analysis was calculated by the standard equation (Given in Chapter 3) and values are ranging from 95.56 to 101.96, and 0.97- 4.43, respectively. The obtained recovery percentage is highly acceptable and more accurate and the error percentages are less on comparing with similar assays [16]. Hence, the good level of statistical parameters implies that the suggested method may provide accurate and reliable results in determination of tetracycline in water samples.

**Table 5.2:** Detection of tetracycline in different water samples

Water sample	Added tetracycline ( $\mu\text{M}$ )	Found ( $\mu\text{M}$ )	Recovery (%)	Error (%)
River water	0	Not Found	--	--
	2.48	2.37	95.56	4.43
	4.97	4.80	96.57	3.42
	7.23	7.37	101.93	1.93
Pond water	0	Not Found	--	--
	2.48	2.39	96.37	3.62
	4.97	4.82	96.98	3.02
	7.23	7.30	100.96	0.97

### 5.3.7 Fluorescence quenching mechanism

As stated earlier the natural fluorescence of LLCs was reduced by addition of tetracycline to the working solution after an incubation of 2 minutes. A number of experiments were carried out to investigate the underlying mechanism of this quenching. In general fluorescence quenching follows five major mechanisms, named as inner filter effect (IFE), dynamic quenching, static quenching, Förster resonance energy transfer (FRET) and photo-induced electron transfer (PET) [27].

Primarily, the chance of inner filter effect was investigated. The present system and quencher does not follow the essential condition for IFE; there no effective overlapping between neither excitation, nor emission spectra of LLCs with absorption spectrum of tetracycline in water.

To further explore the nature of quenching, the fluorescence decay studies were conducted by recording decay spectra of LLCs without and with tetracycline. The results were shown in **Figure 5.14**. The average lifetimes were calculated (As per the equation given in Chapter 3) from the above decay profiles and the obtained values were 7.80 and 7.62 ns, respectively. Reveals that the mechanism was not belongs to FRET, PET or dynamic quenching, since all of them resulting significant change in average lifetime [15,27].

Furthermore, investigation on quenching mechanism was conducted by recording UV-Vis spectra of LLCs, tetracycline, LLCs with tetracycline (LLCs@TC). The results shown in **Figure 5.15**, the summed spectrum does not match with the LLCs@TC spectrum. There are absorption changes to the system on addition of tetracycline. Specifically, it was noted that the tetracycline intensity at around 365 nm was altered and it may be the result of the interaction between LLCs with tetracycline. Besides, there exists a small peak at around 388 nm in the LLCs@TC spectrum, which is not present in LLCs or tetracycline spectrum. These results could indicate the formation of a ground state complex between LLCs and tetracycline.

Altogether the sensing nature of the LLCs with tetracycline meets almost all criteria of static quenching mechanism. As per the static mechanism, a non-fluorescent complex will be formed when a ground state fluorophore (here LLCs) interact with a quencher. Finally, all the results from above discussions guided to the fact that the mechanism behind

the quenching of native fluorescence of LLCs by tetracycline mainly having static quenching nature [16].

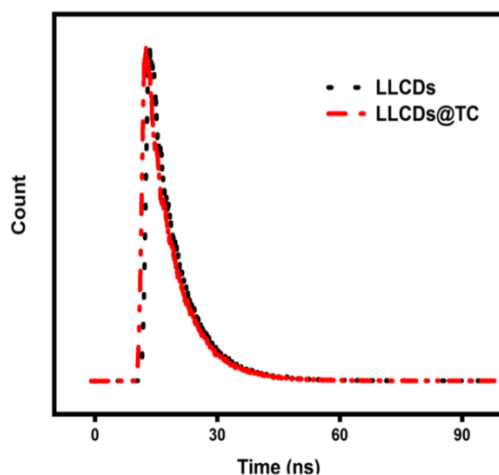


**Figure 5.14:** Fluorescent decay spectra of LLCs and LLCs with tetracycline (LLCs@TC)

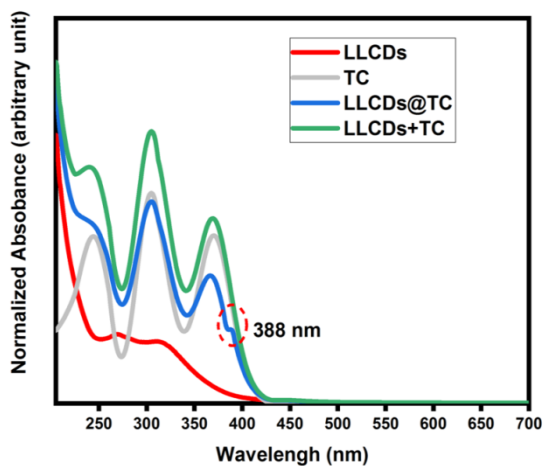


**Figure 5.15:** UV-Vis spectra of LLCs, tetracycline, LLCs with tetracycline (LLCs@TC) and summed spectra of LLCs and tetracycline (LLCs+TC)



## 5.4 Conclusions

In summation, a biogenic, highly fluorescent carbon dots were synthesised by a truly greener methodology through a single step microwave heating process. The nature based precursor wild lemon leaves solely used as the source for the preparation. The as obtained LLCs manifested several excellent features and were explored through various characterisation methods. Investigation results display the selective and sensitive interaction of LLCs with tetracycline antibiotic. The sensing of tetracycline via fluorescence quenching shows comparatively lower limit of detection (0.42  $\mu\text{M}$ ) and maintain a good linear response with concentration of tetracycline.

The quenching was further examined by different methods and finally ascribed to static fluorescence quenching mechanism. Based on this, a simple and facile analytical method was illustrated for the detection of tetracycline in water systems. The synthesis as well as sensing procedures strictly follows green chemistry protocols. The designing of label-free fluorescent probe for the detection of tetracycline in aquatic environment has been done without using any hazardous chemicals or expensive instruments. The real water analysis shows comparatively good statistical parameters. In short, a highly fluorescent, biocompatible, label-free nanoprobe was developed without any chemical reagents in an easiest way and was successfully employed for tetracycline detection in environmental water samples with good recoveries.

## 5.5 References

- [1] T.C. Wareing, P. Gentile, A.N. Phan, Biomass-Based Carbon Dots: Current Development and Future Perspectives, *ACS Nano*. 15 (2021) 15471–15501. <https://doi.org/10.1021/acsnano.1c03886>
- [2] X. Lin, M. Xiong, J. Zhang, C. He, X. Ma, H. Zhang, Y. Kuang, M. Yang, Q. Huang, Carbon dots based on natural resources: Synthesis and applications in sensors, *Microchem. J.* 160 (2021) 105604. <https://doi.org/10.1016/j.microc.2020.105604>
- [3] H. Ding, Y. Ji, J.-S. Wei, Q.-Y. Gao, Z.-Y. Zhou, H.-M. Xiong, Facile synthesis of red-emitting carbon dots from pulp-free lemon juice for bioimaging, *J. Mater. Chem. B*. 5 (2017) 5272–5277. <https://doi.org/10.1039/C7TB01130J>
- [4] N. Chhikara, R. Kour, S. Jaglan, P. Gupta, Y. Gat, A. Panghal, Citrus medica: nutritional, phytochemical composition and health benefits – a review, *Food Funct.* 9 (2018) 1978–1992. <https://doi.org/10.1039/C7FO02035J>
- [5] Y. Dai, M. Liu, J. Li, S. Yang, Y. Sun, Q. Sun, W. Wang, L. Lu, K. Zhang, J. Xu, W. Zheng, Z. Hu, Y. Yang, Y. Gao, Z. Liu, A review on pollution situation and treatment methods of tetracycline in groundwater, *Sep. Sci. Technol.* 55 (2020) 1005–1021. <https://doi.org/10.1080/01496395.2019.1577445>
- [6] J.C. Chee-Sanford, R.I. Mackie, S. Koike, I.G. Krapac, Y.-F. Lin, A.C. Yannarell, S. Maxwell, R.I. Aminov, Fate and transport of antibiotic residues and antibiotic resistance genes following land application of manure waste, *J. Environ. Qual.* 38 (2009) 1086–1108. <https://doi.org/10.2134/jeq2008.0128>
- [7] X. Guo, L. Zhang, Z. Wang, Y. Sun, Q. Liu, W. Dong, A. Hao, Fluorescent carbon dots based sensing system for detection of enrofloxacin in water solutions, *Spectrochim. Acta, Part A*. 219 (2019) 15–22. <https://doi.org/10.1016/j.saa.2019.02.017>
- [8] M.L. Liu, B.B. Chen, C.M. Li, C.Z. Huang, Carbon dots: synthesis, formation mechanism, fluorescence origin and sensing applications, *Green Chem.* 21 (2019) 449–471. <https://doi.org/10.1039/C8GC02736F>

- [9] B. De, N. Karak, A green and facile approach for the synthesis of water soluble fluorescent carbon dots from banana juice, *RSC Adv.* 3 (2013) 8286. <https://doi.org/10.1039/c3ra00088e>
- [10] A. Pal, M. Palashuddin Sk, A. Chattopadhyay, Recent advances in crystalline carbon dots for superior application potential, *Mater. Adv.* 1 (2020) 525–553. <https://doi.org/10.1039/D0MA00108B>
- [11] V. Ramanan, S.K. Thiyagarajan, K. Raji, R. Suresh, R. Sekar, P. Ramamurthy, Outright Green Synthesis of Fluorescent Carbon Dots from Eutrophic Algal Blooms for In Vitro Imaging, *ACS Sustainable Chem. Eng.* 4 (2016) 4724–4731. <https://doi.org/10.1021/acssuschemeng.6b00935>
- [12] P. Murugesan, J.A. Moses, C. Anandharamakrishnan, One step synthesis of fluorescent carbon dots from neera for the detection of silver ions, *Spectrosc. Lett.* 53 (2020) 407–415. <https://doi.org/10.1080/00387010.2020.1764589>
- [13] H. Xu, X. Yang, G. Li, C. Zhao, X. Liao, Green Synthesis of Fluorescent Carbon Dots for Selective Detection of Tartrazine in Food Samples, *J. Agric. Food Chem.* 63 (2015) 6707–6714. <https://doi.org/10.1021/acs.jafc.5b02319>
- [14] S. Zhang, L. Jin, J. Liu, Q. Wang, L. Jiao, A label-free yellow-emissive carbon dot-based nanosensor for sensitive and selective ratiometric detection of chromium (VI) in environmental water samples, *Mater. Chem. Phys.* 248 (2020) 122912. <https://doi.org/10.1016/j.matchemphys.2020.122912>
- [15] M. Wang, R. Shi, M. Gao, K. Zhang, L. Deng, Q. Fu, L. Wang, D. Gao, Sensitivity fluorescent switching sensor for Cr (VI) and ascorbic acid detection based on orange peels-derived carbon dots modified with EDTA, *Food Chem.* 318 (2020) 126506. <https://doi.org/10.1016/j.foodchem.2020.126506>
- [16] D. Uriarte, C. Domini, M. Garrido, New carbon dots based on glycerol and urea and its application in the determination of tetracycline in urine samples, *Talanta.* 201 (2019) 143–148. <https://doi.org/10.1016/j.talanta.2019.04.001>
- [17] J. Peng, W. Gao, B.K. Gupta, Z. Liu, R. Romero-Aburto, L. Ge, L. Song, L.B. Alemany, X. Zhan, G. Gao, S.A. Vithayathil, B.A. Kaiparettu, A.A. Marti, T. Hayashi, J.-J. Zhu, P.M. Ajayan, Graphene

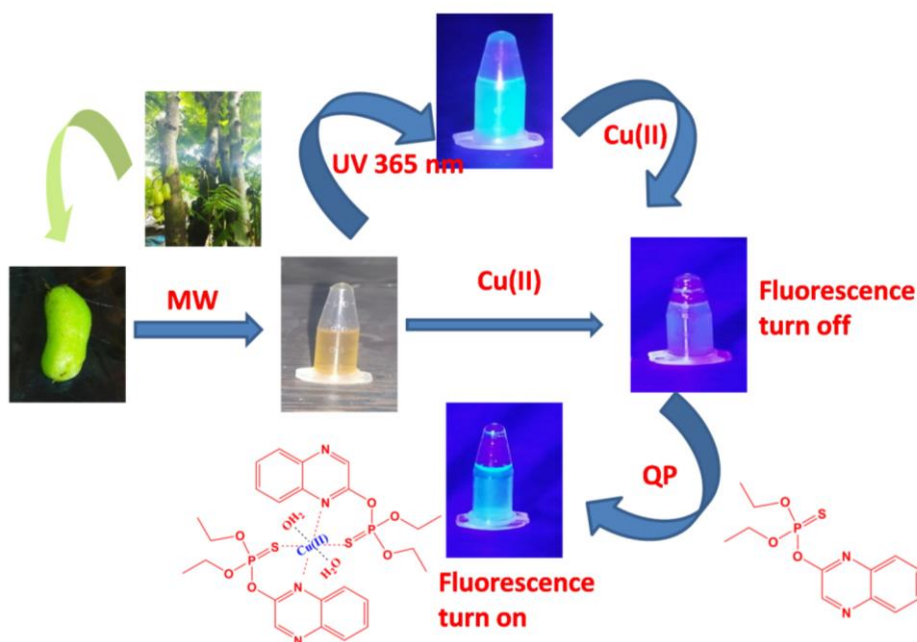
- Quantum Dots Derived from Carbon Fibers, *Nano Lett.* 12 (2012) 844–849. <https://doi.org/10.1021/nl2038979>
- [18] N. Javed, D.M. O’Carroll, Long-term effects of impurities on the particle size and optical emission of carbon dots, *Nanoscale Adv.* 3 (2021) 182–189. <https://doi.org/10.1039/D0NA00479K>
- [19] M. Batool, H.M. Junaid, S. Tabassum, F. Kanwal, K. Abid, Z. Fatima, A.T. Shah, Metal Ion Detection by Carbon Dots—A Review, *Critical Reviews in Analytical Chemistry.* (2020) 1–12. <https://doi.org/10.1080/10408347.2020.1824117>
- [20] W. Shi, F. Guo, M. Han, S. Yuan, W. Guan, H. Li, H. Huang, Y. Liu, Z. Kang, N,S co-doped carbon dots as a stable bio-imaging probe for detection of intracellular temperature and tetracycline, *J. Mater. Chem. B.* 5 (2017) 3293–3299. <https://doi.org/10.1039/C7TB00810D>
- [21] B. Wang, C. Gu, Y. Jiao, Y. Gao, X. Liu, J. Guo, T. Qian, Novel preparation of red fluorescent carbon dots for tetracycline sensing and its application in trace determination, *Talanta.* 253 (2023) 123975. <https://doi.org/10.1016/j.talanta.2022.123975>
- [22] X. Gao, J. Qin, J. Liu, Z. Yang, G. Zhang, J. Hou, Bioinspired Carbon Dots as an Effective Fluorescent Sensing Platform for Tetracycline Detection and Bioimaging, *ChemistrySelect.* 7 (2022) e202104030. <https://doi.org/10.1002/slct.202104030>
- [23] Y. Cao, X. Wang, H. Bai, P. Jia, Y. Zhao, Y. Liu, L. Wang, Y. Zhuang, T. Yue, Fluorescent detection of tetracycline in foods based on carbon dots derived from natural red beet pigment, *LWT.* 157 (2022) 113100. <https://doi.org/10.1016/j.lwt.2022.113100>
- [24] W. Wang, S. Li, P. Yin, J. Li, Y. Tang, M. Yang, Response surface methodology optimization for the synthesis of N, S-codoped carbon dots and its application for tetracyclines detection, *Chemosphere.* 303 (2022) 135145. <https://doi.org/10.1016/j.chemosphere.2022.135145>
- [25] H. Qi, D. Huang, J. Jing, M. Ran, T. Jing, M. Zhao, C. Zhang, X. Sun, R. Sami, N. Benajiba, Transforming waste into value: pomelo-peel-based nitrogen-doped carbon dots for the highly selective detection of tetracycline, *RSC Advances.* 12 (2022) 7574–7583. <https://doi.org/10.1039/D2RA00134A>

- [26] Y. Fan, W. Qiao, W. Long, H. Chen, H. Fu, C. Zhou, Y. She, Detection of tetracycline antibiotics using fluorescent “Turn-off” sensor based on S, N-doped carbon quantum dots, *Spectrochim. Acta, Part A*. 274 (2022) 121033. <https://doi.org/10.1016/j.saa.2022.121033>
- [27] F. Zu, F. Yan, Z. Bai, J. Xu, Y. Wang, Y. Huang, X. Zhou, The quenching of the fluorescence of carbon dots: A review on mechanisms and applications, *Microchim. Acta*. 184 (2017) 1899–1914. <https://doi.org/10.1007/s00604-017-2318-9>



# Chapter 6

## BILIMBI FRUIT DERIVED CARBON DOTS



This work is published in International Journal of Environmental Analytical Chemistry.

P. Venugopalan and N. Vidya, Bilimbi (*Averrhoa bilimbi*) fruit derived carbon dots for dual sensing of Cu(II) and quinalphos, International Journal of Environmental Analytical Chemistry, (2022) 1–14

<https://doi.org/10.1080/03067319.2022.2149331>





## 6.1 Introduction

As previously stated, CDs from biomass and biowaste materials recently received more appraisals. The present chapter deals with the studies on the fluorescent CDs derived from the bilimbi (*Averrhoa bilimbi*) fruit extract. Bilimbi is considered as an acidic fruit enriched with several acids like oxalic and ascorbic acids, various nutrients and numerous carbohydrates. It is considered as an excellent source of antioxidants and minerals and it used as medicine for variety of diseases in the indigenous system of medicine [3,4].

The precursor is selectively opted due to its high acidic content and moreover, the direct materialisation of the extract to fluorescent CDs is not reported yet. The acids present in the fruit extract believe to play an important role in the facile formation of CDs. Especially the presence of excess oxalic and ascorbic acid leads to fast formation CDs from the precursor. Here, materialisation of this biomass is carried out by the aid of greener microwave method, without using any other chemicals. The as prepared CDs is named as BCDs.

From the selectivity study with different metal ions, it is found that the fluorescence of BCDs greatly reduced by the addition of Cu(II) solutions, so the system was used for the sensing of Cu(II) in aqueous medium. The BCDs with Cu(II) is designated as BCDs@Cu(II). In the light of interaction of Cu(II) with some special functionalities, the non-fluorescent BCDs@Cu(II) was again tested for its sensing capacity. Some pesticide molecules were selected for the fluorescence recovery experiments. It is noticed that the fluorescence of BCDs@Cu(II) is enhanced by the addition of quinalphos solution. So, further fluorescence sensing studies were focused with quinalphos.

Quinalphos (O,O-diethyl-O-quinoxalinyolphosphorothioate), is a popular pesticide from the family of organophosphorus pesticides, is frequently applied in different types of crops including rice, tea and variety of fruits etc. [5]. Intoxication of this pesticide occurs through many ways like inhalation, ingestion and skin absorption and all these leads to several health issues such as hypernatremia, pancreatitis, renal failure, weakness, low scoring memory and learning abilities [5,6]. Therefore, precise profiling of this pesticide has been very crucial to ensure safeguarding of crops and appropriate pesticide managements.

BCDs with strong fluorescence was firstly used as selective fluorescent turn-off probe for the sensing Cu(II) and the resulting non-fluorescent system (BCDs@Cu(II) executed as the turn-on fluorescent probe for the organophosphorus pesticide, quinalphos. The quinalphos sensing is also carried out in real rice and tea samples with good recovery percentage. The real samples are purposefully selected because the content of this particular pesticide is frequently noticed in rice and tea; the samples were collected from the local market of Kerala, a popular consumer state in India. The next sections go into the experiment's procedures and results.

## **6.2 Experimental**

### **6.2.1 Synthesis of BCDs**

BCDs were synthesised using a simple, one-step microwave heating procedure with aqueous bilimbi fruit extract as a precursor. This is a description of the full preparation procedure.

Bilimbi fruits were washed thoroughly with water and were cut in to small pieces and crushed using mortar and pestle. The resultant

fruit paste was transferred to a beaker with 30 mL of hot distilled water, and it was magnetically stirred for 30 minutes of time. Afterwards the solution was filtered, centrifuged and 30 mL of this solution was placed in domestic microwave oven at 500 W for 20 minutes of time with frequent cooling in every 5 minutes. The as obtained dry residue was magnetically stirred with 30 mL of distilled water, filtered, centrifuged. Finally the solution was dialysed (dialysis membrane with 3 KDa molecular weight cut off) against distilled water for 48 hrs. The preparation is depicted in **Scheme 6.1**.

The resultant brownish solution of CDs exerts blue fluorescence under UV light of 365 nm and the solution was stored at 4 °C.

### **6.2.2 Cu(II) and quinalphos detection**

Cu(II) and quinalphos sensing was carried out using fluorescence spectra studies. Firstly the fluorescence spectrum of BCDs solution was recorded at an excitation of 430 nm giving emission maxima at 531 nm. The native fluorescence of BCDs was quenched by the addition of different concentration of Cu(II) solution, and the resulting solution is designated as BCDs@Cu(II). This BCDs@Cu(II) was utilised as the probe solution for the quinalphos pesticide sensing.

The sensing probe was developed by the following procedure; 2 mL of BCDs solution was taken in the quartz cuvette and the fluorescence spectra of the bare BCDs was recorded at 430 nm, then different concentration of Cu(II) solution was introduced to the system by using a micropipette. The spectra were recorded after an incubation time of 5 minutes using the same instrument and intensity of emission

spectra were noted down in each addition and all spectra of were recorded at the same excitation wavelength. As concentration of Cu(II) increases the intensity was gradually decreased.

The selectivity of BCDs towards Cu(II) has been identified by the selectivity study, which also follows the same procedure as above. It involves the recording of the spectra of BCDs with different metal ions (Co(III), Ni(II), Hg(II), Pb(II), Al(III), Cd(II) and Fe(III)).

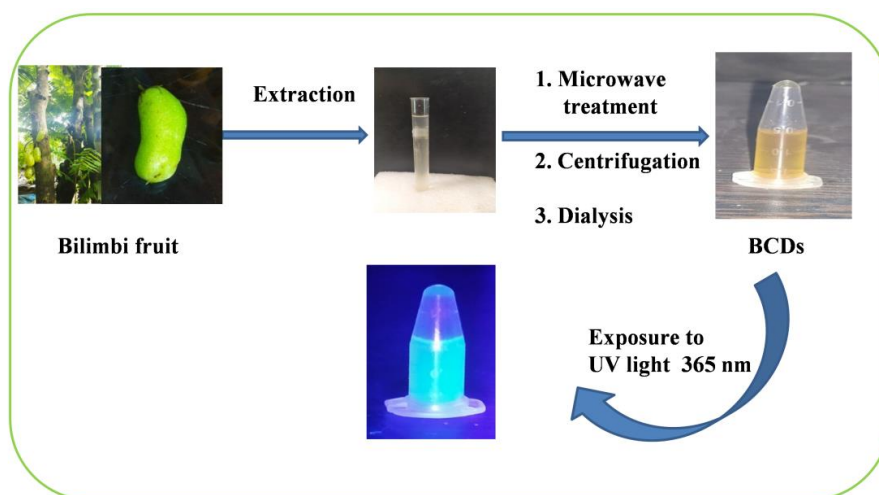
The probe for quinalphos sensing have been developed by the addition of definite concentration of Cu(II) solution to the BCDs and termed as BCDs@Cu(II). Then quinalphos detection by the probe was conducted as follows; about 2 mL of BCDs@Cu(II) was taken in the cuvette, fluorescence spectrum of the probe was recorded. Subsequently different concentrations of quinalphos were added to the probe solution by the aid of micropipette and were kept for 10 minutes as incubation time and spectra were recorded by the same experimental conditions as above. The intensity of emission spectra was monitored.

The fluorescence response of the probe in the absence and presence of quinalphos with different pesticides such as glyphosate, marathion, dichlorovos, chloropyrifos and diethylthiocarbamate were screened to study the selectivity of the probe towards quinalphos. The selectivity investigation follows the same procedure with same concentration and experimental conditions as above.

### **6.2.3 Real sample analysis**

To assert the practicability of the developed probe, the sensing was carried out using real samples. Two different agricultural crops, rice and tea were selected as real samples and were collected from the local market. For this study rice and tea extract were prepared as

follows; about 5 g of each samples were gently grinded and soaked in hot distilled water for 2 hrs of time in two beakers. Later the mixture was filtered and centrifuged. The resulting extracts were spiked with different concentration of quinalphos solution, and were kept stand for 24 hrs. The spectra of the spiked samples with BCDs@Cu(II) probe were recorded at the excitation wavelength of 430 nm after an incubation of 10 minutes. The detection was carried out by monitoring the fluorescence response of the probe. The corresponding recovery percentage was calculated in each case as per the standard equation which is included in Chapter 3.



**Scheme 6.1:** Synthesis of BCDs

## 6.3 Results and discussion

### 6.3.1 Formation of BCDs

As mentioned in the previous chapters, the exact mechanism of CDs formation is still unknown. Since the bilimbi extract consists of plenty of acids and carbohydrates [3,4], the formation mechanism majorly focussed on the carbohydrates. The proposed mechanism for

the formation of CDs falls under the category of bottom-up synthesis, which refers to the process of developing nano-dimensional particles from smaller molecules through condensation, polymerisation, carbonization, and nuclear fusion while being exposed to microwave radiation. The acids presents in the extract, like oxalic acid plays an important role in the initiation of hydrolysis and dehydration of carbohydrates present in the extract by utilising the microwave energy. Then the formation of water soluble fluorescent nano-materials, through various reactions including, decomposition, condensation, carbonization and aromatisation reactions on the dehydrated carbohydrate products [7–9]. Time and energy used for the synthesis was comparatively lesser on comparing similar reports and this may attributed to the contents of the precursor.

### 6.3.2 Characterisation

#### TEM analysis

The TEM images (**Figure 6.1**) were used to examine the morphology and particle size of the BCDs and were found to be nearly spherical in shape (**Figure 6.1(a)**). The size distribution of the particles, with an average size of 4.75 nm and a range of 1.89 to 7.0 nm, as determined by the corresponding histogram, is shown in **Figure 6.1 (c)**. Another TEM image, with particle size markings was also displayed in **Figure 6.1 (d)**, both results reveals that the major population particle size falls under 10 nm. The selected electron diffraction pattern of the particle was used to examine the crystalline or amorphous phase structure of BCDs. As shown in **Figure 6.1 (b)**, it

does not possess bright spots or clear well defined pattern indicating that the crystalline nature of the BCDs is very poor [10].

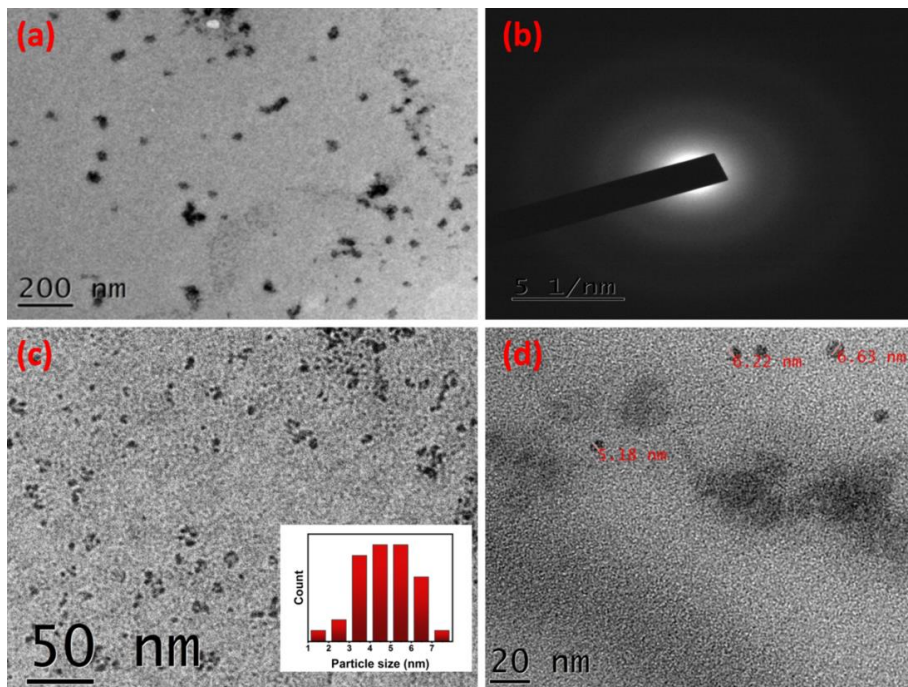


**Figure 6.1:**(a)TEM images of BCDs (b)SAED pattern of BCDs(c)TEM image of BCDs at lower scale (inset: corresponding histogram n= 36) (d) TEM image with particle size markings

### FTIR spectral analysis

Fourier transform infrared spectroscopy has been used to identify the functional groups associated with the prepared BCDs and the spectrum is displayed in **Figure 6.2**. Two bands at 3363 and 3268  $\text{cm}^{-1}$  were arising due to combined effects of O-H and N-H stretching vibrations. A peak at 2930  $\text{cm}^{-1}$  is attributed to stretching vibration of C-H, a medium band at 1719  $\text{cm}^{-1}$  was accredited to C=O stretching. A comparatively strong band appeared at 1625  $\text{cm}^{-1}$  corresponds to

stretching vibration of C=C bond indicating the existence of aromatic  $sp^2$  clusters [9]. Asymmetric and symmetric stretching vibration of  $COO^-$  indicated by the two bands located at 1521 and 1436  $cm^{-1}$ . Bands at 1360 and 1026  $cm^{-1}$  was contributed by the C – N stretching vibrations [9,11], whereas peak centred at 1208  $cm^{-1}$  attributed to the stretching vibrations of C-O group. As a whole the spectral data reveals that the surface of BCDs enriched with plenty of carboxyl, hydroxyl and amine functionalities and these hydrophilic groups plays a vital role in the excellent stability and solubility of the system in aqueous medium.

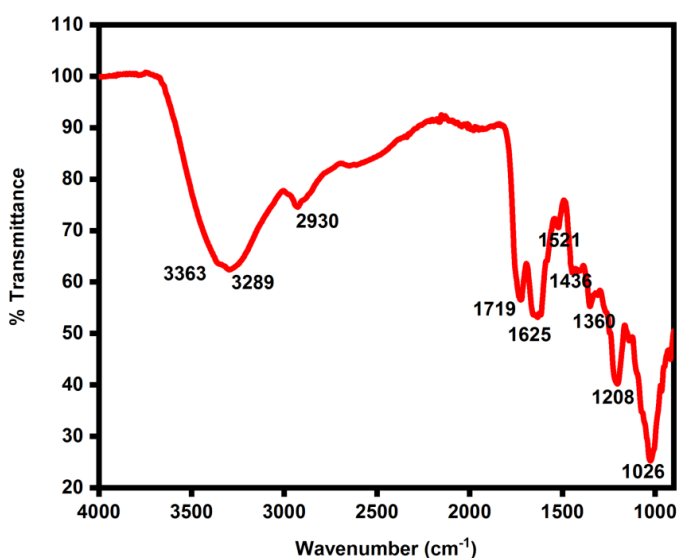


**Figure 6.2:** FTIR spectrum of BCDs

### UV-Vis spectral analysis

The absorbance spectrum of BCDs exhibits a strong peak at 309 nm originated due to the  $n-\pi^*$  transitions of C=O bonds present in



the BCDs [12], and the corresponding spectrum is shown in **Figure 6.3**.

### **Fluorescence spectral analysis**

The fluorescence nature of the BCDs was studied by the fluorescence spectrum and its excitation dependence nature was investigated by recording the spectra at different wavelength ranging from 290 nm to 450 nm (**Figure 6.4**). The results reveals that the system having excitation wavelength dependent nature, and this behaviour may derived from the polydispersity and electronic transitions of surface attached functional groups like C=C and C-NH<sub>2</sub> bonds. This implies that the fluorescence peak is adjustable with excitation wavelength and it shows tuneable nature of the system. Moreover, the full width half maximum of the fluorescence curve was about 90 nm indicating that the range of size distribution of BCDs comparatively narrow [11].

The excitation dependence study also reveals that the BCDs shows maximum emission peak when excited at 430 nm and the emission band is centred at 531 nm (**Figure 6.5**). These values were selected as excitation and emission wavelength for further studies. In addition, the prepared system exhibits strong bluish fluorescence under UV light and the photographs of the BCDs in normal light and UV light of 365 nm is shown in **Figure 6.6** along with the fluorescence excitation and emission graphs of BCDs.

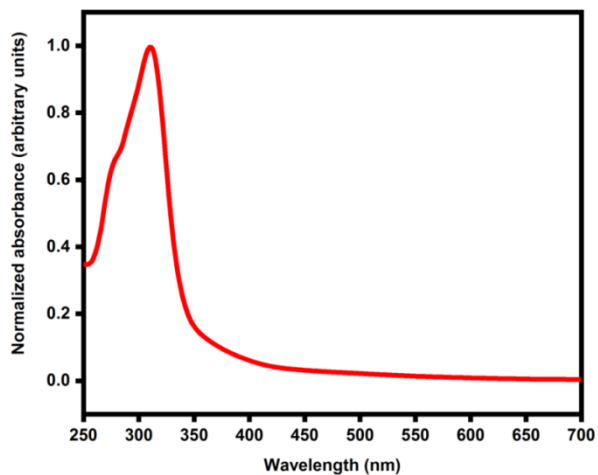


**Figure 6.3:** Normalized UV-Vis absorption spectrum of BCDs

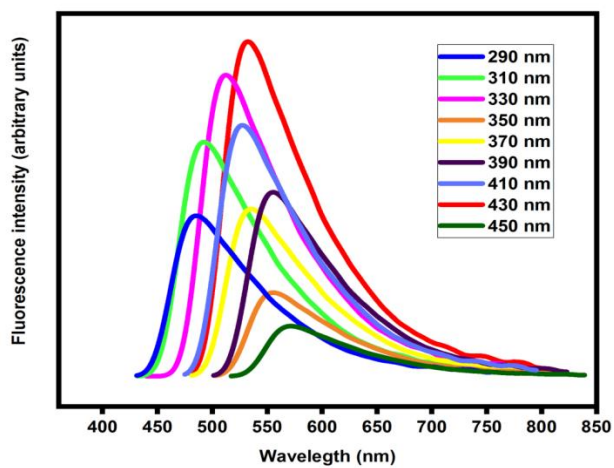


**Figure 6.4:** Excitation dependent emission spectra of BCDs from 290 nm to 450 nm

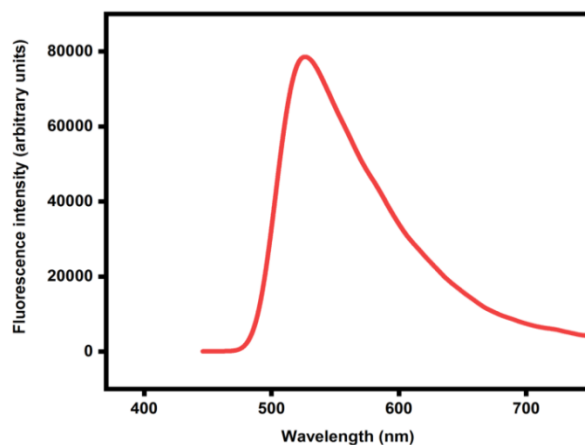


**Figure 6.5:** Fluorescence spectrum of BCDs

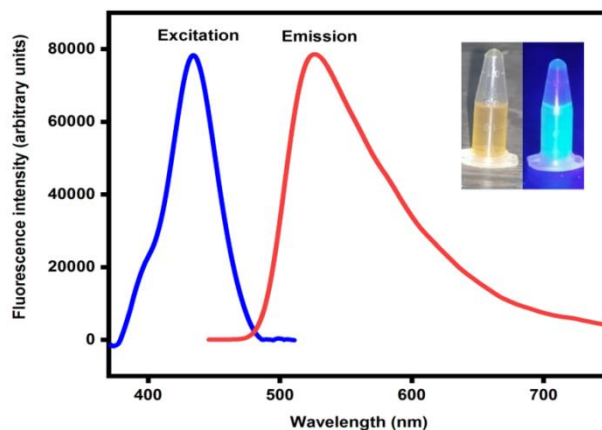


**Figure 6.6:** Excitation and emission spectra of BCDs (inset: BCDs at normal light (left) and BCDs at UV light (right))

### 6.3.3 Fluorescence quantum yield and fluorescence stability of BCDs

The fluorescent quantum yield of the synthesised system was about 3.4 %, determined by using quinine sulphate as standard with quantum yield of 54 %. The stability of the prepared system was

investigated with storage time. It was found to be stable up to nine weeks of time at 4 °C and its stability is comparatively lesser in atmospheric temperature and open atmosphere storage leads lesser stability and kind of fungal infections are noticed over time. Under UV light (365 nm) the system shows apparent stability up to 3 hours of continues irradiation, after that fluorescence slightly reduced. The fluorescence intensity of BCDs not shows any significant effect in presence of different concentration of KCl solution. All these facts reveals that the system have good stability features.

#### **6.3.4 Selectivity studies on BCDs**

Owing to the excellent fluorescence nature of BCDs, its possibility of being act as fluorescence sensor was examined. For that firstly the selectivity of the system was identified through the fluorescence monitoring by the addition of different metal ions like Co(III), Ni(II), Hg(II), Pb(II), Al(III), Cd(II) Fe(III) and Cu(II). The results of this selectivity study are given in **Figure 6.7**. The results shows that the native fluorescence of BCDs is significantly reduced by the addition of Cu(II) ions. It reveals that the quenching efficiency of Cu(II) was comparatively higher than the other metal ions under study. Besides to the selectivity study, the fluorescence response of BCDs with Cu(II) in presence of different metal ions were also conducted for further clarification on selectivity and none of them exerts significant interference in the detection of Cu(II) (**Figure 6.8**). This selectivity was believed to be due to the highest affinity of Cu(II) towards amino and hydroxyl groups for complex formation. This ground state complex formation leads to the fluorescence quenching of

BCDs. So the further sensing studies was conducted with Cu(II).

### 6.3.5 Sensing studies with Cu(II) on BCDs

The fluorescence property of the as prepared BCDs was utilised for dual sensing purpose. Firstly, the fluorescence response of the system with addition of different concentration of Cu(II) solution was studied. A gradual decrease in the native fluorescence of BCDs was observed on increasing Cu(II) concentration. This quenching of fluorescence is shown in **Figure 6.9**, indicating the fluorescence intensity of the emission peak centred at 531 nm decreased with Cu(II).

The plot of  $F_0/F$  with concentration of Cu(II) was shown in **Figure 6.10**, where  $F_0$  and  $F$  was the fluorescence intensity of BCDs before and after the introduction of Cu(II). A good linear relationships between relative fluorescence intensity and concentration of Cu(II) was maintained in the concentration range of 0-20  $\mu\text{M}$  with linear equation  $F/F_0 = 0.06[\text{Cu(II)}] + 0.97$  with  $R^2 = 0.9986$ . Limit of detection (LOD) for Cu(II) was calculated from this linear range and it was found to be 115 nM. LOD value and linear range of the present system with Cu(II) was found to be comparable with reports from the same field of research in literature, and is listed in **Table 6.1**.

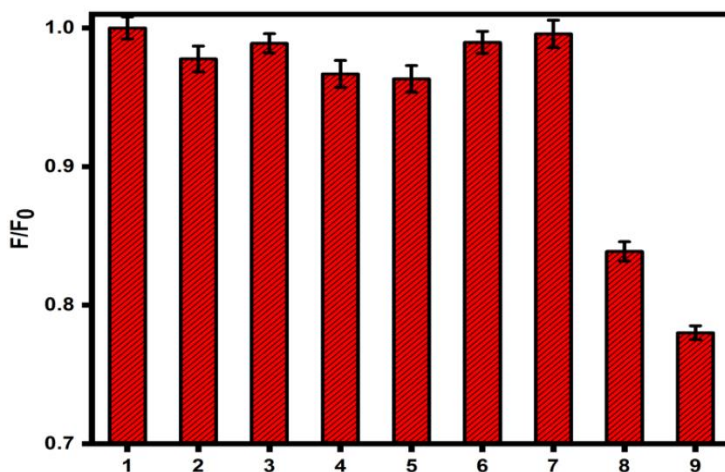


**Figure 6.7.** Relative fluorescence intensity of BCDs with different metal ions (1 to 9 representing BCDs, Co(III), Ni(II), Hg(II), Pb(II), Al(III), Cd(II), Fe(III) and Cu(II))

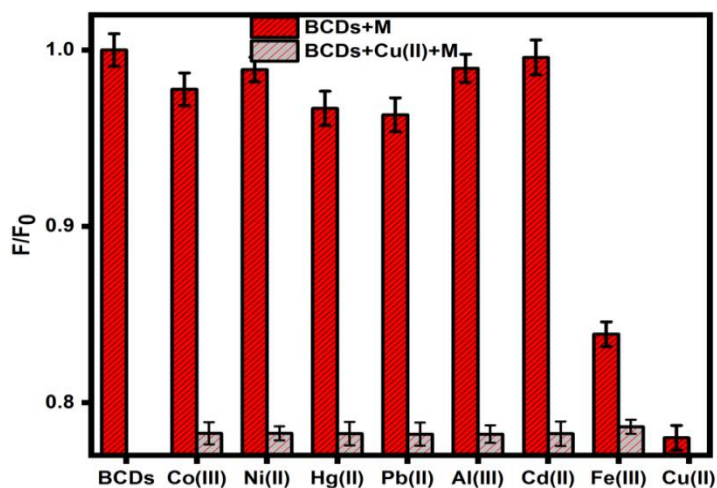


**Figure 6.8:** Relative fluorescence intensity of BCDs with different metal ions in the absence and presence of Cu(II)

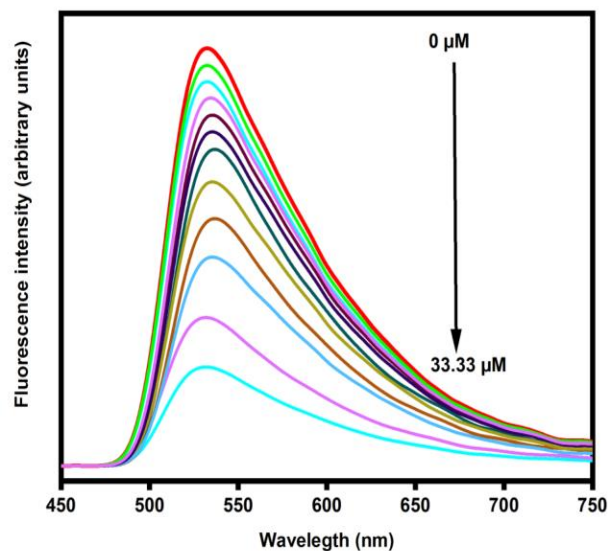


**Figure 6.9:** Fluorescence emission spectra of BCDs with different concentration of Cu(II)

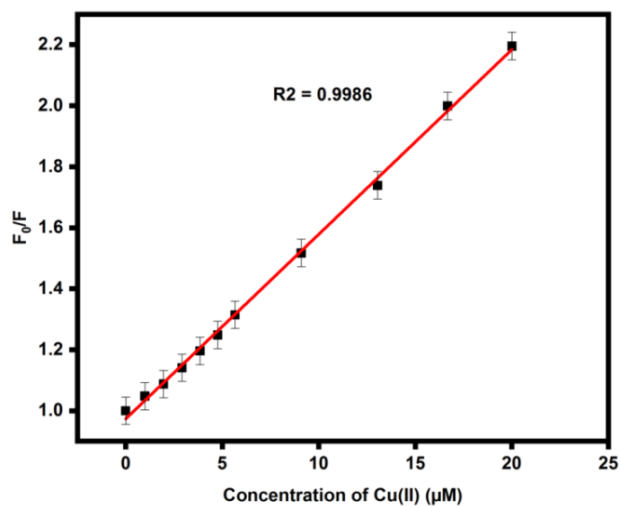


**Figure 6.10:** Relative fluorescence intensity with concentration of Cu(II)

**Table 6.1:** Comparison of different probes for Cu(II) detection

Sensing probe for Cu(II)	LOD ( $\mu\text{M}$ )	Linear range ( $\mu\text{M}$ )	Reference
Radish derived CDs	0.16	0 – 10	[13]
GQDs from humic acid	0.44	1 – 40	[14]
CDs from o-phenyldiamine (OPD)	0.28	1 – 10	[15]
Glyoxylic acid-modified CDs (GA-CDs)	0.21	0 – 10	[16]
Coal derived GQDs	0.29	0 – 8	[17]
Hydrophobic carbon dots (TO-CDs) from triolein	0.21	0.5 – 10	[18]
CDs from peanut shell	4.8	0 – 5	[19]
Banana juice derived CDs	5	16.66 – 13333	[20]
CDs from activated carbon	2.4	5 – 100	[21]
CDs-entrenched chitosan-modified magnetic nanoparticles	0.56	0.01 – 200	[22]
CDs derived from Bilimbi fruit	0.115	0 – 20	This work

### 6.3.6 Selectivity studies on BCDs@Cu(II)

On account to the fluorescence quenching by the addition of Cu(II) a new probe was developed from BCDs. As mentioned earlier the probe was prepared by adding definite concentration of Cu(II) (33.33 $\mu\text{M}$ ) to BCDs solution and termed as BCDs@Cu(II).

The selectivity studies on BCDs@Cu(II) was conducted with different organophosphorous pesticides and out of them quinalphos gives marked recovery of fluorescence to BCDs@Cu(II) system. Interference studies with these pesticides was also conducted by monitoring the fluorescence response of BCDs@Cu(II) in the presence



of quinalphos, results of the same were shown in **Figure 6.11**. The fluorescence enhancement was much higher for quinalphos on comparing with others. So the further sensing studies was conducted with different concentration of quinalphos.

### **6.3.7 Sensing studies with quinalphos on BCDs@Cu(II)**

Fluorescence response of BCDs@Cu(II) with different concentration of quinalphos (0-10.32  $\mu\text{M}$ ) was evaluated and the corresponding spectra is shown in **Figure 6.12**. A significant enhancement of fluorescence intensity was noticed with increasing concentration of quinalphos. This fluorescence turn on behaviour is clear from the figure. The relationships between relative fluorescence intensity with concentration of quinalphos was linear from 0 to 10.32  $\mu\text{M}$  range of quinalphos concentration and it is depicted in **Figure 6.13**, with linear regression equation  $F/F_0 = 0.46[\text{QP}] + 1.09$  ( $R^2 = 0.9977$ ). Where  $F$  and  $F_0$  are the fluorescence intensity of BCDs@Cu(II) after and before the addition of quinalphos, respectively. The corresponding LOD was 510 nM based on  $3\sigma/\text{slope}$  equation, where  $\sigma$  is representing standard deviation and slope is obtained from the linear plot.

LOD value and linear range of the present system with quinalphos were found to be comparable with earlier reports in literature and were listed in **Table 6.2**. It was noted that the quinalphos detection majorly reported by using metal and bimetallic nanoparticles, on comparing with these probes the present system was much more facial, time saving, less expensive and easy to perform. Besides, the

present probe provides close limit of detection and satisfactory level of linear range.

Photographs of BCDs, BCDs@Cu(II) and BCDs@Cu(II)+QP under UV light of 365 nm is given in **Figure 6.14**. The recyclability of the probe was tested by adding definite amount of Cu (II) solution again to BCDs@Cu(II)+QP, the observed decrease in fluorescence indicates the recyclability of the probe for multiple sensing of Cu(II) and quinalphos. Successive operation up to four measurements gave satisfactory results. As the recycled probe is contaminated with the analyte molecules, there is a slight decrease in the performance of the system.

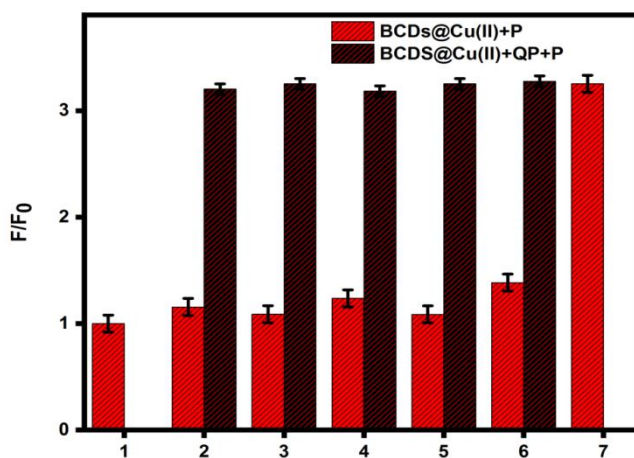


**Figure 6.11:** Relative fluorescence intensity of BCDs@Cu(II) with different pesticides in absence and presence of quinalphos (1 to 7 representing BCDs@Cu(II) without any pesticide, glyphosate, marathion, dichlorovos, chloropyrifos, diethylthiocarbamate and quinalphos)

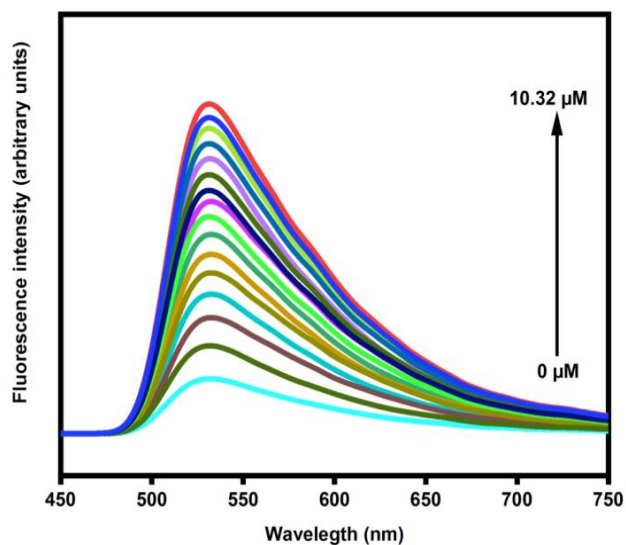


**Figure 6.12:** Fluorescence emission spectra of BCDs@Cu(II) with different concentration of quinalphos

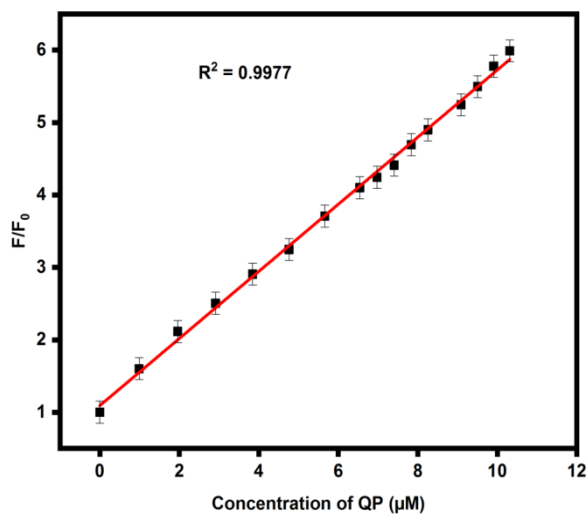


**Figure 6.13:** Relative fluorescence intensity with concentration of quinalphos

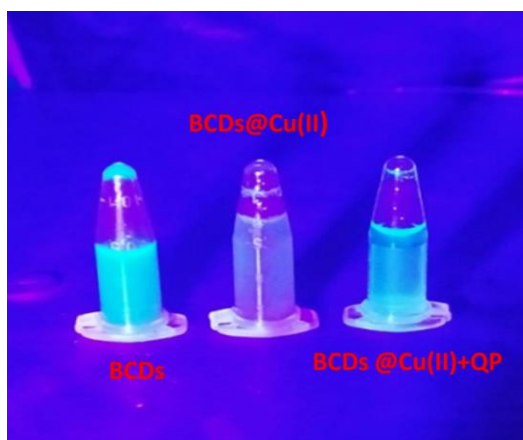


**Figure 6.14:** UV cabinet photographs of BCDs, BCDs@Cu(II) and BCDs@Cu(II)+QP at 365 nm

**Table 6.2:** Comparison of different probes for quinalphos detection

Sensing probe for quinalphos	LOD ( $\mu\text{M}$ )	Linear range ( $\mu\text{M}$ )	Reference
p-nitroanilinedithiocarbamate capped gold nanoparticles (p-NA-DTC-Au NPs)	3.21	10 – 1000	[23]
Trypsin-encapsulated Au-Ag bimetallic NCs	0.32	1 – 100	[24]
2-amino-4-thiadiazoleacetic acid anchored AuNPs	0.048	0.5 – 3.5	[25]
Cationic fluorescein as ion pair complex via spectrofluorometric technique	0.27	x	[26]
CDs derived from Bilimbi fruit	0.510	0 – 10.32	This work

x: Not reported

### 6.3.8 Analysis of quinalphos in rice and tea samples

The feasibility of the probe was assessed for the detection of quinalphos in spiked rice and tea samples, where the quinalphos

content was observed often. The illustrated procedure consists of comparatively simple steps and follows standard addition method. The samples were separately prepared and spiked with different concentration of quinalphos (0, 4, 6, 8  $\mu\text{M}$ ) and were estimated through aforementioned procedure. The results were given in **Table 6.3**, the recovery ranges of the quinalphos in rice and tea samples were determined by standard equation (Chapter 3) and are found to be 95.25 – 97.83 % and 95.33 – 102.12 %, respectively. The corresponding error percentages also show satisfactory levels of accuracy and precision. These results manifested that the fabricated probe could be employed to practical on- field samples.

**Table 3:** Determination of quinalphos in real samples

Sample	Added quinalphos ( $\mu\text{M}$ )	Found ( $\mu\text{M}$ )	Recovery (%)	Error(%)
Rice	0	Not found	--	--
	4	3.81	95.25	4.75
	6	5.87	97.83	2.16
	8	7.75	96.88	3.12
Tea	0	Not found	--	--
	4	3.87	96.75	3.25
	6	5.72	95.33	4.66
	8	8.17	102.12	2.12

### 6.3.9 Probable sensing mechanism

In the present study two different fluorescence responses was encountered. Firstly the fluorescence of BCDs getting reduced by the addition of Cu(II) and this quenching may attributed to non-radiative ground state complex formation between Cu(II) and surface functionalities of BCDs.

FTIR data reveals that the surface contains hydroxyl, carboxyl and amino functional groups. Cu(II) is a ion with paramagnetic nature possessing  $d^9$  system with one unfilled d shell and this make it more susceptible for electron or energy transfer through complex formation with surface group of the nano sensor. Especially the amino group present in the BCDs readily forms cupric amine complexes with Cu(II) and this may result in the fluorescence quenching. The chelation of Cu(II) with oxygen and nitrogen of the surface functionalities bring them close proximity and this also facilitate the complex formation leading to the decrease in fluorescence intensity [27]. This type of quenching falls under the category of static quenching.

To further confirm the mechanism of quenching, absorbance spectra of BCDs, Cu(II) and BCDs@Cu(II) was recorded. The corresponding spectra were displayed in **Figure 6.15**. It is very clear that the spectra of BCDs and BCDs@Cu(II) has differences in absorbance as well as wavelength. Additionally there is an extra peak formation in BCDS@Cu(II) spectra around 345 nm and it may attributed to new complex formation, comprehensively all the obtained

results leads to a conclusion that the quenching of native fluorescence of BCDs by Cu(II) follows static quenching mechanism.

This non-fluorescent complex was further utilised as a probe for quinalphos sensing applications. When quinalphos was introduced to the system a remarkable fluorescence increment was noticed and it could be ascribed to the following.

The non-fluorescent nature of the BCDs@Cu(II) was losses gradually due to the release of BCDs from the complex. The quinoxaliny and phosphorothioate groups present in quinalphos have been profound chelating ability to Cu(II), therefore the quinalphos addition rupture the non fluorescent BCDs@Cu(II) complex and thus resulting to the recovery of native fluorescence of BCDs [5].

The UV-Vis spectra of BCDs, quinalphos, BCDs@Cu(II) and BCDs@Cu(II)+QP (QP is quinalphos) were investigated to further confirm the facts (**Figure 6.16**). The changes in the absorbance of spectrum BCDs@Cu(II)+ QP with that of BCDs@Cu(II) and decrease in absorbance of the newly formed peak by the addition of quinalphos were clear from the spectral data, implies that the formed complex somewhat disturbed by the addition of quinalphos and hence the BCDs recovers its fluorescence.

In consideration of above results the sensing mechanism of the prepared system attributed to static quenching followed by the recovery of fluorescence through release of BCDs from the non-fluorescent complex via competitive chelation of Cu(II) with quinalphos.

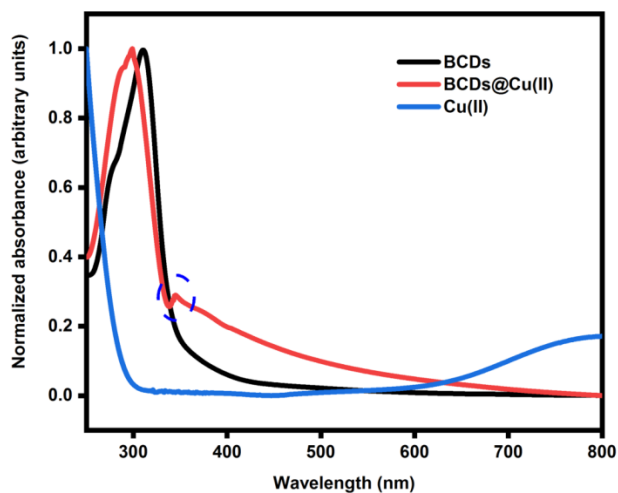


**Figure 15:** Normalized UV-Vis absorption spectra of BCDs, BCDs@Cu(II) and Cu(II)

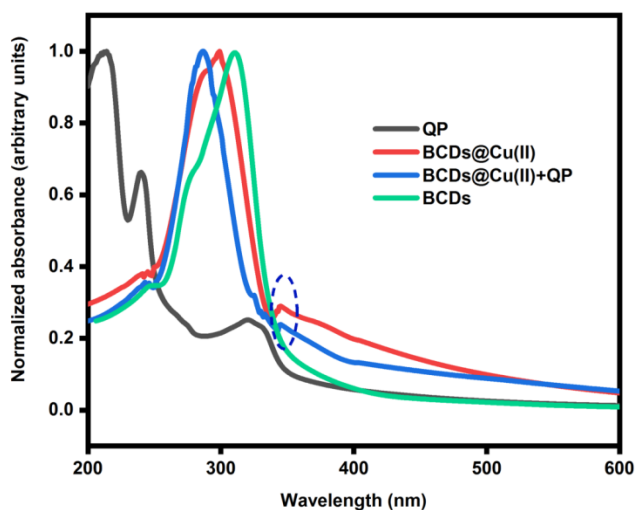


**Figure 16:** Normalized UV-Vis absorption spectra of quinalphos (QP), BCDs@Cu(II), BCDs@Cu(II)+QP and BCDs

## 6.4 Conclusions

In summary, a selective and sensitive dual sensor was developed through a simple one step microwave heating process. The



produced CDs (BCDs) characterised well and owing to the strong fluorescent behaviour, it has been used as a fluorescent probe for the sensing of Cu(II) and quinalphos. In the presence of Cu(II), the native fluorescence of the system gets quenched due to the formation of ground state, non-fluorescent BCDs@Cu(II) complex. This turn-off behaviour of the system was accredited to static quenching mechanism. The fluorescence of the BCDs@Cu(II) gets turn-on by the addition of quinalphos and this fluorescence enhancement is due to the strong chelating interaction between Cu(II) and quinalphos, making the BCDs free from the complex and regain its luminescence. The limit of detection of Cu(II) and quinalphos was found to be about 115 nM and 510 nM, respectively. Based on the simplicity and efficacy of the illustrated method of detection, the BCDs@Cu(II) probe was successfully employed for quinalphos detection in real rice and tea samples. The good level of precision and accuracy with recovery percentage ranging from 95.25 % to 102.12 % are promising to use the system for detecting quinalphos in commercial samples.

## 6.5 References

- [1] T.C. Wareing, P. Gentile, A.N. Phan, Biomass-Based Carbon Dots: Current Development and Future Perspectives, *ACS Nano*. 15 (2021) 15471–15501. <https://doi.org/10.1021/acsnano.1c03886>
- [2] X. Lin, M. Xiong, J. Zhang, C. He, X. Ma, H. Zhang, Y. Kuang, M. Yang, Q. Huang, Carbon dots based on natural resources: Synthesis and applications in sensors, *Microchem. J.* 160 (2021) 105604. <https://doi.org/10.1016/j.microc.2020.105604>
- [3] M. Prasathkumar, S. Anisha, C. Dhriya, R. Becky, S. Sadhasivam, Therapeutic and pharmacological efficacy of selective Indian medicinal plants – A review, *Phytomedicine Plus*. 1 (2021) 100029. <https://doi.org/10.1016/j.phyplu.2021.100029>
- [4] J.K. Suluvoy, V.M. Berlin Grace, Phytochemical profile and free radical nitric oxide (NO) scavenging activity of *Averrhoa bilimbi* L. fruit extract, *3 Biotech*. 7 (2017) 85. <https://doi.org/10.1007/s13205-017-0678-9>
- [5] M.K. Bera, L. Behera, S. Mohapatra, A fluorescence turn-down-up detection of Cu<sup>2+</sup> and pesticide quinalphos using carbon quantum dot integrated UiO-66-NH<sub>2</sub>, *Colloids Surf., A*. 624 (2021) 126792. <https://doi.org/10.1016/j.colsurfa.2021.126792>
- [6] O. Lockridge, L.M. Schopfer, P. Masson, Chapter 64 - Biomarkers of Exposure to Organophosphorus Poisons: A New Motif for Covalent Binding to Tyrosine in Proteins That Have No Active Site Serine, in: R.C. Gupta (Ed.), *Handbook of Toxicology of Chemical Warfare Agents (Second Edition)* Chapter 64 - Biomarkers of Exposure to Organophosphorus Poisons, Academic Press, Boston, 2015: pp. 953–965. <https://doi.org/10.1016/B978-0-12-800159-2.00064-6>
- [7] M.L. Liu, B.B. Chen, C.M. Li, C.Z. Huang, Carbon dots: synthesis, formation mechanism, fluorescence origin and sensing applications, *Green Chem*. 21 (2019) 449–471. <https://doi.org/10.1039/C8GC02736F>
- [8] B. De, N. Karak, A green and facile approach for the synthesis of water soluble fluorescent carbon dots from banana juice, *RSC Adv*. 3 (2013) 8286. <https://doi.org/10.1039/c3ra00088e>
- [9] R. Atchudan, T.N.J.I. Edison, D. Chakradhar, S. Perumal, J.-J. Shim, Y.R. Lee, Facile green synthesis of nitrogen-doped carbon dots using *Chionanthus retusus* fruit extract and investigation of their suitability

- for metal ion sensing and biological applications, *Sens. Actuators, B.* 246 (2017) 497–509. <https://doi.org/10.1016/j.snb.2017.02.119>
- [10] A. Pal, M. Palashuddin Sk, A. Chattopadhyay, Recent advances in crystalline carbon dots for superior application potential, *Mater. Adv.* 1 (2020) 525–553. <https://doi.org/10.1039/D0MA00108B>
- [11] Q. Xiao, Y. Liang, F. Zhu, S. Lu, S. Huang, Microwave-assisted one-pot synthesis of highly luminescent N-doped carbon dots for cellular imaging and multi-ion probing, *Microchim Acta.* 184 (2017) 2429–2438. <https://doi.org/10.1007/s00604-017-2242-z>
- [12] S. Ghosh, A.R. Gul, C.Y. Park, M.W. Kim, P. Xu, S.H. Baek, J.R. Bhamore, S.K. Kailasa, T.J. Park, Facile synthesis of carbon dots from *Tagetes erecta* as a precursor for determination of chlorpyrifos via fluorescence turn-off and quinalphos via fluorescence turn-on mechanisms, *Chemosphere.* 279 (2021) 130515. <https://doi.org/10.1016/j.chemosphere.2021.130515>
- [13] J. Praneerad, N. Thongsai, P. Suphocksoonthorn, S. Kladsomboon, P. Paoprasert, Multipurpose sensing applications of biocompatible radish-derived carbon dots as Cu<sup>2+</sup> and acetic acid vapor sensors, *Spectrochim. Acta, Part A.* 211 (2019) 59–70. <https://doi.org/10.1016/j.saa.2018.11.049>
- [14] X. Liu, J. Han, X. Hou, F. Altincicek, N. Oncel, D. Pierce, X. Wu, J.X. Zhao, One-pot synthesis of graphene quantum dots using humic acid and its application for copper (II) ion detection, *J Mater Sci.* 56 (2021) 4991–5005. <https://doi.org/10.1007/s10853-020-05583-6>
- [15] W. Lv, M. Lin, R. Li, Q. Zhang, H. Liu, J. Wang, C. Huang, Aggregation-induced emission enhancement of yellow photoluminescent carbon dots for highly selective detection of environmental and intracellular copper(II) ions, *Chin. Chem. Lett.* 30 (2019) 1410–1414. <https://doi.org/10.1016/j.ccllet.2019.04.011>
- [16] F. Yan, Z. Bai, Y. Chen, F. Zu, X. Li, J. Xu, L. Chen, Ratiometric fluorescent detection of copper ions using coumarin-functionalized carbon dots based on FRET, *Sens. Actuators, B.* 275 (2018) 86–94. <https://doi.org/10.1016/j.snb.2018.08.034>
- [17] Y. Zhang, K. Li, S. Ren, Y. Dang, G. Liu, R. Zhang, K. Zhang, X. Long, K. Jia, Coal-Derived Graphene Quantum Dots Produced by Ultrasonic Physical Tailoring and Their Capacity for Cu(II) Detection,

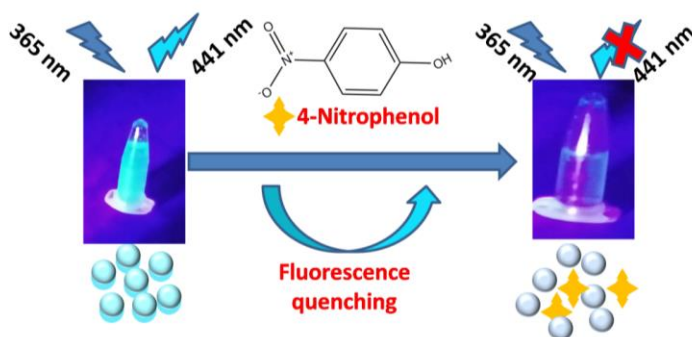
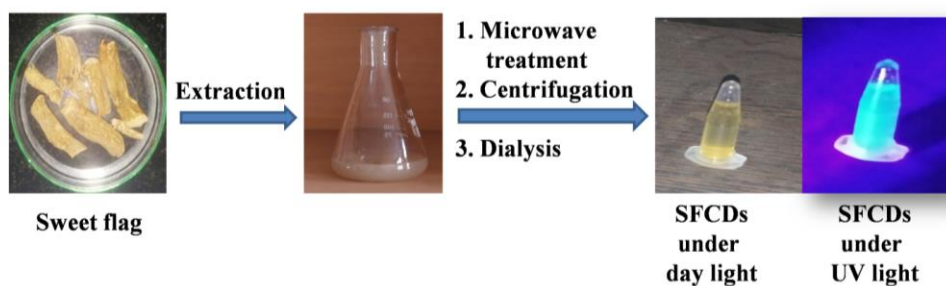
- ACS Sustainable Chem. Eng. 7 (2019) 9793–9799.  
<https://doi.org/10.1021/acssuschemeng.8b06792>
- [18] Y.-S. Lin, Z.-Y. Yang, A. Anand, C.-C. Huang, H.-T. Chang, Carbon dots with polarity-tunable characteristics for the selective detection of sodium copper chlorophyllin and copper ions, *Anal. Chim. Acta.* 1191 (2022) 339311. <https://doi.org/10.1016/j.aca.2021.339311>
- [19] X. Ma, Y. Dong, H. Sun, N. Chen, Highly fluorescent carbon dots from peanut shells as potential probes for copper ion: The optimization and analysis of the synthetic process, *Mater. Today Chem.* 5 (2017) 1–10. <https://doi.org/10.1016/j.mtchem.2017.04.004>
- [20] N. Chaudhary, P.K. Gupta, S. Eremin, P.R. Solanki, One-step green approach to synthesize highly fluorescent carbon quantum dots from banana juice for selective detection of copper ions, *J. Environ. Chem. Eng.* 8 (2020) 103720. <https://doi.org/10.1016/j.jece.2020.103720>
- [21] X. Ma, S. Lin, Y. Dang, Y. Dai, X. Zhang, F. Xia, Carbon dots as an “on-off-on” fluorescent probe for detection of Cu(II) ion, ascorbic acid, and acid phosphatase, *Anal Bioanal Chem.* 411 (2019) 6645–6653. <https://doi.org/10.1007/s00216-019-02038-z>
- [22] A. Kumar, A. Ray Chowdhuri, D. Laha, S. Chandra, P. Karmakar, S. Kumar Sahu, One-pot synthesis of carbon dot-entrenched chitosan-modified magnetic nanoparticles for fluorescence-based Cu<sup>2+</sup> ion sensing and cell imaging, *RSC Adv.* 6 (2016) 58979–58987. <https://doi.org/10.1039/C6RA10382K>
- [23] J.V. Rohit, H. Basu, R.K. Singhal, S.K. Kailasa, Development of p-nitroaniline dithiocarbamate capped gold nanoparticles-based microvolume UV–vis spectrometric method for facile and selective detection of quinalphos insecticide in environmental samples, *Sens. Actuators, B.* 237 (2016) 826–835. <https://doi.org/10.1016/j.snb.2016.07.019>
- [24] S. Akavaram, M.L. Desai, T.-J. Park, Z.V.P. Murthy, S.K. Kailasa, Trypsin encapsulated gold-silver bimetallic nanoclusters for recognition of quinalphos via fluorescence quenching and of Zn<sup>2+</sup> and Cd<sup>2+</sup> ions via fluorescence enhancement, *J. Mol. Liq.* 327 (2021) 114830. <https://doi.org/10.1016/j.molliq.2020.114830>
- [25] C. Loganathan, N.S.K. Gowthaman, S. Abraham John, Chain-like 2-amino-4-thiazoleacetic acid tethered AuNPs as colorimetric and spectrophotometric probe for organophosphate pesticide in water and

- fruit samples, *Microchem. J.* 168 (2021) 106495.  
<https://doi.org/10.1016/j.microc.2021.106495>
- [26] K. Suvardhan, K.S. Kumar, P. Chiranjeevi, Extractive Spectrofluorometric Determination of Quinalphos Using Fluorescein in Environmental Samples, *Environ Monit Assess.* 108 (2005) 217–227.  
<https://doi.org/10.1007/s10661-005-4690-x>
- [27] P. Das, S. Ganguly, M. Bose, S. Mondal, A.K. Das, S. Banerjee, N.C. Das, A simplistic approach to green future with eco-friendly luminescent carbon dots and their application to fluorescent nano-sensor ‘turn-off’ probe for selective sensing of copper ions, *Materials Science and Engineering: C.* 75 (2017) 1456–1464.  
<https://doi.org/10.1016/j.msec.2017.03.045>



# Chapter 7

## SWEET FLAG DERIVED CARBON DOTS



This work is published in Journal of Photochemistry and Photobiology A: Chemistry.

P. Venugopalan and N. Vidya, Microwave assisted green synthesis of carbon dots from sweet flag (*Acorus calamus*) for fluorescent sensing of 4-nitrophenol, Journal of Photochemistry and Photobiology A: Chemistry. 439 (2023) 114625.

<https://doi.org/10.1016/j.jphotochem.2023.114625>





## 7.1 Introduction

Synthesis of CDs from natural resources are gathering much more attention due its merits over the hazardous chemical based CDs and such merits are already discussed in Chapter 2. The present chapter is designed in a fashion, which discuss about the synthesis, characterisation and applications of CDs from pharmacologically important natural precursor, sweet flag (*Acorus calamus*). Sweet flag rhizomes widely accepted in *Ayurvedic* medicinal system and its pharmacological importance are well studied and is discussed in Chapter 2 [1]. However, to the best of our knowledge, its direct materialisation is not reported till date.

Hereby, value addition was applied to the precursor by converting it in to fluorescent CDs. This materialisation was successfully completed with the aid of microwave irradiation without using any hazardous chemicals or sophisticated experimental setups. The CDs prepared is designated as SFCDs and was successfully characterised by TEM, XRD, FTIR, Raman, UV-Vis and fluorescent spectroscopic methods.

From the selectivity studies of SFCDs with different metal ions and phenolic compounds those are commonly encountered as aquatic pollutants, a specific and significant fluorescence quenching of SFCDs was observed by the addition of 4-nitrophenol. So the further sensing studies was majorly done with 4-nitrophenol.

4-Nitrophenol (4-NP) is an important and relevant aromatic

compound, has been well recognised to play major role in the manufacture of several industrial products, like agrochemical products, explosives, textiles, leather, and pharmaceuticals, etc. [2,3]. These products are very much essential for the well-being of the whole society. However, the acute toxicity, lesser biodegradability, high stability and intense water solubility of this compound make it as a dangerous chemical contaminant, and U.S. Environmental Protection Agency (EPA) enlisted it as priority pollutant and maximum accepted level of this contaminant in drinking water has been restricted to be below 0.43  $\mu\text{M}$  [4]. In addition to use for the preparation of many useful pharma chemicals including paracetamol, it is also get released by widely used organophosphate pesticides like parathion, fenitrothion, etc. and thus the reach of this pollutant to water bodies is pretty much easier. Even at small level concentration, 4-NP can exerts its adverse effect; this pollutant has been found to impart hazardous effects on the health of all beings. The accumulation of 4-NP in human body results severe health issues including nervous and ocular system malfunctioning, cyto-embryonic and mutagenic disorders [4].

Based on the selective interaction of SFCDs with 4-NP, a fluorescent probe was developed for the detection 4-NP. The practicability of the probe was tested by employing the sensor towards real water samples. The mechanism of this interaction was also investigated. The methods and outcomes of the experiments are covered in the following sections.

## 7.2 Experimental

### 7.2.1 Synthesis of SFCDs

The aqueous extract of sweet flag rhizomes was used as the precursor in a simple, one-step microwave pyrolysis procedure to create SFCDs. The following describes the whole preparation procedure.

About 10 g of dried sweet flag were magnetically stirred with 30 mL of hot distilled water for 30 minutes of time. The resultant solution filtered and 30 mL of the solution was irradiated with microwaves in a domestic microwave oven for 25 minutes at 500 W with frequent cooling in every 5 minutes. The brownish dry residue obtained was then stirred magnetically with 30 mL distilled water, filtered and centrifuged for 15 minutes to remove large particles. Besides, the resultant solution was dialysed with dialysis membrane of 3 KDa MWCO against distilled water for 48 hours. The preparation is depicted in **Scheme 7.1**.

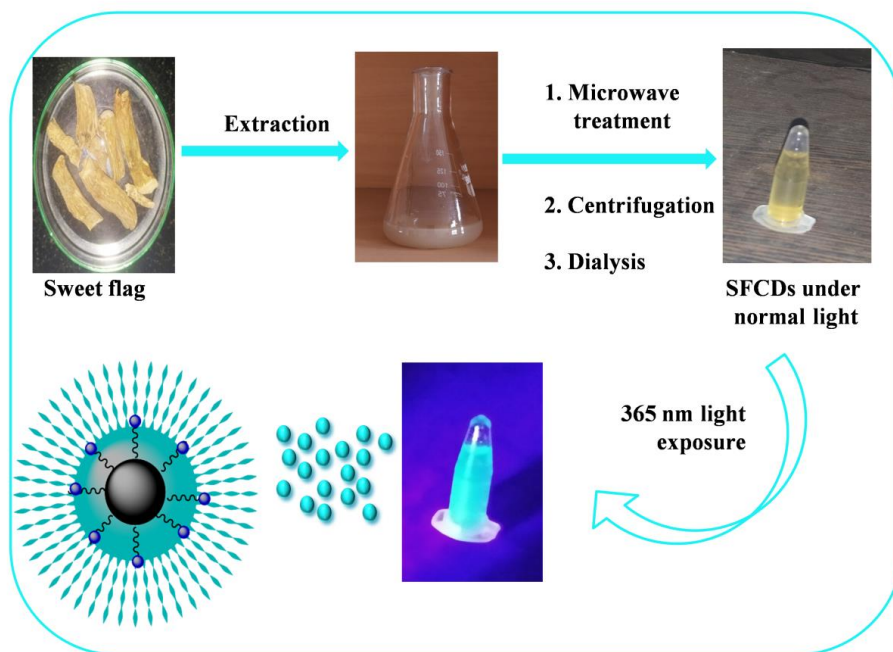
Then the as obtained yellowish brown solution was found to be fluorescent under UV light and it is stored at 4 °C for further use.

### 7.2.2 Detection of 4-NP

The detection of 4-NP was carried out by measuring the fluorescence intensity of the SFCDs in presence of different concentration of 4-NP. In a typical assay, 2 mL of SFCDs solution was taken in quartz cuvette and fluorescence spectrum of the solution

measured. Afterwards different concentrations of 4-NP (0-14.28  $\mu\text{M}$ ) solution were introduced to the system by the use of micropipette and fluorescence spectra of the mixture were monitored after 1 minute of incubation time. The intensity variation up on addition of 4-NP was carefully noticed and recorded.

The same procedure was followed for the selectivity studies by replacing 4-NP with other substances like metal ions ( $\text{K}^+$ ,  $\text{Zn}^{2+}$ ,  $\text{Na}^+$ ,  $\text{Cd}^{2+}$ ,  $\text{Pb}^{2+}$ ,  $\text{Ca}^{2+}$ ,  $\text{Co}^{2+}$ ,  $\text{Hg}^{2+}$ ,  $\text{Cu}^{2+}$  and  $\text{Fe}^{3+}$ ) and phenolic compounds (phenol, resorcinol, 4-chlorophenol, 2-methylphenol, 3-methylphenol, 4-methylphenol, 3-nitrophenol and 2-nitrophenol).



**Scheme 7.1:** Synthesis of SFCDs

### **7.2.3 Real water analysis**

The detection performance of the nanoprobe was practically tested by implementing it for the detection of 4-NP in real water samples collected locally (River water and tap water). River water samples were collected from the nearby Nila River and the tap water samples collected from the laboratory tap. The studies were carried out using standard addition method through spiking process. Firstly, the samples were filtered to remove large particles and then centrifuged for 20 minutes. 1 mL of this sample was spiked with 10  $\mu$ L of standard solution of 4-NP and it was added to 1 mL of SFCDs and after incubation of 1 minute the fluorescence spectrum was recorded using the same instrument and under the same experimental conditions used for all other fluorescence studies. Then again 10  $\mu$ L of the 4-NP was added to the above mixture and fluorescence was monitored and the same process was continued until the total added volume of 4-NP reaches 100  $\mu$ L. The intensity of fluorescence was carefully noted and the calculations are done as per the standard equation as explained in the Chapter 3.

## **7.3 Results and discussion**

### **7.3.1 Formation of SFCDs**

SFCDs were derived from the dried rhizomes of sweet flag by microwave irradiation method. This microwave heating instigates the formation carbon nano particles from the extract; consists with large number of different organic molecules including eugenol acetate, cineole, butyric acid, polyphenolic acids and ester of butyric acids, several amino acids and carbohydrates [1,5]. : The constituents of the

precursor plays vital role in the formation of carbon dots from the extract. The proposed mechanism follows the bottom-up scheme, which involves the formation of nano dimensional particles from smaller molecules when subjected to pyrolysis. The mechanism majorly consists of different steps including condensation, polymerisation, carbonization and nuclear burst resulting into nano products.

In brief, during the microwave irradiation, the carbohydrates present in the extract undergo different chemical reactions such as hydrolysis, dehydration and decomposition. These reactions are facilitated by the polyphenolic acids present in the extract. In general, the furfural derivatives were formed by the above reactions undergoes cascade of reaction including self-condensation and reaction with other reactive molecules in the system leads to the formation of different products and these may get polymerised up on polymerisation reaction. The condensation and aromatisation of these polymerised products leads to the carbon cluster generation and finally the nuclear burst of the cluster gives off the fluorescent carbon dots. All of the reactions proceeds by the aid of microwave energy within a short duration of time [6,7].

### **7.3.2 Characterisation**

#### **TEM analysis**

Surface morphology, size distribution and average size of the as prepared SFCDs were recognized from the TEM images and the corresponding histogram (**Figure 7.1**). This reveals that the size distribution fall under the range of 3.16 to 8.38 nm.

## XRD analysis

The XRD pattern of the system shows a broad diffraction peak centered at  $22.6^\circ$ , which is generally the characteristics of carbonaceous material with  $sp^3$  disorders (**Figure 7.2**). The interlayer spacing of the SFCDs was determined to be 0.37 nm in accordance with the Bragg's equation (Given in Chapter 3). This value is found to be greater than that of bulk graphite (0.33 nm), implies that the synthesised material was less crystalline. Besides, the increase in interlayer spacing directly implies the increase of amorphous character and is accredited to the co-existence of functional groups containing oxygen and functionalities with amine groups [8].

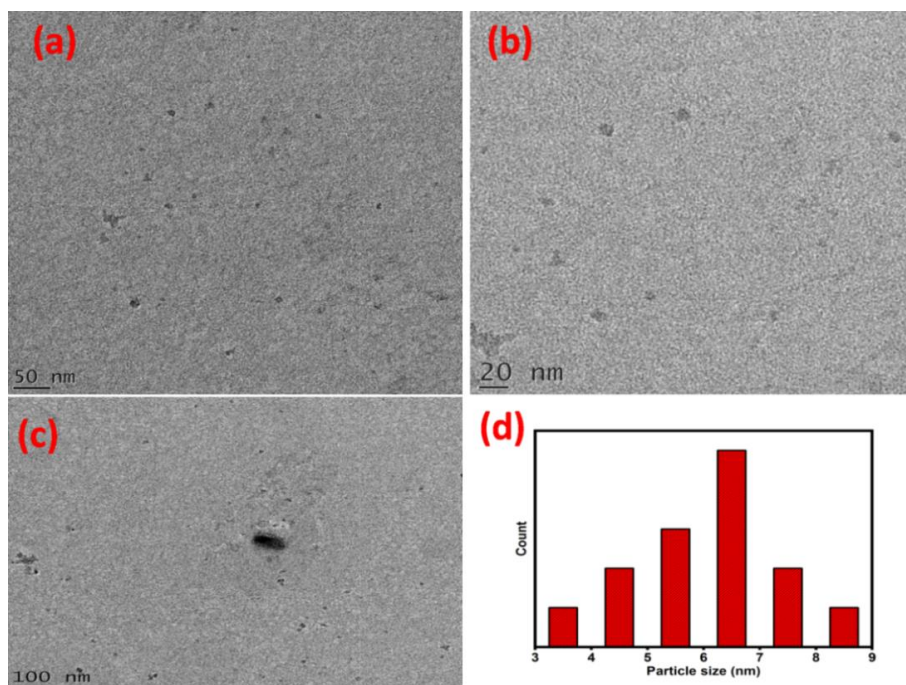


**Figure 7.1:** (a, b,c) TEM images of SFCDs with different scale(d) Histogram from (a) n= 15

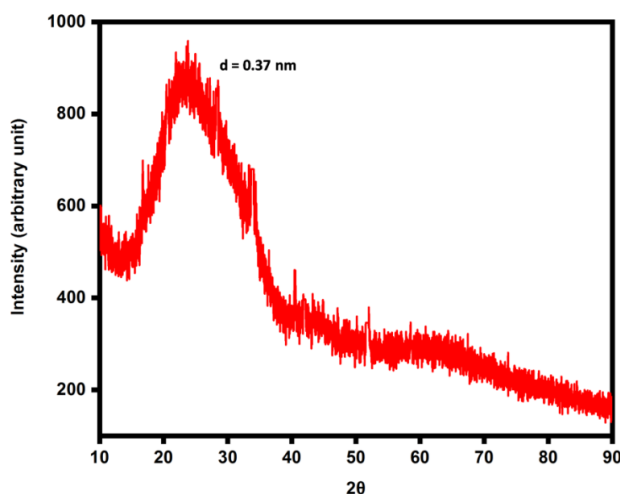


**Figure 7.2:** XRD pattern of SFCDs

### Raman and FTIR analysis

Raman spectrum (**Figure 7.3**) of the SFCDs gives two bands one at  $1362\text{ cm}^{-1}$  and  $1584\text{ cm}^{-1}$ , indicating D and G bands respectively. The D band is related to the vibration of carbon atoms with dangling bonds in the termination plane of disordered graphite or glassy carbon. And it is representing the defects or disorder in the material since it arises due to the activation of  $A_{1g}$  symmetry mode which is generally “forbidden” in perfect graphite. While the G band associated with the  $E_{2g}$  symmetry mode of and is corresponds to the vibration of  $sp^2$  bonded carbon atoms in a two dimensional hexagonal lattice [9,10]. Furthermore, the broadness of the two peaks reveals the poor crystalline behaviour and low graphitization, all these findings were in line with the XRD results [9].

FTIR spectrum of the SFCDs (**Figure 7.4**) was used to identify the functionalities associated with surface of SFCDs. A broad peak centered at  $3292\text{ cm}^{-1}$  corresponds to stretching vibrations of O-H and



N-H bonds. While small peaks at 2932 and 2831  $\text{cm}^{-1}$  were attributed to C-H stretching vibrations [8,11]. A strong band at 1082  $\text{cm}^{-1}$  associated with the C-O stretching vibrations from alcoholic as well as carboxylic groups in the surface of SFCDs. Comparatively strong band at 1578  $\text{cm}^{-1}$  was assumed to be contributed by the combined effect of C=C stretching, N-H bending vibrations and  $\text{COO}^-$  asymmetric stretching vibrations. The symmetric stretching vibration of  $\text{COO}^-$  gives rise to the small band at 1405  $\text{cm}^{-1}$  [12]. Whereas peak at 1452  $\text{cm}^{-1}$  assigned C-N stretching vibrations [13]. Altogether the FTIR data reveals that the surface of SFCDs contains various hydrophilic functionalities including carboxylic, amino and hydroxyl groups. These groups efficiently contribute to the prominent water solubility and stability of SFCDs. This solubility and stability of SFCDs in aqueous medium terribly expands its applicability as sensor in water samples.

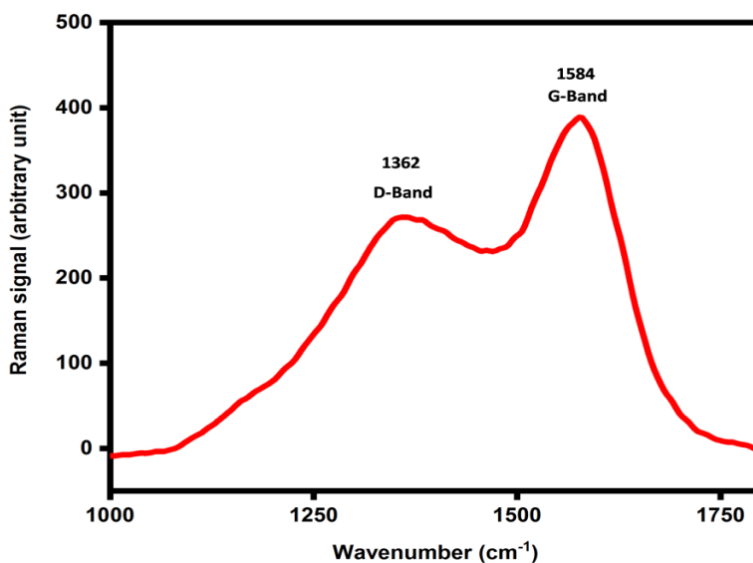


**Figure 7.3:** Raman spectrum of SFCDs

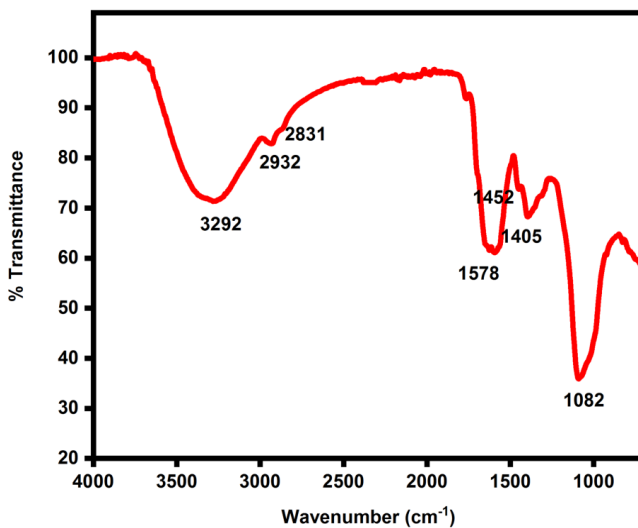


**Figure 7.4:** FTIR spectrum of SFCDs

### UV-Vis spectral analysis

The intriguing optical characteristics of the SFCDs were well explored by the UV-Vis absorption spectra. As given in **Figure 7.5**, there exists two absorption peaks around 227 and 304 nm, the former one assigned to the  $\pi - \pi^*$  transition from the aromatic cores of SFCDs and the latter one ascribed to the electronic transitions originating from the non-bonding electrons of the functionalities present in the system.

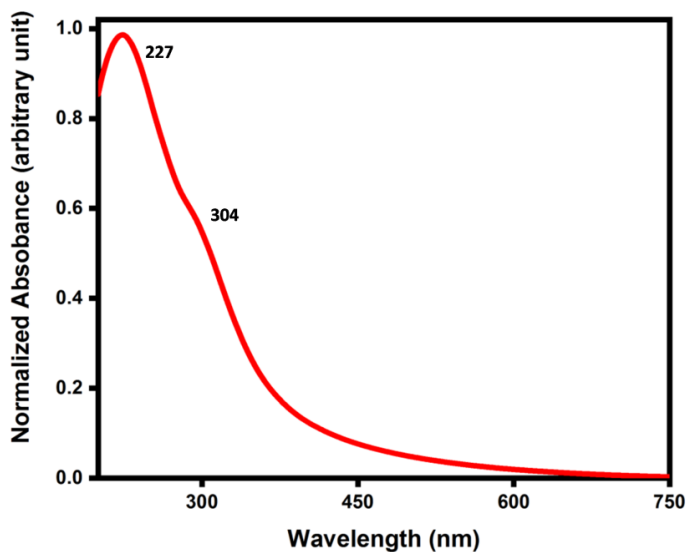


**Figure 7.5:** Normalized UV-Vis absorption spectrum of SFCDs

### Fluorescence spectral analysis

The fluorescence spectrum of SFCDs is presented in **Figure 7.6**. SFCDs exhibits excitation dependent emission behaviour, as the excitation wavelength alters emission wavelength as well as emission intensity also changed and this behaviour of the system may attribute to the polydispersity and surface emissive traps [8]. The fluorescence spectra with excitation wavelength ranging from 325 to 435 nm with interval of 10 nm are given in **Figure 7.7**. From the excitation dependence studies, it reveals that SFCDs possessing highest emission intensity when excited at 365 nm and it was centered at 441 nm. So these values were selected as the excitation and emission wavelength of the present probe for further studies. The system shows yellowish brown colour under normal light but having greenish blue fluorescence

under UV light of 365 nm. The photograph of the same is given in the inset of **Figure 7.8** along with excitation and emission spectra.

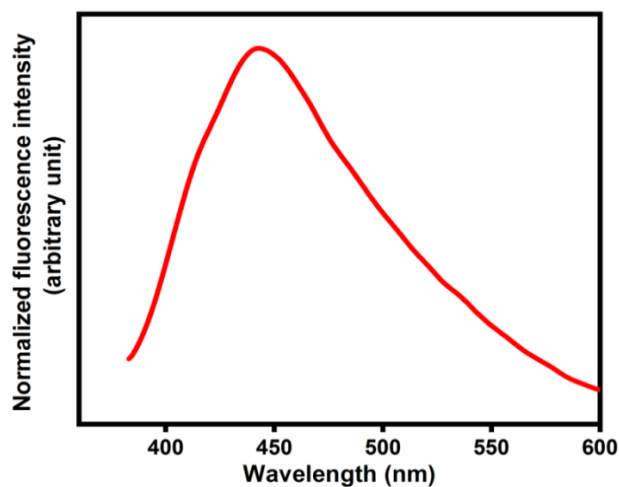


**Figure 7.6:** Fluorescence emission spectrum of SFCDs

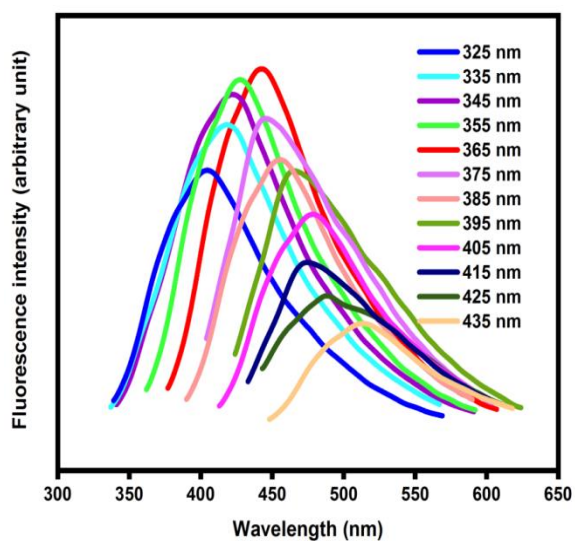


**Figure 7.7:** Excitation dependent emission spectra of SFCDs from 325 to 435 nm

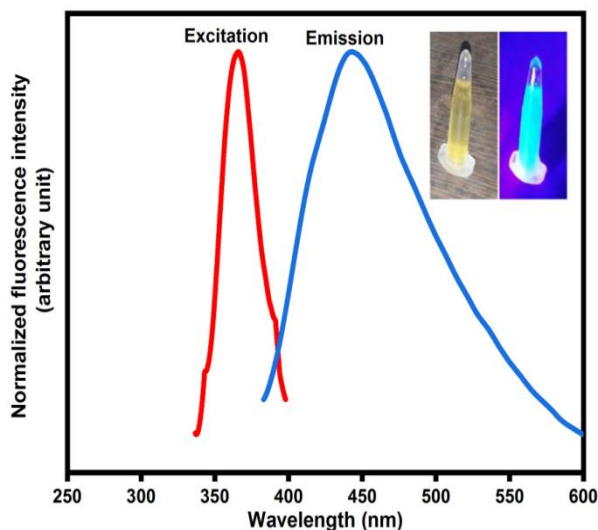


**Figure 7.8:** Excitation and emission spectra of SFCDs (inset: SFCDs at normal light(left) and SFCDs at UV light(right))

### 7.3.3 Fluorescence quantum yield and fluorescence stability of SFCDs

The fluorescence quantum yield of the SFCDs was determined to be about 5.4 % by standard method with quinine sulphate as reference standard

As in the previous cases the fluorescence stability of the system was more than six months at 4 °C and it gets reduced at higher temperature. The photo-stability of the system was tested by placing the solution under UV light of 365 nm for one hour shows no significant fluorescence reduction implies that the system exhibits good level of photo-resistance

### 7.3.4 Selectivity studies

To investigate the possibility of the system as fluorescent sensing probe on account to its prominent fluorescence behaviour, various fluorescent studies were performed. The fluorescence responses of the probe with different metal ions ( $K^+$ ,  $Zn^{2+}$ ,  $Na^+$ ,  $Cd^{2+}$ ,  $Pb^{2+}$ ,  $Ca^{2+}$ ,  $Co^{2+}$ ,  $Hg^{2+}$ ,  $Cu^{2+}$  and  $Fe^{3+}$ ) and different phenolic compound (phenol, resorcinol, 4-chlorophenol, 2-methylphenol, 3-methylphenol, 4-methylphenol, 3-nitrophenol, 2-nitrophenol, 4-NP) were recorded results are depicted in **Figure 7.9 and 7.10**, respectively. The results show that 4-NP exhibits significant fluorescence reduction.

As shown in **Figure 7.10**, among the isomeric mono nitrophenols, 3-nitrophenol shows negligible effect on fluorescence. 4-NP displays highest fluorescence quenching efficiency with 32 % reduction in fluorescence followed by 2-nitrophenol, having only 12 % fluorescence reduction. This confirms the selectivity of the probe towards 4-NP.

The major reason for this selectivity of 4-NP than the other two mononitrophenols is the comparatively stronger interaction of the SFCDs with the 4-NP. The strong acidic nature of the species over the other two plays vital role in the stronger interaction with the surface functionalities of the SFCDs. Stronger electron withdrawing effect of the nitro group in the 4-NP make it more acidic. The electron rich amino groups present in the SFCDs surface interact with the 4-NP and leads to fluorescence quenching [14].

To further ensure the selectivity of the probe, the interference studies were conducted by  $\text{Fe}^{3+}$  and 2-nitrophenol along with 4-NP, since these two species are showing some amount of quenching efficiency on comparing others, and the result displayed in **Figure 7.10** shows that these foreign species does not exerts any significant effect in the sensing of 4-NP. The fluorescence reduction of SFCDs by 4-NP is about three fold higher than the case of 2-nitrophenol and may be due to this it does not exerts much effect in the sensing performance of SFCDs towards 4-NP, similar in the case of  $\text{Fe}^{3+}$  where the reduction in fluorescence of SFCDs is about 20 % as compared to 4-NP. Moreover, the presence of 2-nitrophenol in water resources was comparatively lower than that of 4-NP and this may be due to its lower solubility in water.

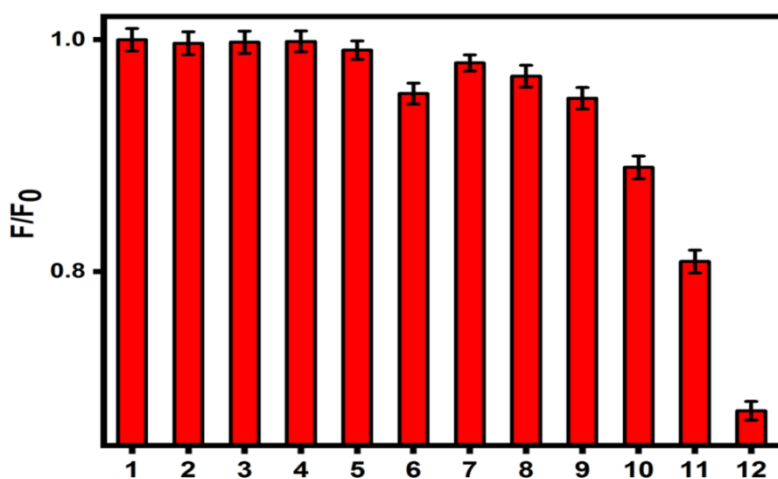


**Figure 7.9:** Relative fluorescence intensity of SFCDs with different metal ions(1 to 12 representing Blank,  $\text{K}^+$ ,  $\text{Zn}^{2+}$ ,  $\text{Na}^+$ ,  $\text{Cd}^{2+}$ ,  $\text{Pb}^{2+}$ ,  $\text{Ca}^{2+}$ ,  $\text{Co}^{2+}$ ,  $\text{Hg}^{2+}$ ,  $\text{Cu}^{2+}$ ,  $\text{Fe}^{3+}$  and 4-NP)

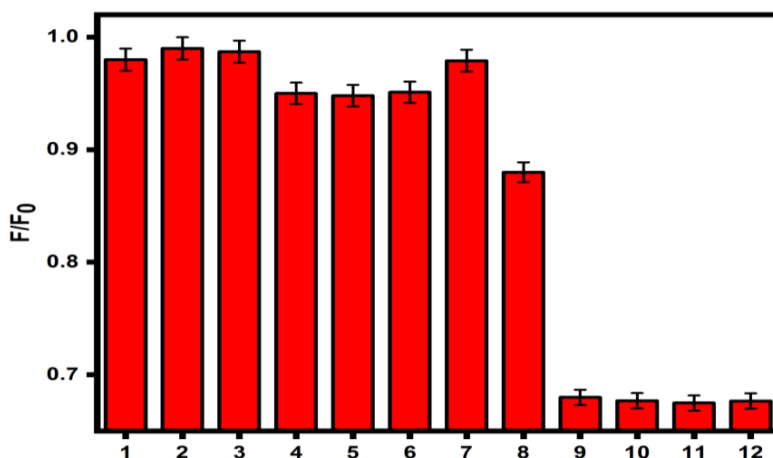


**Figure 7.10:** Relative fluorescence intensity with different phenolic compounds (1 to 12 representing phenol, resorcinol, 4-chlorophenol, 2-methylphenol, 3-methylphenol, 4-methylphenol, 3-nitrophenol, 2-nitrophenol, 4-NP, 4-NP with 2-nitrophenol, 4-NP with  $\text{Fe}^{3+}$  and 4-NP along with  $\text{Fe}^{3+}$  and 2-nitrophenol)

### 7.3.5 Sensing studies with 4-NP

To explore the sensitivity of 4-NP towards the system, fluorescence studies with different concentration of 4-NP were performed. The fluorescence spectrum of the bare SFCDs was recorded initially and then different concentration of 4-NP was introduced to the system. The corresponding fluorescence spectra were monitored after incubation time of 1 minute, after optimisation by trial and error method. **Figure 7.11** clearly reveals the gradual decline of fluorescence intensity of the system by the addition quenching species. As the concentration of quencher increases the intensity fluorescence decreases.



The quenching behaviour follows linear relationships with concentration of the quencher from 0 to 14.28  $\mu\text{M}$ . The linear plot of relative fluorescence intensity with concentration of 4-NP was displayed in **Figure 7.12**. The LOD was found to be 0.207  $\mu\text{M}$  (28.79 ng/mL) and it was calculated by the standard equation  $3\sigma/\kappa$ , where  $\sigma$  is the standard deviation and  $\kappa$  is the slope of linear plot obtained from the linear equation  $F_0/F = 0.0629 [4\text{-NP}] + 0.9889$ . The LOD value and other statistical parameters obtained for this system was comparable with the recent reports in literature and some of them are enlisted in **Table 7.1**. Moreover, the detection limit is lesser than the accepted level (60 ng/mL) of 4-NP in drinking water by US EPA [8], indicates that the probe developed can be implemented to the real water analysis.

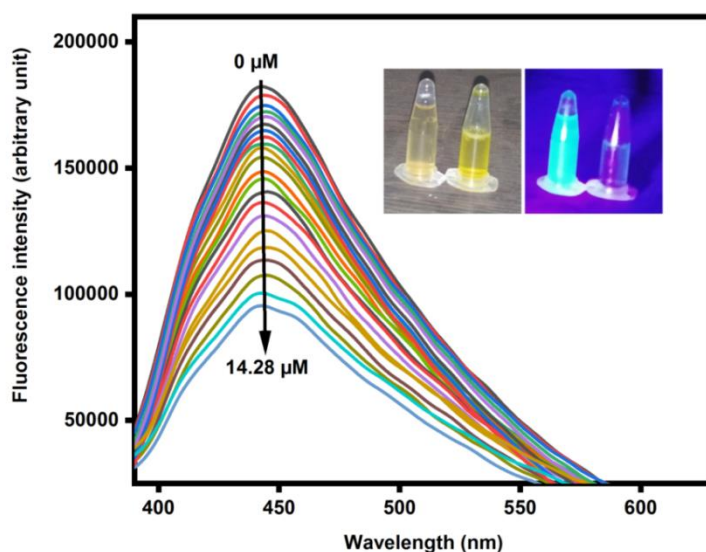


**Figure 7.11:** Fluorescence emission spectra with increasing concentration of 4-NP (inset shows the photographs of SFCDs (left) and SFCDs with 4-NP(right) under normal and UV light)

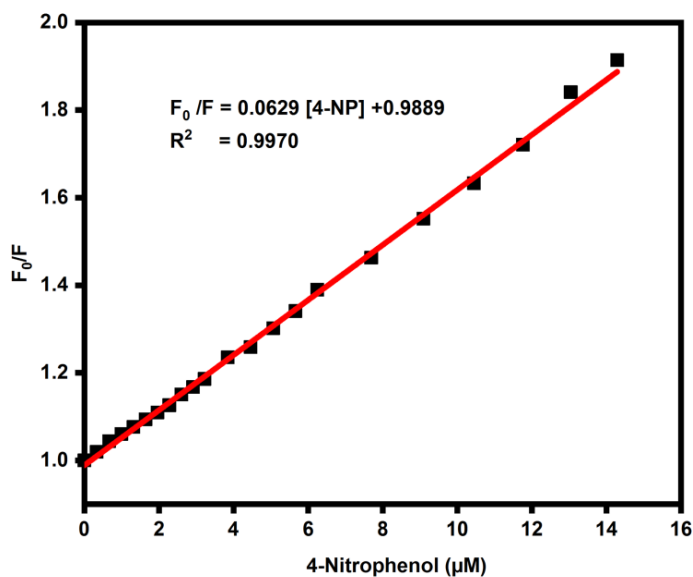


**Figure 7.12:** Linear relationships between relative fluorescence with concentration of 4-NP

**Table 7.1:** Comparison of different sensors for 4-NP detection

Sensing probe	LOD (μM)	Linear range (μM)	Reference
N doped oxidized CDs	2	2.0 – 100	[4]
Chromium(III)-doped CDs	0.27	0.8 – 150	[15]
Nitrogen-doped CDs (N-CDs)	0.201	0.5 – 70	[16]
Boron and nitrogen co-doped CDs (B,N-CDs)	0.2	0.5 – 60	[17]
polymer CDs (PCDs)	0.26	0.5 – 60	[18]
β-cyclodextrin-capped ZnO quantum dots	0.34	1.0 – 40	[19]
CDs derived from sweet flag	0.207	0 – 14.28	This work

### 7.3.6 Detection of 4-NP in real samples

To validate the practicability of this sensing method, SFCs were used for the detection of 4-NP in river and tap water samples by standard addition method. The pre-treated water samples were spiked with standard 4-NP solution and then mixed with SFCs probe. The mixtures were incubated for 1 minute. Afterwards, fluorescence spectrum of the mixture was recorded at excitation of 365 nm. Subsequently, different concentration of 4-NP was added, fluorescence spectra were monitored and recovery and error percentages were calculated (Equation is given in Chapter 3). The results obtained are tabulated in **Table 7.2**. As given, the recovery percentage ranges from 94.80 to 97.20 %.

**Table 7.2** Detection of 4-NP in different water samples

Water sample	Added 4-NP ( $\mu\text{M}$ )	Found ( $\mu\text{M}$ )	Error %	Recovery (%)
River Water	0	Not found	-	-
	0.2	0.1940	3.10	96.90
	0.4	0.3888	2.80	97.20
Tap Water	0	Not found	-	-
	0.2	0.1896	5.20	94.80
	0.4	0.3836	4.10	95.90

### 7.3.7 Fluorescence quenching mechanism

The sensing mechanism behind the selective sensing of 4-NP by the fabricated nanoprobe was thoroughly investigated. In general

fluorescence quenching mechanism can be of four main types, namely static quenching mechanism, dynamic quenching mechanism, IFE and FRET (Förster resonance energy transfer) [20].

The fluorescence decay studies of SFCDs without and with the quenching species helps to reveal the possible mechanism. The results of the same is shown in **Figure 7.13**, The average lifetime of SFCDs was determined by standard equation (Given in Chapter 3) and found out to be 6.891 ns and that of SFCDs@4-NP was 6.783 ns, indicates that there is no significant change in the life time of SFCDs by the addition of 4-NP. This result excludes the chance of dynamic and FRET quenching mechanism from the list [20,21].

Then the quenching may follow static quenching mechanism or IFE mechanism. To reveal this the possibility of complex formation between 4-NP and amino group in the surface of SFCDs was investigated. The electron deficient 4-NP due to strong electron withdrawing effect of nitro group at the *para* position interacts effectively with the electron rich amino group in the surface of SFCDs results in the formation of Meisenheimer complex. This complex formation may leads to the fluorescence quenching through electron transfer induced fluorescence quenching [8].

To furthermore confirming the complex formation, UV-Vis spectra of 4-NP, SFCDs and SFCDs with 4-NP (SFCDs@4-NP) were recorded. As seen in **Figure 7.14**, the absorbance spectrum of SFCDs@4-NP differs from that of SFCDs and 4-NP. Besides, the experimental spectrum of 4-NP with SFCDs was different from the

theoretical spectrum, indicates the presence of effective interaction between the 4-NP and SFCDs. Moreover, there is an extra peak centered at 459 nm in absorbance spectrum of SFCDs@4-NP and it is not present either in the spectrum of SFCDs, 4-NP, or theoretical spectrum of SFCDs+4-NP. Therefore, the new peak in the absorbance spectrum of SFCDs@4-NP may be accredited to the complex formed between the quencher and surface functional groups of SFCDs. Additionally, the quenching effect was also determined by using the Stern-Volmer equation (equation (1)), from the linear plot of relative fluorescence response with concentration of quenching species, by linear regression with fixed intercept at 1.

$$\frac{F_0}{F} = K_{sv} \times [Q] + 1 = K_q \times \tau_0 \times [Q] + 1 \quad (1)$$

Where,  $F_0$  is the fluorescence intensity at zero quencher concentration,  $F$  is the fluorescence intensity at definite concentration of quencher,  $[Q]$  is the concentration of quencher,  $K_{sv}$  is the Stern-Volmer constant,  $K_q$  is the quenching rate constant and  $\tau_0$  is the average life time. The value of  $K_q$  for this probe was determined to be  $8.96 \times 10^{12} \text{ M}^{-1}\text{S}^{-1}$  greater than the highest value of dynamic quenching effect is about  $1.0 \times 10^{10} \text{ M}^{-1}\text{S}^{-1}$ . These finding leads to the conclusion that the mechanism of 4-NP sensing by the system was majorly by the ground state complex formation by the introduction quencher to the fluorescent system. This type of quenching generally belongs to static quenching mechanism.

To test the role of IFE in the quenching mechanism the UV-Vis spectrum of 4-NP was compared with the excitation and emission spectrum of SFCDs. The UV-Vis spectrum of 4-NP consists of two major peaks one at 315 nm accredited to 4-NP and another one centered at 400 nm originates due to the respective phenolate ions, being acidic 4-NP easily forms corresponding phenolate ions in water medium [22]. Surprisingly, as seen in **Figure 7.15**, there is slight overlap between the absorbance peak at 400 nm with both excitation and emission spectrum of SFCDs, so IFE can also contributes to the fluorescence quenching of SFCDs by 4-NP. Therefore, the underlying mechanism of the fluorescence quenching of present system by 4-NP is a combination of static quenching mechanism and slight IFE.

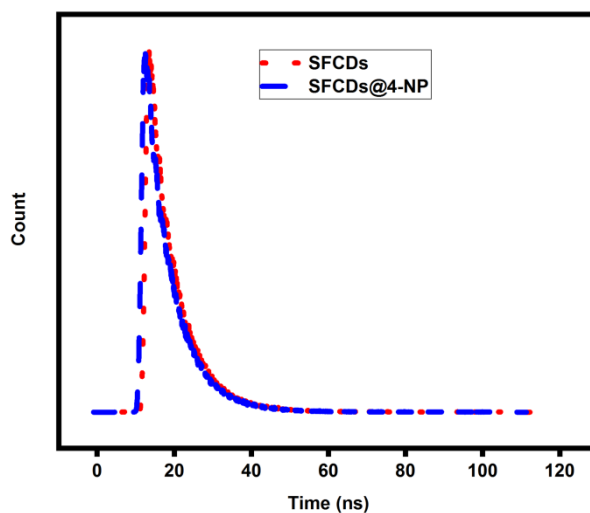


**Figure 7.13:** Fluorescence life time decay curve of SFCDs with and without 4-NP

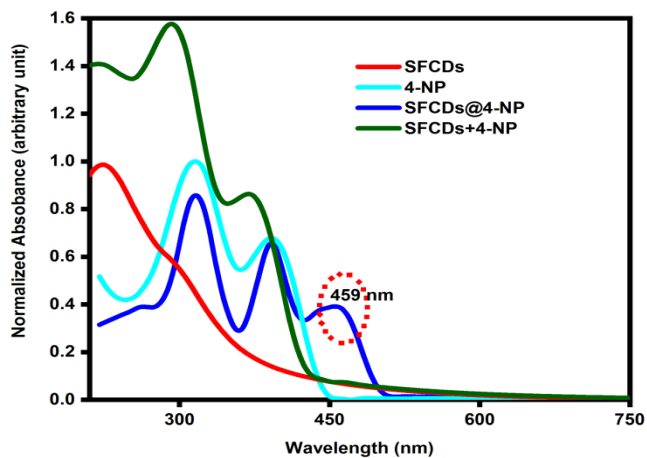


**Figure 7.14:** Normalized UV-Vis absorption spectra of SFCDs, 4-NP, SFCDs@4-NP and SFCDs+4-NP

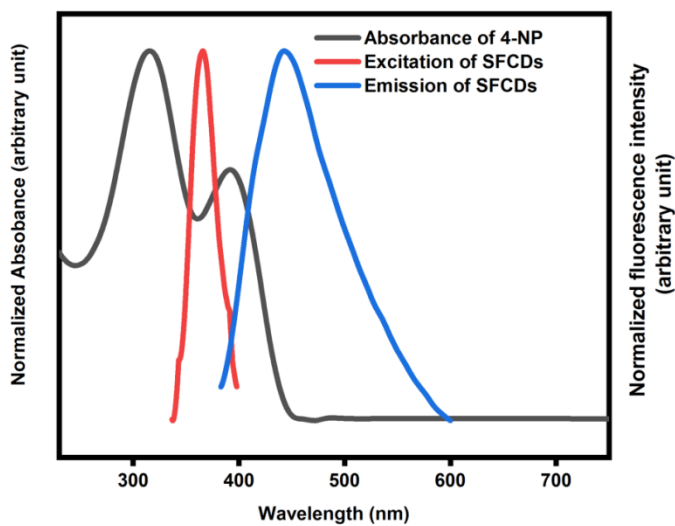


**Figure 7.15:** Spectral overlap of excitation and emission spectra of SFCDs with absorbance spectrum of 4-NP

## 7.4 Conclusions

In summary, a pharmacologically relevant bioprecursor was successfully converted to highly fluorescent carbon dots through facial, cost-effective and simple pathway by truly following green strategies and protocols. Synthesis through microwave irradiation without using any hazardous chemicals or complicated instruments adds more environmental benign colour to the system. The selective interaction of the nano probe with 4-NP with quenching of native fluorescence of the system was utilised to design and fabricate fluorescent sensing tool for the detection of 4-NP. The developed sensor exhibits micromolar level of detection limit and keeps linearity relationships with the concentration of quencher. The quenching mechanism underlying this sensing was thoroughly investigated and attributed to the combination effect of static and IFE mechanism. Moreover the probe was applied to real water analysis to test the potentiality of the tool. The recovery percentage and other parameters give highly acceptable levels, implies that the system can be used as a promising tool for the sensing of 4-NP in natural water systems. Importantly, the proposed method not only gives value addition to the precursor but also give rise to a sensing platform for the detection of aquatic pollutant in natural water resources.



## 7.5 References

- [1] P.K. Mukherjee, V. Kumar, M. Mal, P.J. Houghton, *Acorus calamus*: Scientific Validation of Ayurvedic Tradition from Natural Resources, *Pharmaceutical Biology*. 45 (2007) 651–666.  
<https://doi.org/10.1080/13880200701538724>
- [2] T. Huang, Y. Fu, Q. Peng, C. Yu, J. Zhu, A. Yu, X. Wang, Catalytic hydrogenation of p-nitrophenol using a metal-free catalyst of porous crimped graphitic carbon nitride, *Applied Surface Science*. 480 (2019) 888–895. <https://doi.org/10.1016/j.apsusc.2019.03.035>
- [3] X. Wang, Y. Liu, Q. Wang, T. Bu, X. Sun, P. Jia, L. Wang, Nitrogen, silicon co-doped carbon dots as the fluorescence nanoprobe for trace p-nitrophenol detection based on inner filter effect, *Spectrochim. Acta, Part A*. 244 (2021) 118876. <https://doi.org/10.1016/j.saa.2020.118876>
- [4] N.K.R. Bogireddy, R. Cruz Silva, M.A. Valenzuela, V. Agarwal, 4-nitrophenol optical sensing with N doped oxidized carbon dots, *J. Hazard. Mater.* 386 (2020) 121643.  
<https://doi.org/10.1016/j.jhazmat.2019.121643>
- [5] N.V. Belska, A.M. Guriev, M.G. Danilets, E.S. Trophimova, E.G. Uchasova, A.A. Ligatcheva, M.V. Belousov, V.I. Agaphonov, V.G. Golovchenko, M.S. Yusubov, Y.P. Belsky, Water-soluble polysaccharide obtained from *Acorus calamus* L. classically activates macrophages and stimulates Th1 response, *International Immunopharmacology*. 10 (2010) 933–942.  
<https://doi.org/10.1016/j.intimp.2010.05.005>
- [6] B. De, N. Karak, A green and facile approach for the synthesis of water soluble fluorescent carbon dots from banana juice, *RSC Adv.* 3 (2013) 8286. <https://doi.org/10.1039/c3ra00088e>
- [7] M.L. Liu, B.B. Chen, C.M. Li, C.Z. Huang, Carbon dots: synthesis, formation mechanism, fluorescence origin and sensing applications, *Green Chem.* 21 (2019) 449–471. <https://doi.org/10.1039/C8GC02736F>
- [8] H. Yuan, J. Yu, S. Feng, Y. Gong, Highly photoluminescent pH-independent nitrogen-doped carbon dots for sensitive and selective sensing of p-nitrophenol, *RSC Adv.* 6 (2016) 15192–15200.  
<https://doi.org/10.1039/C5RA26870B>

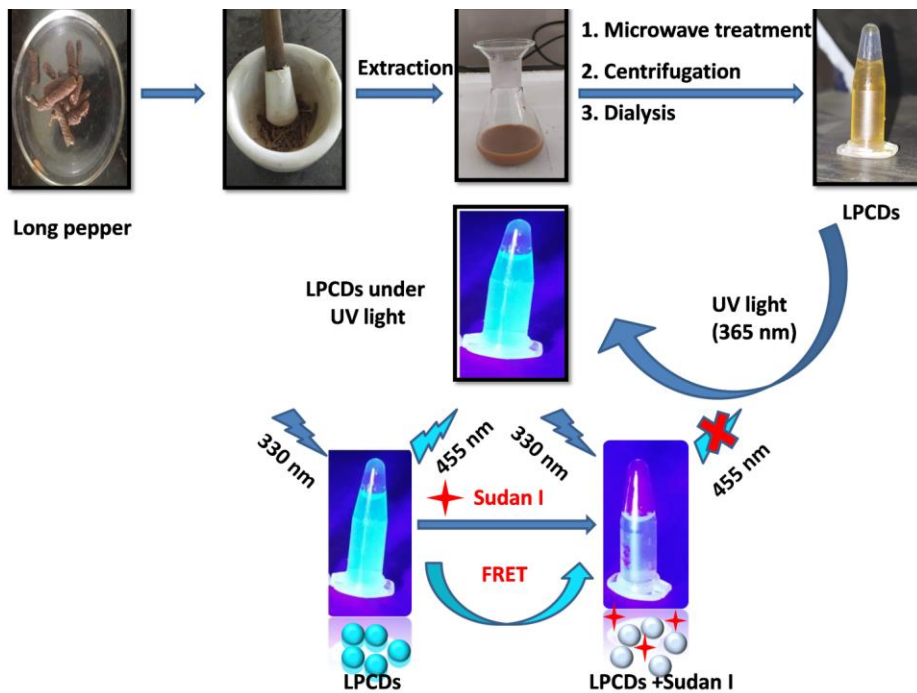
- [9] V. Ramanan, S.K. Thiyagarajan, K. Raji, R. Suresh, R. Sekar, P. Ramamurthy, Outright Green Synthesis of Fluorescent Carbon Dots from Eutrophic Algal Blooms for In Vitro Imaging, *ACS Sustainable Chem. Eng.* 4 (2016) 4724–4731. <https://doi.org/10.1021/acssuschemeng.6b00935>
- [10] K.D. Esmeryan, C.E. Castano, A.H. Bressler, M. Abolghasemibizaki, C.P. Fergusson, A. Roberts, R. Mohammadi, Kinetically driven graphite-like to diamond-like carbon transformation in low temperature laminar diffusion flames, *Diamond Relat. Mater.* 75 (2017) 58–68. <https://doi.org/10.1016/j.diamond.2017.01.014>
- [11] P. Murugesan, J.A. Moses, C. Anandharamakrishnan, One step synthesis of fluorescent carbon dots from neera for the detection of silver ions, *Spectrosc. Lett.* 53 (2020) 407–415. <https://doi.org/10.1080/00387010.2020.1764589>
- [12] H. Xu, X. Yang, G. Li, C. Zhao, X. Liao, Green Synthesis of Fluorescent Carbon Dots for Selective Detection of Tartrazine in Food Samples, *J. Agric. Food Chem.* 63 (2015) 6707–6714. <https://doi.org/10.1021/acs.jafc.5b02319>
- [13] J. Fang, S. Zhuo, C. Zhu, Fluorescent sensing platform for the detection of p-nitrophenol based on Cu-doped carbon dots, *Optical Materials.* 97 (2019) 109396. <https://doi.org/10.1016/j.optmat.2019.109396>
- [14] X. Yang, J. Wang, D. Su, Q. Xia, F. Chai, C. Wang, F. Qu, Fluorescent detection of TNT and 4-nitrophenol by BSA Au nanoclusters, *Dalton Trans.* 43 (2014) 10057–10063. <https://doi.org/10.1039/C4DT00490F>
- [15] C. Li, Y. Zheng, H. Ding, H. Jiang, X. Wang, Chromium(III)-doped carbon dots: fluorometric detection of p-nitrophenol via inner filter effect quenching, *Microchim. Acta.* 186 (2019) 384. <https://doi.org/10.1007/s00604-019-3444-3>
- [16] S. Liao, Z. Ding, S. Wang, F. Tan, Y. Ge, Y. Cui, N. Tan, H. Wang, Fluorescent nitrogen-doped carbon dots for high selective detecting p-nitrophenol through FRET mechanism, *Spectrochim. Acta, Part A.* 259 (2021) 119897. <https://doi.org/10.1016/j.saa.2021.119897>
- [17] N. Xiao, S.G. Liu, S. Mo, N. Li, Y.J. Ju, Y. Ling, N.B. Li, H.Q. Luo, Highly selective detection of p-nitrophenol using fluorescence assay based on boron, nitrogen co-doped carbon dots, *Talanta.* 184 (2018) 184–192. <https://doi.org/10.1016/j.talanta.2018.02.114>

- [18] L. Han, S.G. Liu, J.Y. Liang, Y.J. Ju, N.B. Li, H.Q. Luo, pH-mediated reversible fluorescence nanoswitch based on inner filter effect induced fluorescence quenching for selective and visual detection of 4-nitrophenol, *J. Hazard. Mater.* 362 (2019) 45–52.  
<https://doi.org/10.1016/j.jhazmat.2018.09.025>
- [19] S. Geng, S.M. Lin, S.G. Liu, N.B. Li, H.Q. Luo, A new fluorescent sensor for detecting p-nitrophenol based on  $\beta$ -cyclodextrin-capped ZnO quantum dots, *RSC Adv.* 6 (2016) 86061–86067.  
<https://doi.org/10.1039/C6RA17378K>
- [20] F. Zu, F. Yan, Z. Bai, J. Xu, Y. Wang, Y. Huang, X. Zhou, The quenching of the fluorescence of carbon dots: A review on mechanisms and applications, *Microchim. Acta.* 184 (2017) 1899–1914.  
<https://doi.org/10.1007/s00604-017-2318-9>
- [21] M. Wang, R. Shi, M. Gao, K. Zhang, L. Deng, Q. Fu, L. Wang, D. Gao, Sensitivity fluorescent switching sensor for Cr (VI) and ascorbic acid detection based on orange peels-derived carbon dots modified with EDTA, *Food Chem.* 318 (2020) 126506.  
<https://doi.org/10.1016/j.foodchem.2020.126506>
- [22] S. Liu, A. Qileng, J. Huang, Q. Gao, Y. Liu, Polydopamine as a bridge to decorate monodisperse gold nanoparticles on Fe<sub>3</sub>O<sub>4</sub> nanoclusters for the catalytic reduction of 4-nitrophenol, *RSC Adv.* 7 (2017) 45545–45551. <https://doi.org/10.1039/C7RA09373J>



# Chapter 8

## LONG PEPPER DERIVED CARBON DOTS



---

This work is published in Luminescence.

P. Venugopalan and N. Vidya, Long pepper (*Piper longum*) derived carbon dots as fluorescent sensing probe for sensitive detection of Sudan I, *Luminescence*, 38, (2023), 401-409.

<https://doi.org/10.1002/bio.4459>



## 8.1 Introduction

CDs derived from biobased precursors received greater importance in the past two decades and several reports were coming out from this area [1–9]. Greater bioavailability, very low level of toxicity or null toxicity, renewability, greener nature and low –cost are the key features behind this attractive attention [1,10–14]. Here, a traditionally important medicinal fruit, long pepper, was opted as the precursor for the preparation of CDs.

Long pepper (*Piper longum*) is well renowned for its medicinal applications and *Ayurveda* gives pretty much importance to this fruit and it included in several *Ayurvedic* medicines as a major constituent [15]. The pharmacological activities and applications of this is explained in Chapter 2. However, its materialisation scope was not yet reported.

In the present study, materialization of the long pepper in to fluorescent CDs using microwave energy was designed and executed for the first time and thereby giving value-addition to the precursor. The as prepared long pepper derived CDs is abbreviated as LPCDs. Characterisation of the present system was carried out to explore the physiochemical properties associated with the LPCDs through different analytical methods including TEM, XRD, Raman, FTIR, UV-Vis and fluorescence spectroscopic techniques.

From the investigation for the utilisation of the prepared system as a fluorescent probe, effects of fluorescence intensity of the system

with different food colouring agents was carried out, the results indicates that the native fluorescence of LPCDs is selectively reduced by the interaction with Sudan I dye. Therefore further sensing studies were conducted with Sudan I.

Sudan I is a red coloured azo dye and one of the most widely used colouring agent in various industries. Both natural and synthetic colorants were considered as the major class of food additives in world wide. In food industry, the acceptance for synthetic alternatives much more due to the excellent colouring capability, extreme level of stability, good water solubility and low cost. Beyond all these advantages, it is very essential to consider the higher level of toxicity associated with them [16]. For the case Sudan I the conjugated azo group present in the structure of made it highly carcinogenic and cause potential health problems, including gene mutation, liver and bladder cancers [17] and is listed as category 3 carcinogen by International Agency for Research on Cancer (IARC) so its uses in food products prohibited by all most all countries worldwide [18]. Unfortunately Sudan I is still used in various food products by illegal route, especially in chilli powder, red chilli sauce and tomato sauce to increase the colour appeal of the products. So it is highly required to monitor the presence of such carcinogenic moieties in food products to ensure food safety and public health.

Based on this selective quenching in fluorescence of LPCDs by this carcinogenic dye Sudan I, which is frequently reported as food adulterant in different food products, a fluorescent probe was



fabricated. And the fabricated probe employed for the detection of Sudan I in real chilli powder samples, where it is frequently reported as adulterant. The next parts go into the experimentation techniques and results.

## **8.2 Experimental**

### **8.2.1 Synthesis of LPCDs**

Aqueous long pepper extract was used as a precursor in a straightforward, one-step microwave heating technique to synthesise LPCDs. The entire preparation process is described in the next paragraph.

About 10 g of long pepper was weighed out and grinded into fine powder form by the use of mortar and pestle and allowed to soak in 50 mL of distilled water for 2 hrs. Afterwards, the whole solution was magnetically stirred for 30 minutes, and then it was filtered. 30 mL of the filtered solution was subjected to microwave treatment at 500 W for 15 minutes of time. The irradiation time and power of the synthesis was optimised through different trial and error methods, the fluorescence of the system was thoroughly monitored at definite time intervals and at different irradiation power to find out the best result with minimum time and lesser energy. The dry sticky type residue was mixed with about 30 mL of distilled water, after thorough shaking followed by 30 minutes magnetic stirring, the dark brown solution as obtained was filtered, centrifuged and dialysed against distilled water for 48 hours using dialysis membrane with MWCO of 3 KDa. The

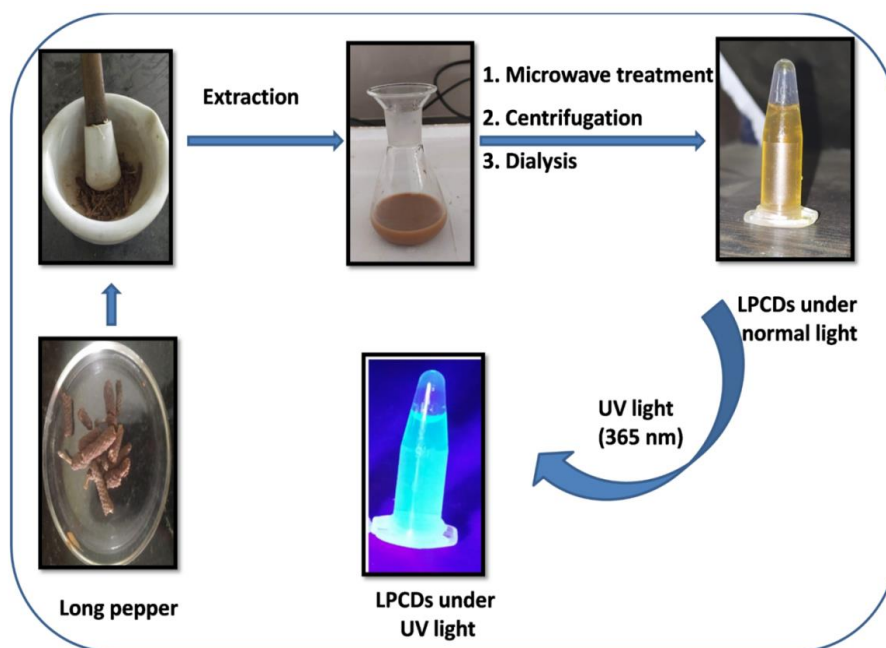
preparation steps are depicted in **Scheme 8.1**.

The as prepared LPCDs exhibits fluorescence under UV light and are stored at 4 °C.

### **8.2.2 Detection of Sudan I**

The fluorescence based detection of Sudan I dye was performed as follows: 1 mM solution of Sudan I was prepared in ethanol. 2 mL of LPCDs solution with 1 mL of ethanol was used as the control for the whole measurements. Emission spectrum of the control was recorded at an excitation wavelength of 370 nm with emission maxima 455 nm. Afterwards different concentration of standard Sudan I in ethanol solution was introduced to the 2 mL of sensing probe solution and was kept in room temperature for about 15 minutes as incubation time. Incubation time of the process was optimised by trial and error method, and a best result obtained at 15 minutes and was selected as the incubation time for the analysis. The spectra of LPCDs solution with different concentration of Sudan I were recorded after the incubation time at an excitation of 370 nm with the same instrumental settings as used for the control. The intensity variations in each addition were carefully monitored.

The same procedure was followed for selectivity testing by replacing Sudan I with different substances including commonly encountered food colorants methyl red, allura red, acid red along with other Sudan dyes (Sudan II, III and IV), some metal salts (NaCl, MgCl<sub>2</sub>, CaCl<sub>2</sub>, KCl and ZnCl<sub>2</sub>) and glucose.



**Scheme 8.1:** Schematic representation of preparation steps and UV cabinet photograph of LPCDs

### 8.2.3 Real sample analysis

Chilli powders were opted as the testing samples, since Sudan dyes were possibly added as an adulterant to it to increase the colour appeal. The testing samples were obtained from the local market in Kerala, India. The pre-treatment of the samples were carried out as follows; about 3 g of chilli powder was added with different concentration of finely powdered Sudan I dye in 3 different beakers, after thorough mixing 30 mL of ethanol was added. The mixture was magnetically stirred for 15 minutes and then it was centrifuged and filtered. The filtrate solution was collected and was subjected for the

determination. Similarly a blank chilli powder sample was also prepared without Sudan I dye by the same procedure as above. The detection was conducted at room temperature and briefly, 2 mL of LPCDs solution was spiked with these pre-treated samples and shaken well, then it was allowed keep for 15 minutes as incubation time. Afterwards fluorescence spectra were recorded at room temperature at an excitation wavelength of 370 nm.

### **8.3. Results and discussion**

#### **8.3.1 Formation of LPCDs**

By the aid of microwave energy LPCDs were synthesised from matured long pepper (*Piper longum*) fruit within a short period of time. Long pepper, a member of *Piperaceae* family and widely distributed in tropical region of the world, especially in India and Sri Lanka. Phytochemicals present in long pepper includes several alkaloids, esters and alcohols like dihydrocarveol [15]. These small molecules are converted into nano dimensional carbon materials by utilising the microwave energy through bottom-up synthetic route. The formation of fluorescent carbon dots involves various steps including condensation, polymerisation and carbonization of the condensed products and finally the nuclear burst of the resulting products. The functional groups present in the precursor believed to be plays a key role in the CDs formation [19,20].

#### **8.3.2 Characterisation**

The analysis below was used to investigate the chemical and optical characteristics of the LPCDs.

## TEM analysis

Particle morphology and size distribution of LPCDs were investigated by TEM and as shown in **Figure 8.1**, major population of the particle size falls within the range of 3.2 to 8.7 nm, which revealed from the histogram based on the TEM results. Besides, spherical nature of the particles was also confirmed from the TEM images. The selected area electron diffraction (SAED) pattern given in **Figure 8.1 (b)** is devoid of bright spots or circles, and are fade in nature indicates the poor crystalline behaviour of the LPCDs.

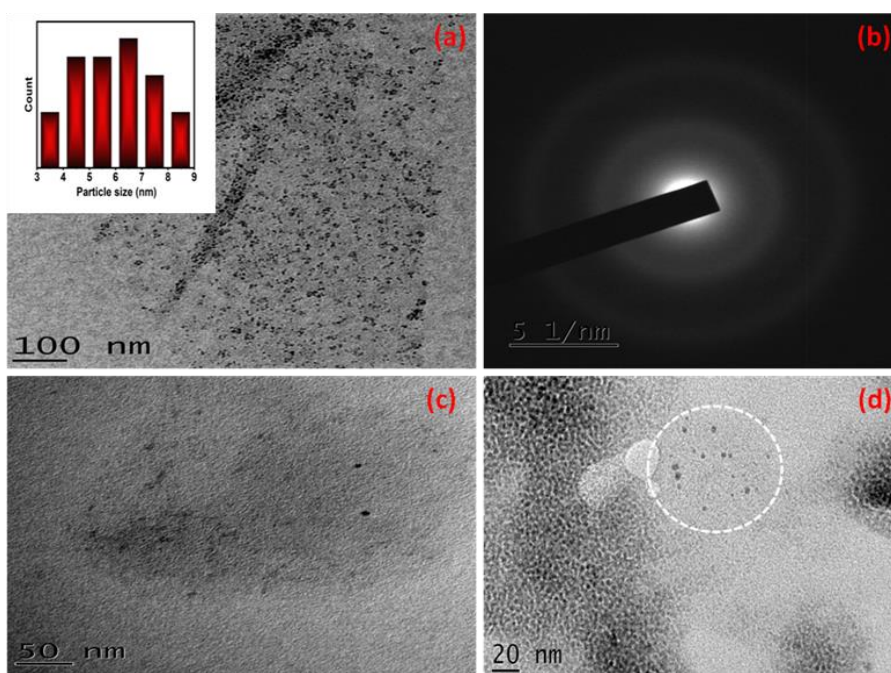


**Figure 8.1:** (a,c,d) TEM images of LPCDs (inset showing histogram  $n=30$ ) (b) SAED pattern of LPCDs

## XRD analysis

The X-ray diffraction (XRD) pattern of the LPCDs (**Figure 8.2**) the pattern exhibiting a single broad peak with  $2\theta = 23.41^\circ$ , which is the characteristics of carbon based material having plenty of  $sp^3$  disorder. The interlayer spacing was calculated by Bragg's equation (Given in Chapter 3) and is of  $3.76 \text{ \AA}$  larger than the spacing of graphite, which is about  $3.3 \text{ \AA}$ , this results also stipulates that the material is less crystalline [7].

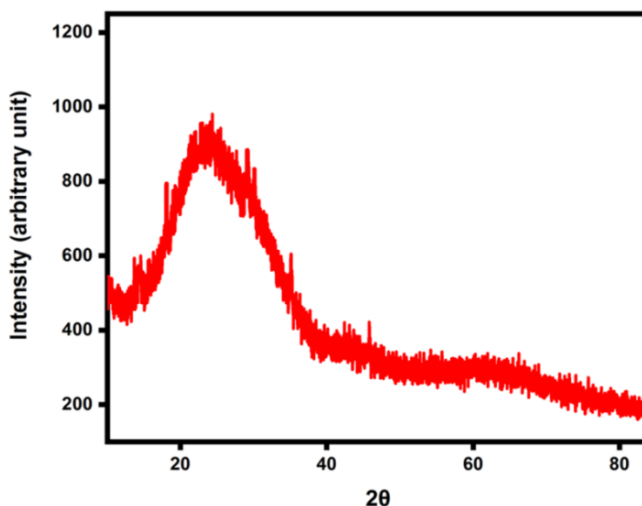


**Figure 8.2:** XRD pattern of LPCDs

## Raman and FTIR analysis

The Raman spectrum of the LPCDs (**Figure 8.3**) giving two broad bands centered at  $1351 \text{ cm}^{-1}$  and  $1568 \text{ cm}^{-1}$ . The former one is attributed to the D band whereas the latter one corresponds to G band. Both bands are observed to be wider, and this wider nature supports

the produced LPCDs' poor crystalline and lower graphitization nature [7].

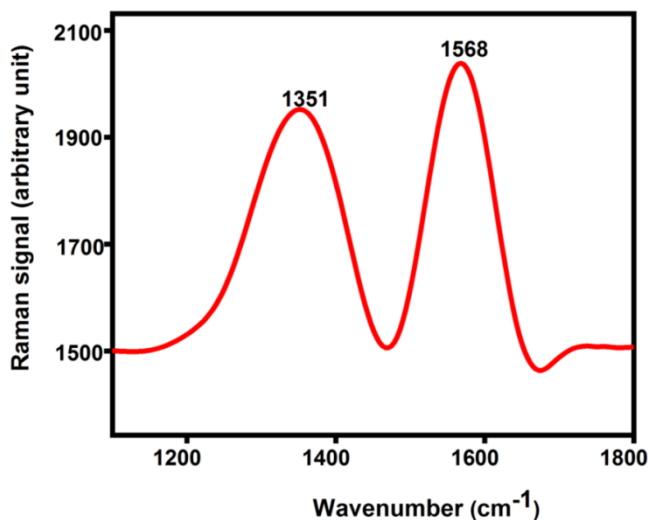


**Figure 8.3:** Raman spectrum of LPCDs

The FTIR spectroscopy was used to demonstrate the surface functionalities associated with LPCDs and the spectrum is given in **Figure 8.4**. A broad peak centered around  $3277\text{ cm}^{-1}$  was attributed to O-H stretching vibrations, whereas a small band at  $2934\text{ cm}^{-1}$  was attributed to the in-plane deformation vibration associated with C-H group [17]. A strong band at  $1560\text{ cm}^{-1}$  was believed to be arises due to the combined effect of symmetric stretching vibrations of  $\text{COO}^-$  and stretching vibration of C=C bond. Moreover a medium band at  $1402\text{ cm}^{-1}$  was ascribed to the asymmetric stretching vibration of  $\text{COO}^-$  [21]. Band at  $1047\text{ cm}^{-1}$  was attributed to the stretching vibration of C-O bond associated with alcoholic and carboxylic functionalities. These characteristic bands signify the presence of plenty of hydrophilic

functionalities such as hydroxyl and carboxylic groups at the surface of LPCDs, which in turn plays a key role in the solubility of LPCDs in aqueous medium.

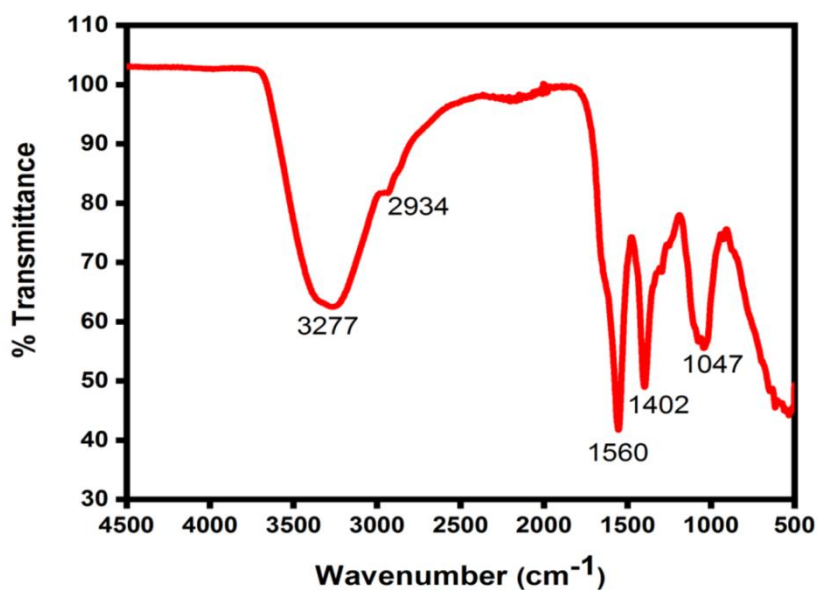


**Figure 8.4:** FTIR spectrum of LPCDs

### UV-Vis spectral analysis

UV-Vis absorbance spectrum of the LPCDs shown in **Figure 8.5**, having two shoulder peaks one is centered at 295 nm corresponds to  $\pi$ - $\pi^*$  transitions majorly contributed by the aromatic parts in the core of LPCDs. Whereas another peak at 349 nm accredited to  $n$ - $\pi^*$  transition associated with the electronic transition of non-bonding electron present in the hetero-atoms present in the LPCDs.



## Fluorescence spectral analysis

The fluorescence spectrum of the LPCDs gives emission maxima at 455 nm, under optimum excitation of 330 nm and is given in **Figure 8.6**. Moreover, order to investigate the dependence of excitation wavelength on emission spectrum, the fluorescence spectra were recorded by altering the excitation wavelength from 310 nm to 400 nm with an interval of 10 nm, the emission maxima of the spectra shows a red shift up on increasing excitation wavelength (**Figure 8.7**). These results reveals that the LPCDs exhibits excitation wavelength dependent emission behaviour, the giant red-edge effect was believed to be the reason behind this characteristics [16]. The intensity of emission peaks shows maximum value at an excitation wavelength of 330 nm and it was opted as the excitation wavelength for the whole studies.

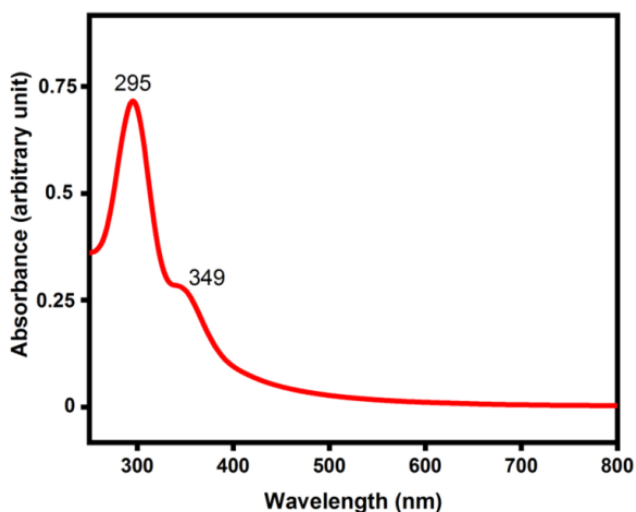


**Figure 8.5:** UV-Vis absorbance spectrum of LPCDs

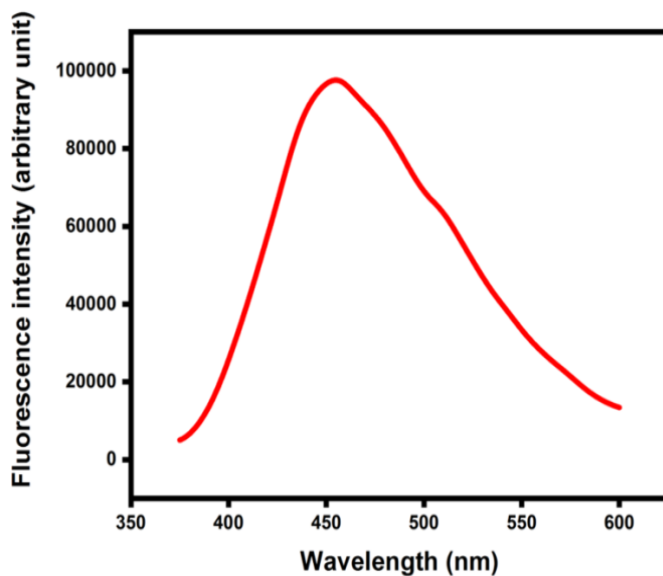


**Figure 8.6:** Fluorescence emission spectrum of LPCDs

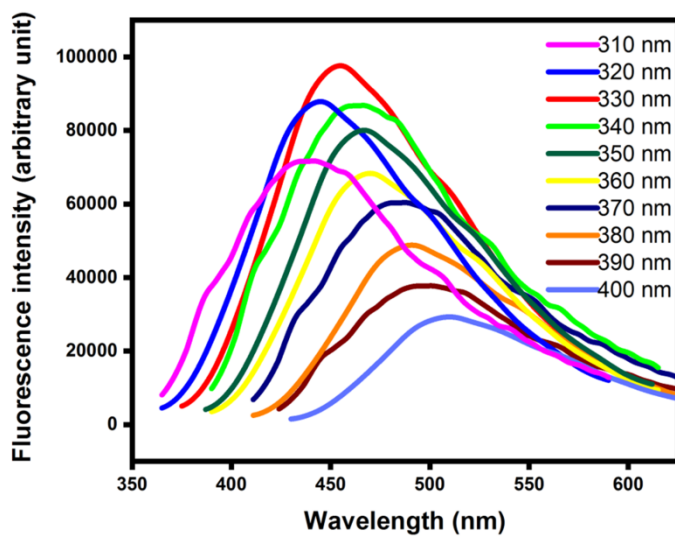


**Figure 8.7:** Fluorescence emission spectrum at different excitation wavelength

### **8.3.3 Fluorescence quantum yield and fluorescence stability of LPCDs**

The quantum yield of the LPCDs was determined and it was found to be 4.3 % by using standard equation (Given in Chapter 3) by taking quinine sulphate as reference standard.

The LPCDs solution at 4 °C was found to be stable up to 6 months of time. Up to this time the analytical performance of the system was not altered. However, after 6 months the fluorescence intensity degraded gradually, and it may be due to particle aggregation over time. These aggregations insert small changes in sensing performance of the probe after this stable period. At room temperature, in enclosed container the stability of LPCDs solution was reduced roughly to 1 month but at open atmosphere, the stability was further reduced to one week. The system was found to be fairly reproducible under the same experimental conditions. The photostability of the system was also highly commendable; that on exposing UV light of 365 nm up to one hour does not alters its fluorescence properties significantly.

### **8.3.4 Selectivity studies**

In order to evaluate the selectivity of the LPCDs the fluorescence spectra of the probe with different substances including commonly encountered food colorants methyl red, allura red, acid red along with other Sudan dyes (Sudan II, III and IV), some metal salts (NaCl, MgCl<sub>2</sub>, CaCl<sub>2</sub>, KCl and ZnCl<sub>2</sub>) and glucose were recorded. The

relative fluorescence response was displayed in **Figure 8.8**. Sudan dyes have comparable quenching efficiency, while it is negligible for other substances.

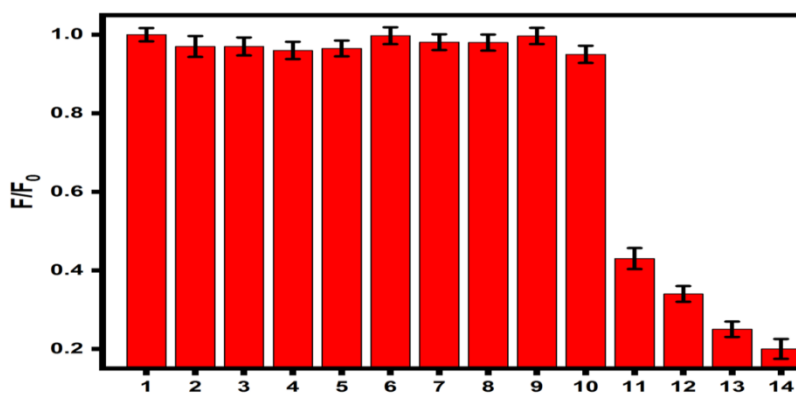


**Figure 8.8:** Relative fluorescence of LPCDs with Sudan I and different interfering substances and other Sudan dyes (1 to 14 represents LPCDs, glucose, methyl red, allura red, acid red, NaCl, MgCl<sub>2</sub>, CaCl<sub>2</sub>, KCl, ZnCl<sub>2</sub>, Sudan IV, Sudan III, Sudan II and Sudan I)

### 8.3.5 Sensing studies with Sudan I

The effects of Sudan I on the fluorescence of LPCDs were comprehensively analyzed by monitoring the fluorescence spectra after introducing different concentration of Sudan I to the system. The fluorescence intensity of the emission peak at 455 nm significantly reduced by the addition of Sudan I. **Figure 8.9** shows the gradual decrease in the fluorescence intensity of LPCDs with increasing concentration of Sudan I from 0 to 27.27  $\mu$ M. With this concentration range about 75 % of the native fluorescence intensity of LPCDs was quenched. The whole fluorescence quenching process was visible to naked eye under UV irradiation of 365 nm and the photograph of the

same is given in the inset of **Figure 8.9**.

Moreover, a good linear relationship was maintained between relative fluorescence intensity ( $F_0/F$ ) with concentration of Sudan I in the whole range from 0 to 27.27  $\mu\text{M}$ . The Stern-Volmer equation was obtained by applying linear fit to the plot with intercept at 1, ( $F_0/F = 0.08116 [C] + 1$ , where  $[C]$  is the concentration of analyte). The limit of detection (LOD) was found to be 0.92  $\mu\text{M}$ , it was determined from the above equation by the  $3\sigma/\text{slope}$  method, where  $\sigma$  is the standard deviation of the measurements. The corresponding plot is given in **Figure 8.10**.

The sensing performance of the system is comparable with reports from literatures and is given in **Table 8.1**. The proposed system exerts good level of detection parameters, on comparing with similar reports from this area. Even though there are reports with lower limit of detection than the proposed system, the present system was found to be greener, completely devoid of hazardous and expensive chemicals or solvents, time saving, less expensive and easy to perform, which are the major features of the presented work.

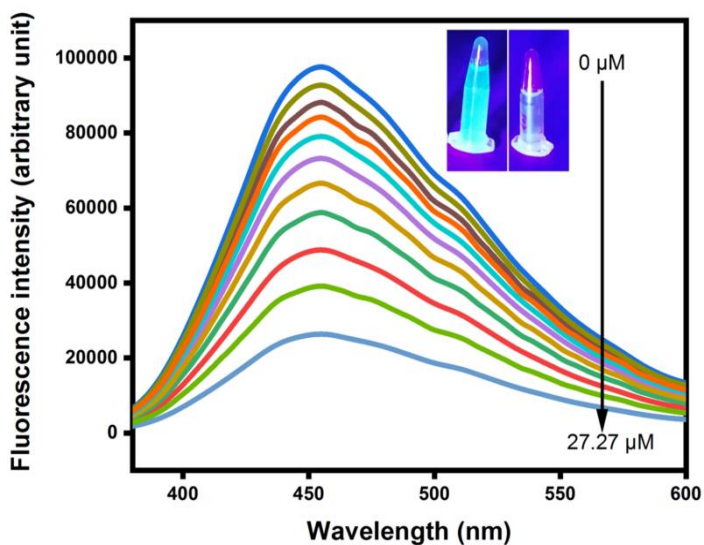


**Figure 8.9:** Fluorescence emission spectra with increasing concentration of Sudan I (inset shows the photographs of LPCDs (left) and LPCDs with Sudan I(right) under UV light)

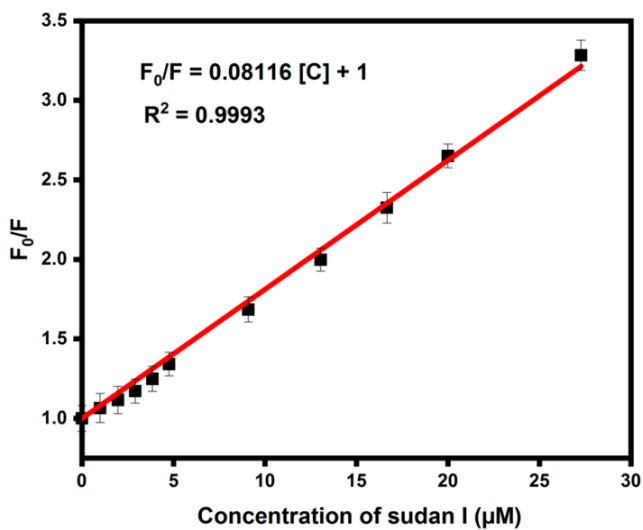


**Figure 8.10:** Linear relationships between relative fluorescence with concentration of Sudan I

**Table 8.1:** Comparison of different sensors for Sudan I detection

<b>Sensing probe for Sudan I</b>	<b>LOD (<math>\mu\text{M}</math>)</b>	<b>Linear range (<math>\mu\text{M}</math>)</b>	<b>Reference</b>
Carbon quantum dots from cigarette filters	0.95	2.40 – 104.0	[16]
Carbon dots from lignin and sulfuric acid	0.12	0 – 40	[17]
Rubber tires and ammonium persulphate derived carbon dots	0.62	0.5 – 60	[22]
Triphenylamine functionalized polyhedral oligomeric silsesquioxane	0.36	0.48 – 29.84	[23]
Carbon dots derived from long pepper	0.92	0 – 27.27	This work

### 8.3.6 Analysis of Sudan I in chilli powder

The practicability of the developed method using the prepared probe was tested by employing the system for Sudan I detection in commercial chilli powders. As mentioned earlier, known concentrations of Sudan I were added to the sample and determined as per the procedure, the corresponding results were shown in **Table 8.2**. The recovery percentage for this sample analysis falls in the range from 93.51 % to 103.83 %.

**Table 8.2:** Detection of Sudan I in chili powder

<b>Chili powder Samples</b>	<b>Added Sudan I (<math>\mu\text{M}</math>)</b>	<b>Found (<math>\mu\text{M}</math>)</b>	<b>Recovery (%)</b>	<b>Error (%)</b>
Sample 1	0	NF <sup>a</sup>	--	--
	2	1.92	96.00	4.00
	4	3.79	94.75	5.25
	6	6.23	103.83	3.83
Sample 2	0	NF <sup>a</sup>	--	--
	2	1.87	93.80	6.2
	4	3.86	96.50	3.5
	6	5.69	94.8	5.16
Sample 3	0	NF <sup>a</sup>	--	--
	2	1.94	97.00	3.00
	4	3.74	93.51	6.5
	6	5.94	99.00	1.00

a: NOT FOUND

### 8.3.7 Fluorescence quenching mechanism

Generally the fluorescence quenching can be accomplished through charge transfer and energy transfer. The first type mechanism is arises by the transfer of charge between the fluorophore and the quencher moiety, the second one resulted through the absorption of fluorescence by the quenching species. For the most part, fluorescence quenching of CDs by organic compounds feasibly explained through energy transfer mechanism [16,17].

The energy transfer based quenching could be happen only when there is sufficient overlap between either excitation or emission spectrum of the fluorophore with absorbance spectrum of the quencher.



This type of quenching can be either inner filter effect (IFE) or Förster resonance energy transfer (FRET). An essential condition for the FRET quenching mechanism was the energy absorption or simply absorbance spectrum of the quencher acts as acceptor, should be overlapped by the energy emission spectrum of the fluorophore as donor.

In this piece of work, donor of energy was the LPCDs, while acceptor of energy was the Sudan I dye. By the irradiation of UV light, LPCDs will give rise to resonance energy then the transfer of this energy take place between the donor and the Sudan I molecule once they were close to each other [17].

To confirm this, the absorbance spectrum of the Sudan I and emission spectrum of the LPCDs were scanned. The emission spectra of LPCDs having a fluorescence maximum centered at 455 nm with excitation of 330 nm, at the same time the maximum absorbance of Sudan I dye is located at the 480 nm, and the two spectra overlapped effectively, the spectral overlap between these two is given in **Figure 8.11**.

Due to structural similarity, other Sudan dyes having the absorbance maxima near to 480 nm also exerted some quenching in fluorescence as shown in **Figure 8.8** and it can be attributed to the small spectral overlapping of the absorbance spectrum of the quencher with emission spectrum of the probe [24]. From previous reports there exists a red shift of absorbance maxima from Sudan I to IV [24], and

hence a decrease in the extent of spectral overlapping from Sudan I to IV which is reflected in their quenching efficiency.

The present study mainly focuses on the sensing of Sudan I as it is most commonly reported in commercial chilli powders than the other Sudan dyes, probably due to its lesser price and availability than others. The extent of spectral overlap affects the efficiency of energy transfer between these two moieties. There is substantial amount of overlap between emission spectrum of LPCDs with absorbance spectrum of Sudan I. So from the above discussed results the quenching mechanism may be attributed to FRET or IFE.

To distinguish them, the fluorescence life time decay curve of the sample with and without Sudan I was recorded and the average life time of LPCDs and LPCDs with Sudan I was calculated (Equation is given in Chapter3) and found to be 3.11 ns and 1.64 ns, respectively. The results were displayed in **Figure 8.12**. There is a significant decrease in the fluorescence life time of the sample by the addition of Sudan I. Since efficient spectral overlap between emission peak of donor and absorbance peak of quencher and significant decrease in fluorescence life time by the addition of quenching moiety are the essential requirements for the FRET mechanism of quenching to be happening. Therefore, the obtained results suggest that the mechanism behind this fluorescence quenching of LPCDs with Sudan I can be attributed to FRET. The maximum fluorescence energy transfer efficiency of the system with Sudan I was calculated by the equation (1) [25].

$$E = 1 - \frac{F_D}{F_D'} \quad (1)$$

Where, E representing fluorescence energy transfer efficiency,  $F_D$  and  $F_D'$  are the integrated fluorescence intensity of the LPCDs in the presence and absence of the quencher, respectively. The value was determined as 72.96 %. Comparatively good value of fluorescence energy transfer efficiency further confirms the FRET mechanism.

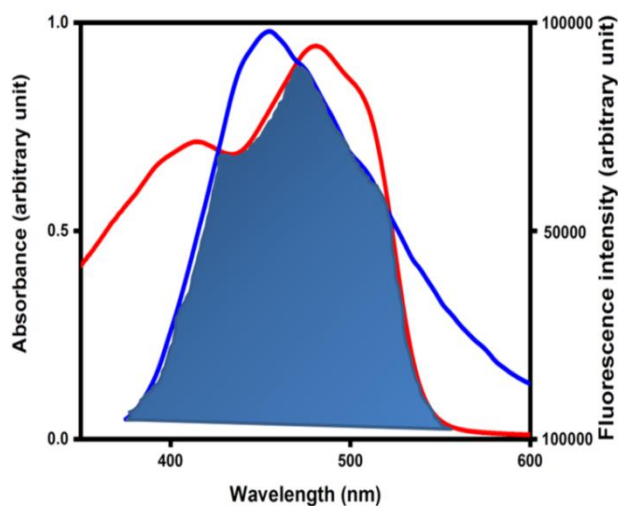


**Figure 8.11:** Spectral overlap of emission spectrum (blue line) of LPCDs with absorbance spectrum (red line) of Sudan I

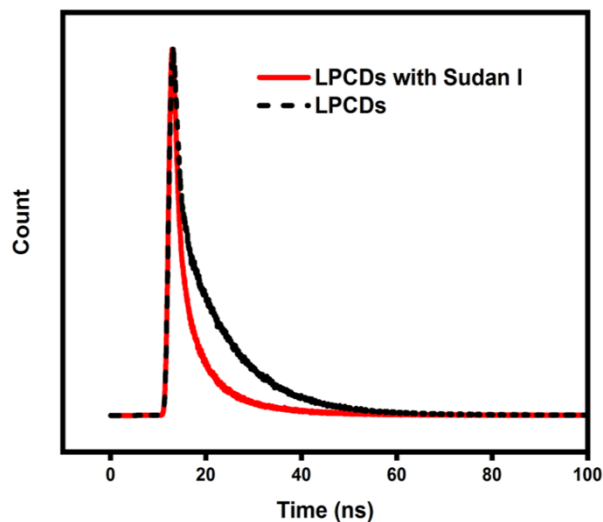


**Figure 8.12:** Fluorescence life time decay curve of LPCDs with and without Sudan I

#### 8.4 Conclusions

In summary, a widely available biomass, long pepper was successfully converted to fluorescent carbon dots through microwave pyrolysis, without using any harsh chemicals. Various characterisation methods were utilised to inspect the properties associated with LPCDs. The as synthesised LPCDs with excellent photo-luminescent properties selectively interact with Sudan I dye resulting the quenching of native fluorescence of LPCDs was made to propose it as a fluorescent turn-off probe for Sudan I. The sensing of Sudan I follow FRET mechanism and it was found out from various experimental investigations. The sensing methodology was extremely simple and cost-effective with good level of statistical parameters such as limit of detection of 0.92  $\mu\text{M}$  and linear range from 0 to 27.27  $\mu\text{M}$ . On regard to this, the sensing

method was implemented for the sensing of Sudan I in commercial chilli powder, where the presence of Sudan I dye was reported frequently in past few years. The results obtained are promising to fabricate a reliable fluorescent probe for the detection of the food adulterant Sudan I in different food products.

## 8.5 References

- [1] R. Atchudan, T.N.J.I. Edison, K.R. Aseer, S. Perumal, N. Karthik, Y.R. Lee, Highly fluorescent nitrogen-doped carbon dots derived from *Phyllanthus acidus* utilized as a fluorescent probe for label-free selective detection of  $\text{Fe}^{3+}$  ions, live cell imaging and fluorescent ink, *Biosens. Bioelectron.* 99 (2018) 303–311. <https://doi.org/10.1016/j.bios.2017.07.076>
- [2] R. Atchudan, T.N.J.I. Edison, D. Chakradhar, S. Perumal, J.-J. Shim, Y.R. Lee, Facile green synthesis of nitrogen-doped carbon dots using *Chionanthus retusus* fruit extract and investigation of their suitability for metal ion sensing and biological applications, *Sens. Actuators, B.* 246 (2017) 497–509. <https://doi.org/10.1016/j.snb.2017.02.119>
- [3] R. Atchudan, T.N.J.I. Edison, Y.R. Lee, Nitrogen-doped carbon dots originating from unripe peach for fluorescent bioimaging and electrocatalytic oxygen reduction reaction, *J. Colloid Interface Sci.* 482 (2016) 8–18. <https://doi.org/10.1016/j.jcis.2016.07.058>
- [4] R. Atchudan, T.N.J.I. Edison, S. Perumal, R. Vinodh, Y.R. Lee, Betel-derived nitrogen-doped multicolor carbon dots for environmental and biological applications, *J. Mol. Liq.* 296 (2019) 111817. <https://doi.org/10.1016/j.molliq.2019.111817>
- [5] R. Atchudan, T.N.J.I. Edison, S. Perumal, N. Muthuchamy, Y.R. Lee, Hydrophilic nitrogen-doped carbon dots from biowaste using dwarf banana peel for environmental and biological applications, *Fuel.* 275 (2020) 117821. <https://doi.org/10.1016/j.fuel.2020.117821>
- [6] R. Atchudan, T.N. Jebakumar Immanuel Edison, suguna perumal, N. Muthuchamy, Y. Lee, Hydrophilic nitrogen-doped carbon dots from biowaste using dwarf banana peel for environmental and biological applications, *Fuel.* 275 (2020) 117821. <https://doi.org/10.1016/j.fuel.2020.117821>
- [7] V. Ramanan, S.K. Thiyagarajan, K. Raji, R. Suresh, R. Sekar, P. Ramamurthy, Outright Green Synthesis of Fluorescent Carbon Dots from Eutrophic Algal Blooms for In Vitro Imaging, *ACS Sustainable Chem. Eng.* 4 (2016) 4724–4731. <https://doi.org/10.1021/acssuschemeng.6b00935>
- [8] K. Raji, V. Ramanan, P. Ramamurthy, Facile and green synthesis of highly fluorescent nitrogen-doped carbon dots from jackfruit seeds and

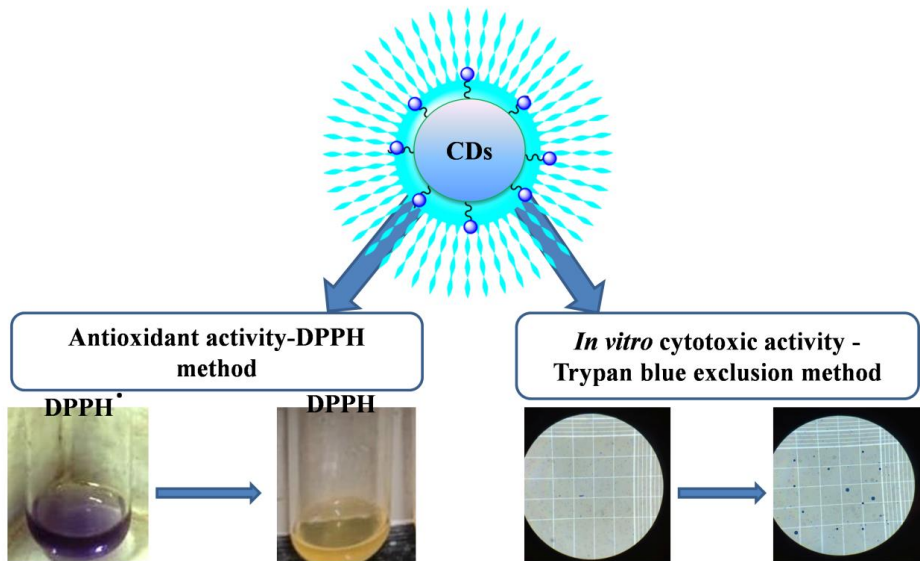
- its applications towards the fluorimetric detection of Au<sup>3+</sup> ions in aqueous medium and in in vitro multicolor cell imaging, *New J. Chem.* 43 (2019) 11710–11719. <https://doi.org/10.1039/C9NJ02590A>
- [9] A. Sachdev, P. Gopinath, Green synthesis of multifunctional carbon dots from coriander leaves and their potential application as antioxidants, sensors and bioimaging agents, *Analyst.* 140 (2015) 4260–4269. <https://doi.org/10.1039/C5AN00454C>
- [10] T.C. Wareing, P. Gentile, A.N. Phan, Biomass-Based Carbon Dots: Current Development and Future Perspectives, *ACS Nano.* 15 (2021) 15471–15501. <https://doi.org/10.1021/acsnano.1c03886>
- [11] M. Kurian, A. Paul, Recent trends in the use of green sources for carbon dot synthesis—A short review, *Carbon Trends.* 3 (2021) 100032. <https://doi.org/10.1016/j.cartre.2021.100032>
- [12] X. Lin, M. Xiong, J. Zhang, C. He, X. Ma, H. Zhang, Y. Kuang, M. Yang, Q. Huang, Carbon dots based on natural resources: Synthesis and applications in sensors, *Microchem. J.* 160 (2021) 105604. <https://doi.org/10.1016/j.microc.2020.105604>
- [13] H. Liu, J. Ding, K. Zhang, L. Ding, Construction of biomass carbon dots based fluorescence sensors and their applications in chemical and biological analysis, *TrAC, Trends Anal. Chem.* 118 (2019) 315–337. <https://doi.org/10.1016/j.trac.2019.05.051>
- [14] W. Meng, X. Bai, B. Wang, Z. Liu, S. Lu, B. Yang, Biomass-Derived Carbon Dots and Their Applications, *Energy Environ. Mater.* 2 (2019) 172–192. <https://doi.org/10.1002/eem2.12038>
- [15] A. Khandhar, S. Patel, A. Patel, M. Zaveri, S. Lecturer, Chemistry and pharmacology of Piper Longum L, *Int. J. Pharm. Sci. Rev. Res.* Volume 5 (2010) 67–76. <https://www.researchgate.net/publication/257299404>
- [16] S. Anmei, Z. Qingmei, C. Yuye, W. Yilin, Preparation of carbon quantum dots from cigarette filters and its application for fluorescence detection of Sudan I, *Anal. Chim. Acta.* 1023 (2018) 115–120. <https://doi.org/10.1016/j.aca.2018.03.024>
- [17] X. Yang, Y. Guo, S. Liang, S. Hou, T. Chu, J. Ma, X. Chen, J. Zhou, R. Sun, Preparation of sulfur-doped carbon quantum dots from lignin as a sensor to detect Sudan I in an acidic environment, *J. Mater. Chem. B.* 8 (2020) 10788–10796. <https://doi.org/10.1039/D0TB00125B>

- [18] E. Mejia, Y. Ding, M.F. Mora, C.D. Garcia, Determination of banned sudan dyes in chili powder by capillary electrophoresis, *Food Chem.* 102 (2007) 1027–1033. <https://doi.org/10.1016/j.foodchem.2006.06.038>
- [19] B. De, N. Karak, A green and facile approach for the synthesis of water soluble fluorescent carbon dots from banana juice, *RSC Adv.* 3 (2013) 8286. <https://doi.org/10.1039/c3ra00088e>
- [20] M.L. Liu, B.B. Chen, C.M. Li, C.Z. Huang, Carbon dots: synthesis, formation mechanism, fluorescence origin and sensing applications, *Green Chem.* 21 (2019) 449–471. <https://doi.org/10.1039/C8GC02736F>
- [21] H. Xu, X. Yang, G. Li, C. Zhao, X. Liao, Green Synthesis of Fluorescent Carbon Dots for Selective Detection of Tartrazine in Food Samples, *J. Agric. Food Chem.* 63 (2015) 6707–6714. <https://doi.org/10.1021/acs.jafc.5b02319>
- [22] Y. Hu, Z. Gao, Sensitive detection of Sudan dyes using tire-derived carbon dots as a fluorescent sensor, *Spectrochim. Acta, Part A.* 239 (2020) 118514. <https://doi.org/10.1016/j.saa.2020.118514>
- [23] D. Li, P. Zhou, Y. Hu, G. Li, L. Xia, Rapid determination of illegally added Sudan I in cake by triphenylamine functionalized polyhedral oligomeric silsesquioxane fluorescence sensor, *Spectrochim. Acta, Part A.* 282 (2022) 121673. <https://doi.org/10.1016/j.saa.2022.121673>
- [24] C.V. Di Anibal, M. Odena, I. Ruisánchez, M.P. Callao, Determining the adulteration of spices with Sudan I-II-III-IV dyes by UV–visible spectroscopy and multivariate classification techniques, *Talanta.* 79 (2009) 887–892. <https://doi.org/10.1016/j.talanta.2009.05.023>
- [25] K. Yang, F. Li, W. Che, X. Hu, C. Liu, F. Tian, Increment of the FRET efficiency between carbon dots and photosensitizers for enhanced photodynamic therapy, *RSC Adv.* 6 (2016) 101447–101451. <https://doi.org/10.1039/C6RA20412K>



# Chapter 9

## BIOLOGICAL STUDIES ON LPCDs AND SFCDs



---

The antioxidant and *in vitro* cytotoxic properties of LPCDs (long pepper derived CDs) and SFCDs (sweet flag derived CDs) are discussed in this chapter.



## 9.1 Introduction

CDs have long been known to have biological applications, and scholarly research firmly supports this claim [1–6]. The great biocompatibility, water solubility, and improved surface functionalities of CDs were thought to make this application conceivable [1,6]. Also, each precursor employed in the current study to make CDs had favourable pharmacological characteristics, which strongly prompted to evaluate the biological effects of all the CDs and extracts they had produced.

This Chapter focuses on the CDs' antioxidant and *in vitro* cytotoxic properties, particularly those of LPCDs (long pepper derived CDs) and SFCs (sweet flag derived CDs), because these CDs produce effective outcomes.

Antioxidants are substances that can prevent other molecules from oxidation. It can effectively interact with and neutralise free radicals, and prevent the oxidative mechanism that leads to damage cells. The therapeutic value of antioxidants for treating oxidative stress-related illnesses such as cancer, diabetes mellitus, and neurodegenerative disorders has recently gained a lot of attention [7]. In a similar fashion, using biocompatible antioxidant materials that might have therapeutic applications is given significant weight.

One of the most often used methods to assess the antioxidant activity is the DPPH (1,1-diphenyl-2-(2,4,6-trinitrophenyl)hydrazine)

based test. It is a simple and fast method to evaluate a compound's antioxidant potential.

DPPH is a well known radical to monitor chemical reactions involving radicals and it is a nitrogen-containing free radical with a long half-life that turns yellow when it interacts with an antioxidant. When a DPPH solution with a strong absorption at 520 nm is mixed with a substance that can donate a hydrogen atom (AH), the reduced form of DPPH is formed, which can be monitored by measuring the absorbance at 520 nm. Lower absorbance at 520 nm represents higher DPPH scavenging activity [8].

The percentage of DPPH radical scavenging activity of sample was calculated from the decrease in absorbance at 520 nm. The oxidized and reduced form of DPPH is given in, **Figure 9.1**, AH indicates the sample with antioxidant potential.

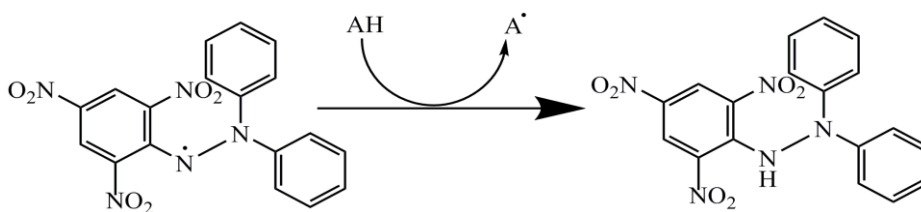


**Figure 9.1:** Oxidised and reduced form of DPPH

*In vitro* cytotoxicity is the term indicating the viability of the cells with the testing samples. For the case of cancerous cell lines the term cytotoxicity directly indicates the anticancer activity of the testing samples. MTT assay and trypan blue exclusion method are the widely used methods for the assessment of *in vitro* cytotoxicity [9–11].

The increasing incidence and mortality of cancer have made it a major health burden worldwide. So the search on anticancer products receives paramount importance. Due to their distinct optical characteristics and inherent theranostic qualities, CDs have been acknowledged as viable prospects in nanotheranostics for anticancer applications for concurrent bioimaging and other therapies [12].

Here, we assess the anticancer efficacy of the selected CDs systems using Dalton's Lymphoma Ascites (DLA) cell lines using the simplest trypan blue exclusion approach. In which the cytotoxicity was determined through the addition of trypan blue dye, since only dead cell lines can absorb the blue colour of the dye. This makes it possible to count both live and dead cells after the cell line interaction with testing samples.

## **9.2 Experimental**

### **9.2.1 Antioxidant activity–DPPH method**

The antioxidant activity of the all the CDs and extracts were carried out through DPPH radical scavenging assay. The common procedure adopted for the assay is described as follows:

Standard solution of DPPH (0.3 mM) was prepared in ethanol and kept under dark for 30 minutes. Then add about 370  $\mu$ L of this DPPH solution in to test tubes containing different concentration of CDs and extracts (20, 40, 60, 80, 100  $\mu$ L). Made up all the solutions in the test tubes to 2 mL and kept under dark for 30 minutes of time as incubation time at 37 °C. A blank solution was also prepared by avoiding the test samples. After the incubation period, each solution was tested for absorbance at 520 nm since pure DPPH has an obvious

peak that is almost at this wavelength. The absorbance studies were conducted using UV-Vis spectrophotometer. Same procedure was used to determine the DPPH scavenging activity of ascorbic acid taken as standard. The scavenging percentage (S %) and effective concentration of test samples for achieving 50 % of scavenging (EC<sub>50</sub>) were calculated from the absorbance data, the equation for the S % value calculation was incorporated in Chapter 3.

### **9.2.2 *In vitro* cytotoxicity – Trypan blue exclusion method**

The *in vitro* cytotoxicity of the CDs and extracts were analysed through the Trypan blue exclusion method using DLA as the model cell lines. This is a standard procedure; the assay was conducted as follows:

The tumour cells were aspirated from the peritoneal cavity of tumour bearing mice were washed thrice with phosphate buffered saline (PBS). Viable cells suspension was added to tubes containing various concentrations of the test samples (10, 20, 50, and 100 µL) and the volume was made up to 1 mL using PBS. These assay mixtures were incubated at 37 °C for 3 hours of time. After that the cell suspension was mixed with 100 µL of 1 % trypan blue solution and kept aside for 2-3 minutes. Then it was loaded on a haemocytometer for cell counting process. Dead cells in the suspension take up the blue colour of typan blue dye where as the live cells do not. The numbers of stained and unstained cells were counted separately. From these numbers the cytotoxicity of the samples were evaluated as % of cytotoxicity. The equation for the % of cytotoxicity was given in the

Chapter 3. Similarly, a control was also conducted by the same procedure and the control tube contained only cell suspension.

### **9.3 Results and discussion**

#### **9.3.1 Antioxidant activity of LPCDs and SFCDs**

As mentioned earlier, the antioxidant activity of the selected CDs and their corresponding extracts are going to be discussed here.

LPCDs (long pepper derived CDs) and SFCDs (sweet flag derived CDs) give the better results out of all prepared CDs. For comparative studies, the antioxidant screening of the corresponding precursor extracts was also conducted. In both cases, the radical scavenging percentage, S % of the CDs were found to be higher than that of corresponding extracts LPE (long pepper extract) and SFE (sweet flag extract). The results of DPPH assay were tabulated in **Table 9.1**.

As the concentration of samples increased the DPPH free radical scavenging activity also got increased. However, their activity is found to be varied depending on the physiochemical properties of the samples. LPCDs and SFCDs showed 85.71 % and 88.09 % free radical scavenging activity. The comparison of S % value of the graph is given in **Figure 9.2**.

The effective concentration of the test samples for acquiring 50 % of scavenging activity, the  $EC_{50}$  values were found out from the above graph by extrapolation and are depicted in **Figure 9.3**. Lower  $EC_{50}$  values signify samples with more antioxidant potential. The lower  $EC_{50}$  value from the tested samples is displayed by SFCDs.

Therefore, SFCDs have the highest level of antioxidant capacity and it may be due to the existence of the activity of pharmacological constituents in the CDs from the precursor. Its comparatively higher activity than the SFE may be attributed to its nanodimensionalities.

**Table 9.1:** DPPH assay results

Volume (μL)	Absorbance of control	Absorbance of sample	S%
Ascorbic acid			
20	0.84	0.64	23.8
40	0.84	0.532	36.66
60	0.84	0.416	50.47
80	0.84	0.328	60.95
100	0.84	0.236	71.9
LPE			
20	0.84	0.69	17.85
40	0.84	0.45	46.42
60	0.84	0.32	61.90
80	0.84	0.25	70.23
100	0.84	0.17	79.76
SFE			
20	0.84	0.61	27.38
40	0.84	0.42	50.00
60	0.84	0.30	64.28
80	0.84	0.21	75.00
100	0.84	0.15	82.14
LPCDs			
20	0.84	0.514	38.81
40	0.84	0.348	58.57
60	0.84	0.25	70.23
80	0.84	0.16	80.95
100	0.84	0.12	85.71
SFCDs			
20	0.84	0.455	45.83
40	0.84	0.289	65.59
60	0.84	0.223	73.45
80	0.84	0.136	83.89
100	0.84	0.1	88.09



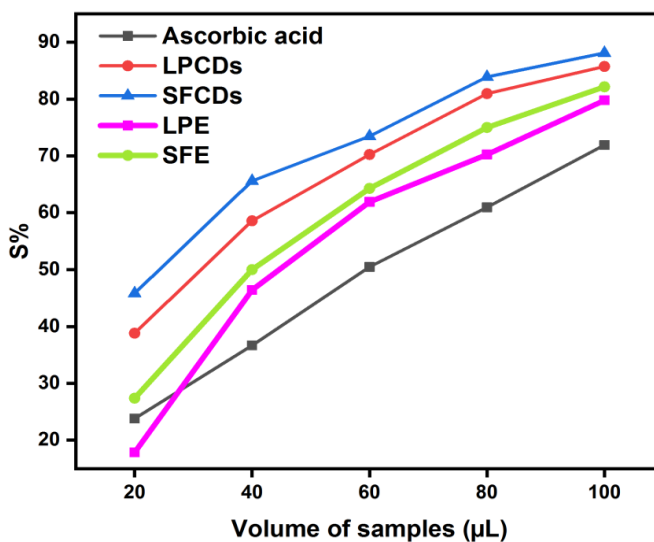


**Figure 9.2:** DPPH scavenging activity of ascorbic acid, LPCDs, SFCDs, LPE and SFE

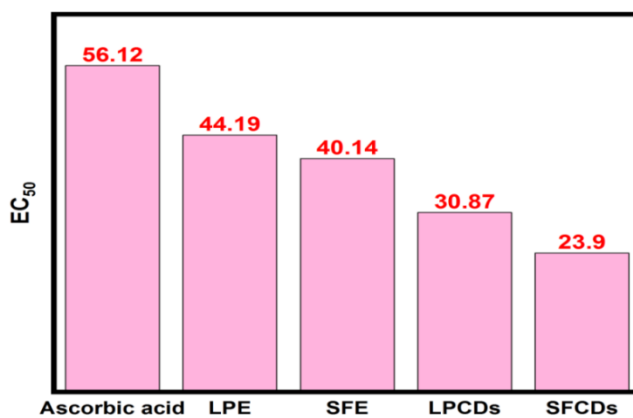


**Figure 9.3:** EC<sub>50</sub> values of ascorbic acid, LPCDs, SFCDs, LPE and SFE

### 9.3.2 Mechanism of DPPH scavenging by CDs

The exact mechanism of DPPH scavenging by CDs has not yet been identified [13]. Here, a possible mechanism is described based on the research that is currently accessible.

The generation of hydrogen donation and radical adducts may all play a role in the DPPH scavenging mechanism in nanocarbon-based materials [14–16]. It is well known that carbonyl and hydroxyl groups are typically found on the edges of CDs. Due to their positions; they may exhibit additional covalent bonding-like defects [16,17]. Earlier studies noted that the many functional groups at CDs' edge sites mostly hydroxy and carboxyl groups were the source of their high hydrogen donor activity [16,18].

According to the FTIR study, both CDs (LPCDs and SFCDs) systems have hydroxyl, carboxyl, and amino groups on their surfaces. The DPPH free radical (DPPH•) was converted to DPPH-H by absorbing H• from the CDs. Any of the functional groups on the surface of CDs can donate this H•, and the resulting unpaired electron in the CDs can subsequently be delocalized via resonance within their aromatic domains of the CDs [13].

Rather than surface functional sites, most investigations concluded that radical adducts originated at  $sp^2$  sites [16,19]. Altogether, the main processes for DPPH scavenging of CDs are hydrogen donation and adduct formation. Different kinds of surface oxygen groups showed various scavenging strategies. Higher antioxidant activity is seen in CDs with hydroxyl or carbonyl surface functionalities [16].

### **9.3.3 *In vitro* cytotoxicity of LPCDs and SFCDs**

In the current work, anticancer efficacy of CDs in DLA tumour cell lines is examined *in vitro*. Swiss albino mice were chosen, and intraperitoneal injection was used to sustain the cells *in vivo*. Saline

was used to aspirate DLA cells, which are converted into tumour cells. For the analysis, four different CD concentrations (10  $\mu\text{L}$ , 20  $\mu\text{L}$ , 50  $\mu\text{L}$ , and 100  $\mu\text{L}$ ) were chosen. The identical analysis was carried out using precursor extracts following the same steps.

Treatment with both CDs systems resulted in noticeable decrease in the number of live cells. As the volume of the CDs increases, the number of dead cells also increases indicating the concentration dependent effect of CDs towards the cancer cells. It also implies the anti-proliferative activity of CDs against tumour cells [11]. The dead cells get stained by the addition of trypan blue dye and there by dead cells and living cells can be counted using the haemocytometer [20,21]. From the number of dead cells and total cells the % of toxicity can be found out using the equation as mentioned before. The results of the study were tabulated in the **Table 9.2 and 9.3**.

At a concentration of 100  $\mu\text{L}$  of LPCDs from LPE, destroy only 38.25 % where as for SFCDs 36.86 %. This proves that the anticancerous activity is more predominant with LPCDs from long pepper compared to SFCDs. This is the first report on the activity of sweet flag and long pepper derived CDs against DLA tumour cells.

On comparison with parent extracts LPE (100  $\mu\text{L}$ ) exerts 23.28 % of cytotoxicity which lower than the LPCDs system in the same conditions. Similarly cytotoxicity % of SFE is 20.52 % and this value was also lower than the corresponding SFCDs system. This increment in anticancer activity of CDs systems on comparing with precursor

extract may be attributed to the increased activity of the active sites by the transformation in to nano forms. The CDs' excellent antioxidant capabilities and existence of pharmacologically active groups even after materialisation treatment might be the cause of their antitumor effects. The prevalence is unpredictable and it can be dependent up on several factors including type of extraction, reaction conditions and post reaction treatments. There is still some mystery about the precise cause of CDs' notable anticancer action.

**Table 9.2:** *In vitro* cytotoxic activity of LPE and LPCDs

Drug concentration( $\mu\text{L}$ )	% of cytotoxicity	
	LPE	LPCDs
10	5.23 $\pm$ 0.7	10.59 $\pm$ 0
20	7.89 $\pm$ 1.2	15.39 $\pm$ 0
50	10.83 $\pm$ 1.2	23.29 $\pm$ 1.6
100	23.28 $\pm$ 1.5	38.25 $\pm$ 1.4

**Table 9.3:** *In vitro* cytotoxic activity of SFE and SFCDs

Drug concentration( $\mu\text{L}$ )	% of cytotoxicity	
	SFE	SFCDs
10	6.23 $\pm$ 0.5	10.25 $\pm$ 0.4
20	8.24 $\pm$ 0	12.59 $\pm$ 0.7
50	15.29 $\pm$ 12	22.75 $\pm$ 0.14
100	20.52 $\pm$ 17	36.86 $\pm$ 1.5

## 9.4 Conclusions

The antioxidant activity of the prepared CDs systems and corresponding extracts were studied by DPPH assay and results indicate that CDs possessing excellent antioxidant activity with lower  $EC_{50}$  value than the respective precursors. The *in vitro* cytotoxicity activity with DLA cell lines shows that the cytotoxicity increases with concentration of CDs and both are exerts good level of performance than the corresponding extracts. It may be due to the combined effect of existence of pharmacological activity from the precursor and nano dimensional size. The produced CDs' *in vitro* cytotoxicity and antioxidant activities lay the door for a more thorough investigation of the biological applications of CDs systems as future work.

## 9.5 References

- [1] H. Liu, J. Ding, K. Zhang, L. Ding, Construction of biomass carbon dots based fluorescence sensors and their applications in chemical and biological analysis, *TrAC, Trends Anal. Chem.* 118 (2019) 315–337. <https://doi.org/10.1016/j.trac.2019.05.051>
- [2] R. Atchudan, T.N.J.I. Edison, D. Chakradhar, S. Perumal, J.-J. Shim, Y.R. Lee, Facile green synthesis of nitrogen-doped carbon dots using *Chionanthus retusus* fruit extract and investigation of their suitability for metal ion sensing and biological applications, *Sens. Actuators, B.* 246 (2017) 497–509. <https://doi.org/10.1016/j.snb.2017.02.119>
- [3] R. Atchudan, T.N.J.I. Edison, S. Perumal, R. Vinodh, Y.R. Lee, Betel-derived nitrogen-doped multicolor carbon dots for environmental and biological applications, *J. Mol. Liq.* 296 (2019) 111817. <https://doi.org/10.1016/j.molliq.2019.111817>
- [4] R. Atchudan, T.N. Jebakumar Immanuel Edison, suguna perumal, N. Muthuchamy, Y. Lee, Hydrophilic nitrogen-doped carbon dots from biowaste using dwarf banana peel for environmental and biological applications, *Fuel.* 275 (2020) 117821. <https://doi.org/10.1016/j.fuel.2020.117821>
- [5] K. kanthi Gudimella, G. Gedda, P.S. Kumar, B.K. Babu, B. Yamajala, B.V. Rao, P.P. Singh, D. Kumar, A. Sharma, Novel synthesis of fluorescent carbon dots from bio-based *Carica Papaya* Leaves: Optical and structural properties with antioxidant and anti-inflammatory activities, *Environ. Res.* 204 (2022) 111854. <https://doi.org/10.1016/j.envres.2021.111854>
- [6] G. Ge, L. Li, D. Wang, M. Chen, Z. Zeng, W. Xiong, X. Wu, C. Guo, Carbon dots: synthesis, properties and biomedical applications, *J. Mater. Chem. B.* 9 (2021) 6553–6575. <https://doi.org/10.1039/D1TB01077H>
- [7] S. Rodríguez-Varillas, T. Fontanil, Á.J. Obaya, A. Fernández-González, C. Murru, R. Badía-Laíño, Biocompatibility and Antioxidant Capabilities of Carbon Dots Obtained from Tomato (*Solanum lycopersicum*), *Appl. Sci.* 12 (2022) 773. <https://doi.org/10.3390/app12020773>
- [8] A. Sachdev, P. Gopinath, Green synthesis of multifunctional carbon dots from coriander leaves and their potential application as

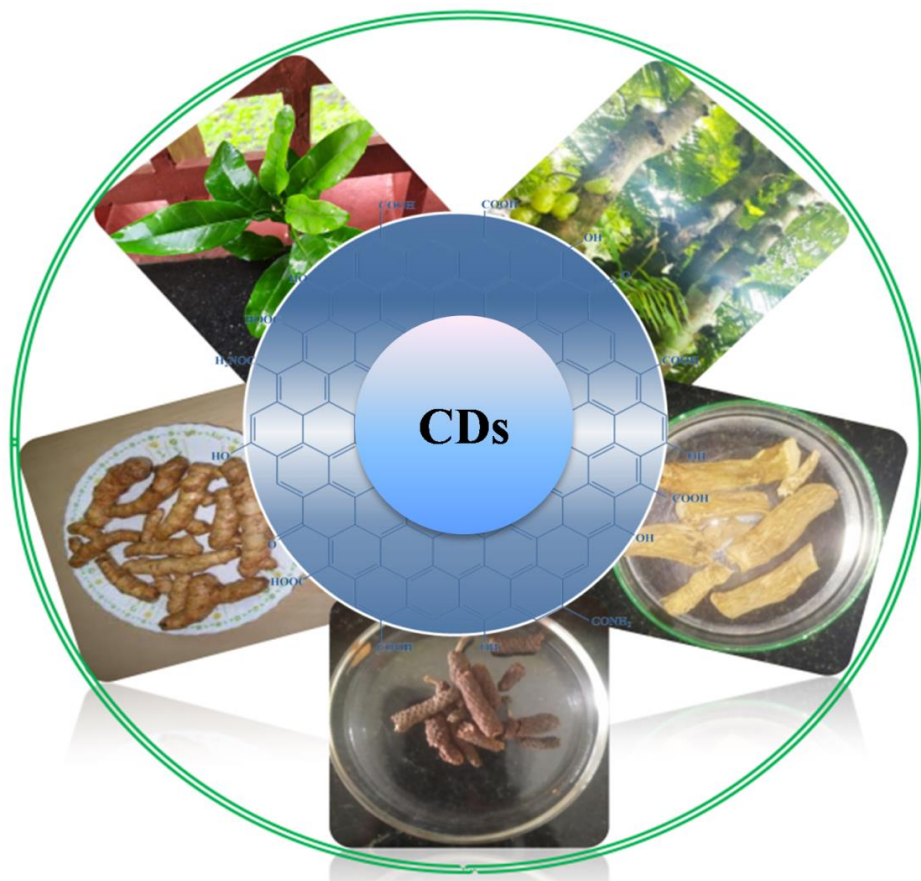
- antioxidants, sensors and bioimaging agents, *Analyst*. 140 (2015) 4260–4269. <https://doi.org/10.1039/C5AN00454C>
- [9] Y.-Y. Chen, W.-P. Jiang, H.-L. Chen, H.-C. Huang, G.-J. Huang, H.-M. Chiang, C.-C. Chang, C.-L. Huang, T.-Y. Juang, Cytotoxicity and cell imaging of six types of carbon nanodots prepared through carbonization and hydrothermal processing of natural plant materials, *RSC Adv.* 11 (2021) 16661–16674. <https://doi.org/10.1039/D1RA01318A>
- [10] S. Mishra, K. das, S. Chatterjee, P. Sahoo, S. Kundu, M. Pal, A. Bhaumik, C.K. Ghosh, Facile and Green Synthesis of Novel Fluorescent Carbon Quantum Dots and Their Silver Heterostructure: An In Vitro Anticancer Activity and Imaging on Colorectal Carcinoma, *ACS Omega*. 8 (2023) 4566–4577. <https://doi.org/10.1021/acsomega.2c04964>
- [11] A. Paul, M. Kurian, Facile synthesis of nitrogen doped carbon dots from waste biomass: Potential optical and biomedical applications, *Cleaner Engineering and Technology*. 3 (2021) 100103. <https://doi.org/10.1016/j.clet.2021.100103>
- [12] Q. Jia, Z. Zhao, K. Liang, F. Nan, Y. Li, J. Wang, J. Ge, P. Wang, Recent advances and prospects of carbon dots in cancer nanotheranostics, *Mater. Chem. Front.* 4 (2020) 449–471. <https://doi.org/10.1039/C9QM00667B>
- [13] C. Murru, R. Badía-Laiño, M.E. Díaz-García, Synthesis and Characterisation of Green Carbon Dots for Scavenging Radical Oxygen Species in Aqueous and Oil Samples, *Antioxidants*. 9 (2020) 1147. <https://doi.org/10.3390/antiox9111147>
- [14] Y.-T. Shieh, W.-W. Wang, Radical scavenging efficiencies of modified and microwave-treated multiwalled carbon nanotubes, *Carbon*. 79 (2014) 354–362. <https://doi.org/10.1016/j.carbon.2014.07.077>
- [15] Y. Zhao, H.-S. Hsieh, M. Wang, C.T. Jafvert, Light-independent redox reactions of graphene oxide in water: Electron transfer from NADH through graphene oxide to molecular oxygen, producing reactive oxygen species, *Carbon*. 123 (2017) 216–222. <https://doi.org/10.1016/j.carbon.2017.07.048>
- [16] Y. Wang, W. Kong, L. Wang, J.Z. Zhang, Y. Li, X. Liu, Y. Li, Optimizing oxygen functional groups in graphene quantum dots for

- improved antioxidant mechanism, *Phys. Chem. Chem. Phys.* 21 (2019) 1336–1343. <https://doi.org/10.1039/C8CP06768F>
- [17] X. Shi, B. Jiang, J. Wang, Y. Yang, Influence of wall number and surface functionalization of carbon nanotubes on their antioxidant behavior in high density polyethylene, *Carbon*. 50 (2012) 1005–1013. <https://doi.org/10.1016/j.carbon.2011.10.003>
- [18] W. Zhang, Z. Zeng, J. Wei, Electrochemical Study of DPPH Radical Scavenging for Evaluating the Antioxidant Capacity of Carbon Nanodots, *J. Phys. Chem. C*. 121 (2017) 18635–18642. <https://doi.org/10.1021/acs.jpcc.7b05353>
- [19] B.R. Bitner, D.C. Marcano, J.M. Berlin, R.H. Fabian, L. Cherian, J.C. Culver, M.E. Dickinson, C.S. Robertson, R.G. Pautler, T.A. Kent, J.M. Tour, Antioxidant Carbon Particles Improve Cerebrovascular Dysfunction Following Traumatic Brain Injury, *ACS Nano*. 6 (2012) 8007–8014. <https://doi.org/10.1021/nn302615f>
- [20] B.S. Thavamani, M. Mathew, D.S. Palaniswamy, Anticancer activity of *Cocculus hirsutus* against Dalton's lymphoma ascites (DLA) cells in mice, *Pharm. Biol.* 52 (2014) 867–872. <https://doi.org/10.3109/13880209.2013.871642>
- [21] J. Kavya, G. Amsaveni, M. Nagalakshmi, K. Girigoswami, R. Murugesan, A. Girigoswami, Silver Nanoparticles Induced Lowering of Bcl2/Bax Causes Dalton's Lymphoma Tumour Cell Death in Mice, *J. Bionanosci.* 7 (2013) 276–281. <https://doi.org/10.1166/jbns.2013.1135>



# Chapter 10

## CONCLUSION AND RECOMMENDATION



---

In this chapter, concluding remarks and future scope of the present study has been discussed



## 10.1 Conclusions

In the present work, synthesis of five different CDs systems were accomplished through ecofriendly microwave assisted synthesis from natural resources without using any hazardous chemicals or sophisticated instruments. The adopted synthetic method is extremely simple with comparatively effortless separation process thereby saving energy and time. And moreover, the entire process strictly follows the green protocols make the current work more environmental friendly. The synthesised CDs revealed excellent fluorescent properties which made them amenable for the fabrication of fluorescent nano sensor. Significant conclusions can be outlined in light of the experimental results.

The five systems were well characterised and depending up on the properties associated with them each CDs was fabricated as fast responsive, and economical fluorescent probe for the selective detection of different aquatic pollutants and food adulterants, with good level of statistical parameters.

The first system designated as MGCDs prepared from the unique spice mango ginger and is effectively used as a fluorescent sensor against toxic aquatic pollutant, hexavalent chromium in aqueous medium. The LOD and linear range of the detection was comparable with the recent reports from the area. Real sample analysis was also successfully carried out by this probe. Apart from this the fluorescence quenching mechanism

behind this sensing was investigated with different methods and accredited to inner filter effect (IFE).

The second system is LLCs synthesised from the leaves extract of wild lemon and the fluorescence of the system utilised for the fabrication of tetracycline sensor in water. The sensing is based on the selective interaction of LLCs with tetracycline leads to the fluorescence quenching. The real environmental water samples analysis was also worked out with good results. Besides, the mechanism of the fluorescence quenching was also examined and ascribed to static quenching mechanism.

The third one is an interesting piece of work and it is named as BCDs, synthesised from bilimbi fruit extract for the first time. The BCDs was used for multiple sensing purposes. Primarily, it is designed as a Cu(II) sensor in water medium based on the fluorescence quenching. And this BCDs with Cu(II) (designated as BCDs@Cu(II)) was again used as a sensor against quinalphos pesticide by the fluorescence recovery method and the mechanism of quenching as well as fluorescence recovery was studied and attributed to static quenching. The real sample quinalphos analysis was also conducted with rice and tea samples with good results.

The next work is based on the CDs from sweet flag rhizomes and is abbreviated as SFCDs. This fluorescent CDs system was designed and executed as 4-NP sensor in water based on the special interaction of SFCDs with 4-NP. The LOD and

linear range of the detection was comparable with the recent reports from this area. Real sample analysis was also employed with good results. The mechanism of sensing by fluorescence quenching was thoroughly investigated with available techniques and finally attributed to combination of static and IFE mechanism.

The last system was prepared from long pepper for the first time, designated as LPCDs. The fluorescence of this system was used for the development of nano sensor against Sudan I, a carcinogenic dye commonly encountered as food adulterant. Real sample analysis was also conducted with chilli powder samples. The mechanism behind the fluorescence quenching was accredited to FRET.

Apart from the above fluorescence based applications, the systems were also subjected for the evaluation of biological properties like antioxidant and *in vitro* cytotoxicity against DLA cell lines. The better results were obtained for the last two systems.

In summary, five different natural products were successfully transformed in to fluorescent nanoparticles. Through this direct materialisation, a value addition was also incorporated. The entire process of preparation was simple, economical and completely greener. And all the systems are successfully employed as sensors against different pollutants.

## 10.2 Recommendations

Other further works were also planned, taking into account the promising future of CDs in numerous fields. The present preparation strategies can be extended to commercialisation of the fluorescent probes. The following list includes a few of the possible thrust zones.

- The biological studies of the prepared systems are at pioneer stage and is planned to explore more with many other methods like, bioimaging, *in vivo* anticancer studies, photo therapy, drug delivery etc.
- New methods can be developed to increase the fluorescence quantum yield and stability.
- As the surface of CDs contains a wide range of functions, precise labelling with certain specific molecules can increase the selectivity of sensing.
- The photocatalytic activity of CDs can be extended for the degradation of several pollutants.